X-Box Binding Protein-1 is Important in Maintenance of Endothelial Integrity and Migration

Martin, Daniel

Awarding institution:
King's College London

Title: X-Box Binding Protein-1 is Important in Maintenance of Endothelial Integrity and Migration

Author: Daniel Martin

X-Box Binding Protein-1 is Important in Maintenance of Endothelial Integrity and Migration

A thesis submitted to King's College London for the degree of Doctor of Philosophy

Daniel Martin

June 2012

Abstract

Background – Sustained activation of spliced x-box binding protein-1 (XBP1), an endoplasmic reticulum stress response transcription factor, results in the development of atherosclerosis in apoE -/- mice. Histone deacetylases (HDACs) play a crucial role in transcriptional regulation through modulation of chromatin structure. In particular, HDAC3 is involved in maintaining endothelial integrity. HDAC3 and XBP1 are similarly expressed in the bifurcation regions of aorta. Unspliced XBP1 (XBP1u) is expressed in a similar manner in endothelial cells. In the present study we investigated the role of XBP1u and XBP1s in the maintenance of endothelial integrity and endothelial cell migration. Furthermore, the crosstalk between HDAC3 and XBP1 signalling pathways was examined.

Methods and Results – Our study demonstrated that disturbed flow upregulated HDAC3 and XBP1u protein production through the VEGF receptor 2 / PI-3-kinase pathway. Knockdown of XBP1 by shRNA lentiviral transfection ablated disturbed flow-induced HDAC3 upregulation. Similarly to HDAC3, overexpression of XBP1u by adenoviral gene transfer increased Akt phosphorylation at serine 473 and haem oxygenase 1 gene transcription, which showed a protective role in hydrogen peroxide-induced apoptosis of endothelial cells. Co-immunoprecipitation assays demonstrated that HDAC3 physically associates with XBP1u and Akt. The use of truncated HDAC3 constructs demonstrated that XBP1 binds to the central section of HDAC3, which is predicted to contain a nuclear export signal. Furthermore, we identified a role for XBP1 in mediating endothelial cell migration. Overexpression of both XBP1u and XBP1s enhanced the ability of endothelial cells to migrate. Ablation of XBP1 expression and XBP1 splicing, through knockdown of IRE1α expression, reduced endothelial cell migration; however this was without a corresponding decrease in eNOS expression and NO production. Further studies using XBP1-null endothelial cells demonstrated that XBP1 is crucial for mediating migration and that this may occur through mediating focal adhesion kinase expression. These studies were aided through the isolation of coronary microvascular endothelial cells from wild type and heterozygous mice hearts.

Conclusions **–** These results suggest that XBP1u protects endothelial cells from oxidative stress, including that produced by disturbed flow. The interaction with HDAC3 could be crucial for this effect. The ratio between XBP1u and XBP1s is also crucial for correct endothelial cell migration. Modulation of this balance and the interaction with HDAC3 may provide novel therapeutic strategies in vascular disease whilst maintaining endothelial integrity.

Acknowledgments

I wish to express my sincere appreciation to my supervisors Professor Qingbo Xu and Dr. Lingfang Zeng for their support, guidance and advice with all aspects of the project. I would like to thank both my supervisors for their patience and encouragement throughout my PhD.

I would like to thank all the members of Professor Xu's lab, past and present, for their support and encouragement. I would particularly like to thank Dr. John-Paul Kirton and Dr. Saydul Alam for keeping me entertained.

I am appreciative to my parents for their unwavering support during my PhD. I would also like to thank Dr. Thomas Murray, for being a fantastic housemate and cheering me up at every opportunity. I would also like to thank Alyssa Bobst; without whose support this PhD would not have been written.

Finally, I would like to thank the MRC and the BHF for funding this project and my PhD.

Declaration

I, Daniel Martin, confirm that the work presented in this thesis is my own and I have been involved in the design, planning and conduct of all the experiments and the thesis writing.

Expert assistance was provided in some aspects of the project by the following colleagues from the Cardiovascular Division of King's College London.

Dr. Lingfang Zeng created the HDAC3 mutation constructs and was responsible for designing and characterising the mice lines.

Dr. Saydul Alam created the HDAC3 lentivirus.

Dr Yanhua Hu performed the arterial graft experiments.

Several figures have previously been presented in academic journals and these have been referenced in the figure legends. Gifts of reagents and constructs have been acknowledged in the text.

Table of Contents

List of Figures

List of Tables

Abbreviations

ABC	ATP-binding cassette
Ad	Adenovirus
ADP	adenosine diphosphate
AP	adipocyte fatty acid-binding protein
Apo	apolipoprotein
ARE	antioxidant response element
ASK	arabidopsis SKP-like
ATF	activating transcription factor
ATP	adenosine triphosphate
BSA	bovine serum albumin
bZIP	basic leucine zipper
Ca^{2+}	calcium
CETP	cholesterol ester transfer protein
CMEC	coronary microvascular endothelial cell
CO	carbon monoxide
CO_2	carbon dioxide
CPE	cytopathic effect
Cre	cre recombinase
CRLR	calcitonin receptor-like receptor
D	aspartate
Dll	drosophila delta-like
DMEM	dulbecco's modified eagle medium
DNA	deoxyribonucleic acid
E	enhancer
EC	endothelial cell
eIF	eukaryotic initiation factor
ER	endoplasmic reticulum
ERAD	endoplasmic reticulum associated degradation
ERSE	endoplasmic reticulum stress response element
eNOS	endothelial nitric oxide synthase
EPC	endothelial progenitor cell
Erk	extracellular-signalling related kinase

ESC	embryonic stem cell
FAK	focal adhesion kinase
FBS	foetal bovine serum
Fe^{2+}	iron
f/f	floxed mice
GAPDH	glyceraldehyde-3-phosphate dehydrogenase
Grp	glucose regulated protein
GSK	glycogen synthase kinase
HBSS	hank's buffered salt solution
HCl	hydrochloric acid
HDAC3	histone deacetylase
HDL	high density lipoprotein
HEK	human embryonic kidney
HLA	human leukocyte antigen
HO	haem oxygenase
HRP	horseradish peroxidase
HUVEC	human umbilical vein endothelial cell
IRE	inositol requiring enzyme
kDa	kilodalton
KLF	kruppel-like factor
LDL	low density lipoprotein
LO (LOX)	lipoxygenase
LXR	liver X receptor
MAPK	mitogen activated kinase
MEF	myocyte enhancer factor
MEK	MAP kinase / Erk kinase kinase
MKK	mitogen activated protein kinase kinase
MMP	matrix metalloproteinase
mRNA	messenger ribonucleic acid
NADPH	nicotinamide adenine dinucleotide phosphate
NF	nuclear factor
NO	nitric oxide
NOS	nitric oxide synthase
Nrf	nuclear factor E2-related factor

NT	non-targeting
PBS	phosphate buffered solution
PCSK	proprotein convertase subtilisin / kexin-type
PDGF	platelet dependent growth factor
PDK	protein dependent kinase
PECAM (CD31)	platelet endothelial cell adhesion molecule
PERK	RNA-dependent protein kinase-like ER kinase
PH	plekstrin homology
PI-3-kinase	phosphatidyl inositol 3 kinase
PIP	phosphatydyl inostiol phosphate
PPAR	peroxisome proliferator activated receptor
ROS	reactive oxygen species
S	serine
shRNA	short hairpin ribonucleic acid
SMC	smooth muscle cell
snPPIX	tin protoporphyrin IX
SR	scavenger receptor
T	threonine
TGF	transforming growth factor
Th	helper T cell
TOR	target of rapamycin
TNF	tumour necrosis factor
tRNA	transfer ribonucleic acid
TX	thromboxane
UPR	unfolded protein response
VCAM	vascular cell adhesion molecule
VE	vascular endothelial
VEGF	vascular endothelial growth factor
VEGFR	vascular endothelial growth factor receptor
vWF	von Willebrans factor
XBP1s	spliced X-box binding protein
XBP1u	unspliced X-box binding protein

Chapter 1 – Introduction

1.1 The vascular system

The cardiovascular system is a complex organ involved in the transport of blood around the body, providing nutrients and oxygen and removing waste products and carbon dioxide. The human embryonic vasculature is the earliest organ to develop. Once the embryo exceeds a specific size passive diffusion is no longer sufficient to supply nutrients to all cells. The embryonic vasculature develops from progenitor cells that migrate and differentiate into endothelial cells (ECs). These form a vascular plexus alongside smooth muscle cells (SMCs), which are recruited by ECs, to form the arterial and venous systems (Carmeliet, 2000a). *De novo* vascular development occurs in three processes: vasculogenesis, the formation of new blood vessels from progenitor cells and predominantly occurs during embryogenesis (Risau and Flamme, 1995); angiogenesis, the sprouting of new vessels from pre-existing vessels which can be induced by hypoxia and occurs in multiple diseases, including many forms of cancer (Carmeliet, 2003); and arteriogenesis, induced by physical forces such as shear stress, and involves remodelling of the existing vasculature and expansion of collateral vessels (Carmeliet, 2000b; Heil et al., 2006).

1.1.1 The vascular structure

Large arteries have three distinct layers; the intima, the media and the adventitia. The intima, the layer in closest proximity to the lumen, is bordered on the lumenal side by a layer of ECs and on the basal side by an elastic basal lamina. Surrounding the ECs is a mixture of extracellular connective tissue matrix, predominantly composed of proteoglycans and collagen. The media is composed primarily of SMCs. SMCs have a contractile role and influence vasodilation and vasoconstriction of arteries thereby controlling vessel diameter and influencing blood pressure. The adventitia, the outermost layer, is predominantly composed of connective tissue although SMCs and fibroblasts are also present. Large arteries only contribute to a small percentage of the total human vasculature. The majority of the

vascular system is composed of small capillary networks, which form widespread meshes. Capillaries differ in structure to arteries as they are not surrounded by SMCs and therefore only passive changes in diameter are possible. Although capillaries contribute to the majority of the vascular system, disruption of the larger arteries and arterioles is of greater interest for research. Dysfunction of these vessels results in more serious complications due to the larger areas of the body reliant on the blood supply provided by these vessels. Venules and veins are responsible for the return of blood to the heart. They have a poorly developed media layer, allowing for an easier flow of low-pressure blood into them.

1.1.2 Endothelial cells

ECs are crucial cellular components located on the intima of all blood vessels, where they function as a selectively permeable barrier between blood and tissues. They are one of the largest organs of the human body covering an approximate surface area of 4000 – 7000 m^2 (Wolinsky, 1980). The endothelium can display different structures depending on the vessel type. Arteries and veins have a more continuous, thicker endothelium as compared to the more fenestrated endothelium of capillaries. The endothelial monolayer is actively involved in several regulatory processes and controls vascular function in response to various stimuli. It forms a semi-permeable barrier for the transport of blood-borne solutes to the underlying tissues, regulates haemostasis, vascular tone, cellular cholesterol and lipid homeostasis.

ECs are polar with apical and basal surfaces. The basal surface is surrounded by extracellular matrix proteins and enclosed by the basal lamina, which together are enveloped by mural cells. The mural cells can be SMCs, cardiomyocytes or pericytes depending on the size and location of the vessel that they help form. Under normal physiological conditions, ECs are in close contact, growth inhibited and protected from apoptosis. ECs in the tubular regions of arteries, where blood flow is laminar, are ellipsoid in shape, aligned in the direction of flow and express a range of anti-apoptotic genes (Hahn and Schwartz, 2009; Malek et al., 1999). The magnitude and direction of endothelial shear stress, caused by the force of contacts between

components of the blood and the endothelial wall, is detected by mechanosensors in the EC membrane and results in specific gene expression patterns, such as KLF2 instigated signalling (Fledderus et al., 2008; Fledderus et al., 2007). The regions of the vasculature subjected to high shear stress during laminar, pulsatile flow express factors that promote growth arrest and prevent apoptosis. ECs exposed to low, oscillatory or disturbed flow have only intermittent activation of these pathways (Chatzizisis et al., 2007; Dekker et al., 2005). To maintain the permeability barrier ECs form intercellular junctions which mediate intercellular signalling and regulate homeostasis (Bazzoni and Dejana, 2004; Mehta and Malik, 2006). In the advent of endothelial damage, growth factors and chemokines are released which increase EC proliferation and motility in an attempt to reduce neointima formation, caused by deposition in the denuded area. Recent studies have also identified that endothelial precursor cells (EPCs), which circulate in the blood, may target and repair damaged endothelial regions (Xu, 2008; Xu et al., 2003). Endothelial dysfunction is hypothesised to be the initial stage in many cardiovascular diseases, such as atherosclerosis.

1.1.3 Endothelial cell development

ECs and SMCs were initially thought to derive from distinct precursor cells through multiple rounds of cell division and specialisation. ECs were thought to derive from the angioblast, (an exclusively endothelial prescursor) or the haemangioblast (both EC and blood cell precursor) during embryonic development (Carmeliet, 2003). In addition to these precursors, in both embryos and adults, new ECs can also derive from circulating EPCs (Asahara et al., 1997). Adult EPCs have also been postulated to play a role in vascular repair as well as disease progression. Recent reports have demonstrated the existence of a common, vascular endothelial growth factor receptor-2 (VEGFR-2)$^{+}$, precursor from which both ECs and SMCs can be derived (Yamashita et al., 2000). EC or SMC differentiation from the common VEGFR-2^{+} precursor has been demonstrated to occur after vascular endothelial growth factor (VEGF) and platelet derived growth factor-BB treatment, respectively (Xiao et al., 2007; Xiao et al., 2006).

The isolation and characterisation of EPCs has proved very difficult and is therefore a controversial subject, with many differences in the methods of isolation, culture and characterisation. However, despite these issues EPCs have the potential to be extremely important in vasculogenesis, angiogenesis (both therapeutic and pathologic) and as an agent of repair for damaged endothelium (Zampetaki et al., 2008). EC precursors are initially characterised by VEGFR-2 expression. Stimulation of VEGFR-2 and downstream signalling initiates cell migration and division. For the initiation of the majority of differentiation events towards ECs VEGF is the stimulus. VEGF is produced in close proximity to regions of newly forming vessels allowing progenitor cells to create the vascular plexus which forms a template for vascular development. Further development and differentiation produces mature ECs. Mature ECs can be characterised through the expression of von Willebrand Factor (vWF), platelet endothelial cell adhesion molecule (PECAM-1 or CD31), VEGFR1, VEGFR2, Tie2, endothelial nitric oxide (eNOS) and many other factors. Although some of these factors are not limited to ECs, detection of multiple factors is considered sufficient to identify ECs. There is an additional level of regulation during EC differentiation which involves formation of arterial and venous endothelium.

1.1.4 Endothelial cell function

The endothelium is a semi-permeable barrier that lines the vasculature and regulates the conduction of blood and the passage of fluids and solutes between the blood and the interstitial space. The permeability of the barrier is tightly regulated. There are two pathways that allow the passage of solutes: the paracellular pathway, involving passage between adjacent ECs through the intercellular junctions; and the transcellular pathway, involving passage through the cell via uptake and export machinery. The intercellular junctions are crucial for the correct formation of blood vessels. The most important intercellular junctions are adherens junctions and tight junctions. Adherens junctions are formed by vascular endothelial (VE)-cadherin, which is a calcium dependent transmembrane receptor. Tight junctions are formed by occludin and members of the claudin family and function as a size barrier to prevent the passage of solutes larger than 3nm in diameter, but allow passive diffusion of

smaller solutes. Adherens junctions are also involved in signalling events and can regulate specific gene transcription (Bazzoni and Dejana, 2004). The intercellular junction is a dynamic structure and can respond to agonists which alter permeability. Dynamic regulation allows infiltration of cells, such as leukocytes, through the endothelium and can alter the flow of solutes between the blood and the interstitial space during specific events (Mehta and Malik, 2006; Vandenbroucke et al., 2008). Intercellular junctions are even more important in the formation and maintenance of the blood-brain barrier. The blood-brain barrier contains multiple adenosine tri-phosphate (ATP)-binding cassette (ABC) transporters, preventing the accumulation of harmful anionic compounds within the brain.

ECs also have an anti-thrombotic role, which prevents / slows the progression of the thrombotic response after endothelial damage. Coagulation is prevented through the release of tissue factor pathway inhibitor, which binds activated coagulation pathways and inhibits the activation of tissue factor. Platelet aggregation is prevented by nitric oxide (NO), prostacyclin and prostaglandin-E_2 synthesis, which also induce vasodilation. Fibrinolysis is stimulated by synthesis of plasminogen activators, which lyse the developing thrombus before the advent of damage (van Hinsbergh, 2001). The endothelium is also responsible for inhibiting leukocyte adhesion, inhibiting SMC proliferation and regulating vascular tone.

The balanced production of vasodilation and vasoconstriction factors by the endothelium maintains the basal vascular tone. The vasodilatory factors produced by the endothelium include NO, prostacyclin and endothelium derived hyperpolarising factor. The vasoconstrictive factors include TXA_2. NO production in ECs occurs through the action of the enzyme nitric oxide synthase (NOS), of which there are three isoforms; neuronal, inducible and endothelial. The ability of a blood vessel to dilate is mainly dependent upon the activity of eNOS. Agonists of eNOS (bradykinin, acetylcholine, ATP, ADP, substance P and thrombin) increase the cytosolic concentration of Ca^{2+} inducing the association of Ca^{2+} with calmodulin, which binds to and activates eNOS. Phosphorylation, by kinases, and acetylation of eNOS can also increase its activity (Butt et al., 2000; Jung et al., 2010). NO diffuses from the EC into the adjacent vascular SMCs, where it reduces their contraction.

1.1.5 Endothelial cell dysfunction

Endothelial dysfunction is thought to be the initiation point for many diseases. The healthy endothelium may be considered 'a defender' and through expression and release of NO, prostacyclin, bradykinin, carbon monoxide (CO) and others reduce inflammation and thrombosis. Endothelial dysfunction results in the cell becoming 'an offender', increasing superoxide, prostaglandin-D_2, cytokine, chemokines and adhesion molecule production. Formation of this state increases inflammation and thrombosis which ultimately leads to disease formation and progression. Endothelial dysfunction can be initiated by low density lipoprotein (LDL) levels, smoking, diabetes, hypertension, infection and haemodynamic forces. Perturbation of EC function leads to EC dysfunction, which often precedes vascular disease, such as atherosclerosis.

1.1.6 Endothelial cells and atherosclerosis

Cardiovascular diseases are a major contributor to mortality, especially in North America and Europe. The most recent statistics demonstrate that cardiovascular disease is the main cause of death in Europe, contributing to over four million deaths per year, equivalent to 48% of total deaths. In North America, the 2009 statistics released by the Centres for Disease Control and Prevention, state that over 33% from a total of 2.5 million deaths were as a result of heart disease or stroke. Cardiovascular diseases include, but are not limited to aneurysms, arteriosclerosis, cerebrovascular disease, coronary heart disease, heart failure, hypertension, myocardial infarction and stroke. Atherosclerosis is the most common form of arteriosclerosis and is the primary cause of coronary heart disease and cerebrovascular disease.

Atherosclerosis is the generic term to describe pathologies which cause a hardening of the arterial wall and a reduction in elasticity. Atherosclerosis is considered a chronic inflammatory disease, associated with endothelial dysfunction and other profound changes to the vascular system (Sandoo et al., 2010; Sima et al.,

2009). ECs are involved at all stages of atherogenesis and their dysfunction is a key early event in atherosclerotic plaque formation. Atherosclerosis predominantly manifests in specific regions of the vasculature and develops due to interactions between modified lipoproteins, macrophages, endogenous SMCs and ECs and immune cells. The aetiology of atherosclerosis is extremely complex and its acquisition is not attributable to any single factor, rather it results from and requires multiple risk factors. It is difficult to classify atherosclerosis as a single disease process, as at various stages different processes such as endothelial dysfunction, inflammation and autoimmune responses are activated and predominate. Only elevated levels of cholesterol have been demonstrated to be sufficient to drive the formation of atherosclerotic lesions in mice in the absence of other risk factor. Multiple risk factors have been characterised by epidemiologic and animal studies (table 1).

The exposure of the endothelial wall to these risk factors triggers changes in endothelial cell functions. In atheroprone regions, ECs have increased permeability, secretory function, hyperplasia of the basement membrane, transcytosis of lipoproteins and increased expression of cell adhesion molecules on their surface and increased cytokine production (Sima et al., 2009). Atheroprone regions of the vasculature occur where there is disturbed flow. ECs are sensitive to changes in blood flow, which can change their morphology and signalling cascade activation (World et al., 2006). There is also a positive correlation between areas of disturbed flow and sites of LDL accumulation and lesion formation (Ross, 1999; Zand et al., 1999).

Atherosclerosis can lead to an acute clinical event by occlusion of the lumen of a vessel, usually through thrombosis after plaque rupture. The progression of atherosclerosis, although incompletely understood, can be classified into several stages (figure 1). Briefly, formation of a fatty streak through retention and oxidation of low density lipoprotein (LDL) within the endothelium activates ECs at the atheroprone region. This leads to the activation of an inflammatory response by inducing the exposure of adhesion molecules on the apical surface of the endothelium. Monocytes are subsequently recruited and penetrate into the subendothelial space. Oxidised LDL is engulfed by macrophages, through recognition by scavenger

receptors. The excessive uptake of oxidised LDL and reduced clearance by macrophages results in a morphological change into a foam cell.

Table 1: Atherosclerotic risk factors

Component	Association with atherosclerosis
Genetic Factors	
Elevated levels of LDL / vLDL	Increased accumulation of LDL in the vasculature results in LDL accumulation in the subendothelial space and leads to increased oxLDL production (Tamminen et al., 1999). Circulating LDL levels can increase due to abrogated expression of ApoE or LDL receptors.
Reduced levels of HDL	Decreased removal of LDL from peripheral tissues leads to increased accumulation of oxLDL in macrophages. ABCA1 is a cholesterol transporter implicated in LDL export from macrophages (Hobbs and Rader, 1999).
Increased blood pressure / hypertension	Increased blood pressure and the rennin – angiotensin – aldosterone pathway are implicated in atherosclerotic lesion formation. Angiotensin II induced hypertension resulted in increased lesion formation (Assmann et al., 1999; Weiss et al., 2001).
Diabetes and Obesity	Aberrant ratio of cholesterol molecules increases the risk of cardiovascular disease and atherosclerosis (Assmann et al., 1999).
Systemic inflammation	Increased activation of the inflammatory response leads to faster progression of fatty streaks into lesions. Elevated levels of inflammatory proteins are linked to atherosclerosis (Bisoendial et al., 2007).
Environmental Factors	
High-fat diet	Increased circulating LDL levels, increases LDL accumulation in subendothelial regions (Assmann et al., 1999).
Smoking	Reduction in endothelial integrity. Smoking is a risk factor for atherosclerosis and other cardiovascular diseases (Assmann et al., 1999).
Lack of exercise	Increased ratio of LDL to HDL levels (Assmann et al., 1999).

.

The foam cells have high intracellular levels of cholesterol which after time induces apoptosis releasing the fatty contents into the subendothelial space and

driving the formation of the atherosclerotic lesion. The lesion progresses through growth of a fibrous cap, formed from SMC-produced extracellular matrix proteins. The cap fills around the core and continued expansion of the lipid-filled interior leads to the formation of a lipid-filled necrotic core (Glass and Witztum, 2001; Rader and Daugherty, 2008). Atherosclerotic plaques can either be stable or unstable, a status that is dependent on their composition and location. Stable plaques can continue to grow until the lumen is completely occluded or unstable plaques can rupture, which is usually precipitated by proteolytic degradation at the edges of the fibrous cap, resulting in thrombogenesis and the occlusion of the lumen at the site of rupture. Atherosclerosis has primarily been studied through the use of knockout animals and epigenetic studies. Although mice are naturally resistant to atherosclerosis, lesions can be induced through a combination of ApoE knockdown and a high fat diet. However, atherosclerotic lesions in mice are different from human lesions as they take weeks rather than years to form and are much more cellular in structure. These differences must be taken into account when extrapolating data from studies on atherosclerosis in mice.

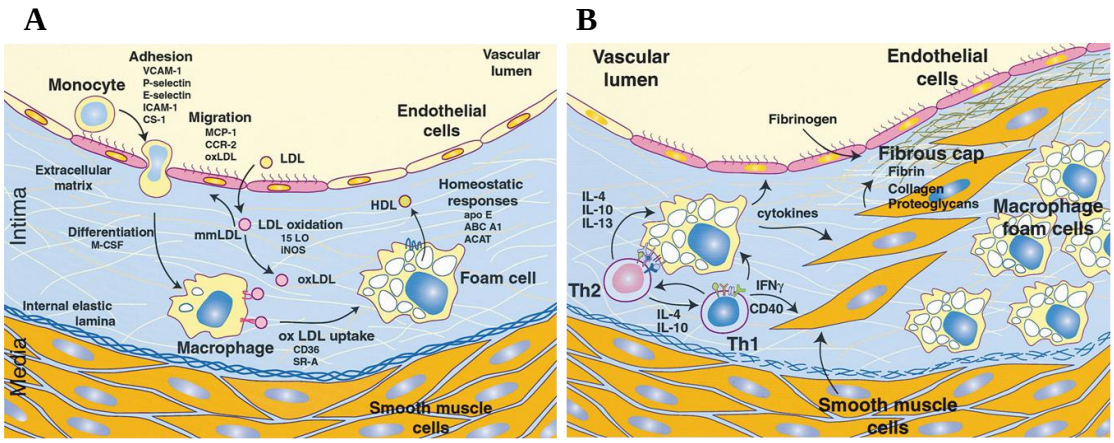

Figure 1: The initial stages of atherosclerotic lesion formation.

A. Formation of the fatty streak and initiation of the inflammatory response. LDL infiltrates the subendothelial space where oxidation occurs. Oxidised LDL stimulates adhesion molecule production by ECs and monocyte recruitment. Macrophages engulf oxidised LDL after recognition by scavenger receptors leading to foam cell formation. **B.** Progression of the atherosclerotic lesion and formation of the necrotic core. The accumulation and apoptosis of foam cells leading to exposure of modified self-antigens such as oxLDL activates an immune response. Th1 cells are activated which increase local inflammation, initially in a beneficial manner. Progression of the lesion involves SMC migration, formation of a fibrous cap and development of a chronic inflammatory state. Adapted from (Glass and Witztum, 2001).

The formation of the initial fatty streak is considered to be the initiating event in the formation of an atherosclerotic lesion and is also the atherosclerotic event towards which EC activity and function is most important. Although it is important to note that fatty streak formation has been observed from the first decade of life and does not necessarily lead to atherosclerosis. This stage is characterised by the accumulation of LDL within the subendothelial space and macrophage recruitment (figure 1A). The increased transcytosis of lipoproteins leads to their accumulation and retention in the intimal space by modification through oxidation, glycation and other enzymatic reactions. LDL is able to passively diffuse through intercellular junctions; however, the oxidation of these molecules in the permissive subendothelial environment prevents retrograde transfer due the formation of more stable interactions with extracellular matrix proteins. These modified lipoproteins have been identified in early thickenings of the human aorta (Tirziu et al., 1995). Oxidised LDL stimulates ECs, in part through the activation of signalling through the LOX-1 endothelial LOX-1 receptor. This leads to NADPH oxidase activation and the production of superoxide radicals (Xu et al., 2007). Endothelial activation involves the synthesis and secretion of cytokines such as monocyte chemotractant protein-1, interleukins, vascular endothelial growth factor (VEGF) and the expression of cell adhesion molecules; vascular cell adhesion molecule 1, intercellular cell adhesion molecule 1 and E- and P- selectins (Nakashima et al., 1998). The expression of these proteins is specifically activated in response to oxidised LDL (Khan et al., 1995). The expression of adhesion molecules and chemokines recruits and activates monocytes to the intimal space. Oxidised LDL is a high affinity substrate for the macrophage scavenger receptors; SR-1 and CD36. Therefore macrophage recruitment by activated endothelial cells initially works to reduce the presence of oxidised LDL in the subendothelial space. However, there is no negative feedback regulation of the scavenger receptor-mediated uptake and therefore if there are large quantities of oxidised LDL present then the macrophages will eventually overload and form foam cells. Foam cells have a dramatically reduced ability to migrate and are retained in the subendothelial space where they eventually undergo apoptosis and the start of the atherosclerotic lipid-filled core is formed.

The progression of atherosclerosis is characterised by fibrous plaque formation (figure 1B), which involves an accumulation in extracellular lipid, infiltration of

SMCs into the intima and activation of an immune response. Th1 and Th2 cells are activated by macrophage foam cells and dendritic cells presenting modified self antigens, such as oxLDL. Published studies suggest that Th1 cells, which initiate a pro-inflammatory response, predominate in atherosclerosis, with the role of Th2 cells suggested to be anti-inflammatory (Nilsson and Hansson, 2008). Therapeutic modulation of the Th1 and Th2 response and ration may be beneficial in patients suffering from atherosclerosis. Activated Th1 cells release cytokines which increase the level of local inflammation.

SMCs pass through the basal lamina, proliferate and secrete extracellular matrix proteins that form a fibrous plaque. The lesion continues to grow as more macrophages are recruited and more cholesterol is deposited in the core. Initially the lesion grows towards the basal lamina, however after a threshold is passed the lesion extends into the lumen of the vessel. During the early growth phase the lumen of the vessel remains constant as the vessel is remodelled through expansion of the local artery wall. Although complete occlusion of the lumen is possible, most complications of atherosclerosis are caused by plaque rupture and resulting thrombosis. Plaque rupture exposes thrombotic factors present in the lesion core. The stability of the lesion is influenced by many factors such as cellular composition of the necrotic core, macrophage activation and expression of metalloproteinase's (Newby, 2007, 2008). Metalloproteinase's have been demonstrated to be particularly active in the edge regions of atherosclerotic lesions, which are the regions most likely to rupture.

There are several therapeutic targets for the treatment of atherosclerosis (table 2). Atherosclerosis has also been targeted as an autoimmune disease initiated by the immune response to oxLDL. Studies have been performed that demonstrate the incidence of atherosclerosis is reduced after immunisation of ApoE knockout mice with peptide fragments generated from ApoB100, which is conserved in all LDL molecules (Nilsson et al., 2007). Much of the information obtained on atherosclerosis derives from studies on animal models. The usefulness of these models is subject to much debate. In the ApoE mice atherosclerotic lesions develop, however they have a much more cellular content than lesions formed in humans. These lesions take only weeks to form compared to years, even decades in humans. The incidence of plaque

rupture is also very different in mice lesions, as plaque rupture is thought to depend on the composition of the lesion and not the size. Finally, lipoprotein metabolism and inflammatory responses differ greatly between mice and humans suggesting that the therapeutic response observed in mice may not be conserved in humans.

Table 2: Therapeutic targets for the treatment of atherosclerosis.

Target	Aim of Therapy	Function
PCSK2	↓	Targets LDL receptors in hepatocytes for degradation rather than recycling resulting in increased circulating LDL.
ApoB	↓	Major protein component of LDL molecules. Reduced ApoB expression would decrease LDL levels.
Lipoprotein lipase	↓	Catalyses the conversion of vLDL to LDL molecules.
15-LO	↓	Catalyses the oxidation of LDL, promoting LDL accumulation and initiating the inflammatory response.
CETP	↓	Catalyses the conversion of HDL molecules to LDL.
LXR	↑	Activates expression of ABCA1 and ABCG1, increasing clearance of LDL from macrophages into HDL molecules.
ABCA1 / ABCG1	↑	Transport cholesterol from macrophages to nascent and mature HDL molecules respectively.
VCAM1	↓	Expressed on the surface of ECs, involved in monocyte recruitment and expressed in response to oxLDL.
MMP9	↓	Involved in degradation of the extracellular matrix proteins in the fibrous cap leading to plaque rupture.

1.1.7 Endothelial cell migration, angiogenesis and focal adhesion kinase

The growth of new blood vessels occurs through a process termed neovascularisation. This process is critical during development and growth and for wound healing and tissue repair. Angiogenesis, a form of neovascularisation involves the migration, recruitment and connection of ECs. Unwanted angiogenesis has been associated with the development of atherosclerosis (Carmeliet, 2003). The early vascular tree occurs through the sprouting of ECs from angioblasts. This process requires the activation of VEGFR, cell-cell and cell-matrix signalling. The cells will

then migrate, interconnect and divide before eventually forming tube-like structures (Risau, 1997). There are three main forms of angiogenesis vasculogenesis, arteriogenesis and angiogenesis. Vasculogenesis is the formation of new blood vessels from circulating or tissue-resident EC stem cells, which proliferate to form new vessels. This predominantly occurs during development. Arteriogenesis is the formation of larger blood vessels, possessing an intima, media and adventitial layer. Angiogenesis is the formation of thin-walled EC-lined structures, which extensively occur during the repair of damaged tissues. The new growth of blood vessels supports tissue growth and organ function during development and disease. If a lack of nutrients or oxygen is detected then angiogenic sprouting occurs, which is the growth of new vessels from an existing vessel. The signals that activate angiogenic sprouting include growth factors and chemokines that are released by hypoxic tissue (Phng and Gerhardt, 2009). EC migration during angiogenesis involves several major stages. The EC senses a pro-migratory signal, such as VEGF and filopodia are formed through the activation of Cdc42 and WASP signalling. PI-3-kinase phosphorylation and activation of focal adhesion kinase signalling result in the extension of lamellipodia. The extended region of the EC then reattaches to the surrounding matrix through focal adhesion assembly. The cell then contracts through stress-fibre mediated contractions and the rear end of the cell is released from its attachments by degradation of focal adhesions. These steps require the precise remodelling of the EC in response to a hypoxic signal (Lamalice et al., 2007). One particular mechanism through which EC migration can be abrogated is through ROS-dependent signalling. ROS produced via the activation of NADPH oxidase, subsequent to VEGF stimulus has been hypothesised to activate several protein tyrosine phosphatases, including SHP-1 and SHP-2. These dephosphorylate VEGFR2 and attenuate the effects of VEGF signalling (Ushio-Fukai, 2006).

There are multiple pro and antiangiogenic signals that originate within the body. These contribute to and control blood vessel density and function. The insufficient supply of nutrients and oxygen in any tissue results in the formation of new vessels from the walls of existing vessels. Angiogenic sprouting occurs after quiescent ECs receive signals from growth factors and cytokines released by surrounding hypoxic tissue. These signals enhance the migratory capacity of ECs and a new network of vasculature is formed, until the hypoxic signalling is reduced by

correct blood flow to the affected area. VEGF, VEGFR2 and focal adhesion kinase (FAK) are crucial during the formation of blood vessels. Activation of VEGFR2 expression promotes EC elongation, motility and proliferation. The detection of VEGF by ECs results in delta-like ligand 4 (Dll4) expression which is a crucial protein of 'tip cells', which are ECs with a highly motile phenotype thought to form at the migrating end of newly forming vessels. Activation of Dll4 signals to the proceeding ECs to induce a phenotypic change into 'stalk cells' to promote new vessel formation (Jakobsson et al., 2010). The migration of all ECs does not occur in the same manner. The migration of ECs is spearheaded by the 'tip cells' which exude long filopodia composed of multiple tyrosine kinase receptors to sense the surrounding environment (Gerhardt and Betsholtz, 2003; Gerhardt et al., 2003). These cells have a reduced interaction with surrounding cells, which is necessary to increase their ability to migrate. Stalk cells produce fewer filopodia and proliferate when stimulated with VEGF-A. These cells also contribute to lumenal formation through form intercellular interactions via adherens and tight junctions (Dejana et al., 2009). The specification of these ECs and the signals that are required to produce tip and stalk cells are highly regulated and elucidating not only these signals but the way in which they interact will contribute toward our understanding of the angiogenic process which is so important during so many disease processes.

One of the crucial components during EC migration is the formation and degradation of focal adhesions. FAK is widely expressed in ECs and its signalling regulates fundamental aspects of neovascularisation and is involved in EC adhesion and migration (Wary et al., 2012). FAK signalling can be initiated by both integrins and through VEGF / VEGFR2 signalling, thus implicating FAK as a signal component of EC migration and survival pathways (Zhao and Guan, 2009). FAK is ubiquitously expressed and the promoter has been demonstrated to contain AP-2, NF-κB and p53 regulatory sites (Golubovskaya et al., 2004).

In the adult vasculature, ECs form a quiescent monolayer, where the cells are no longer dividing and form a network of intercellular attachments. Upon stimuli, such as a loss of shear stress a subset will respond and form tip cells, which are responsible for new vessel formation (figure 4). Tip cells have reduced interconnections with surrounding ECs and extracellular matrix, and the cells are

therefore able to proliferate, elongate and migrate (Wary et al., 2012). Stalk cells have also been identified which proliferate to increase the length of the blood vessel. The formation of both of these cell types is regulated through the activation of VEGF signalling on VEGFR2 receptors (Gerhardt et al., 2003).

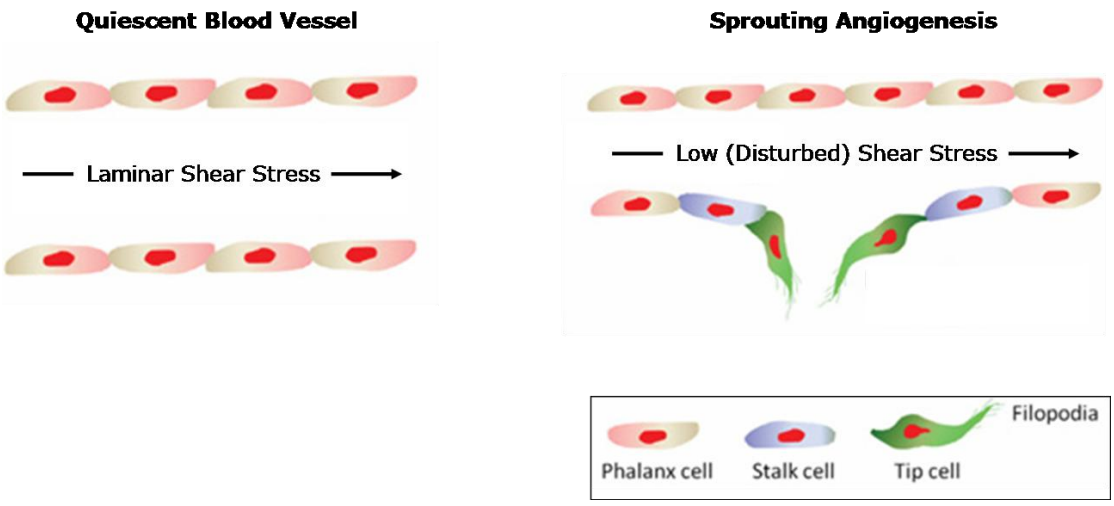

Figure 2: Tip cell formation during angiogenesis.
The formation of a new blood vessel due to a loss of shear stress and VEGF signalling. Tip cells form filopodia and 'push' the new vessel forwards. Stalk cells are in a proliferative state and maintain EC-cell contacts. Phalanx cells are in a quiescent anti-proliferative, anti-migratory state. This figure has been adapted from (Zhuang et al., 2011).

FAK can regulate the migratory process and the formation of tip cells through several mechanisms. Firstly in FAK-null cells there are increased numbers of focal adhesions and FAK was also shown to regulate cell survival (Ilic et al., 2003). Secondly FAK-deficient cells cannot form functional vascular networks, whilst overexpression of FAK increased angiogenesis in a transgenic mouse model (Ilic et al., 2003; Zhao and Guan, 2009). These results indicate a key role for FAK in angiogenesis and EC migration. During EC migration it is necessary for ECs to partially detach from the extracellular matrix, which increases the likelihood of the cell undergoing apoptosis. Previous studies have shown that FAK acts to prevent EC apoptosis through the recruitment and activation of PI-3-Kinase and its subsequent downstream pathways, including Akt (Vivanco and Sawyers, 2002).

1.1.8 Endothelial cells and shear stress

Despite the systematic nature of atherosclerotic risk factors, atherosclerosis lesions only occur at predisposed sites. The propensity for atherosclerotic lesion development therefore differs between regions of the vasculature. A higher incidence of atherosclerosis was observed in curved regions and lateral walls of branch points than in linear segments of vessels (Ku et al., 1985). Atherosclerotic lesions predominantly formed in regions of the vasculature which have low time-averaged shear stress (the amplitude of the total flow observed over time in a single direction) and high spatial shear stress (the total force of the shear stress observed at a single location in multiple directions). These different forces are caused by the non-uniform flow of blood through the vascular system. In regions of the vasculature that are straight and around the outer curves of bends the laminar blood flow sensed by the endothelium is unidirectional and pulsatile. In humans the shear stress sensed by the endothelium in these regions is between 15 – 70 dynes / cm^2. Regions of the vasculature predisposed to atherosclerotic lesion formation, such as the insides of arterial curves and bifurcation points continue to sense pulsatile flow, however it is highly turbulent and bidirectional. The endothelium in these regions senses an oscillatory shear stress of 0 - 10 dynes / cm^2. High shear stress induces an atheroprotective and anticoagulant endothelial phenotype. Studies into the rate of EC apoptosis on visible (laminar shear stress) and occluded (disturbed shear stress) sections of atherosclerotic lesions demonstrated an 85% decrease in EC apoptosis in regions with elevated shear stress (Tricot et al., 2000). Meanwhile, disturbed shear stress is associated with endothelial dysfunction and atherosclerosis development. The inside walls of arterial curves and lateral branch points demonstrated increased monocyte adhesion and EC apoptosis (Boon and Horrevoets, 2009).

1.1.8.1 Protective Cell Signalling

Steady laminar shear stress activates mechanosensitive, atheroprotective signalling pathways, responsible for maintaining endothelial integrity. Atheroprotective flow patterns limit oxidative stress, inflammation and apoptosis. In regions of disturbed flow these pathways may only be transiently activated (Berk,

2008; Chatzizisis et al., 2007). In healthy regions of the vasculature mechanical forces and chemical ligands are sensed by receptors on the apical surface of ECs. This initiates a signalling cascade that ultimately resolves in altered gene expression. These result in altered cell function; in this case increasing the protection of ECs against apoptosis and reducing the expression of monocyte attachment proteins. There are several crucial signalling pathways that are activated through mechanical force; including redox-mediated inhibition of ASK1 / jun-terminal kinase signalling and activation of KLF2 and Nrf2 signalling.

Kruppel-like transcription factor 2 (KLF2) is specifically induced by laminar shear stress in ECs (Dekker et al., 2002). KLF2 expression promotes anti-inflammatory and pro-survival signalling through suppressing the activation of the apoptotic molecule TGF-β, by inducing Smad7 expression and reducing baseline expression levels of AP-1 (Boon et al., 2007). Global expression studies showed that KLF2 is also important for the integration of multiple endothelial functions associated with vascular regions that are resistant to atherogenesis such as inflammation, thrombosis/haemostasis, vascular tone and blood vessel development (Parmar et al., 2006). Shear stress induces KLF2 expression through both transcriptional activation and stabilisation of KLF2 mRNA (Dekker et al., 2002; van Thienen et al., 2006). Shear stress leads to the induction of MEK5-ERK5-MEF2C signalling, leading to MEF2C binding to the KLF2 promoter (Parmar et al., 2006). Histone deacetylases have been linked to the regulation of MEF2 activity at the KLF2 promoter (Kumar et al., 2005).

Nuclear factor erythroid 2-like 2 (Nrf2) is a shear induced transcription factor responsible for antioxidant gene expression. Nrf2 binds directly to the antioxidant response element (ARE) of antioxidant enzymes like haem oxygenase 1 (HO-1) and NAD(P)H dehydrogenase quinone 1. Activation of these enzymes reduces the oxidative burden on the endothelium (Chen et al., 2003b). Nrf2 is activated by shear stress through activation of PI-3-Kinase and Akt signalling, which increases the nuclear localisation of Nrf2 (Dai et al., 2007).

Laminar flow also promotes a reducing state in ECs due to the presence of glutathione. Glutathione is a substrate for glutathione peroxidase to allow the

elimination of hydrogen peroxide and lipid hydroperoxides. Steady laminar flow has been shown to inhibit hydrogen peroxide-induced jun-terminal kinase activation by increasing the reduced glutathione levels in a glutathione reductase-dependent manner (Hojo et al., 2002).

1.1.8.2 Atherogenic cell signalling

In contrast to endothelium subjected to laminar flow, regions of the vasculature exposed to disturbed flow have very different gene expression patterns. Disturbed flow attenuates NO and prostacyclin production, reducing the vasodilatory and atheroprotective role of these molecules (Chien, 2008a). Disturbed flow also promotes oxidative stress by increasing the transcription and activity of nicotinamide adenine dinucleotide phosphate (NADPH) oxidase and downregulating the expression of reactive oxygen species (ROS) scavengers. Disturbed flow has also been shown to enhance inflammation by upregulating NF-κB-mediated VCAM and monocyte chemoattractant protein expression. Disturbed flow also promotes SMC migration, differentiation and proliferation; extracellular matrix degradation and synthesis in fibrous plaques; and has potential roles in neovascularisation, calcification and thrombogenecity (Chatzizisis et al., 2007; Cunningham and Gotlieb, 2005).

1.2 Oxidative stress in the vasculature

Oxidative stress has been implicated in cardiovascular dysfunction and many cardiovascular diseases, including atherosclerosis. Oxidative stress is a state in which ROS overwhelm the endogenous antioxidant capabilities of cells and tissues. ROS play an important role in endothelial dysfunction. ROS molecules include hydrogen peroxide, superoxide radical, hydroxyl radicals and reactive nitrogen species, such as peroxynitrate and nitrogen oxide radicals. ROS are oxygen molecules capable of easily reacting with other molecules to produce further detrimental products and reactions. Superoxide is formed from the univalent reduction of oxygen, which can be performed by NADPH oxidases and xanthine oxidases. Superoxide is itself functional within the cell; however it is also required to generate the more harmful peroxynitrate, the nitrogen oxide radicals and the less harmful hydrogen peroxide

molecules. Hydrogen peroxide can be converted into water or into the highly reactive hydroxyl radical. All of these species initiate signalling responses in the vasculature (Taniyama and Griendling, 2003). ROS can be generated endogenously or in response to environmental stress and are involved in initiating apoptotic signalling. HO-1 has been a major focal point of research due to its ability to counter proapoptotic stimuli and thereby prevent apoptosis (Ryter et al., 2007).

1.2.1 Apoptotic signalling through oxidative stress

Maintaining the correct balance of ROS levels is crucial in preserving endothelial function. For example nitrogen oxide is required for arterial vasodilation and a reduction in nitrogen oxide levels resulting from increased interactions with superoxide radicals impairs vasodilation. ROS are of particular importance in maintaining EC integrity. The incubation of ECs with superoxide or hydrogen peroxide induces apoptosis, which damages the endothelial wall and initiating a proatherogenic state. The overproduction of hydrogen peroxide in mice was also demonstrated to increase atherogenesis (Cai, 2005). ROS are also involved in promoting adhesion molecule production and the subsequent attachment of monocytes to the endothelial wall. In humans, the higher expression of NADPH subunit proteins is associated with increased superoxide production and severity of atherosclerosis (Sorescu et al., 2002). NADPH oxidase deficient ApoE -/- mice also have significantly less atherosclerotic lesions formation than their wild type counterparts (Barry-Lane et al., 2001). Furthermore interleukin-1 beta activation of VCAM-1 expression was almost completely abolished by co-incubation with antioxidants, suggesting that VCAM-1 expression can be induced by ROS (Marui et al., 1993). Shear stress, apoptotic signalling through TNFα, VEGF and cellular injury can all result in the activation of ROS producing enzymes. These activate ECs and lead to impaired vessel relaxation, an increase in apoptosis and increased monocyte adhesion. This primes regions of the vasculature and makes them more sensitive to hypertension and atherogenesis (Taniyama and Griendling, 2003).

1.2.2 ROS, atherosclerosis and shear stress

Shear stress plays a critical role in the production of ROS in the vasculature. Shear stress has been shown to activate NADPH oxidase resulting in the production of superoxide (De Keulenaer et al., 1998; Hwang et al., 2003a; Hwang et al., 2003b). This increases the ability of monocytes to adhere to the endothelium thereby increasing the likelihood of atherosclerotic lesion formation (Hwang et al., 2003b). Xanthine oxidoreductase is also activated in response to disturbed flow and promotes the production of superoxide molecules (McNally et al., 2003). NO is also a key molecule in the vascular system and can result in increased oxidative stress. eNOS is induced in ECs by pulsatile and laminar shear stress (Metaxa et al., 2008). The production of NO can be beneficial and result in vasodilation of the vasculature; however it is also able to interact with superoxide molecules to form the highly reactive peroxynitrate molecule. Peroxynitrate induces oxidative damage and enhances adhesion molecule expression inducing a pro-atherogenic EC phenotype (Shelton et al., 2008). The expression of these molecules is heavily influenced by the type of flow that ECs are subjected to. High laminar shear stress enhances the NO production and reduces superoxide molecule production, whereas oscillatory shear stress enhances superoxide expression to a greater extent than laminar flow (De Keulenaer et al., 1998; Takabe et al., 2011). These studies demonstrate a clear link between shear stress, the production of ROS and the development of atherosclerotic lesions.

1.2.3 Haem oxygenase 1

Haem oxygenase is the rate limiting enzyme in the degradation of haem. HO-1 is inducible whilst the expression of HO-2 is constitutive in certain cell types. HO catalyses the conversion of haem into carbon monoxide (CO), biliverdin and iron (Fe^{2+}). HO-1 plays a central role in the response of cells to stress, particularly oxidative stress. The expression of HO-1 has been associated with anti-inflammatory effects and the suppression of proliferation, apoptosis and inflammation (Ryter et al., 2007). The various contributions of HO-1 towards preventing apoptosis are

demonstrated in figure 3. Although iron is pro-oxidative, HO-1 induces the export of iron from the cell and the formation of ferritin. Ferritin neutralises the reactive iron and reduces apoptosis. Iron has also been shown to activate NF-κB which initiates an anti-apoptotic signalling cascade (Choi et al., 2004). Biliverdin and bilirubin also prevent apoptosis by scavenging ROS molecules. Bilirubin and biliverdin may also initiate anti-inflammatory and anti-proliferative signalling (Ryter et al., 2006). CO is the most interesting and therefore most studied product of the HO-1-mediated degradation of haem. Initially thoughts towards the function of CO were heavily influenced by the perception generated by CO poisoning leading to death due to its ability to permanently displace oxygen from haemoglobin. However, recent studies have demonstrated a role for CO in many signalling events (Kaczorowski and Zuckerbraun, 2007). CO was demonstrated to inhibit TNFα-mediated apoptosis in mouse ECs. The activation of MKK3 and p38 MAPK were necessary for this function (Brouard et al., 2000). CO was also determined to have a direct anti-inflammatory effect by inhibiting cytokine-mediated apoptosis. HO-1 is therefore a potent inhibitor of oxidant mediated apoptosis and inflammation in cells.

1.2.3.1 Induction of haem oxygenase 1 gene expression

HO-1 can be highly induced by haem, heavy metals, TGFβ, PDGF, VEGF, NO, peroxynitrate, modified lipids, hypoxia and cytokines (Ryter et al., 2006). HO-1 can also be induced in response to many atherosclerotic risk factors such as high blood pressure, shear stress, smoking and oxidised lipids (Chen et al., 2003a; Favatier and Polla, 2001; Ishikawa et al., 2001; Ishizaka et al., 1997). It has been suggested that HO-1 is a relevant target in pharmacologic intervention in atherosclerosis (Stocker and Perrella, 2006). There are several critical regulatory domains present in the 10kb proximal promoter region, upstream of the HO-1 initiation site. This region contains multiple confirmed and putative enhancer sites of which E1 and E2 are the most studied. These regions contain stress response elements that are able to bind proteins belonging to the bZIP superfamily of transcription factors. HO-1 gene transcription can be induced by a wide-range of stimuli and therefore its regulation is highly complex (Ryter et al., 2006).

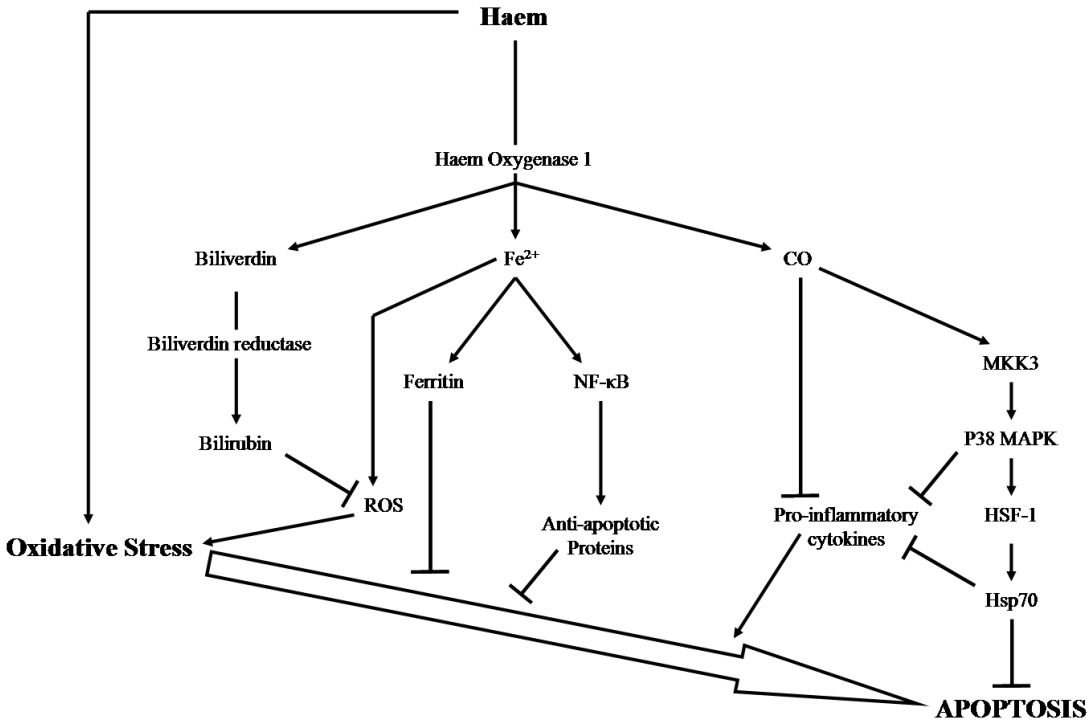

Figure 3: Anti-apoptotic signalling pathways initiated by haem oxygenase-1.
HO-1 catalyses the conversion of haem into biliverdin, Fe^{2+} and CO. Haem and ROS are inducers of oxidative stress which leads to apoptosis and inflammatory responses. Biliverdin is converted into bilirubin by biliverdin reductase. Both bilirubin and biliverdin function as antioxidant molecules and scavenge free ROS. Fe^{2+} is an inducer of ROS, however, HO-1 induced Fe^{2+} is either exported from the cell or forms aggregations, termed ferritin. Ferritin inhibits the apoptotic effect of Fe^{2+}. Fe^{2+} may also be involved in suppressing apoptosis through activating transcription of anti-apoptotic proteins mediated by NF-κB. CO has been demonstrated to indirectly inhibit pro-inflammatory cytokine production as well as inhibitng apoptosis through an MKK3, p38 MAP kinase signalling cascade. Adapted from (Ryter et al., 2007).

1.3 X-box binding protein 1

The human X-box binding protein (XBP1) belongs to the basic region / leucine zipper (bZIP) superfamily of transcription factors. Members of the bZIP transcription superfamily contain a basic peptide region, responsible for non-covalent interactions with the major groove of DNA molecules and a leucine zipper region, containing a leucine residue every seven amino acid residues, responsible for protein dimerisation and necessary for gene transcription. XBP1 was initially characterised through its ability to bind the HLA DRα promoter in B cells. Early studies into XBP1

demonstrated that guanine residues in the X-box motif and the interspace element, the nucleotides located between the X and Y boxes, contributed towards the interaction of XBP1 with the DNA molecule (Liou et al., 1990). These early studies only identified a single 261 amino acid structure of XBP1, containing a basic domain in which 45% of the residues are arginine or lysine and a leucine zipper region, containing six leucine residues spaced seven amino acid residues apart (figure 4). The consensus target DNA sequence for XBP1 was identified as 5'-TGCGTCA-3'. XBP1 also contains an acid-rich domain, a glutamine-rich domain and a serine-threonine-rich domain. XBP1 retains a high degree of sequence homology with other members of the bZIP transcription family, in particular c-*jun* (Liou et al., 1990).

Subsequent studies identified two isoforms of XBP1, which arise due to unconventional splicing. The region of the genome encoding XBP1 has coding sequences present in two distinct reading frames (figure 4). Both of these reading frames are transcribed and are incorporated into a single XBP1 mRNA molecule. Under normal physiologic conditions the first reading frame is translated and the unspliced XBP1 (XBP1u) protein is synthesised. Unconventional splicing of XBP1 mRNA, which is mediated by IRE-1α homodimerisation and activation, results in the removal of a 26 nucleotide fragment from the central section of XBP1 mRNA. This splicing event results in the translational machinery bypassing the first stop codon, allowing the synthesis of a second, spliced XBP1 protein (XBP1s). XBP1s has a unique C-terminal domain (figure 4B). Unconventional splicing occurs in the cytoplasm and does not require the nuclear spliceosome machinery. Unconventional splicing has been more fully described via experimentation on the yeast homologue of XBP1 (Yoshida, 2007). In order for the splicing of XBP1 to occur IRE-1α, a resident endoplasmic reticulum membrane protein, undergoes homodimerisation in response to endoplasmic reticulum (ER) stress. Conformational changes in the IRE-1α cytoplasmic region result in the formation of an active endoribonuclease site. IRE-1α catalyses the removal of a 26 nucleotide fragment from XBP1u mRNA. The remaining RNA sequence is subsequently ligated through an as yet undetermined mechanism in humans, or by Rlg1p in yeast cells to produce XBP1s mRNA. The mature XBP1u protein is a 261 amino acid peptide and contains an N-terminal DNA-binding domain, a nuclear import and export signal and a motif that targets the protein for proteosome-mediated degradation. The mature XBP1s protein contains a 376

amino acid sequence and contains the identical N-terminal domains (the DNA-binding site and the nuclear localisation signal), but has an altered C-terminal domain. This region contains an activation domain responsible for inducing the transcription of ER stress response genes, such as endoplasmic reticulum associated protein degradation (ERAD) and chaperone proteins (figure 4B). The mature XBP1u protein is predicted to be 35 kDa in size, whilst the spliced isoform produces a protein of 56 kDa, allowing identification of the expression of each individual isoform.

1.3.1 ER stress

The accumulation of unfolded proteins within the ER results in the induction of ER stress. Activation of ER stress results in an intracellular signalling cascade called the unfolded protein response (UPR). There are three mechanistically distinct pathways involved in the correct signal transduction of the UPR (figure 5). These pathways are mediated by activating transcription factor 6 (ATF6); inositol requiring enzyme 1α (IRE-1α); and double-stranded RNA-activated protein kinase (PKR)-like endoplasmic reticulum kinase (Reimold et al.) (Reimold et al.). The activation of the UPR alters gene expression, including the induction of genes involved in lipid synthesis, ERAD and protein folding. The specific functional and gene expression changes generate an adaptation to normal cell physiology which allows cells to compensate and then overcome the demands imposed by ER stress (Schroder and Kaufman, 2005). ER stress can be defined as a consequence of an imbalance between the load of unfolded proteins in the ER and the capacity of the unfolded protein machinery to deal with that load (Ron and Walter, 2007). Once an increase in the load of unfolded proteins is detected within the lumen of the ER, three discrete pathways are activated which initiate signal transduction events. Activation of the unfolded protein response results in a transient reduction in normal protein production, a medium-term upregulation of the protein folding machinery and an increase in the degradation machinery and if unfolded protein response stimulation is long-term initiate apoptosis. These three pathways are controlled by the integral ER membrane proteins, ATF6, PERK and IRE-1α, which can assess the folding state in the ER lumen through interactions with BiP and initiate a co-ordinated response (Ron and Walter, 2007) (figure 5).

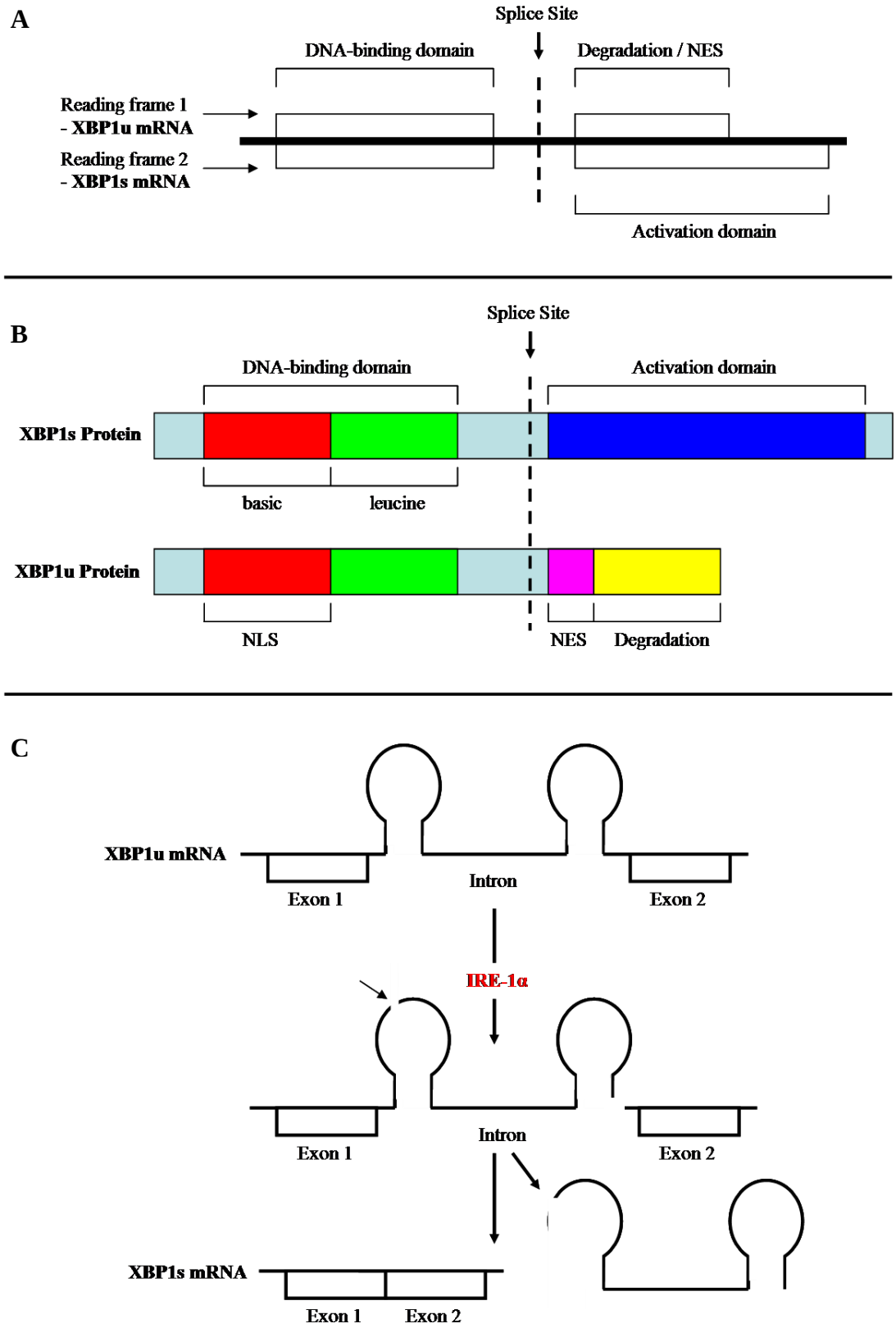

Figure 4: XBP1u and XBP1s mRNA and protein structure.

A. The mRNA structure of XBP1u and XBP1s. **B.** The protein domain structure of XBP1u and XBP1s. **C.** The predicted mechanism of XBP1u splicing through IRE-1α. The removal of the 26 nucleotide sequence and re-ligation results in the translation of a second open-reading frame.

Transient activation of the ER stress response abrogates the derogatory effects of an increase in protein load. However, chronic ER stress results in cell death by apoptosis (Ferri and Kroemer, 2001; Rodriguez et al., 2011).

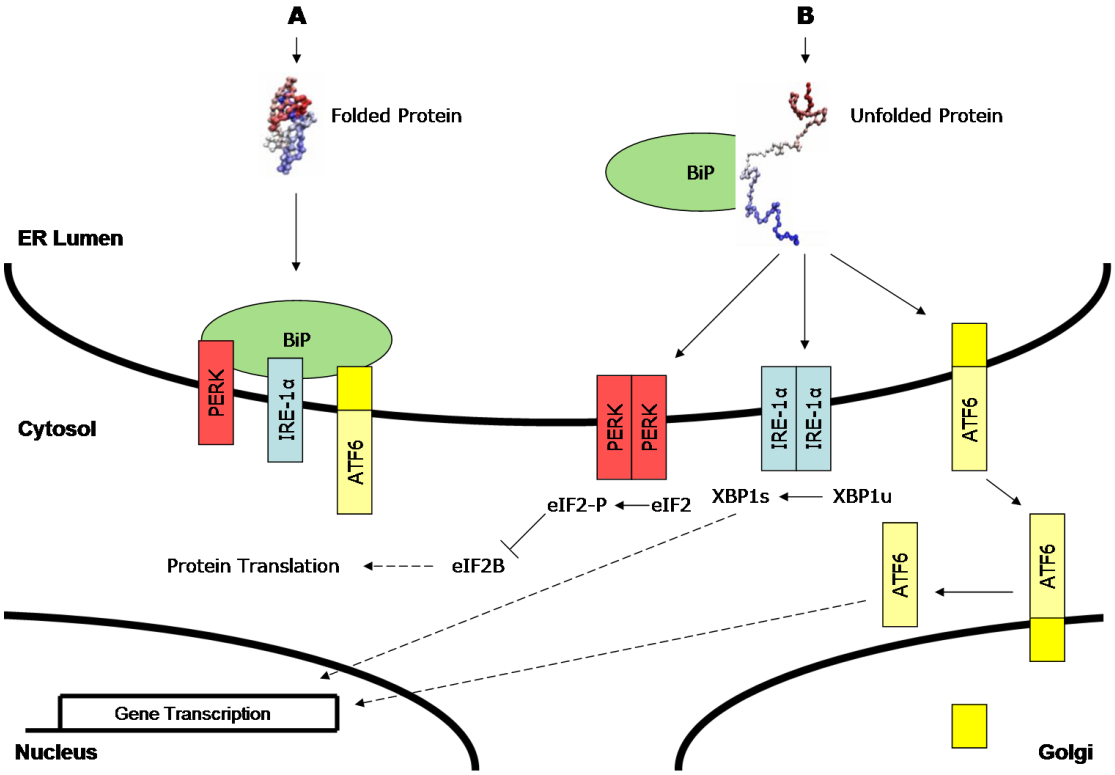

Figure 5: The unfolded protein response signalling cascade.

A. Under normal physiological conditions proteins fold normally and the association of BiP with PERK, IRE-1α and ATF6 prevents their dimerisation (PERK and IRE-1α) and their transport to the golgi (ATF6). **B.** When the unfolded protein load exceeds the capability of the protein folding machinery the level of unfolded proteins is increased. BiP preferentially associates with the unfolded proteins, liberating the oligomerisation domains of IRE-1α and PERK and allowing the transfer of ATF6 from the ER membrane to the golgi. ATF6 is then spliced in the golgi by S1P and S2P, releasing activated ATF6, which translocates to the nucleus and induces gene transcription. PERK oligomerisation induces autophosphorylation exposing its endogenous kinase activity. PERK phosphorylates eIF2, which inhibits eIF2B, which is an activator of translation. IRE-1α oligomerisation exposes its endogenous endoribonuclease activity. XBP1u is spliced allowing the translation of XBP1s protein. XBP1s is targeted to the nucleus and inducing gene transcription. There are several points where cross talk between the three pathways occurs. The mechanism of BiP activity is also yet to be confirmed.

1.3.2 IRE-1α activation

IRE-1α initiates the most conserved signalling pathway of the UPR, although very little is known about its biochemical regulation. IRE-1α is a serine / threonine kinase that catalyses the unconventional splicing of XBP1. A 26 nucleotide intron of XBP1 mRNA is spliced out by IRE-1α. There have been several models suggested to explain the activation of IRE-1α by ER stress. The initial model suggested that BiP binds to the lumenal domain of IRE-1α and maintains it in an inactive state. BiP release during ER stress results in IRE-1α dimerisation and subsequent activation (Bertolotti et al., 2000). Mutagenesis analysis of the IRE-1α lumenal domain indicated that unfolded proteins may bind directly to IRE-1α and promote its aggregation (Credle et al., 2005). Further mechanisms suggested two other mechanisms through which BiP and IRE-1α may interact. BiP could potentially recruit unfolded proteins and target them towards IRE-1α to promote dimerisation, or BiP, when not associated with unfolded proteins can interact with IRE-1α to prevent its dimerisation (Hetz et al., 2011). Recent studies have indicated that IRE-1α may form oligomers instead of dimmers and that the formation of these oligomers is crucial for XBP1 splicing (Li et al., 2010).

Only two groups have looked at the mechanisms involved in targeting XBP1 mRNA to IRE-1α. It has been shown that the XBP1u protein itself may be involved in mediating the interaction between XBP1 mRNA and IRE-1α (Yanagitani et al., 2009). It has been shown that XBP1u mRNA localises to the ER membrane and it is released to the cytosol after splicing. The membrane localisation of XBP1u mRNA required a hydrophobic region within the XBP1u protein, as demonstrated by biochemical mutation analysis. These data served to demonstrate that the nascent XBP1u polypeptide serves to recruit its own mRNA to the membrane for subsequent splicing and translation events. During searches to identify other IRE-1α substrates it was noticed that a subset of genes were downregulated during ER stress in an XBP1-independent, IRE-1α-dependent manner. It was suggested that IRE-1α was involved in the selective degradation of mRNA molecules (Hollien et al., 2009; Hollien and Weissman, 2006). The reports describing IRE-1α-dependent mRNA decay indicate that mRNA decay is cell specific and no consensus target sequence was identified.

1.3.3 XBP1s and ER stress

The translation of XBP1s in response to ER stress induces physiologic changes to the cell which decrease the build up of ER stress (Yoshida et al., 2001). XBP1s can bind to *cis*-acting response elements in promoter regions such as the ERSE, ERSE-II and UPRE elements (Figure 6). The targets of XBP1s include the ER chaperones: BiP, ERdj4, ERdj5, HEDJ, GRP58 and PDI-P5. Induction of expression of these genes increases the ability of the protein folding machinery in the ER to bind, process and fold misfolded proteins. The ERAD components EDEM and OS9 are transcribed increasing the degradation of misfolded proteins. Finally components of the secretory pathway are increased by XBP1s activation which increases the speed of protein transport from the ER to target compartments. XBP1u was initially demonstrated to be a precursor molecule to allow fast transcription of XBP1s in response to ER stress. Recent studies demonstrated that XBP1u could bind to XBP1s, translocate from the nucleus to the cytoplasm and target XBP1s for degradation (Yoshida et al., 2006).

1.3.4 Functional roles of XBP1u

Previous studies have identified a role for XBP1 in antibody production, lipid synthesis, liver function, cancer and inflammation. XBP1 was initially identified through its ability to bind to the promoter region of MHC class II genes. XBP1 was subsequently demonstrated to be required for the differentiation of plasma cells (Brunsing et al., 2008; Schebesta et al., 2002). XBP1 was linked with cancer through its similarity to hepatocarcinogenesis-related transcription factor. XBP1 splicing was also detected in hepatocellular carcinoma. The interior of the cancer is predicted to be hypoxic which can induce the unfolded protein response and XBP1 splicing. XBP1 has been speculated as a therapeutic target for the treatment of cancer (Koong et al., 2006). XBP1 has also been linked to atherosclerosis through its role in ER stress (Gargalovic et al., 2006).

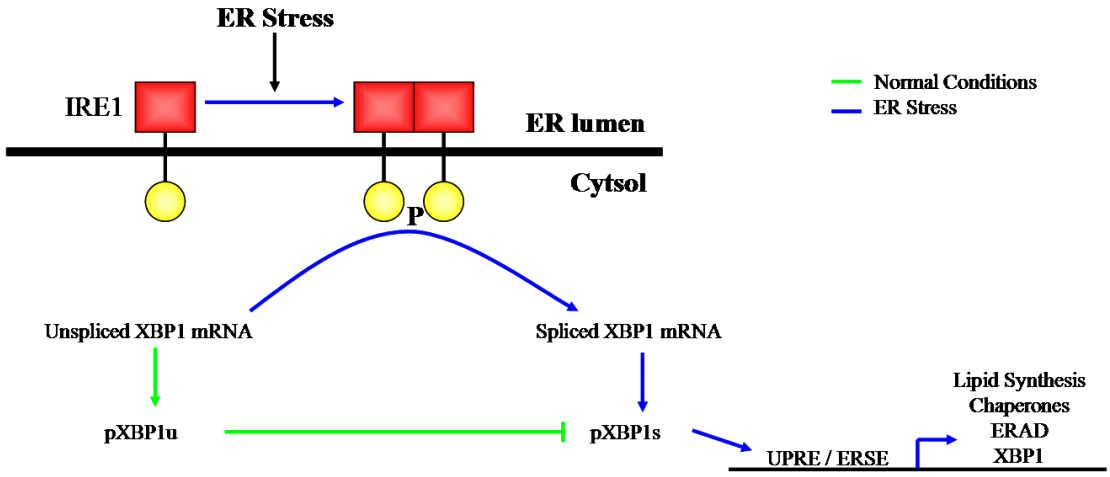

Figure 6: The IRE1 / XBP1 pathway in response to ER stress.

ER stress is initiated after the accumulation of unfolded proteins in the ER. BiP dissociates from IRE1 exposing an oligomerisation domain. Homodimerisation of IRE1 leads to conformational changes in the cytosolic domain of IRE1 exposing the endogenous endoribonuclease activity. A 26 nucleotide fragment of XBP1 pre-mRNA, which is constitutively expressed as XBP1u, is cleaved resulting in an altered reading frame. XBP1s is encoded by the mature mRNA and when expressed results in gene transcription via binding to ER stress response elements in the promoter regions of enzymes and proteins involved in ER membrane lipid synthesis, chaperone proteins, ERAD proteins and the promoter of XBP1. When ER stress has been reduced XBP1 pre-mRNA is no longer spliced and the XBP1u isoform binds to XBP1s and targets it for degradation.

Two recent studies have identified very important roles for XBP1 in hepatic lipogenesis and intestinal inflammation. XBP1 was identified to have a central role in normal fatty acid synthesis in the liver, distinct from its role in augmenting lipid synthesis for ER expansion. XBP1 synthesis was elevated after feeding mice with carbohydrates. This corresponded with an XBP1-dependant induction of genes involved in fatty acid synthesis. This study demonstrated that XBP1 is able to regulate a subset of genes involved in fatty acid synthesis (Lee et al., 2008). A second study identified the role of XBP1 and ER stress in intestinal inflammation. The authors demonstrate that induction of cell-specific ER stress through activation of XBP1 can lead to organ inflammation, a process requiring XBP1 (Kaser et al., 2008). Both of these studies involve processes that occur during progression of atherosclerosis. Further study on the role of XBP1 in EC and during atherosclerosis is necessary, perhaps to identify a novel therapeutic target for the disease.

Interestingly, a study published in the last few years has identified a novel role for XBP1u in preventing oxidative stress (Liu et al., 2009). XBP1-deficient mouse embryonic fibroblasts were exposed to hydrogen peroxide to promote oxidative stress. It was determined that XBP1-null cells were more susceptible to oxidative stress than their wild type counterparts, as demonstrated by assessing mitochondrial membrane potential and apoptosis. ROS generation in XBP1-null cells was also enhanced. The expression of catalase was strongly linked to XBP1u expression and indeed XBP1u was shown to bind to the catalase promoter via CCAAT boxes. These studies are very similar in nature to the ones performed in our studies and therefore support the principle that XBP1u prevents oxidative stress.

1.4 Akt and cell survival signalling

Akt is a serine / threonine kinase that has an amino-terminal PH domain, a central catalytic domain and a carboxyl-terminal regulatory domain. There are three members of the Akt family; Akt1, Akt2 and Akt3. Akt is activated via a dual regulatory mechanism (Vivanco and Sawyers, 2002). Firstly Akt must be translocated to the plasma membrane. Secondly activation of Akt requires the phosphorylation of serine-473 and threonine-308 (Bellacosa et al., 1998) (figure 7). Akt is recruited to the plasma membrane through the activation of PI-3-Kinase. PI-3-Kinase catalyses the conversion of phosphatidylinositol-4,5-bisphophate (PIP_2) into phosphatidylinositol-3,4,5-trisphosphate (PIP_3). PIP_3 recruits Akt to the plasma membrane through its ability to interact with its PH domain. Once Akt has been recruited to the plasma membrane kinases are able to induce the phosphorylation of Akt at S473 and T308. 3-phosphoinositide-dependent protein kinase-1 (PDK1) catalyses the phosphorylation of Akt at T308, which is sufficient to induce its activation (Stokoe et al., 1997). In order for Akt to be fully activated the phosphorylation of S473 by a second protein kinase is required (Alessi et al., 1997). The MTORC2 complex, that consists of multiple proteins including mTOR, rictor, mLST8, DEPTOR and Sin1, has been demonstrated to induce phosphorylation of this site (Oh and Jacinto, 2011).

The activation of Akt results in increased cell survival, proliferation and growth. Akt is also important during VEGF-mediated endothelial cell migration during angiogenesis. Akt promotes cell survival through a multi-factorial manner, by phosphorylating several components of the cell death machinery. For example, Akt has been shown to inhibit the pro-apoptotic action of caspase-9 through phosphorylation of serine-196 (Cardone et al., 1998). Akt also promotes cell survival through its indirect ability to alter the functionality of NF-κB and p53. Akt enhances the anti-apoptotic activity of NF-κB through phosphorylation and activation of IκB Kinase, which induces the degradation of the NF-κB inhibitor IκB. NF-κB is subsequently released and translocates to the nucleus to induce the transcription of target genes (Romashkova and Makarov, 1999). Activated Akt can also phosphorylate MDM2, which is a negative regulator of p53 function, thereby reducing pro-apoptotic signalling through p53 (Mayo and Donner, 2001). Akt is also highly important in regulating proliferation signals. One of the targets of Akt is glycogen synthase kinase 3β (GSK3β). Phosphorylation of GSK3β by Akt, blocks its kinase activity and prevents the phosphorylation of cyclin D1 kinase, thereby preventing its degradation and ensuring progression through the G1 to S-phase transition (Diehl et al., 1998).

Interestingly, several studies have implicated redox regulation of Akt activation. The phosphorylation of Akt has been demonstrated to be both positively and negatively influenced by ROS signalling. In the same study, hydrogen peroxide increases Akt activity at low concentrations and acts in an inhibitory manner at higher concentrations (Antico Arciuch et al., 2009). Furthermore, direct redox regulation of Akt is suggested to regulate its function. Oxidation of Akt and the subsequent disulphide bond formation between cysteine 293 and cysteine 311 in cardiac H9C2 cells exposed to hydrogen peroxide led to an increased association with the inhibitory phosphatase PP2A and a reduction in serine 473 phosphorylation and Akt signalling (Murata et al., 2003).

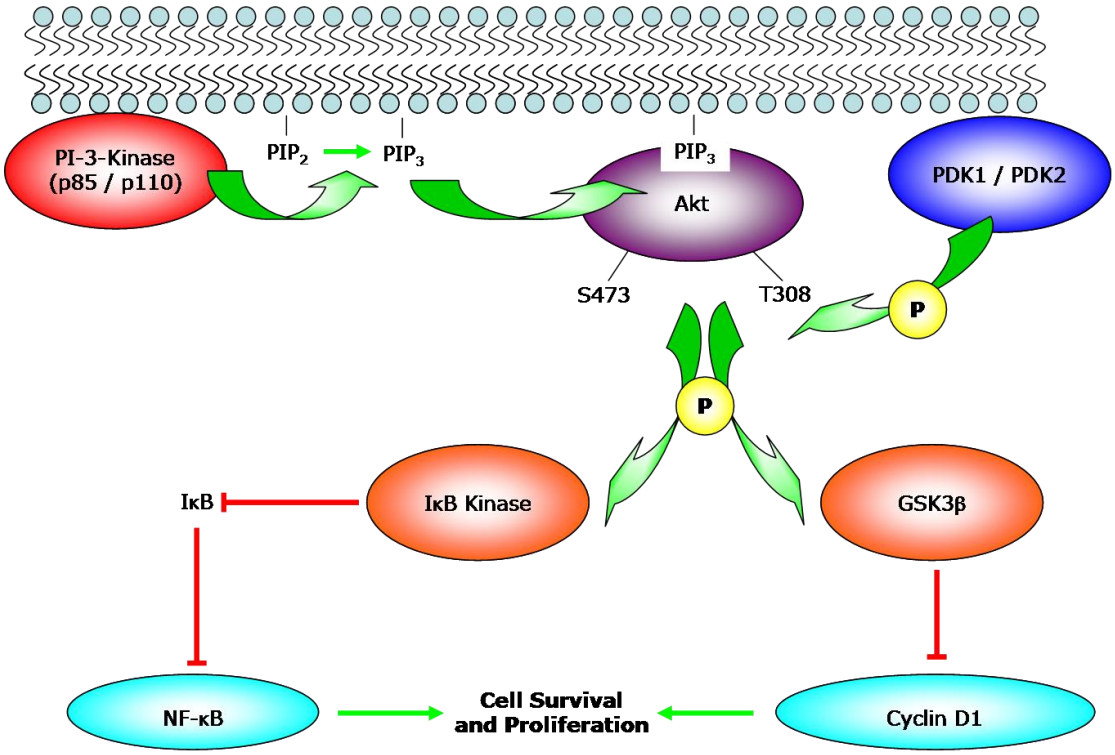

Figure 7: Akt activation and downstream signalling cascades.

Pi-3-Kinase induces the phosphorylation of PIP2 into PIP3. Akt binds to PIP3 at the cell membrane through its PH domain. This allows the phosphorylation of Akt at T308 and S473 leading to Akt activation and downstream signalling cascades to induce cell survival and proliferation.

1.4.2 Akt induced activation of HO-1

The PI-3-Kinase / Akt pathway has been reported to activate HO-1 expression and enhance cell survival. Previous reports have demonstrated that the activation of Akt is required for HO-1-mediated protection against carnosol-induced oxidative stress (Martin et al., 2004). The levels of the ARE-binding transcription factor Nrf2 are also raised during the protective response against carnosol. Akt has also been demonstrated to directly phosphorylate HO-1 at serine-188. Point mutations of HO-1 at this site to represent the effect of phosphorylation result in enhance enzymatic activity of HO-1 both *in vitro* and *in vivo* (Salinas et al., 2004). Recent studies have also shown that HO-1 expression is mediated by activation of Akt signalling by a mitochondrial redox-dependent pathway in ECs. Celecoxib, a cyclooxygenase-2 selective inhibitor, activates HO-1 expression through an Akt-dependent manner

(Hamdulay et al., 2010). These results indicate that activation of Akt is a key event in regulating the induction of HO-1 in response to cytokines and growth factors.

1.5 Histone deacetylases

Histone deacetylases (HDACs) are protein lysine deacetylases with pivotal roles in numerous biological processes; largely through their repressive influence on transcription. There are four classes of HDACs; I, IIa, IIb and IV, which separate HDACs according to phylogenetic analysis and sequence homology. The activity of HDACs is zinc-dependent and they can all be inhibited by pan HDAC inhibitors.

Human cells show distinct gene expression profiles which are modulated in response to physiological and pathological signalling. This requires multiple levels of transcriptional control and occurs through transcriptional regulators that bind specific DNA sequences. These modify the chromatin structure allowing DNA transcriptional machinery to access the genome. The main factor influencing chromatin structure is the state of the histone amino acid tails that serve as targets for many reversible post-translational modifications. The acetylation status of the lysine residues at the protruding N-termini of histones acts to regulate, both positively and negatively, gene transcription (Shahbazian and Grunstein, 2007). HDACs are responsible for the removal of acetyl groups from these residues. The loss of the acetyl group increases the positive charge of the histone N-terminal domain and tightens its interaction with the negatively charged DNA, thus compacting the DNA and reducing the access of the transcriptional machinery (Shahbazian and Grunstein, 2007).

HDACs can also promote the upregulation of gene expression (Nusinzon and Horvath, 2005). HDACs are predicted to exert this function through the utilisation of their deacetylase activity on non-histone proteins, such as heat shock and structural proteins. HDACs are often found in multi-protein complexes associated with specific co-repressors and modifiers to assert their function (Haberland et al., 2009).

1.5.1 HDAC3 structure

The class I HDAC3 family, of which HDAC3 is a member, are ubiquitously expressed, predominantly found in the nucleus and display a high enzymatic activity towards histone substrates. They have a conserved C-terminal deacetylase domain and short C- and N-terminal extensions.

HDAC3 is a 428 amino acid protein with a predicted molecular weight of 49kDa (Yang et al., 1997). HDAC3 has a variable C-terminal domain that differentiates it from other class I HDACs. HDAC3 is present in the both the nucleus and the cytoplasm and is located at the cell membrane (Longworth and Laimins, 2006; Takami and Nakayama, 2000). The nuclear export signal responsible for this ability is present within the amino acid sequence 180-313. HDAC3 is also reported to contain domains responsible for: deacetylase activity, which requires the C-terminal region; transcriptional repression, encoded by amino acids 421-428; nuclear localisation signal, present in amino acids 313-428; protein-protein interactions, which requires the N-terminal 1-122 amino acids (figure 8) (Yang et al., 2002).

HDAC3 does not exist in isolation within the cell and can form large multi-protein complexes through protein-protein interactions. One of these complexes is the NCoR SMRT repression complex. The formation of this complex alongside the recruitment of other proteins, such as GSP2 stabilises and potentiates HDAC3 enzymatic activity (Oberoi et al., 2011). The activity of HDAC3 is also regulated by protein-protein interactions, phosphorylation status and cellular localisation. CK2 kinase and PP4 phosphatase mediate antagonistic effects on S424 of HDAC3. Phosphorylation at this site increases HDAC3 activity (Zhang et al., 2005). HDAC3 is also able to localise to the plasma membrane through interactions with the membrane bound tyrosine kinase, c-Src (Longworth and Laimins, 2006). Through these different interactions HDAC3 is able to mediate signalling pathways promoting proliferation, differentiation, development, metabolism and inflammation.

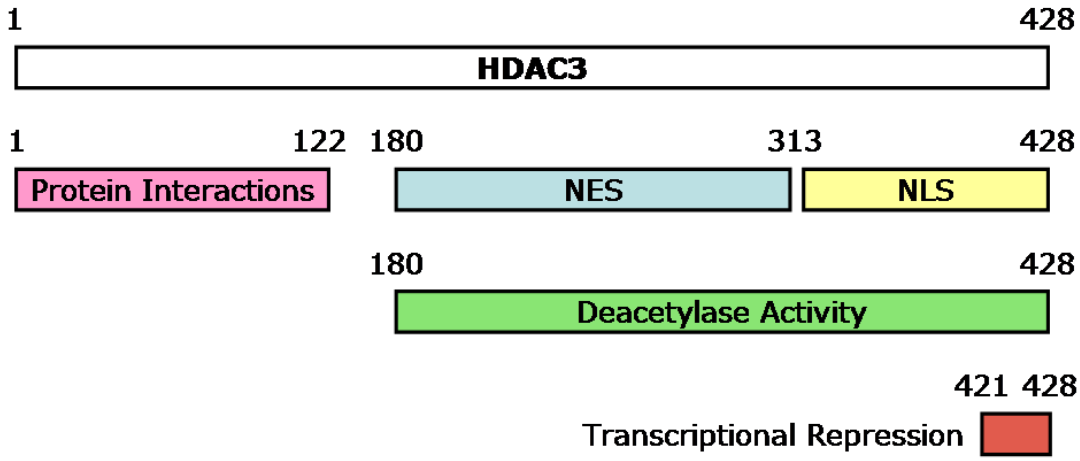

Figure 8: HDAC3 structural domains.

HDAC3 is a 428 amino acid protein containing a protein-protein interaction domain, a nuclear export and nuclear import signal, deacetylase activity and a domain responsible for transcriptional repression.

1.5.2 HDAC3 function in endothelial cells

HDAC3-null mice die before embryonic day 9.5 owing to defects in gastrulation; possibly due to the loss of DNA double-stranded break repair (Bhaskara et al., 2008). Several studies into cardiac specific deletion of HDAC3 have also been performed. Cardiac-specific HDAC3 deletion resulted in increased expression of genes associated with fatty acid uptake, fatty acid oxidation and oxidative phosphorylation. This induced myocardial accumulation of lipids and triglycerides, leading to the mice dying 3-4 months after birth from cardiac hypertrophy (Montgomery et al., 2008). Transgenic overexpression of HDAC3 in the heart also leads to severe defects. Overexpression of HDAC3 led to increased myocardium thickness and reduced ventricular cavity space (Trivedi et al., 2008). These studies indicate that the role of HDAC3 is tightly regulated in cardiomyocytes to promote normal development and function.

Several studies have also demonstrated a crucial role for HDAC3 in maintaining endothelial integrity. Our lab has shown that HDAC3 can mediate the differentiation of embryonic stem cells (ESCs) to endothelial-like cells that are capable of vascular repair. VEGF and shear stress induced differentiation requires p53 deacetylation and activation of p21 (Xiao et al., 2006; Zeng et al., 2006).

Furthermore, knockdown of HDAC3 in ECs inhibits TNFα-induced VCAM1 expression and reduced the adhesion of monocytes to ECs (Inoue et al., 2006). Increased leukocyte adhesion is one of the initiating steps during atherogenesis. Therefore inhibition of HDAC3 has been suggested as a potential mechanism to attenuate the inflammatory response in ECs and thereby reduce atherosclerotic lesion formation. HDAC3 can also regulate blood coagulation. Inhibition of HDAC3 abolished TNFα-induced tissue factor expression in ECs (Wang et al., 2007). HDAC3 has also been demonstrated to transcriptionally and post-translationally regulate eNOS expression and activity. The recruitment of HDAC3 and subsequent deacetylation of the eNOS promoter histone tails leads to the repression of eNOS transcription (Zhang et al., 2008). Recently, acetylation of lysine 609 of eNOS was shown to stimulate NO production. Overexpression of HDAC3 inhibited the acetylation event and reduced eNOS activity and NO production. Knockdown of HDAC3 resulted in increased lysine 609 acetylation and thereby increased the generation of NO (Jung et al., 2010). These studies demonstrate the important role of HDAC3 in the vasculature and suggest that its regulation is crucial to maintain EC function and integrity.

There is therefore clearly an important role for HDAC3 in mediating various endothelial functions. Recently, and crucial to this study, our lab has demonstrated that the correct regulation of HDAC3 function aids in the maintenance of endothelial integrity and prevents atherosclerosis formation (Zampetaki et al., 2010). The expression of HDAC3 is enhanced in regions of the vasculature subjected to disturbed flow, whilst knockdown of HDAC3 led to reduced EC survival in both *in vitro* and *ex vivo* experiments. Disturbed flow-mediated stabilisation of HDAC3 was shown to be impaired in the presence of vascular endothelial growth factor receptor (VEGFR2) and phosphatidyl inositol-3-kinase (PI-3-K) inhibitors. Akt, a downstream mediator of PI-3-K signalling is also enhanced by disturbed flow and interacts with HDAC3 to form a complex. This interaction is enhanced in the presence of disturbed flow, as well as increased phosphorylation of HDAC3 serine and threonine residues, although HDAC3 is not a target for Akt-mediated phosphorylation. HDAC3 deletion constructs identified that residues 136-206 of HDAC3 mediate the interaction with Akt. Further experiments suggested that reduced NO levels, which occur in regions of the vasculature subjected to disturbed flow, are crucial in increasing the binding of

Akt to HDAC3. Furthermore, overexpression of HDAC3 enhances the phosphorylation, and therefore activation, of Akt at serine 473 and threonine 308. Overexpression of constitutively active Akt can partially rescue the apoptotic response observed after HDAC3 knockdown. Finally, knockdown of HDAC3 in aortic isografts experiments led to significant increases in neointima formation. These studies provide evidence that HDAC3 acts as a prosurvival factor in the vasculature and that its interaction with Akt is critical for EC survival (Zampetaki et al., 2010).

1.6 Project Aims

XBP1 is a key signal transducer in the ER stress response yet its potential role in endothelial cell function and atherosclerosis development is unknown. This study aimed to investigate the role of XBP1 in the endothelium. To explore the role of XBP1 in the vascular system the expression of XBP1 was determined in linear and bifurcation regions of mice aortas. It was previously known that XBP1 is expressed in ECs, however it was unknown if XBP1 expression correlated with the microenvironment of particular vascular locations. The expression of XBP1 protein was detected in the linear and bifurcation regions of *ApoE*$^{-/-}$ / *Tie2-LacZ* mice aorta by *en face* staining (figure 9). Staining of mice aortic segments with an anti-XBP1 antibody that binds to both isoforms of XBP1 revealed that XBP1 was highly expressed in vascular regions exposed to disturbed blood flow. There was very little XBP1 protein detected in linear regions of the vasculature. Linear and bifurcation segments were also stained with X-gal to demonstrate the morphology of ECs in linear and bifurcation regions. ECs in linear vasculature regions demonstrate a smooth 'wave-like' pattern, whilst those near bifurcation regions have a disorganised morphology.

Furthermore the expression of XBP1 in atherosclerotic lesions of *ApoE*$^{-/-}$ / *Tie2-LacZ* mice was examined. Staining of mouse aortic segments containing atherosclerotic lesions demonstrated that XBP1 is highly expressed in these regions (figure 9).

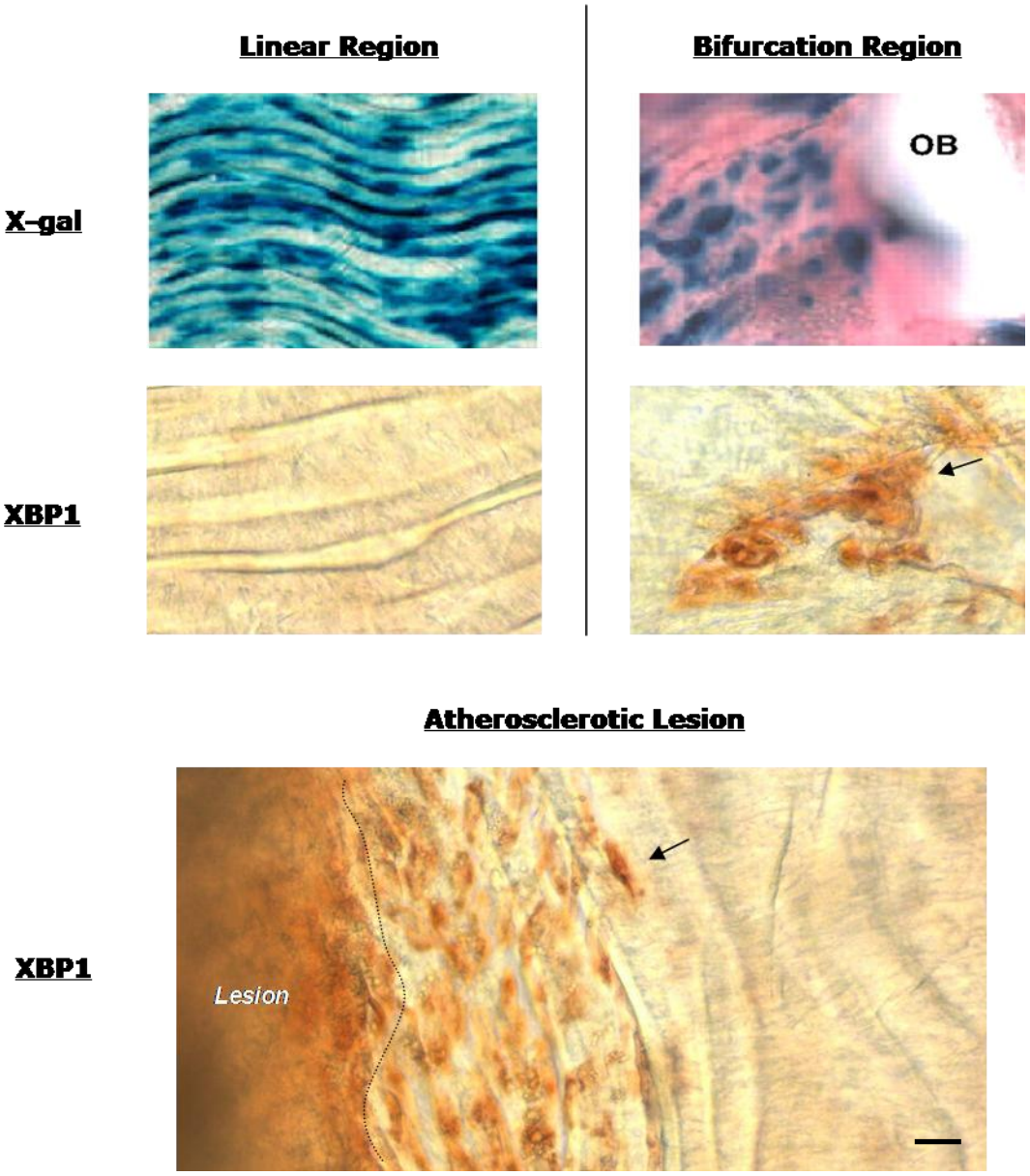

Figure 9: XBP1 is highly expressed in bifurcation regions and atherosclerotic lesions.

Aortas from *Tie2-LacZ / ApoE*$^{-/-}$ were harvested and prepared for *en face* staining. Aorta sections from linear and bifurcation regions (OB) were developed with X-gal to demonstrate the morphology of ECs in these regions. *En face* immunostaining for XBP1 showed that XBP1 was highly expressed in the branch points and regions of atherosclerotic lesion development in mice arteries. Minimal XBP1 staining was observed in linear regions of the vasculature. Scale bar: 100μm. The data is representative of three independent experiments. This is data is reproduced with permission from Dr. Lingfang Zeng and has been adapted from (Zeng et al., 2009).

Laminar flow induces EC quiescence and survival, whilst disturbed flow has been linked to EC proliferation and apoptosis. Having observed that XBP1 is upregulated in bifurcation regions of the vasculature, which are prone to increased EC turnover we hypothesised that shear stress-induced modulation of XBP1 could push ECs towards an atheroprone or atheroprotective phenotype. In order to differentiate the role of XBP1u from XBP1s two separate expression vectors were constructed and their roles in EC integrity were examined individually. In order to observe the role of XBP1s on EC survival, XBP1s was overexpressed in *ex vivo* aorta sections from *Tie2-LacZ* mice (figure 10A) and in *in vivo* aortic isograft experiments with *ApoE*$^{-/-}$ mice (figure 10B). Overexpression of XBP1s in *ex vivo* aorta sections dramatically reduced EC survival. Similarly, the overexpression of XBP1s in aortic isograft experiments significantly increased the size of atherosclerotic lesion formation. These results, alongside further studies performed in our laboratory, demonstrate that XBP1s promotes a pro-apoptotic, pro-atherogenic EC phenotype. Further studies into the role of XBP1s demonstrated that EC apoptosis is promoted by XBP1s via caspase activation and down-regulation of VE-cadherin through transcriptional suppression and matrix metalloproteinase-mediated degradation (Zeng et al., 2009).

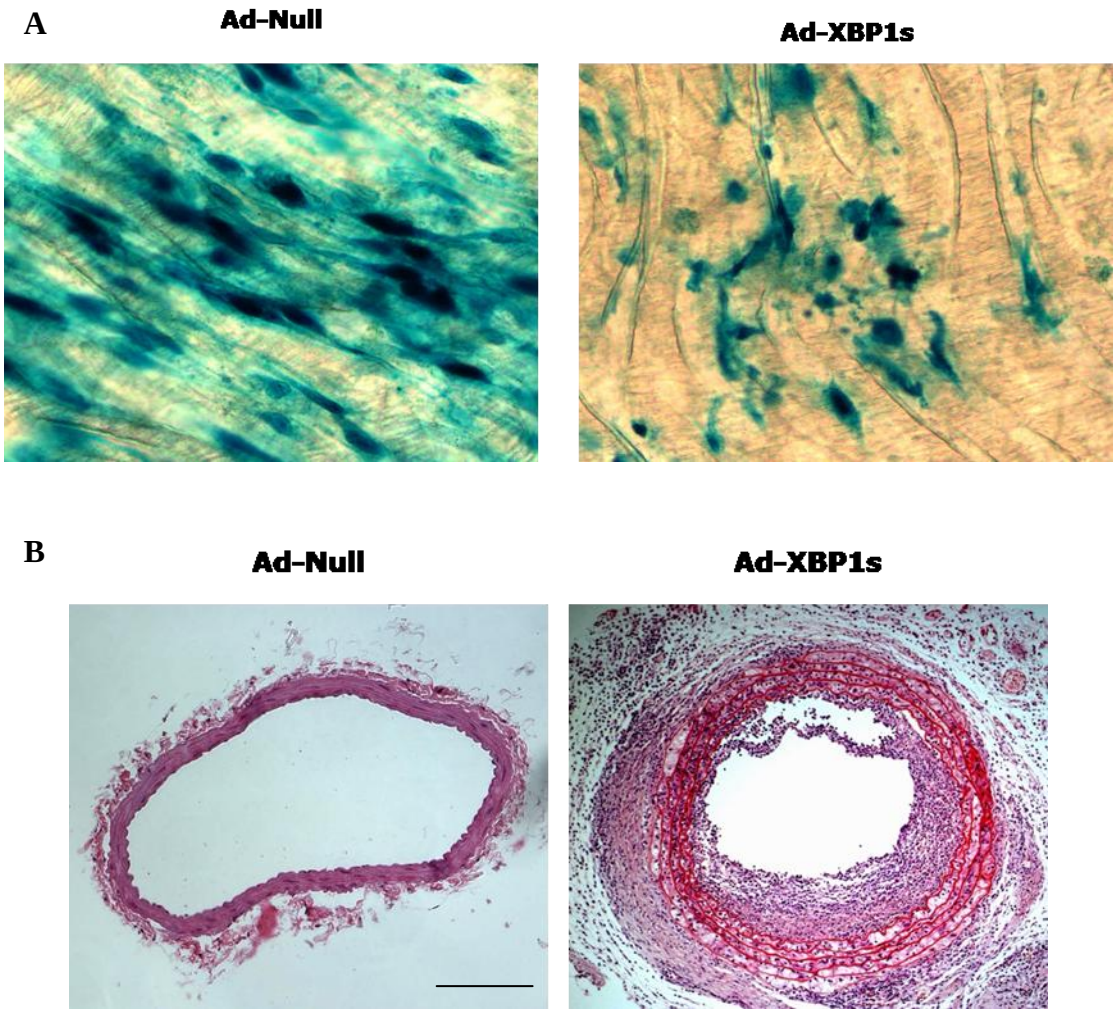

Figure 10: XBP1s promotes EC apoptosis and atherosclerotic lesion formation.

A. Overexpression of XBP1s induced EC loss from the vessel wall. Artery segments from *Tie2-LacZ / ApoE*$^{-/-}$ mice were infected with Ad-Null or Ad-XBP1s adenovirus at 5 x 10^7 pfu/mL and cultured for 4 days. The surviving ECs were revealed by X-gal staining. The images are representative of six independent experiments. **B.** Overexpression of XBP1s induced atherosclerosis development. Thoracic aortas were isolated from donor *ApoE*$^{-/-}$ mice and infected with Ad-Null or Ad-XBP1s adenovirus at 1 x 10^6 pfu/mL *in vitro*. The aortas were then grafted into the same background recipient *ApoE*$^{-/-}$ mice. Neointima formation was checked on the grafts four weeks later. The images are representative of six independent experiments. There were significant differences observed after quantification of the data between Ad-Null and Ad-XBP1s treated samples. This figure has been reproduced with permission from Dr. Lingfang Zeng and has been adapted from (Zeng et al., 2009).

Under normal conditions, XBP1 exists as a 29 kDa unspliced isoform. Although XBP1u is reported to modulate the level of XBP1s via proteosome-mediated degradation, other functions are predicted (Nekrutenko and He, 2006). The physiological function of the unspliced isoform remains unclear. In our previous

study, it was shown that XBP1u was the main isoforms present in cultured HUVECs and could be upregulated by disturbed flow. XBP1u was also revealed to be expressed in regions prone to atherosclerosis and the expression correlated with the severity of lesion formation in ApoE-/- mice. ECs in regions prone to atherosclerosis or under disturbed flow are believed to be undergoing proliferation and apoptosis. Considering that XBP1u contains an intact N-terminal domain and DNA binding domain, it may bind to DNA sequences and recruit other co-activators or co-repressors via interactions with its N-terminal domain, modulating gene transcription. Indeed, we found that XBP1u bound to the promoter of VE-cadherin in living cells. Thus, our hypothesis is that besides antagonising XBP1s, XBP1u may exert its own function in the modulation of cell proliferation and apoptosis.

To facilitate our study, unspliced XBP1 has been cloned and an adenoviral expression vector (Ad-XBP1u) has been created. Overexpression of XBP1u will be mediated via adenoviral gene transfer. On the other hand, knockdown of XBP1 will be mediated through shRNA lentiviral vectors. In this study, we aim to decipher the potential role of XBP1u in EC survival under oxidative stress and the underlying mechanism. We will investigate the effect of overexpression and knockdown of XBP1u on ECs under hydrogen peroxide challenge and the signalling pathways involved. We will also screen XBP1u regulated survival genes by microarray assay and explore how XBP1u regulates the expression of these genes.

Importantly, this study focuses on the role of XBP1u. The physiological switch between the production of XBP1u and XBP1s can happen very quickly as unconventional splicing of XBP1u occurs in the cytoplasm. Therefore, upon ER stress the production of XBP1s protein occurs very rapidly. To aid our study we use Ad-XBP1u to produce large exogenous quantities of XBP1u. However, when we knock down XBP1 using shRNA this is targeted to both isoforms of XBP1 and therefore the role that each isoforms play in the cell is more difficult to establish. Under normal conditions very little XBP1s is produced and therefore the XBP1u isoforms predominates. During ER stress the activation of IRE-1α results in a large induction of XBP1u pre-mRNA splicing and the expression of the XBP1s protein. Our study aims to elucidate the contribution of the XBP1u isoforms towards EC function. However, the role of XBP1s cannot be ignored due to their close interaction.

Chapter 2 - Materials and Methods

2.1 Materials

2.1.1 Chemicals and Reagents

2-Mercaptoethanol
β-EC growth factor
Bovine serum albumin (BSA)
Collagen-1
Collagenase, type 2 (Worthington Biochemical Corporation)
Dulbecco's modified eagle media (DMEM) (Gibco)
EC growth supplement from bovine neural tissue
Fibronectin
Foetal bovine serum (FBS)
Gelatin
Glucose
Hanks' balanced salt solution (HBSS)
Heparin
Hydrocortisone
Insulin-like growth factor 1
L-glutamine (Gibco)
M199 (Gibco)
Magnesium chloride
Murine epidermal growth factor
Phosphate buffered solution (PBS) (Gibco)
Penicillin (Invitrogen)
Streptomycin (Invitrogen)
Taurine
Thymidine
Trypsin-EDTA (Gibco)
VEGF

2.1.2 ELISAs, Assays and Kits

Qiaprep Miniprep Kit (Qiagen)

Qiaquick Gel Extraction Kit (Qiagen)

RNeasy Mini Kit (Qiagen)

CellTiter 96 Aqueous One Solution Cell Proliferation Assay (Promega)

Nitric Oxide Biometric Assay Kit (BioVision)

Apo-Direct Flow Cytometry Kit for Apoptosis (Chemicon)

Cell Surface Protein Isolation Kit (Pierce)

2.1.3 Buffers and Solutions

HUVEC media	M199 media 3ng/mL β-EC growth factor 3μg/mL EC growth supplement from bovine neural tissue 10U/mL heparin 1.25μg/mL thymidine 10% (v/v) FBS 2mM L-glutamine 100U/mL penicillin 100μg/mL streptomycin
HBSS + additions	HBSS 2mg/mL glucose 2.5mg/mL taurine 1% (w/v) BSA 1.4mM magnesium chloride
HBSS + collagenase	HBSS + additions 0.8mg/mL collagenase, type 2
HBSS + trypsin	HBSS 0.05% trypsin 2mg/mL glucose
CMEC media	DMEM 10% (v/v) FBS 100U/mL penicillin 100μg/mL streptomycin 2mM L-glutamine

	10μg/mL EC growth supplement 5U/mL heparin 1μg/mL hydrocortisone 1μM 2-mercaptoethanol 10ng/mL murine epidermal growth factor 1μg/mL ascorbic acid 0.5ng/mL VEGF 10ng/mL insulin-like growth factor 1
Fixation Solution	37% Formaldehyde 25% Gluteraldehyde in PBS
X-gal staining solution	1 mg/mL X-gal solution 5mM Potassium ferricyanate 5mM Potassium ferrocyanate 2mM Magnesium chloride in PBS
HEK 293 media	Dulbecco's modified eagle medium (DMEM) 10% (v/v) FBS 2mM L-glutamine 100U/mL penicillin 100μg/mL streptomycin
5X SDS loading buffer	10% SDS 50% glycerol 0.05% bromophenol blue 10mM β-mercaptoethanol 500mM Tris-hydrochloride (pH 6.8)
6X DNA loading buffer	30% glycerol 0.3% bromophenol blue Distilled water
Protein lysis buffer	1mM EDTA 50mM tris-hydrochloride (pH7.4) 150mM NaCl 1% Triton X Protease Inhibitor cocktail (Roche – 1 tablet in 50 mL)
Transfer buffer	25mM Tris 192mM glycine 10% methanol in distilled water
Tris buffered saline	0.9% sodium chloride 500mM Tris base (pH8.4)

Phosphate buffered saline	137mM sodium chloride 2.7mM potassium chloride 8.1mM Na_2HPO_4 1.76mM KH_2PO_4 to pH7.4
Buffer 1	25 mM Tris-HCL (pH8.0) 10mM EDTA 50mM glucose
Buffer 2	0.2M NaOH 1% SDS
Buffer 3	5M KOAc
Buffer 4	10 mM Tris-HCL (pH8.0) 1mM EDTA 20 μg/mL RNASE

2.1.4 Antibody list and dilutions

Antibody	Company	Dilution (Application)
Rabbit polyclonal anti-HDAC3	Abcam, ab7030	1:500 (WB)
Rabbit polyclonal anti-HDAC3	SIGMA, H3034	1:50 (IF) 1:50 (IP)
Rabbit polyclonal anti-Akt	Santa-Cruz, sc-8312	1:200 (WB)
Rabbit polyclonal anti-T308 Akt	Santa-Cruz, sc-16646r	1:200 (WB)
Rabbit polyclonal anti-S473 Akt	Santa-Cruz, sc-7985r	1:200 (WB) 1:50 (IF)
Rabbit polyclonal anti-HO-1	Abcam, ab13243	1:500 (WB) 1:50 (IF)
Mouse monoclonal anti-ATF3	Abcam, ab54854	1:200 (WB)
Rabbit polyclonal (M-186) anti-XBP1	SantaCruz, sc-7160	1:200 (WB) 1:50 (IF)
Rabbit polyclonal snti-IRE-1α	SantaCruz, sc-20790	1:200 (WB)

Rabbit polyclonal anti-CRLR	SantaCruz, sc-30028	1:200 (WB)
Rabbit polyclonal anti-PPARγ	SantaCruz, sc-7196	1:200 (WB)
Mouse monoclonal anti-p53	SantaCruz, sc126	1:200 (WB)
Mouse monoclonal anti-CD144	SantaCruz, sc-101580	1:200 (WB)
Goat polyclonal anti-vWF	SantaCruz, sc-8068	1:200 (WB)
Goat polyclonal anti-β tubulin	Santa-Cruz, sc-31782	1:1000 (WB)
Rabbit polyclonal anti-GAPDH	SantaCruz, sc-25778	1:2000 (WB)
Rabbit polyclonal snti-eNOS	SantaCruz, sc-653	1:200 (WB)
Goat polyclonal anti-CD31	SantaCruz, sc-1506	1:200 (IF)
Swine anti-rabbit IgG-HRP	Dako, P0160	1:3000 (WB)
Polyclonal rabbit anti-goat IgG-HRP	Dako, P0447	1:3000 (WB)
Polyclonal goat anti-mouse IgG-HRP	Dako, P0401	1:3000 (WB)
Donkey anti-rabbit IgG Alexa Flur 488	Invitrogen, A-21206	1:300 (IF)
Rabbit anti-goat TRITC	Dako, F0250	1:200 (IF)
Mouse anti-Flag M2-affinity agarose conjugate	SIGMA. A2220	40μL (IP)
Rabbit polyclonal anti-HA agarose conjugate	SantaCruz, sc-805AC	40μL (IP)

2.1.5 Semi-quantitative PCR primers

Primers specific to our PCR template were designed from human mRNA sequences using the Primer-BLAST tool. All the primers were ordered from SIGMA.

Primer	Sequence 5' – 3'	Annealing temperature (°C)	Cycles	Product size (bp)
HDAC3-f	CCCCGACGTGGGCAACTTCC	60	28	271
HDAC3-r	GAGCCCGGGAAACACTGGGC			
HO-1-f	CTTCTTCACCTTCCCCAACA	60	33	197
HO-1-r	GCTCTGGTCCTTGGTGTCAT			
ATF3-f	GCCATTGGAGAGCTGTCTTC	60	32	228
ATF3-r	GGGCCATCTGGAACATAAGA			
XBP1-f	CCTTGTAGTTGAGAACCAGGAG	60	32	XBP1u – 252 XBP1s – 226
XBP1-r	GGTCCAAGTTGTCCAGAATGC			
eNOS-f	GAACCTCAGTCATCTCTGTG	60	30	392
eNOS-r	TGCTGAATGCAGAGCTCGGTG			
GAPDH-f	ACAGTCAGCCGCATCTTCTT	60	28	299
GAPDH-r	TGGAAGATGGTGATGGGATT			
β-actin-f	AGCCATGTACGTTGCTATCC	60	28	207
β-actin-r	CGCTCGGCCGTGGTGGTGAA			
XBP1-gen1	GTTTCTAGGCATTGCCACATTTACGTCC			270bp WT 388bp Flpd

XBP1-gen2	ATCCTGTCTTGAAATGGCAAGTGTTGG		
XBP1-gen3	TGGCAAGGCTGAGCCTGATCG		265bp WT 315bp Flped
XBP1-gen4	GGAACTAGAGATACCACTGAG		
XBP1-gen5	CCCTGTGCTCAGACAGAAATGAGA		
XBP1-gen6	CGCATAACCAGTGAAACAGCATTGC		

2.1.6 Real-time PCR primers

Primer	Sequence 5' – 3'	Product size (bp)
HO-1-f	GCCAGCAACAAAGTGCAAGATT	97
HO-1-r	TGAGTGTAAGGACCCATCGGAG	
PPARγ-f	ATGCTGGCCTCCTTGATGAAT	101
PPARγ-r	TCACCAAAGGCTTTCGCAG	
ATF3-f	AAAGATGCACTTGCCCTGGTC	94
ATF3-r	CCAGCAGCAGAGAACCATCAA	
XBP1(total)-f	GTGAGCTGGAACAGCAAGTGGT	98
XBP1(total)-r	CCAAGCGCTGTCTTAACTCCTG	
XBP1u-f	AGCACTCAGACTACGTGCACCT	100
XBP1u-r	TGCCCAACAGGATATCAGACTC	
18S ribosomal-f	CCCAGTAAGTGCGGGTCATAA	106
18S ribosomal-r	CCGAGGGCCTCACTAAACC	

2.2 Methods

2.2.1 Cell Culture

All cell culture techniques were performed in sterile conditions in a tissue culture class II safety cabinet. Cell cultures were maintained in a humidified atmosphere of 5% CO_2 and 95% air at 37°C. Cell centrifugation steps were performed using a Thermo Scientific Sorvall Legend RT centrifuge with the 75006445 rotor, unless stated otherwise.

2.2.1.1 Human Umbilical Vein Endothelial Cell (HUVEC) Culture

Primary ECs were isolated from postnatal human umbilical vein and were kindly donated by Dr. Gillian Cockerill. HUVECs were isolated on three distinct occasions and were named HUVEC-A, HUVEC-B and HUVEC-C. Primary HUVECs are labelled when used during experiments. Pre-screened HUVECs were also obtained from PromoCell (C-12205). HUVECs from all sources were maintained under identical conditions and used up to passage 8. HUVECs were cultured on flasks pre-incubated with 10μg/mL collagen-1 for 1hr at 37°C. HUVECs were cultured in HUVEC media and sub-cultured when 70-80% confluent, usually every three days, at a ratio of 1:4. The media was changed every one to two days.

HUVECs were sub-cultured through the addition of trypsin and incubated in a humidified incubator for 90 seconds until cell detachment was observed. HUVEC growth media was added to the flask to prevent over-trypsinisation and the cell solution was transferred to a falcon tube and the cells were centrifuged at 400 x g for 5 minutes, before resuspension and transfer to fresh collagen-coated flasks.

2.2.1.2 Human embryonic kidney 293 cell culture

HEK 293 (ATCC, CRL-1573) and 293T (ATCC, CRL-11268) cells were maintained in HEK 293 media in a humidified incubator with 5% CO_2. The cells

were passaged at a ratio of 1:6 every three days. Trypsin-mediated detachment was used to subculture the cells

2.2.1.3 Mouse coronary microvascular EC (CMEC) isolation and culture

CMECs were isolated and characterised using a method adapted from Li *et al* (Li et al., 2001). Each batch of CMECs was isolated from at least 4 hearts that were harvested from mice between 6 and 10 weeks old. The isolation process does not involve selection; instead cardiomyocytes are removed by treatment with collagenase. CMECs are removed with trypsin and then separated from SMCs due to the different length of time required for adhesion of the cells to the gelatin-coated flask.

Isolation:

1. Prepare a 15mL falcon tube containing 10mL PBS for each batch of hearts
2. The mice were sacrificed by cervical dislocation and the hearts were removed whilst still beating and placed in PBS
3. Briefly dip the hearts into 70% ethanol to devitalise the epicardial mesothelial cells
4. Wash in PBS and trim all the fat and connective tissue. Remove the atria and valve tissue from the heart and remove all clots
5. Cut open the ventricles and repeat the wash in PBS
6. Chop the remaining tissue into $1mm^2$ pieces and suspend in 20mL HBSS + additions
7. Centrifuge at 500rpm for 1 minute
8. Resuspend in 6mL HBSS + collagenase, digest for 5 minutes (shear for the first 3 minutes by passing through a 10mL pipette at least 10 times, leave for the final 2 minutes to settle (no centrifugation))
9. Discard the supernatant and repeat a further three times
10. Resuspend the pellet in 6mL HBSS + trypsin and digest for 3 minutes (shear for the first 2 minutes by passing through a 10mL pipette at least 10 times, leave for the final minute to settle (no centrifugation))
11. Remove the supernatant and mix with 1mL FBS
12. Repeat a further three times

13. Combine the four trypsin digestions with 22mL complete media and centrifuge at 1200rpm for 8 minutes.
14. Resuspend in 10mL CMEC media and plate on a 75cm2 flask pre-coated with 1% (v/v) gelatin for 1hr
15. Change the media gently after 2hrs to remove non-adherent cells

Culture:

CMECs were characterised by CD31, CD144 and vWF immunocytochemistry staining. Vimentin and SM22were used as controls for fibroblast and muscle cell contamination. Acetylated-LDL uptake was also assessed. CMECs were cultured and used until passage 3, whilst the media was changed daily during culture. Shear and immunocytochemistry experiments were performed with CMECs plated on flasks and slides pre-coated with 10ng/mL fibronectin.

2.2.1.4 Cell Subculture

1. Remove and discard culture medium
2. Briefly rinse the cell layer with PBS and discard
3. Add 3mL of 0.05% Trypsin-EDTA per $75cm^2$ of cell layer for 3 minutes
4. Add 7mL of complete growth medium and aspirate the cells
5. Centrifuge at 400 x g for 5 minutes
6. Resuspend and aliquot appropriate cell numbers to new flasks

2.2.1.5 Cell Counting

Cell numbers were determined using a haemocytometer. Cells were resuspended in complete media and 10μL of the cell suspension was mixed with 10μL 0.4% Trypan blue. 10μL of this mixture was used to assess cell number in the original suspension whilst excluding dead cells from the count.

2.2.1.6 Harvesting cells

Cells were scraped off the culture flasks with the medium present and decanted into 15 mL centrifuge tubes. The cells were pelleted by centrifugation at 600 x g for 5 minutes. The medium was decanted and the cell pellet was resuspended in 1 mL of cold (4°C) PBS. The PBS-cell solution was then used to extract RNA or protein.

2.2.2 Viral Gene Transfer

The adenoviruses used for this project were constructed using the Adeno-X expression system (BD Biosciences).

2.2.2.1 XBP1u-FLAG Adenoviral Gene Construction

Unspliced XBP1 cDNA was cloned by RT-PCR from untreated HepG2 cell mRNA using the primer set: 5'-GGA GCT GGT ACC CTG GTG GTG GTG GCA GCC-3' and 5'-TCT GAG TCT AGA ACA GTA TTG GAT CAT TCC-3'. The insert was cloned into Kpn I / Xba I sites of the modified pShuttle 2 vector, in which the FLAG tag is fused to the N-terminal of the target protein. The resulting plasmid was designated as pShuttle2-XBP1u-FLAG and verified by DNA sequencing. The adenoviral vector Ad-XBP1u was created using the pShuttle2-XBP1u plasmid and a commercial kit (Clontech). The initial step was to construct the recombinant adenoviral-XBP1u-FLAG DNA by subcloning from the pShuttle2-XBP1u-FLAG vector. A double digestion of the pShuttle2-XBP1u-FLAG vector with the restriction endonucleases PI-*Sce* I / I-*Ceu* I was carried out to provide the XBP1u-FLAG expression cassette. This expression cassette was purified with the Qiagen Gel extraction kit after running on a 1% agarose gel. The XBP1u-FLAG expression cassette was then ligated into the Adeno-X genome by an *in vitro* ligation reaction at 16°C overnight in a microcentrifuge tube. The ligated adenoviral XBP1u-FLAG DNA was then purified using the phenol : chloroform : isoamyl alcohol method. 90μL of 1X TE buffer (pH8.0) was added to 100 μL of phenol : chloroform : isoamyl alcohol (24:25:1) and the ligation mixture and mixed by vortexing gently. The phases

were separated by centrifugation at 10,000 x g for 5 minutes at 4°C. The aqueous phase was transferred to a new tube and 1 / 10 volume of 3M NaOAc and 1 μL glycogen (20 mg/mL) was added and vortexed gently. The supernatant was discarded after centrifuging at 10,000 x g for 5 minutes at 4°C. The pellet was overlayed with 300 μL of 70% ethanol and centrifuged at 10,000 x g for 2 minutes and the supernatant carefully removed. The pellet was air dried for 15 minutes at room temperature and the DNA precipitate was resuspended in 15 μL of 1X TE buffer (pH8.0).

The ligated Adeno-XBP1u-FLAG vector was then propagated and purified. Adeno-XBP1u-FLAG was transformed into JM109 competent cells and ampicillin resistant positive colonies were identified by PCR screening with the primer sets provided in the kit. Positive colonies were amplified overnight in LB medium (100 μg / mL ampicillin) with shaking at 37°C. Purification of the adeno-XBP1u-FLAG plasmid was then carried out using the mini scale purification kit provided. The bacterial cell pellet was resuspended in 150 μL of buffer 1 by gently pipetting up and down. 150 μL of buffer 2 was then added to the suspension and mixed gently by inversion several times. After 5 minutes of incubation at room temperature, 150 μL of buffer 3 was added to the chilled suspension and mixed gently by inverting the tube several times and placing on ice for 5 minutes. The suspension was centrifuged at 10,000 x g for 5 minutes at 4°C and the supernatant was transferred to a clean microcentrifuge tube. An equal volume of phenol : chloroform : isoamyl (25:24:1) was added to the supernatant and mixed by inversion. The suspension was centrifuged for 5 minutes at 4°C to separate the phases and the top aqueous layer was transferred to a clean 1.5 mL microcentrifuge tube. After thorough mixing with 1 mL of 95% ethanol through inversion, the mix was centrifuged at 10,000 x g for 10 minutes at 4°C and the supernatant was discarded. 1 mL of 70% ethanol was added to the mix and centrifuged for 2 minutes at room temperature. The supernatant was discarded and the pellet was air dried at room temperature. The DNA precipitate was then dissolved in 15 μL of buffer 4 and vortexed gently. PCR screening was performed to check that XBP1u-FLAG was correctly inserted, using the primers provided with the Adeno-X kit.

For the production of recombinant Adenovirus, the adeno-XBP1u-FLAG DNA was first linearised by *PacI*, before transfection into HEK 293 cells. Post digestion with *PacI*, 60 µL 1X TE buffer (pH8.0) and 100 µL phenol : chloroform : isoamyl alcohol (25:24:1) was added to the mix and vortexed gently. The tubes were centrifuged at 10,000 x g for 5 minutes at 4°C to separate the phases. The top aqueous layer was transferred to a new microcentrifuge tube. Subsequently 400 µL of 95% ethanol, 1/10 volume of 3M NaOAc and 1 µL glycogen (20mg/mL) was added and vortexed gently. The tubes were then centrifuged at 10,000 x g at 4°C for 5 minutes and the supernatant was removed and discarded. The pellet was washed with 300 µL of 70% ethanol and centrifuged at 10,000 x g for 2 minutes. The supernatant was carefully aspirated and the pellet was airdried for 15 minutes at room temperature. The DNA precipitate was dissolved with 10 µL of 1 X TE buffer (pH 8.0).

One T75 flask of subconfluent HEK 293 cells was transfected with 10 µL of the linearised DNA using Fugene 6 transfection reagent according to the manufacturer's protocol. When the cytopathic effect (CPE) was observed, approximately 1 week post-transfection, the cells were dislodged by pipetting and transferred to a 15 mL conical tube and centrifuged at 1,500 x g for 5 minutes at room temperature. The cell pellet was resuspended in 500 µL PBS and lysed with three consecutive freeze-thaw cycles (-80°C to room temperature). 250 µL of this viral solution was used to transfect a second T75 of HEK 293 cells. When 50% CPE was observed the virus was harvested as previously mentioned. The concentration of the virus was increased through subsequent infections of large quantities of HEK 293 cells and resuspension in the same volume of PBS. The final viral concentration was determined through an end-point dilution assay.

24 hours prior to the titration protocol, 100 HEK 293 cells / well were plated into every well of a 96-well plate in 100 µL growth medium. Serial dilutions of the virus stock were done as follows: 1:100 dilution by adding 10 µL virus stock to 990 µL growth medium. Serial dilutions were performed to create a viral dilution range from 10^{-3} to 10^{-10}. 100 µL of each dilution was added to 10 wells, with the remaining wells left with 100 µL growth medium to act as negative control wells to demonstrate the viability of non-transfected cells. The cells were then incubated in a humidified 5% CO_2 incubator for 10 days at 37°C. Using a microscope the cells in each well

were checked for CPE. A well is scored as showing CPE even if only a few cells show CPE. The number of wells demonstrating CPE was calculated (as a fraction of 1 for each viral dilution) and the viral titre was calculated using the formula: Titre (pfu/mL) = 10 (x + 0.8) based on the Apearman-Karber method where x is the sum of the fractions of CPE-positive cells. Dilutions of 10^{-1} and 10^{-2} are assumed to all show CPE and therefore contribute 1.0 and 1.0 to the final value for x.

2.2.2.2 Adenoviral XBP1u gene transfer

For adenoviral gene transfer, ECs were cultured as described and transduced with the adenoviral vector for 24 hours. The cells were then harvested at the stated timepoints post-infection. The cells were transduced with different multiplicity of infections (MOI) indicating the number of viral particles per cell used for each experiment. An adenoviral tetracycline-controlled transactivator (Ad-Null) was used as the control virus. This adenovirus expresses tTa, a regulatory protein that switches on genes expressed under the control of a tetracycline response element promoter. No such genes under this control were used under our current system and this adenovirus thus served as the control virus. Ad-Null was used to compensate for MOI, to ensure that all cells were treated with adenoviral vectors to compensate for the effect of infection on cell attributes.

2.2.2.3 Constitutively active and dominant-negative AKT gene transfer

The adenovirus encoding the constitutively active myrAkt cDNA (Ad-Akt) and the dominant-negative (Ad-Akt(d/n)) was a generous gift from Professor Justin Mason at the Bywaters Centre for Vascular Inflammation, Imperial College, Hammersmith Hospital, London, W12 0NN, UK. Ad-Akt expresses a constitutively active Akt mutant in which point mutations of threonine 308 and serine 473 are substituted with aspartic acid (T308D / S473D) and has the c-Src myrisolytion sequence for membrane targeting fused in frame to the N terminus. For adenoviral gene transfer, ECs were seeded the day before transfection and transfected at the stated MOI for 24 hours with the virus and harvested at the stated time points. Ad-Null was used as the infection control.

2.2.2.4 XBP1 lentiviral particle production

Knockdown of XBP1 was achieved through lentiviral infection in HUVECs with small hairpin RNA (shRNA) complementary to XBP1. Lentiviral particles were produced using MISION shXBP1 lentiviral pLKO.1 plasmid according to the protocol provided by the RNA consortium. The shRNA non-targeting pLKO.1 plasmid was used as a negative control. Fugene 6 is a lipid-based transfection reagent allowing nucleic acid delivery into the host cell. This method was employed for the transfection of lentiviral plasmids and the packaging plasmids, required to make a functional lentivirus, into HEK 293T cells. 24 hours prior to transfection 1.5 x 10^6 HEK 293T cells / T75 flask were seeded to achieve 70 % confluency after 24 hours growth. A ratio of 3:1 (Fugene: μg plasmid) was used during the transfection. Co-transfection was performed using 4 μg shRNA-XBP1 (or HDAC3, IRE-1α or NT), 3.5 μg pCMV-dR8.2 packaging plasmid and 0.5 μg pCMV-VSV-G envelope plasmid (both Addgene). 24 μL Fugene 6 was added directly to 46 μL Opti-MEM serum free media in a microcentrifuge tube for 5 minutes at room temperature. 8 μg of plasmids were then added to 30 μL of serum-free Opti-MEM in a separate tube. The plasmids were then added to the Fugene mixture and incubated at room temperature for 30 minutes to allow the lipid – plasmid complex to form. This complex was then added drop wise to the HEK 293T cells in serum-free media. The media was changed 4-6 hours later and the supernatant, containing the lentivirus particles was harvested 24, 48 and 72 hours after transfection, pooled and then filtered through a 0.45 μm filter and then the concentration was detected via p24 antigen ELISA.

The p24 antigen ELISA (Zeptometrix) was used to determine the viral titre. The microwells are coated with a monoclonal antibody specific for the p24 *gag* gene product of HIV-1. The viral antigen present in our lentivirus particles is specifically captured onto this immobilised antibody during specimen incubation. The shRNA-XBP1 sample was diluted 1:1000 and 200 μL of this dilution was added to the microwells in duplicate. Simultaneous addition of the inactivated p24 antigen standard was added to the microwells with 8 dose points (0-125 pg/mL) and incubated overnight at 37°C. The captured antigen was then reacted with a high titred human anti-HIV-1 antibody conjugated with biotin for 1 hour at 37°C. Subsequent incubation at 37°C for 30 minutes with streptavidin conjugated to horseradish

peroxidase binds it to biotin, a blue colour is developed as the bound enzyme reacts with the addition of the substrate, tetramethylbenzidine/H_2O_2 in citrate buffer, for a further 30 minutes at room temperature. The reaction was halted and a yellow colour develops. The optical density was observed at 450 nm and this is proportional to the amount of HIV-1 p24 antigen present in the specimen. The transducing unit (TU) was calculated using the conversion factor recommended by the manufacturer (10^4 physical particles per pg of p24 and 1 TU per 10^3 physical particle for a VSV-G pseudotyped lentiviral vector), with 1pg of p24 antigen converted to 10TU.

2.2.2.5 XBP1 shRNA lentivirus particle transduction

For lentiviral transduction, 1.5 x 106 HUVECs were seeded on Collagen I-coated plates and left to adhere overnight. The following day the cells were incubated with 100 TU/cell shRNA-XBP1 (HDAC3, IRE-1α or NT) in complete growth media with 10 mg/mL polybrene for 16 hours. Subsequently fresh medium was added to the cells and the plates were harvested at the stated time points after transduction. shRNA-NT was used as a transduction control.

2.2.3 Cell Treatments

2.2.3.1 MTT-Cell Proliferation Assay

HUVECs were grown until 60% confluent. The media was replaced and the HUVECs were incubated for 16 hours with the stated multiplicity of infection (MOI) of control adenovirus (Ad-Null; tetracycline controlled transactivator) and Flag-tagged XBP1u containing adenovirus (Ad-XBP1u). 24 hours after infection the HUVECs were subcultured into 96 well plates at a density of 1 x 10^4 HUVECs per well. The HUVECs were grown for a further 42 hours before cell proliferation was assessed using the CellTiter 96 Aqueous One Solution Cell Proliferation assay kit (Promega). HUVECs were treated with 50 μM hydrogen peroxide or 50 μM SnPPIX where stated. The MTS tetrazolium compound is bioreduced by cells to form a coloured formazan product that is detectable using a luminometer at 490 nm. Only metabolically active cells produce the NADPH (NADH) dehydrogenase enzymes

necessary to carry out this conversion. The absorbance was observed 2 hours after the application of the MTS compound using a luminometer. The induction or reduction in proliferation was assessed relative to the rate of proliferation of untreated HUVECs which was set to 1.0.

2.2.3.2 Hydrogen peroxide treatment

Hydrogen peroxide treatment was used to induce cell death as a model of oxidative stress. HUVECs and aorta sections were treated with 50 μM (or in some cases 20 μM) hydrogen peroxide. All hydrogen peroxide treatments took place for 24 hour time periods. Hydrogen peroxide was stored at 4°C and fresh dilution aliquots were prepared before each experiment.

2.2.3.3 Flow cytometry detection of apoptosis

Apoptosis was determined using the Apo-Direct flow cytometry kit (Chemicon). This is a single step staining method that detects apoptotic cells through labelling DNA breaks. Wild type and XBP1-null embryonic cells were isolated as stated previously. The cells were left untreated or treated with hydrogen peroxide to induce apoptosis, followed by fixation through suspension in 1% paraformaldehyde on ice for 1 hour. The cell suspension was then centrifuged at 300 x g and the supernatant was discarded, before washing in 5 mL PBS and subsequent centrifugation. This wash step was repeated 3 times. The pellet was resuspended in the residual PBS by gentle vortexing. DNA breaks were detected by staining with 50 μL of staining solution (TdT reaction buffer, TdT enzyme, Fluorescin-dUTP) and incubated for 60 minutes at 37°C, with shaking every 15 minutes. The reaction was stopped through the addition of 1 mL rinse buffer and the cells were pelleted through centrifugation at 300 x g for 5 minutes. The supernatant was removed and discarded. This rinse stage was repeated 3 times. The cell pellet was resuspended in 500 μL of propidium iodide/RNase A solution and incubated in the dark at room temperature for 30 minutes.

Apoptosis was observed by flow cytometry. As fluorescein fluoresces at 520 nm, using the positive and negative apoptotic cells and a 488 nm Argon Laser as a

light source it was possible to identify apoptotic cells. The number of detected fluorescein events was recorded and as the cell numbers in the samples were kept constant it was possible to determine the level of apoptosis for all the different cell samples.

2.2.3.4 Actinomycin D and cyclohexamide treatment

To determine if changes in gene expression are transcriptionally and translationally dependent Actinomycin D and cyclohexamide treatment can be used to inhibit transcription and translation, respectively. Actinomycin D binds DNA at the transcription initiation complex and prevents elongation of the RNA chain by RNA polymerase. Cyclohexamide blocks translation by preventing the correct translocation of tRNA and mRNA molecules and thereby preventing peptide elongation. HUVECs were pre-treated with DMSO (as a control), 25 nM Actinomycin D and 50 μg / mL cyclohexamide for 6 hours prior to subsequent experimentation.

2.2.3.5 Tin protoporphyrin treatment

The effect of HO-1 on cell survival was determined using an inhibitor of HO-1. Tin protoporphyrin (SnPPIX) is a competitive inhibitor of HO-1. HUVECs were treated with DMSO as a control and 50 μM SnPPIX 6 hours prior to any subsequent treatments.

2.2.3.6 Inhibition of VEGFR2, PI-3-Kinase and MEK

To determine if changes in cell function require VEGFR2, PI-3-Kinase or MEK activation inhibitors of these proteins were used. HUVECs were pre-treated with 5μM LY294002 (an inhibitor of PI-3-Kinase), 5μM SU1498 (an inhibitor of VEGFR2) and 10μM PD98059 (an inhibitor of MEK1) or DMSO controls 6 hours prior to further experimentation.

2.2.3.7 Disturbed flow

HUVECs were plated at stated quantities in 25 cm^2 collagen-1 coated flasks and grown overnight. Disturbed flow was created by placing flasks longitudinally on a platform shaker (Labnet, model Rocker 25). A measurable and constant parameter for disturbed flow was maintained by ensuring a conserved 2.0 mm depth in culture medium, a 10 cm flask length, a ± 7° rotating angle and a frequency of 0.5 Hz (2 seconds per cycle). The magnitude of the shear stress experienced by the cells is approximately 4.5 dyn/cm^2. However, during each cycle the magnitude of the shear stress perceived by the cells is subjected to spatial and temporal variability. In each rotating cycle the spatial gradient of shear stress ranges between 0 and 20 (dyn/cm^2)/cm, whilst the average temporal gradient of the shear stress is 4.5 (dyn/cm^2)/sec. These values have been estimated based on numerical simulation of the oscillatory flow system using computational fluid dynamics software. It is important to note that HUVECs are subjected to reduced, oscillatory, disturbed flow as opposed to just disturbed flow. The HUVECs were subjected to disturbed flow for the stated time points.

2.2.3.8 HO-1 and ARE luciferase promoter assay

The HO-1 promoter sequence was identified using the UCSC genome browser programme. Forward and reverse primers were designed to clone the promoter region.

Forward: 1.003kb: 5'-ACTGTG-GGTACC-GAATCATCTGGTCCATTC-3'
4.014kb: 5'-AGCGTA-GGTACC-ACCTGCATTTCTGCTGCG-3'

Reverse: 5'-AGGATC-CTCGAG-TGCGCTGAGGACGCTCGA-3'

XhoI and KpnI were not present within the promoter region and were therefore introduced into the primer sequence. The HO-1 promoter was amplified using Accuprime Taq via PCR as stated previously. The sequence was then restriction digested with the aforementioned restriction enzymes and inserted into a linearised PGL3 basic plasmid. The sequence was then verified and the plasmid was transfected into HUVECs as detailed below.

The ARE-promoter luciferase construct was kindly donated by Professor Josef Dulak, Jagellonian University, Krakov, Poland.

HUVECs were plated 24 hours prior to treatment at a density of 100,000 cells per $10cm^2$. Prior to transfection cells were cultured in low serum (2%), additive-free media. Fugene was used at a 3:1 ratio (Fugene : μg DNA). For 1 x T25 of HUVECs 2 μg of the promoter plasmid was combined with 0.5 μg of the renilla transfection control and 7.5 μL of Fugene 6 reagent. These are then combined in 100 μL of DMEM and left at room temperature for 30 minutes to form a complex. The DNA-lipid complex was then added drop wise to cells and incubated for 6 hours, before the media was changed. The cells were then grown for a further 48 hours before treatment was initiated.

The cells were washed with ice-cold PBS and then following the addition of RLB buffer were subjected to three rounds of freeze-thaw cycles (-80°C to room temperature). The cell suspension was then centrifuged at 10,000 x g for 5 minutes and the supernatant was removed to a fresh tube. This can then be used to measure the luciferase and renilla activity present in the sample. Renilla and luciferase activity is measured by combining 100 μL of the cell supernatant and 30 μL of luciferase and renilla substrate (Promega). Each sample is then normalised to renilla to account for transfection efficiency and then compared against the untreated control samples.

2.2.3.9 Wound healing assay

To perform the wound healing assay HUVECs were plated in 6-well plates and allowed to grow until confluent. A 1 mL pipette tip was then used to create a consistently sized scratch across the confluent monolayer. A permanent marker was used to characterise individual sections of the scratch that would be studied over a time course experiment. Images were taken after 0, 4 and 8 hours and the area of the wound relative to the starting area was calculated using AxioVision 4.7 software.

2.2.3.10 Induction of migration

To study the expression of genes at the initial stages of migration, HUVECs were grown until confluent. The confluent monolayer was then subjected to multiple scratch wounds so that >75% of the HUVECs would have reduced contacts with surrounding cells. The HUVECs were then allowed to migrate for the stated time points before they were harvested for gene expression studies.

2.2.3.11 Determination of nitrate in HUVEC supernatant

Determination of the nitrate concentration in the supernatant of HUVECs allowed a determination of eNOS activity and NO production. HUVECs were treated and then grown until confluent. They were then incubated in the minimum possible media (4 mL for a T75 flask) for 24 hours to increase the detectable concentration of nitrate. Nitrate was detected using a two-step process. The initial step converts nitrate to nitrite using nitrate reductase, whilst the second step uses Greiss reagents to convert nitrate to a detectable purple Azo compound (BioVision). The assay was performed according to the manufacturer's protocol. The absorbance at 540 nm was detected and using the standard curve created by the supplied standards the nitrate concentration was calculated using the following formula: nitrate concentration = ((sample absorbance – blank absorbance) / slope of standard curve) / μL of sample measured. The nitrate was then compared against the amount of nitrate found in the control samples.

2.2.3.12 Tube formation assays

Tube formation assays involve the plating of ECs on matrigel and observing the outgrowth and ability of the ECs to form tube-like structures. For the tube formation assays matrigel (Morsi et al.) was removed from -80°C and defrosted overnight on ice. 100μL was plated per well of an 8-well chamber slide. 20,000 HUVECs were plated and the tube formation was observed via microscope after 8 hours.

2.2.4 In vivo and ex vivo experiments

2.2.4.1 Creation of *Tie2-Cre XBP1$^{f/f}$* mice

The conditional knockout XBP1 mouse was developed through collaboration with genOway. The aim was to develop a floxed mouse line, by inserting a *loxP* site together with an FRT flanked neomycin selection cassette within the intron 2 and a single distal *loxP* site within the upstream of exon 1. The mouse line was then bred with deleter mice, which constitutively express Flp recombinase to remove the neomycin selection cassette and thus create a line of floxed mice in which exons 1-2 are flanked by *loxP* sites. The floxed XBP1 mouse is then bred with a mouse line expressing Cre recombinase under the control of the Tie2 promoter, so XBP1 is only knocked out in cells expressing Tie2. The specific process and genotyping are demonstrated in figure 11.

2.2.4.2 *En face* X-gal staining

Mice aortas were removed from the donor animals and cut into 2-4 mm^2 sections. Each section was then washed with PBS and fixed in fixation solution at room temperature for 5 minutes. The sections were then washed in PBS before the application of X-gal staining solution overnight at 37°C. The sections were then washed in 3% DMSO and water was added to dissolve any remaining X-gal crystals. The sections were then mounted on slides with the inner surface facing upwards and the surviving endothelial cells were observed to have a blue colouration when placed under a light microscope.

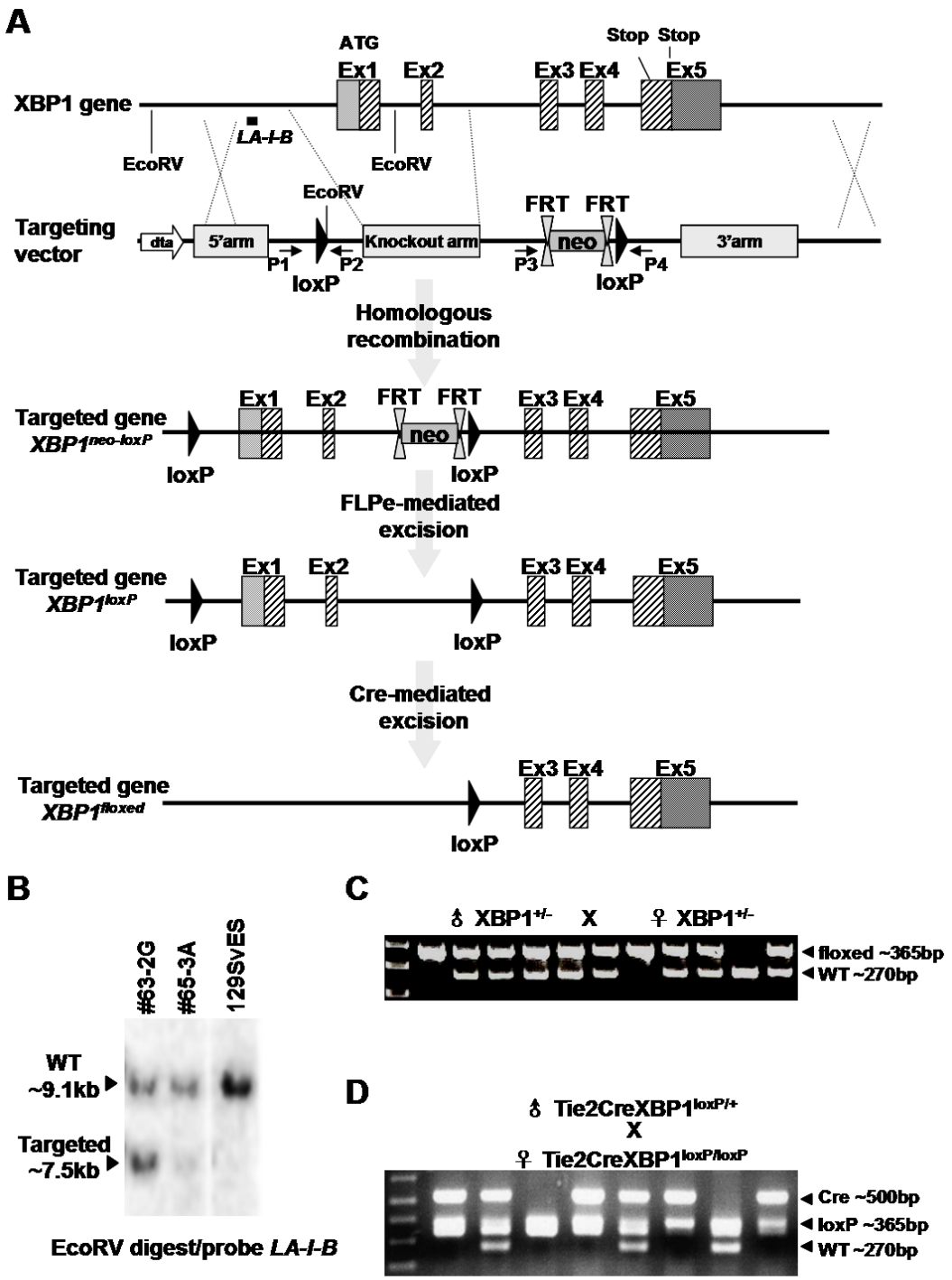

Figure 11: Creation of Tie2-Cre XBP1f/f mice.

A. Schematic diagram of the creation of XBP-conditional knockout mice. Initially homologous recombination of the XBP1 and the targeting vectro occur to introduce two *loxP* sites and an FRT-flanked neomycin gene. FLPe-meditaed excision of the neomycin fragment follow. Finally after brreding with a Tie2-Cre mouse Cre recombinase induced excision results in abrogated XBP1 expression. **B. C.** and **D.** Genotype analysis of Cre recombinase and XBP1 floxed mice.

2.2.4.3 Indirect Immunofluorescence staining of aorta segments

Mice were anaesthetised and perfused with 4% paraformaldehyde to fix the ECs. The aortas were then harvested from wild type and *Tie2-Cre XBP1*$^{f/f}$ mice. These were cut into approximately 2 mm^2 sections and mounted lumen side up on rubber sections. The sections were then washed in PBS briefly before a further fixing stage at room temperature for 20 minutes in 4% paraformaldehyde. The sections were then washed three times in PBS for 5 minutes. The cells were then permeabilised with 0.1% Triton X-100 for 40 minutes at room temperature. The sections were again washed in PBS for 5 minutes. The sections were then blocked in 10% swine serum for 1 hour at 37°C. The sections were then incubated with the primary antibody in 10% swine serum overnight at 4°C. The primary antibody was removed through washing in PBS and the secondary antibody was applied for 1 hour at 37°C. The sections were washed three times in PBS and counterstained with DAPI (1:1000) for 2 minutes at room temperature. The cells were then mounted with fluorescent mounting media (Dako) and images were taken with the axio imager M2 microscope and AxioVision Digital Imaging Sytem (Carl Zeiss).

2.2.4.4 *En face* staining of aorta segments

Tie2-LacZ / ApoE$^{-/-}$ mice or *Tie2-LacZ / ApoE*$^{+/+}$ mice were perfused with 4% paraformaldehyde to fix ECs, followed by dissection of the artery vessel. After removing the fatty tissues the artery was mounted on rubber with the lumen opened and facing upwards. The *en face* staining procedure detailed above was used, using rabbit anti-XBP1 antibody. Images were assessed by Zeiss Axioplan 2 Imaging microscope with Plan-NEOPLUAR 10x/0.3 objective lenses, AxioCam camera and Axiovision software at room temperature and were processed by Adobe Photoshop software. Scale bars are demonstrated in the images.

2.2.4.5 Isolation of XBP1-null embryonic cells

XBP1 heterozygous mice were cross bred and the embryos were harvested at day 13.5. A portion of the embryo was used for genotype analysis. The embryos from XBP1$^{+/+}$ and XBP1$^{-/-}$ embryonic day 13.5 mice were removed from the embryo

sac and gently homogenised. The cells were then strained via passage through a cell strainer. The cells were plated on flasks coated with 10μg/mL collagen-1 for 1hr at 37°C and cells that did not adhere after 2 hours were discarded. Those cells that adhered were maintained for further analysis.

2.2.4.6 Artery graft experiments

Arteries were isolated from donor *ApoE*$^{-/-}$ mice. The ends and main branches were banded. 300 μL of virus solution (1 x 10^6 pfu/mL diluted in M199 + 15% FBS) was injected into the lumen and incubated at 37°C for 2 hours with the whole artery immersed in M199 medium and 15% FBS. Each artery was then cut into two pieces and grafted into two recipient *ApoE*$^{-/-}$ mice. Four weeks later, the recipient mice were sacrificed humanely and the grafts were harvested for formalin-fixed sections. The sections were stained with H.E. and neointima formation was observed under a microscope.

2.2.4.7 Ring outgrowth

Arterial sections from wild type and *Tie2-Cre / XBP1*$^{f/f}$ mice were harvested and cut into narrow ring sections. These were then plated onto low-growth factor matrigel (Morsi et al.) and the outgrowth of ECs was assessed after 8 hours by microscopy.

2.2.5 Nucleic Acid Analysis

All solutions used in the isolation and manipulation of nucleic acids were prepared using molecular biology grade chemicals and distilled water or ethanol. The solutions were sterilised by autoclaving or filtration through a 0.22 μm filter. RNA degradation by contaminating RNases was minimised through the use of diethylamine pyrocarbonate (DEPC) treated water (Invitrogen). All techniques that required the handling of RNA were performed with RNA-grade reagents and RNA-free plastic ware. All centrifugation steps using 1.5 mL tubes were performed using an Eppendorf Centrifuge 5415R with an FE014 rotor.

2.2.5.1 RNA Extraction and Purification

RNA was extracted from cultured cells to study the expression pattern of genes in HUVECs subjected to various treatments. RNA expression patterns of specific genes were analysed using semi-quantitative PCR, real-time PCR and microarray analysis.

The cell medium was removed and the cells were washed briefly with ice-cold PBS. The cells were then mechanically detached, using a cell scraper, into 0.1 mL of PBS per cm^2 cell surface area. The cell suspension was pelleted in a 15 mL tube through centrifugation, in a Thermo Scientific Sorvall Legend RT centrifuge, at 600 x g for 5 minutes at 4°C. The cells were resuspended in 1 mL ice-cold PBS, transferred to a 1.5 mL tube and centrifuged at 13,400 rpm for 30 seconds at 4°C. The supernatant was removed and the cells were resuspended in RLT buffer (Qiagen) supplemented with 10 μL 14.3 M β-mercaptoethanol per 1 mL (Sigma). RNA was purified using the Qiagen RNeasy mini kit. Briefly, cell lysis was ensured by centrifugation through a QIAshredder column. The cell lysate was mixed with 1 volume of 70% ethanol. RNA was bound to the RNeasy column and several wash steps were used to remove contaminants. Purified RNA was eluted in 30-50 μL DEPC-treated water.

Genomic DNA contamination was prevented by treatment with DNase I (Ambion). 0.1 volume of 10X DNase buffer was mixed with RNA and 1 μL DNase I at 37°C for 25 minutes. 0.1 volume of DNase inactivation reagent was added to inhibit DNase activity and chelate ions which may have interfered with subsequent steps. The solution was centrifuged at 10,000 rpm for 1.5 minutes and the supernatant was transferred to a fresh tube. The RNA concentration (ng/μL) was assessed in duplicate using a NanoDrop 1000 (Thermo Scientific). Only RNA with an A_{260}/A_{280} nm value greater than 1.8 was used in subsequent experiments.

2.2.5.2 Reverse Transcription

RNA was converted into cDNA using reverse transcriptase. A typical reverse transcriptase reaction was performed in 25 μL total volume. Initially 1 μg RNA was made up in 10 μL DEPC-treated water. Reaction mix A containing RT buffer, dNTPs (Invitrogen), random primers and magnesium chloride (all Promega, Southampton, UK) was mixed with the RNA, incubated at 70°C for 5 minutes and then cooled to 4°C. Reaction mix B containing RNasin plus RNase inhibitor and reverse transcriptase was subsequently added (Promega). The final reaction mix contained: 1 μg RNA, 1X (v/v) RT buffer, 1 μM dNTP, 4 μg/mL random primers, 3mM magnesium chloride, 1 U/μL RNasin and 0.2 U/μL reverse transcriptase. This mixture was incubated at 25°C for 5 minutes, 42°C for 1.5 hours and finally the reverse transcriptase was inactivated by incubating the mixture at 72°C for 5 minutes before cooling to 4°C. The reverse transcription was performed in a Techne thermo cycler 512. Assuming that all the RNA was converted into cDNA the mixture was then diluted to create 10 ng/μL cDNA solutions. Negative control reverse transcription experiments were also performed. These contained the above reagents with the exclusion of reverse transcriptase. The purpose of these was to determine that no genomic DNA contamination had occurred.

2.2.5.3 Microarray Analysis

RNA was purified from HUVECs as detailed above and analysed by the genomics group, Oxford. Briefly, 500 ng total RNA was provided at 45.5 ng / μL and the samples were quantified using an Agilent Bioanalyser. The amplification and labelling was performed using the Ambion total prep Illumina Amplification kit, the quality was then checked using the Agilent Bioanalyser. The sample was then hybridised to the chip and scanned. The output consisted of a report file containing the intensity data per probe. This was analysed using BeadStudio software. 500 ng of total RNA (45 ng/μL) was quantified by the Agilent Bioanalyser. Total RNA is amplified and labelled with biotin during *in vitro* transcription with the Ambion Illumina TotalPrep RNA Amplification kit. The amplified RNA is hybridised overnight to the array. The array is then washed and stained with Cy3-streptavidin complex which can be seen by the scanner. The arrays are made up of

oligonucleotides probes attached to beads which are randomly introduced to the Illumina chip. Each array will contain up to 30 replicates of the bead type and therefore 30 replicates of each probe. Each oligomer is made up of the 50-base gene-specific probe and 29-base address sequence used to identify the randomly placed bead (www.well.ox.ac.uk/expression-profiling). Three HUVEC cell lines (A, B and commercial (promocell)) were infected with 5 MOI of Ad-Null and Ad-XBP1u adenoviral vectors. Samples were harvested 24 and 72 hours post-infection. The variation in intensity for each gene, as determined through binding to specific probes was assessed. Genes demonstrating a 2-fold change were selected for further study.

The subsequent analysis was performed by Ingenuity statistical calculations. Ingenuity statistical software uses a specific test to determine gene expression profile changes that correspond to particular cellular functions. The genes identified to have two-fold changes were entered into the online statistical calculation software. The right-tailed Fishers exact test was used to analyse gene expression profiles as it considers: the number of roles that the gene plays in each cell function; the total number of genes in the particular cell function analysed known to be associated with that cell function; the total number of genes in the data sample; the total number of genes in the reference set. There is then a significance threshold of 0.05 under which a particular cell function is deemed to have been significantly altered by the overexpression of XBP1u.

2.2.5.4 Semi-quantitative Polymerase Chain Reaction (PCR)

DNA amplification using the polymerase chain reaction (PCR) was used to amplify specific sequences within the genes of interest to analyse gene expression changes. A typical PCR was performed in 25 μL total volume. Prior to each experiment a master mix containing PCR reaction buffer, magnesium chloride, dNTPs, Taq DNA polymerase and primers was prepared (all Invitrogen). 50 ng of cDNA is used per reaction. The final concentration of reagents in the reaction mixture is 1X PCR reaction buffer, 2 mM magnesium chloride, 0.166 μM dNTP, 0.5 U Taq DNA polymerase and 0.666 μM forward and reverse primers all diluted in DEPC-treated water. The generic reaction protocol involved an initial 5 minute incubation at 94°C, followed by repeating cycles of 94°C denaturation and annealing for 30 seconds, and

72°C extension for 1 minute. The number of cycles and the annealing temperature is stated in Table 4.1. The reaction was terminated by a final extension of 10 minutes at 72°C and the mixture was cooled to 4°C. The PCR was performed in a Techne thermo cycler 512. The specific sequences, cycle numbers and annealing temperatures for each primer used are shown in Table 4.1. Lyophilised primers were diluted in 10 mM EDTA to a concentration of 100 μM. Further dilutions were all performed in DEPC-treated water.

2.2.5.5 Agarose Gel Electrophoresis of DNA

DNA was separated by electrophoresis on a 1% (w/v) agarose gel made in 1X TBE buffer supplemented with 0.1 μg/mL of ethidium bromide. DNA samples were mixed 1:5 with 6X gel loading buffer (50% glycerol, 1% bromophenol blue) and loaded into wells. The samples were electrophoresed in 1X TBE buffer at 195 V for approximately 25 minutes. The DNA bands were visualised using ultraviolet light using a UVP biosphere AC imaging system and vision works software. The size of the DNA fragments was estimated by comparison to a 1 kb plus DNA ladder (0.1-10kb; Invitrogen).

2.2.5.6 Real-time PCR

Total RNA was isolated as previously described. Each real-time PCR reaction was performed in duplicate. Real-time PCR primers were designed as stated previously. Each real-time reaction contained 20 ng cDNA, 9 uL DEPC-treated water, 0.75 uL of 0.3 μM forward and reverse primers and 12.5 uL of sybr green reaction mix (Applied Biosystems). The reaction mixture was placed in one well of a 96-well plate and placed into a Sequence Detection System 7000 (Applied Biosystems). A dissociation protocol was run using 60°C as the annealing temperature. Results were analysed using ABI prism software and compared to 18S ribosomal expression levels.

2.2.5.7 Genotyping

Genotyping of total knockout XBP1-null mice was performed on the mixed population of embryonic cells whose isolation has previously been described. $1/40^{th}$ of the cell pellet was resuspended in PBS and centrifuged at 500 x g for 5 minutes at 4 °C. The cell pellet was resuspended in 200 µL DNA extraction buffer containing 200 µg / mL proteinase K and incubated overnight at 55°C. The DNA was extracted using 200 µL phenol/chloroform and centrifuged at 10,000 x g for 5 minutes at 4°C. The supernatant was then transferred to a fresh tube and 200 µL was added, followed by subsequent mixing and centrifugation at 10,000 x g for 5 minutes at 4°C. The supernatant was then transferred to a fresh tube. 1/10 volume NaAc, 2.5 volumes of ethanol were added to the supernatant, mixed and incubated at room temperature for 1 hour. The sample was then centrifuged at 10,000 x g for 5 minutes at 4°C. The supernatant was discarded and the DNA was resuspended in 50 µL water. Semi-quantitive PCR was performed using three primer sets (XBP1-gen-1/2/3) with a 55°C annealing temperature for 35 cycles. The products were then run on a 2% agarose gel. $XBP1^{-/-}$ = 365bp, $XBP1^{+/-}$ = 365bp and 265bp, $XBP1^{+/+}$ = 265bp.

To genotype the conditional XBP1-null mice (*Tie2-Cre / $XBP1^{f/f}$*) the DNA was extracted from tail sections as previously stated above. However the semi-quantitative PCR reaction utilises 4 primer sets, (XBP1-gen-1/4/5/6). These will identify the presence of both $XBP1^{f/f}$ and *Tie2-Cre*. Cre^{+} = 500bp, $XBP1^{+/+}$ = 270bp, $XBP1^{f/+}$ = 270bp + 388bp, $XBP1^{f/f}$ = 388bp.

2.2.6 Protein Analysis

2.2.6.1 Whole Lysate Protein Extraction and Purification

Cells were washed with PBS to remove cell debris. The cells were mechanically removed using a cell scraperand centrifuged to form a cell pellet. The cell pellet was resuspended in the appropriate volume of lysis buffer (50mM Tris-HCl pH 7.5, 150mM NaCl, 1mM EDTA pH 8), supplemented with protease inhibitors (Roche) and 0.5% triton (all others Sigma). The samples were incubated at 4°C for

15 minutes before sonication for 10 seconds. The samples were incubated for a further 30 minutes at 4°C. The samples were then centrifuged at 13,000rpm for 10 minutes at 4°C and the supernatant was removed to a clean tube. The protein concentration was calculated using BSA of known concentrations to form a standard curve and Bradford reagent (BioRAD) to determine protein concentrations of the samples.

2.2.6.2 Western Blot Protein Analysis

Western blots were run using 25 μg of protein samples and the Precision Plus protein ladder (BioRAD). SDS-PAGE was performed using 4-12% Bis-Tris gels (Invitrogen) using 1 L running buffer (Invitrogen). The gels were run for 1 hour at 180 V. Proteins were transferred onto a nitrocellulose membrane (Whatman) and transferred at 25 V for 2.5 hours. The membrane was blocked for two hours in 5% Milk diluted with PBS-T. Primary antibody incubation was performed overnight at 4°C. Primary antibodies are listed in Table 2.4. The blot was washed 3 times for 10 minutes with PBS and then incubated with secondary antibody for 1 hour (Dako). The blot was washed as stated previously, incubated with ECL reaction mixture for 3 minutes and exposed to Hyperfilm (GE Healthcare) and developed. The blots were analysed using Adobe Photoshop software.

2.2.6.3 Cell membrane protein isolation

Membrane protein isolation was carried out using Pierce Cell Surface Protein Isolation Kit (Thermo Scientific) according to the manufacturer's instructions. HUVEC treated in T175 flasks were washed twice with ice cold PBS. The membrane proteins were first biotinylated with the membrane impermeable EZ-link Sulfo-NHS-SS-Biotin, a thiol-cleavable amine-reactive biotinylation reagent with gentle agitation on a rocker for 30 minutes at 4°C. The Sulfo-NHS-SS-Biotin reagent forms a stable covalent linkage with an extended spacer arm for avidin binding. 500 μL of quenching solution was then added to stop the reaction and cells were centrifuged at 500 x g for 3 minutes and the cell pellet was subsequently lysed via sonication in 500 μL lysis buffer in a microcentrifuge tube at 4°C. After incubation on ice for 30 minutes the cell lysate was centrifuged at 10,000 x g for 2 minutes at 4°C and the

supernatant was transferred to a new microcentrifuge tube. The following step isolates the labelled proteins with NeutrAvidin Agarose. 500 μL of the NeutrAvidin slurry was added to the columns provided and centrifuged for 1 minute at 1,000 x g and the flow-through was discarded. 500 μL of wash buffer was then added to the gel and centrifuged for 1 minute at 1,000 x g and the flow-through was again discarded. The washing process was repeated 3 times. The cell lysate was then added to the gel and incubated for 60 minutes on a rotator at room temperature. The column was then added to a collection tube and centrifuged for 1 minute at 1,000 x g and the flow-through discarded. 500 μL wash buffer was added and mixed by inverting the column and centrifuged for 1 minute at 1,000 x g. This wash was repeated 3 times. The final step was carried out to release the bound proteins by incubating them with 200 μL SDS-PAGE sample buffer containing 50 mM DTT with rotation at room temperature. The columns were then centrifuged for 2 minutes at 1,000 x g and the protein concentration of the eluted sample was then measured as previously stated. 50 μg of the eluted protein was then analysed by Western blotting.

2.2.6.4 Isolation of nuclear and cytosolic fractions

HUVECs were treated in T175 flasks and then washed in ice-cold PBS, before they were scraped and pelleted into a microcentrifuge tube at 500 x g for 2 minutes. The supernatant was removed and 400 μL of hypotension buffer (10 mM Tris hydrochloride (pH7.4), 10 mM potassium chloride and 10 mM EDTA) was used to resuspend the cell pellet. 12 μL of NP40 was added to disrupt the outer cell membrane and the solution was vortexed for 10 seconds. The solution was then centrifuged at 10,000 x g for 10 seconds. The supernatant was recovered and then designated as the cytoplasmic fraction. The pellet was the resuspended and washed with PBS three times before being resuspended in 200 μL buffer C. The solution was then sonicated for 3 seconds and was designated as the nuclear fraction. 50 μg of protein was then analysed by Western blotting.

2.2.6.5 Co-immunoprecipitation

For immunoprecipitation studies HUVECs in T175 flasks were transfected with the adenoviral vectors for 48 hours. The cells were then harvested as previously

stated and the cell pellet was resuspended in 400 μL immunoprecipitation buffer-A (IP-A) in a microcentrifuge tube. After incubation on ice for 45 minutes the cell suspension was centrifuged at 8,000 x g for 5 minutes and the lysate was transferred to a new microcentrifuge tube. The cell pellet was resuspended in 100 μL IP-A and sonicated with a Branson Sonifier 150 at the lowest setting for 5 seconds. The solution was then incubated on ice for a further 30 minutes. The cell lysate was then centrifuged at 8,000 x g for 5 minutes and the supernatant was pooled with the previous lysate. The protein concentration was determined as stated previously and 1 mg of protein was transferred to fresh microcentrifuge tubes. 3 times the volume of IP-B was added to the lysate which was then incubated overnight with 40 μL of the agarose conjugated antibody on a rotator at 4°C. The mix was then centrifuged at 5000 x g and the supernatant carefully removed and discarded with a narrow pipette tip. The resin was then washed 3 times with 500 μL TBS. The bound proteins were then eluted with 20 μL 2 x SDS-sample elution buffer by boiling for 3 minutes. The samples were then centrifuged at 5,000 x g for 30 seconds to pellet any undisolved agarose and the supernatant was transferred to a new microcentrifuge tube. The samples were then loaded simultaneously with 50 μg of the total lysate sample and analysed by Western blotting.

2.2.7 Data and statistical analysis

Data was expressed as mean and standard deviation of three individual experiments. Statistical analysis was carried out using the unpaired Student's *t* test. All statistical analysis was carried out using the Prism GraphPad 4.0 software. A P value < 0.05 was considered significant.

Chapter 3 - Results

The X-box binding protein-1 (XBP1) is a key signal transducer in the endoplasmic reticulum stress response yet its potential role in endothelial cell (EC) function and atherosclerosis development is unknown. This study aims to explore the impact of XBP1 on maintaining EC integrity related to atherosclerosis and to delineate the underlying mechanisms. Under normal conditions, XBP1 exists as a 29 kDa unspliced isoform (XBP1u). Although XBP1u is reported to modulate the level of spliced XBP1 (XBP1s) via proteosome-mediated degradation, other functions are predicted (Nekrutenko and He, 2006; Yoshida et al., 2006). The physiological function of the unspliced isoform remains unclear. In our previous study, it was shown that XBP1u was the main isoforms present in cultured HUVECs and could be upregulated by disturbed flow. XBP1u was also revealed to be expressed in regions prone to atherosclerosis and the expression correlated with the severity of lesion formation in ApoE-/- mice (Zeng et al., 2009). ECs in regions prone to atherosclerosis or under disturbed flow undergo increased proliferation and apoptosis. Considering that XBP1u contains an intact N-terminal domain and DNA binding domain, it may bind to DNA sequences and recruit other co-activators or co-repressors via interactions with its N-terminal domain, thereby modulating gene transcription. Indeed, we have found that XBP1u binds to the promoter of VE-cadherin in living cells (data not shown). Thus, our hypothesis is that besides antagonising XBP1s, XBP1u may exert its own function in the modulation of cell proliferation and apoptosis.

To facilitate our study, XBP1u has been cloned and an adenoviral expression vector (Ad-XBP1u) has been created. Overexpression of XBP1u will be mediated via adenoviral gene transfer. On the other hand, knockdown of XBP1 will be mediated through shRNA lentiviral vectors (shRNA-XBP1). In this study, we aim to decipher the potential role of XBP1u in EC survival under oxidative stress and the underlying mechanism. We will investigate the effect of overexpression and knockdown of XBP1u on ECs under hydrogen peroxide challenge and the signalling pathways involved. We will also screen XBP1u regulated survival genes by microarray assay and explore how XBP1u regulates the expression of these genes.

3.1 XBP1u Enhances EC Survival in Response to Oxidative Stress

3.1.1 Disturbed flow enhances XBP1 expression

The bifurcation regions of the vasculature are subjected to lower, more turbulent, oscillatory or even reversed shear stress (commonly termed disturbed flow) caused by the non linear flow of blood. Linear regions of the vasculature are subjected to higher, unidirectional haemodynamic forces (laminar flow). Due to the nature of blood flow bifurcation regions are more susceptible to the formation of atherosclerotic lesions caused by alterations in the phenotype of local ECs (Malek et al., 1999). Due to the differences in the shear stress exerted by blood flow between linear and bifurcation regions we speculated that the expression of either XBP1 isoform could be driven by differences in shear stress and that these could act to induce an atheroprotective or atheroprone EC phenotype. Disturbed flow was applied to HUVECs *in vitro* and the expression of XBP1u and XBP1s was assessed at the mRNA and protein level (figure 12). The expression of XBP1s protein is transiently and significantly upregulated by 1 and 2 hours of disturbed flow in comparison to static controls. The increased expression of XBP1s protein is quickly reduced after 2 hours (figure 12A, 12C). The expression of XBP1u is differently modulated by disturbed flow. The expression of XBP1u at the protein level is consistently upregulated by 1 to 8 hours of disturbed flow, with the observed expression dropping slightly, although remaining above that of the static control, after 24 hours (figure 12A, 12B). These studies show that disturbed flow induces a prolonged increase in the expression of XBP1u and a more acute increase in the expression of XBP1s.

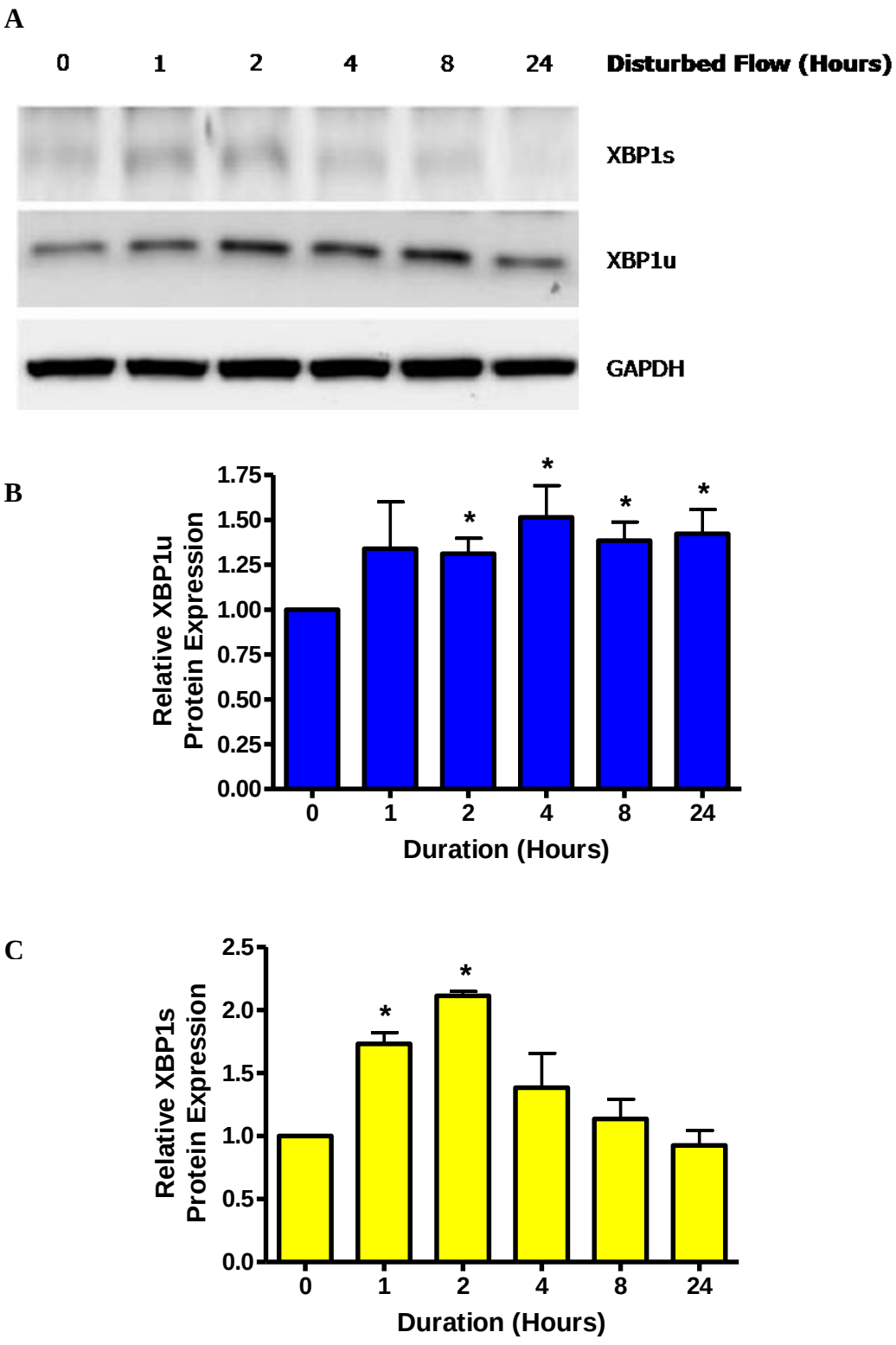

Figure 12: Disturbed flow upregulates XBP1 expression at the protein level.

HUVECs were subjected to disturbed flow for 0, 1, 2, 4, 8 and 24 hours. **A.** The expression of XBP1u and XBP1s at the protein level was detected by Western blotting. The images are representative of three independent experiments. **B.** and **C.** The expression changes in XBP1u and XBP1s at the protein level were quantified by densitometry. * $P < 0.05$.

3.1.2 Overexpression of XBP1u increases HUVEC proliferation

Overexpression of XBP1s 'pushes' ECs towards an apoptotic phenotype, however, XBP1s is only expressed under certain conditions and the expression of XBP1u predominates in ECs. The expression of the spliced isoforms of XBP1 is minimal under quiescent conditions. However, during ER stress and in response to redox fluctuations the activity of IRE-1α and therefore the expression of XBP1s is dramatically upregulated (Yoshida, 2007; Yoshida et al., 2001; Zeng et al., 2009). Therefore determining the role of XBP1u in ECs is crucial to a more complete understanding of vascular integrity. Previous reports show that XBP1u can function through antagonistic interactions with XBP1s (Yoshida et al., 2006). XBP1u binds to XBP1s, sequesters it in the cytosol and targets it for proteosome-mediated degradation. Due to its antagonistic effects on XBP1s, XBP1u could promote EC survival.

Additionally, other XBP1u functions have been predicted, yet remain unexplored (Nekrutenko and He, 2006). Furthermore, the mature XBP1u protein contains an intact N-terminal domain, comprising a DNA-binding element and therefore has the potential to act as a co-activator or co-repressor during gene transcription. Indeed, previous work in our lab has demonstrated that XBP1u binds to the VE-cadherin promoter (data not shown). Similarly to XBP1s, XBP1u is also upregulated in bifurcation regions of the vasculature. We hypothesised that XBP1u is upregulated in ECs to promote survival and protect against mechanical stress induced apoptosis and that this occurs separately to its role in antagonising XBP1s.

Overexpression of XBP1u was achieved by cloning the XBP1u gene fused to a FLAG tag into an adenoviral expression vector (Ad-XBP1u). The adenoviral vector was produced and HUVECs were transduced with Ad-XBP1u alongside Ad-Null, which contains a tTa gene as a control for transduction. The infection of HUVECs with Ad-XBP1u adenovirus augmented the expression of XBP1u at the mRNA and protein level (figure 13A-B).

The overexpression of XBP1u also altered HUVEC morphology in comparison to Ad-Null transduced cells (figure 13C-D). Overexpression of XBP1u

induced HUVECs to acquire an elongated and unidirectional appearance, similar to that observed when healthy ECs are subjected to laminar shear stress. HUVECs subjected to the overexpression of XBP1u also demonstrated a more quiescent morphology.

ECs subjected to laminar shear stress demonstrate increased cell survival and are less likely to undergo apoptosis. We hypothesised that XBP1u enhances EC growth and survival. To determine if XBP1u is involved in EC survival XBP1u was overexpressed via adenoviral gene transfer and the proliferation of HUVECs was determined via an MTS tetrazolium assay. The overexpression of XBP1u in HUVECs significantly increased HUVEC proliferation (figure 13E). These data indicate that the overexpression of XBP1u in ECs contributes to changes in EC morphology and an enhancement in EC survival.

3.1.3 XBP1u protects ECs against oxidative stress

Disturbed flow promotes oxidative stress leading to EC apoptosis (Chatzizisis et al., 2007). Disturbed flow also increases ROS production by enhancing gene expression and post-transcriptional activity of NADPH and xanthine oxidase at the endothelial membrane (Hwang et al., 2003b; McNally et al., 2003). Disturbed flow also downregulates ROS scavengers and degrades the atheroprotective NO molecule and its cofactors further enhancing the production of ROS (Harrison et al., 2006). We have demonstrated that XBP1u is upregulated in regions of disturbed flow, which are prone to increased oxidative stress and EC apoptosis. Secondly, we have demonstrated that the overexpression of XBP1u enhances EC proliferation. Therefore, we hypothesised that XBP1u is upregulated by disturbed flow to mediate against augmented ROS production.

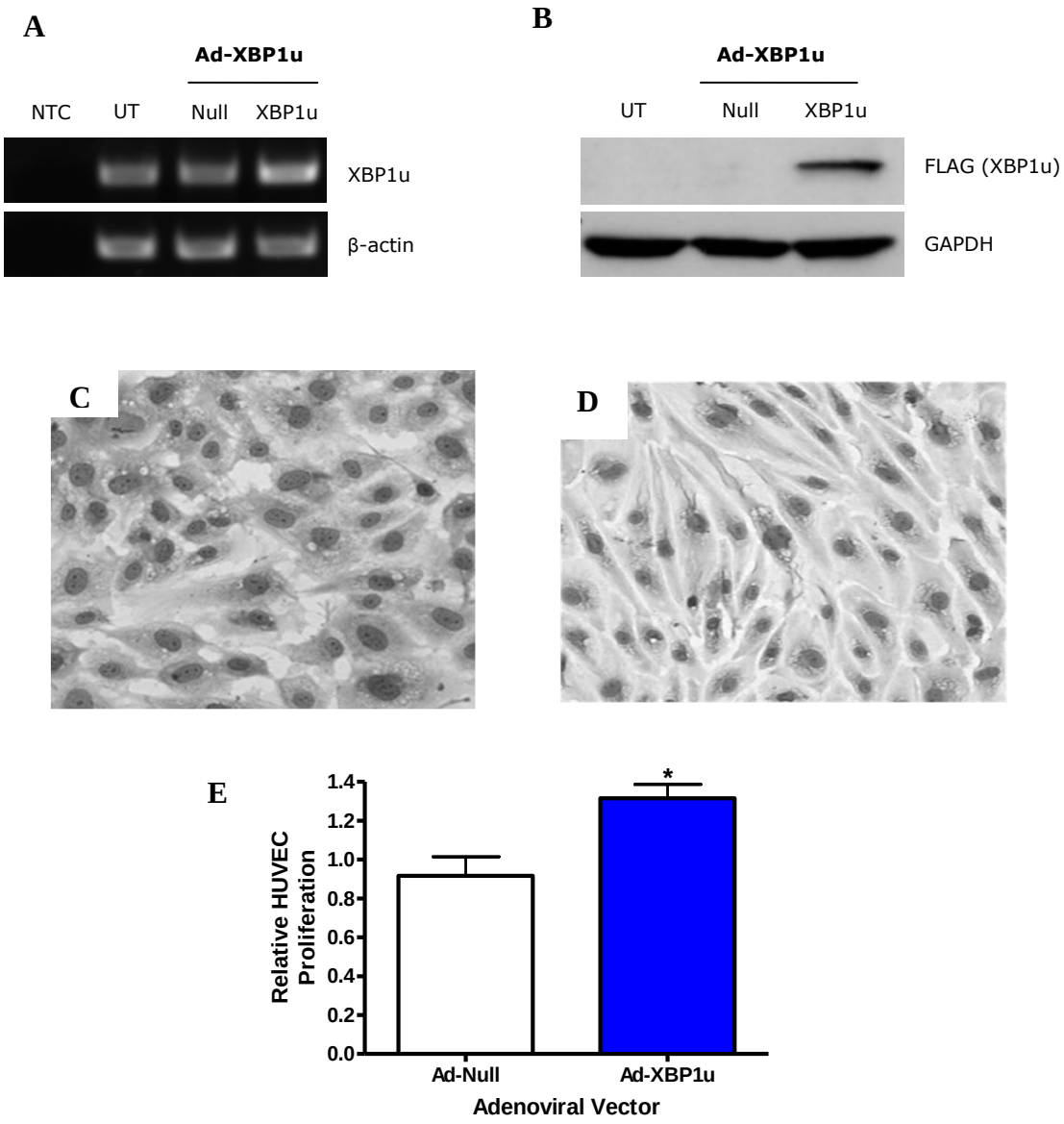

Figure 13: XBP1u enhances HUVEC proliferation.

A. and **B.** HUVECs were left untreated or transduced with 10 MOI of Ad-Null or Ad-XBP1u adenoviruses. The mRNA and protein was harvested 48 hours post-transduction and the expression of XBP1u at the (**A**) mRNA and (**B**) protein level was detected by semi-quantitative PCR and Western blotting respectively. **C.** and **D.** The morphology of HUVECs transduced with (**C**) Ad-Null and (**D**) Ad-XBP1u adenoviruses was observed by imaging 72 hours post-infection. **E.** HUVECs were transduced with 10 MOI of Ad-Null or Ad-XBP1u adenoviruses. The proliferation was detected via an MTS tetrazolium assay 72 hours after transduction. The images are representative and histogram depicts averages and standard deviation of six independent experiments. ***** $P < 0.02$.

The balance of hydrogen peroxide production and degradation is tightly controlled within a cell. Excess hydrogen peroxide induces oxidative stress and leads to apoptosis. Hydrogen peroxide treatment of cells can be used as a model to study the effects of oxidative stress of cell survival. In order to test this hypothesis HUVECs were treated with Ad-Null and Ad-XBP1u adenoviruses. The HUVECs were subsequently treated with 50μM hydrogen peroxide for 24 hours, a dose that has previously been shown to promote HUVEC apoptosis. The proliferation of HUVECs was observed via an MTS tetrazolium assay subsequent to hydrogen peroxide treatment (figure 14). HUVECs under control conditions demonstrated significant cell loss after hydrogen peroxide treatment. However, the overexpression of XBP1u significantly suppresses hydrogen peroxide-induced cell loss. There is a two-fold increase in HUVEC proliferation in cells expressing exogenous XBP1u after treatment with hydrogen peroxide. This data implicates XBP1u has a protective role against oxidative stress.

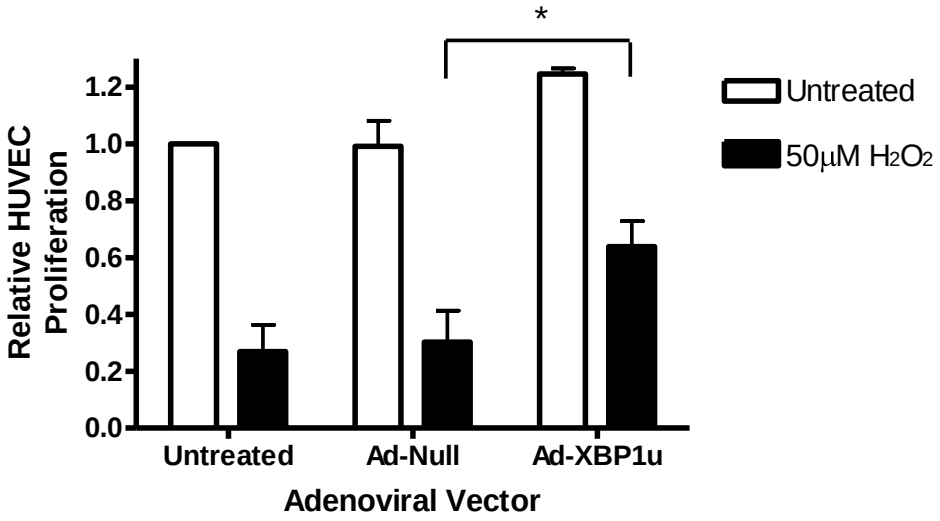

Figure 14: XBP1u protects ECs against oxidative stress.

HUVECs were left uninfected, infected with 10 MOI Ad-Null or 10 MOI Ad-XBP1u adenoviral vectors. 48 hours after transduction the cells were left untreated or treated with 50μM hydrogen peroxide for 24 hours. HUVEC proliferation was assessed using an MTS tetrazolium compound assay. ***** $P < 0.05$. The histogram depicts the average and standard deviation of four independent experiments.

The regions of the vasculature subjected to disturbed flow and at increased risk of atherosclerotic lesion formation are exclusively found in the arterial system. Our *in vitro* cell model, HUVECs, are part of the venous system, therefore it was necessary to determine that XBP1u retains this protective effect in arterial ECs. To this end, aortas from *Tie2-LacZ* mice were harvested and cut into 1-2 mm^2 sections. These were then immediately treated with Ad-Null or Ad-XBP1u adenovirus. The sections were subsequently treated with 50μM hydrogen peroxide for 24 hours. Surviving ECs were detected by X-gal staining (figure 15). Hydrogen peroxide treatment of uninfected or Ad-null infected aortic sections resulted in significant EC death. The overexpression of XBP1u in aortic ECs significantly protected ECs from hydrogen peroxide mediated apoptosis. In fact a two-fold increase in EC survival was observed after exogenous overexpression of XBP1u and hydrogen peroxide treatment.

3.1.4 Knockdown of XBP1 increases EC apoptosis

XBP1u increases EC survival during oxidative stress; therefore a loss of XBP1u could decrease the ability of ECs to survive stimulation with oxidative stress. Total XBP1 was knocked down through the creation and application of a lentiviral construct containing a short-hairpin RNA (shRNA) directed at the mature XBP1 mRNA molecule (shRNA-XBP1). To control for the effects of lentiviral infection a lentivirus containing a randomly generated non-targeting RNA sequence was used (shRNA-NT). HUVECs were transduced with shRNA-NT or shRNA-XBP1 lentiviral vectors. After 72 hours, HUVECs were treated with 20μM hydrogen peroxide and the proliferation was observed via an MTS tetrazolium assay (figure 16C). shRNA-mediated knockdown of total XBP1 resulted in an 80% reduction in XBP1u detection at the mRNA level (figure 16A) and a 70% reduction in XBP1u at the protein level (figure 16B). The treatment of the control cells with hydrogen peroxide resulted in a significant (50%) reduction in EC proliferation. Knockdown of XBP1 had no effect on the level of HUVEC proliferation after hydrogen peroxide treatment. We also observed that knockdown of XBP1 had no effect on HUVEC proliferation in the absence of hydrogen peroxide treatment. This data implies that the knockdown of XBP1 does not further enhance oxidative stress-mediated apoptosis and that XBP1u is only sufficient to enhance EC proliferation not necessary.

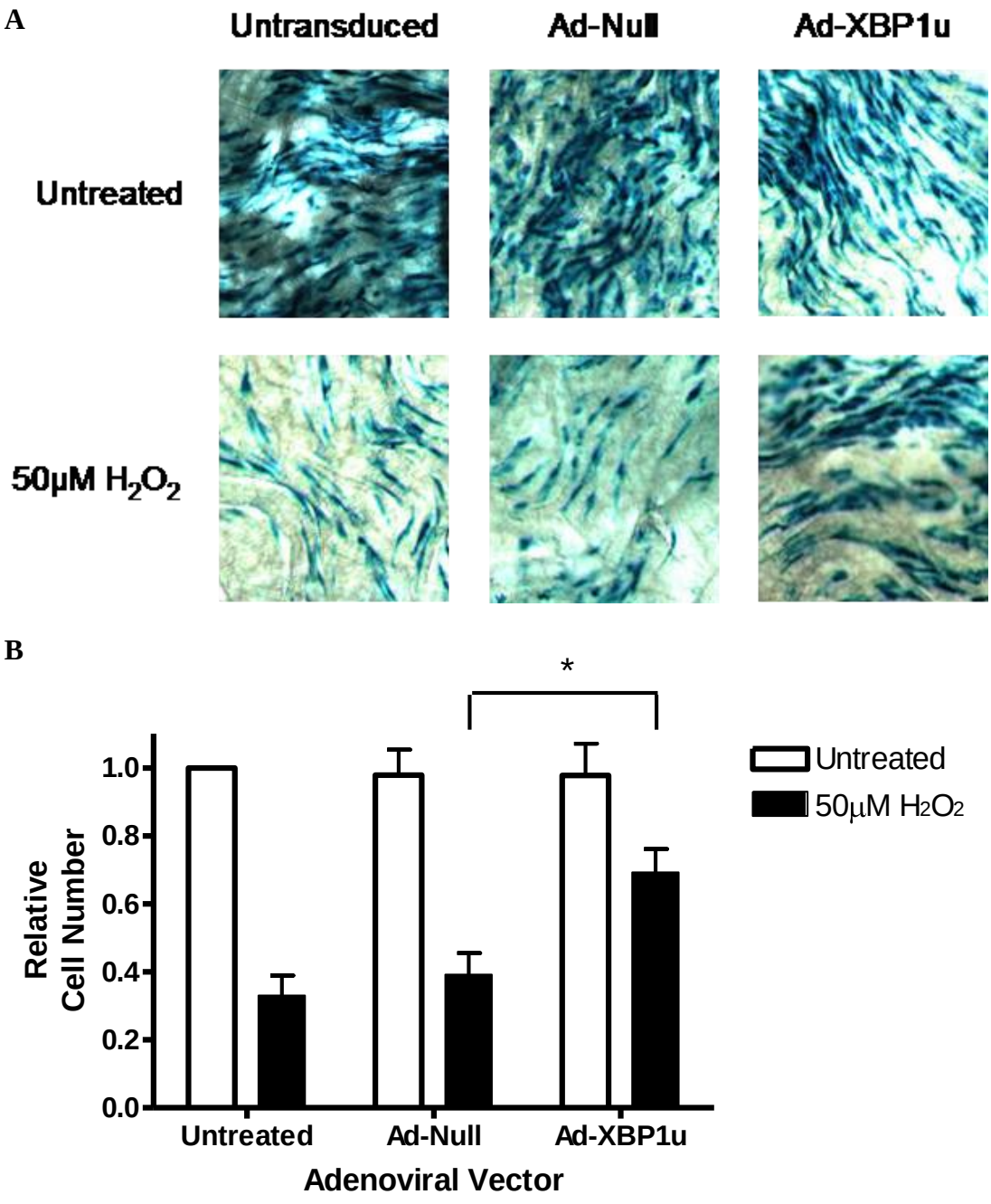

Figure 15: XBP1u protects ECs from hydrogen peroxide-induced apoptosis in ex vivo aorta sections.

Aortic sections from 8-10 week old *Tie2-LacZ* mice were left untreated or treated with $1x10^7$ pfu/mL of Ad-Null or Ad-XBP1u adenoviral vectors. The aortic sections were treated with 50μM hydrogen peroxide for 24 hours, 48 hours after transduction. **A.** Surviving ECs were observed by X-gal staining. **B.** Surviving ECs were counted from 10 random segments of the aortic sections. The number of surviving ECs was calculated relative to the number of surviving ECs in the uninfected, untreated artery sections. ***** $P < 0.01$. The data is representative of six independent experiments.

We had anticipated that knockdown of XBP1 would enhance the susceptibility of HUVECs to oxidative stress; however the previous data does not confirm this. We wished to confirm this data using a different cell population. XBP1-null mice are embryonic lethal after day 15.5 due to hypoplastic liver formation, which results in reduced haematopoiesis and death from anaemia (Reimold et al., 2000). Therefore, to examine XBP1-null cells from these embryos it is necessary to harvest them at an earlier time point. Heterozygous $XBP1^{+/-}$ mice were crossbred and harvested as embryos at day 13.5. At this time point the wild type and heterozygous embryos are significantly larger when compared to homozygous XBP1-null embryos. An adherent XBP1-null cell population was extracted from these embryos.

The heterozygous $XBP1^{+/-}$ mice were generated by Dr. Lingfang Zeng and Dr. Yanhua Hu through the insertion of a stop codon in exon 2. The wild type, heterozygous and XBP1-null mice were genotyped and the presence of XBP1 in these animals has been demonstrated by semi-quantitative PCR (figure 17A). The adherent cell population was generated according to the protocol stated in the methods section and the morphology of these cells is demonstrated in Figure 17B. These cells have not been further characterised, therefore they represent a population of cells isolated from wild type, heterozygous and XBP1-null animals that have been selected for based on their adherence to collagen after 1 hour of incubation.

Wild type and XBP1-null cells were treated with 20μM hydrogen peroxide to induce apoptosis. The cells were stained with dUTP-fluorescein to identify DNA breaks. The number of DNA breaks as compared to total cell number for XBP1 and XBP1-null cells was determined by FACS analysis (figure 17A-B). The percentage of apoptotic cells from each sample was quantified (figure 17C). There was very little apoptosis observed in the untreated wild type cell population. The treatment of wild type cells with 20μM hydrogen peroxide increased the observed apoptosis from 0.3% of the cell population to 3% of the cell population. XBP1-null cells, under normal conditions, exhibited a higher level of apoptosis than untreated wild type cells (4.5% to 0.3% respectively). Significantly the treatment of XBP1-null cells with hydrogen peroxide significantly increased the observed apoptosis when compared to XBP1-null untreated cells and wild type cells treated with hydrogen peroxide. This data

counteracts the previous experiment and implies that XBP1 is required to promote EC survival in response to oxidative stress.

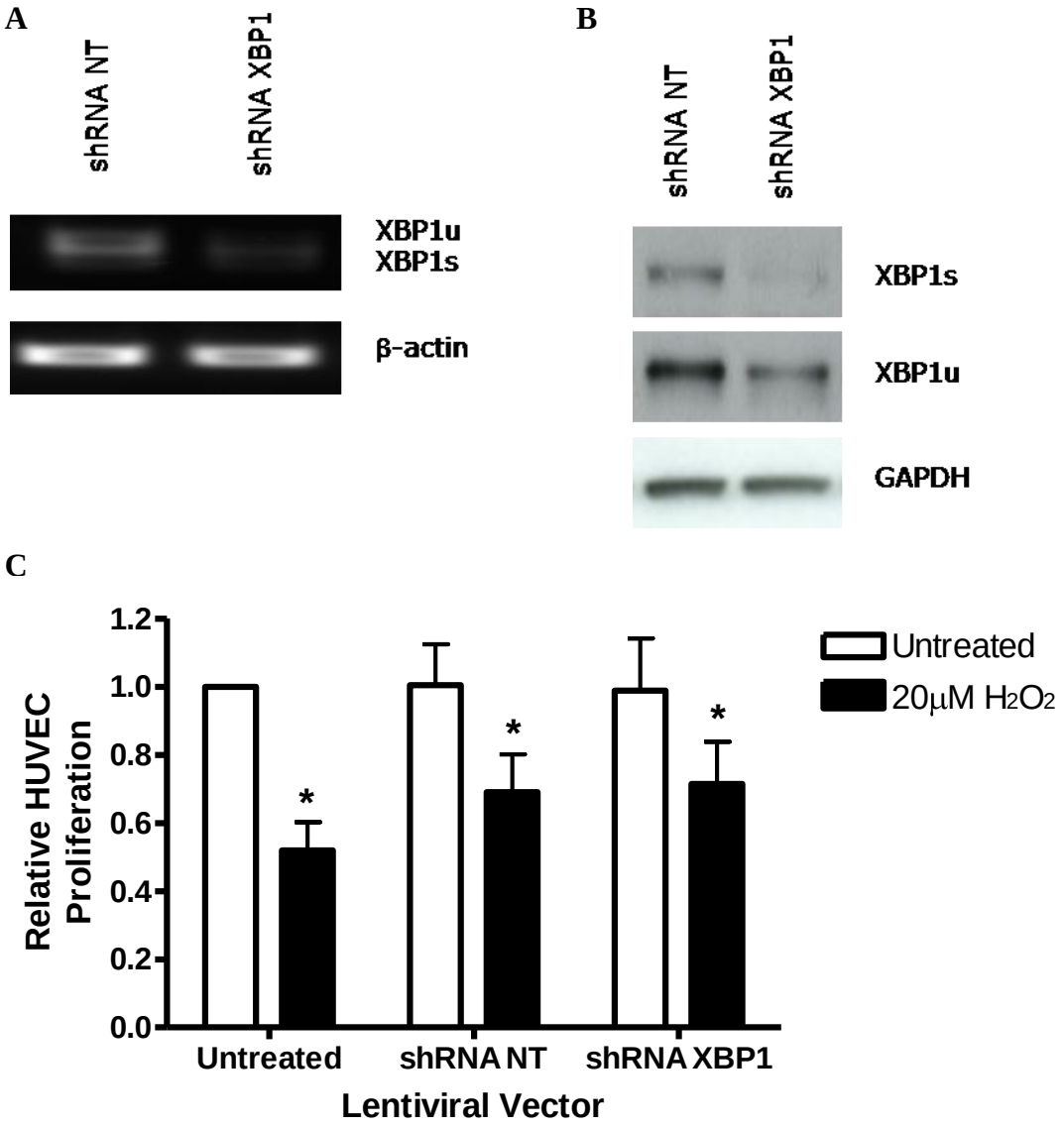

Figure 16: Knockdown of XBP1 does not enhance oxidative stress-mediated survival.

HUVECs were left untreated or transduced with 100 TU/cell of lentivirus containing a non-targeting (shRNA NT) or XBP1 targeting (shRNA XBP1) shRNA particle. The (**A**) mRNA and (**B**) protein was harvested and the expression of XBP1u, XBP1s, GAPDH and β-actin was assessed by RT-PCR and Western blotting respectively. **C.** 48 hours after transduction HUVECs were treated with 20 μM hydrogen peroxide for 24 hours and the proliferation was assessed using an MTS tetrazolium compound assay. The images are representative and the histogram depicts mean and standard deviation of four independent experiments. * $p < 0.05$.

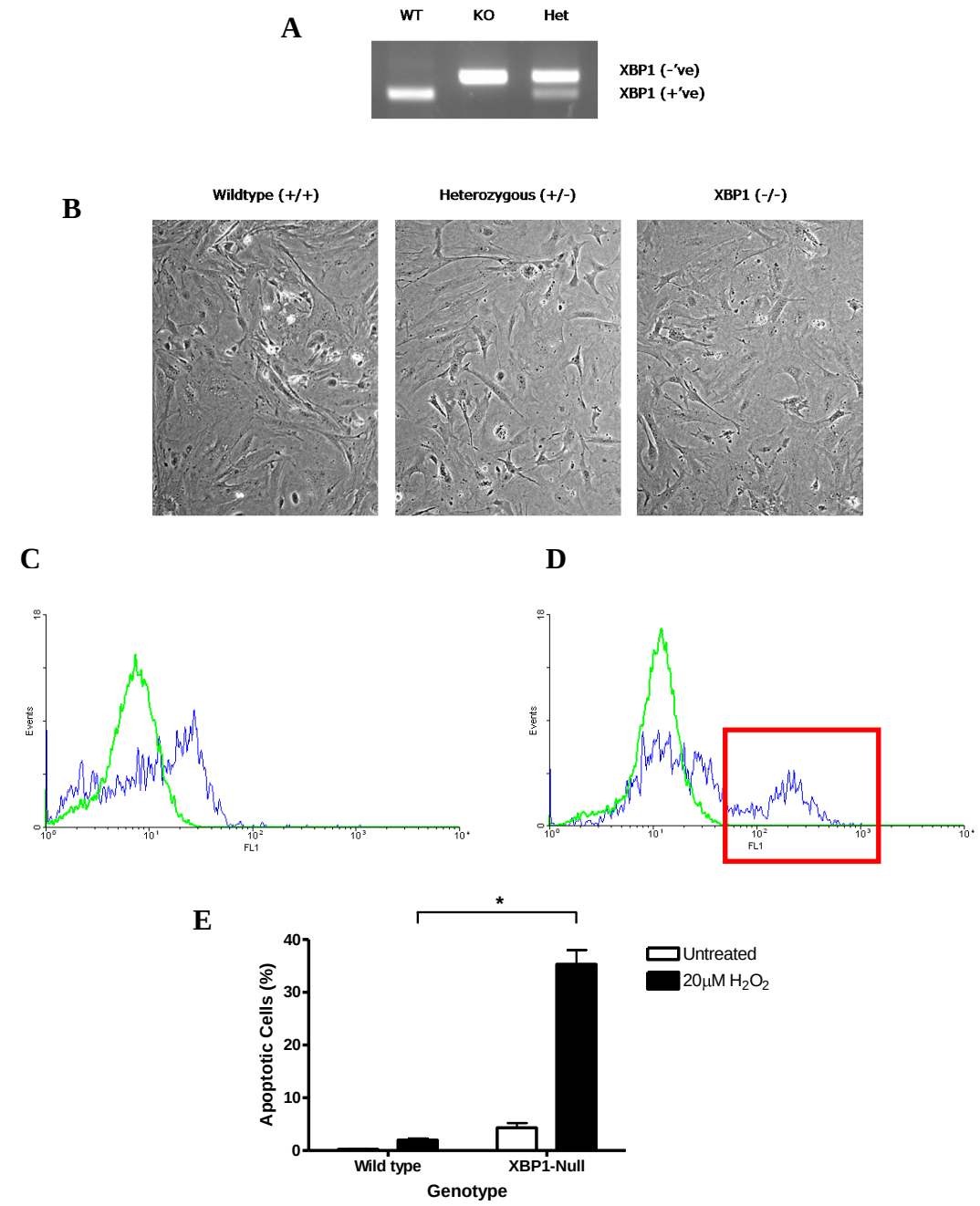

Figure 17: XBP1 knockdown increases hydrogen peroxide-induced apoptosis in XBP1-null mouse embryonic cells.

Wild type and XBP1-null Embryos from E13.5 were harvested and an adherent cell population was isolated. **A.** Wild type, heterozygous and XBP1-null embryos were genotyped and the presence of XBP1 was demonstrated by PCR. **B.** The morphology of the isolated population was demonstrated through imaging. Wild type and XBP1-null cells were treated with 20μM hydrogen peroxide. Apoptosis was determined via detection of dUTP-fluorescein by FACS. Cell populations of wild type (Oberoi et al.) and XBP1-null (blue) in (**C**) untreated and (**D**) 20μM hydrogen peroxide treated samples. The XBP1-null cell population positive for apoptosis is highlighted in red. **E.** Histogram depicting the changes in apoptotic cells present in wild type and XBP1-null cell populations. The data is representative and the histogram depicts mean and standard deviation of three independent experiments.

We have demonstrated that XBP1 is highly expressed in bifurcation regions and atherosclerotic lesions. Disturbed flow is able to transiently upregulate the expression of XBP1s and more permanently upregulate the expression of XBP1u. Our previous studies have demonstrated that XBP1s enhances EC apoptosis and atherosclerotic lesion formation. This data demonstrates that the overexpression of XBP1u in ECs significantly enhances their ability to proliferate and to survive after stimulation with oxidative stress. The importance of XBP1 in survival was further demonstrated as XBP1-null cells undergo increased apoptosis after hydrogen peroxide treatment. Our future studies focused on the signalling pathways initiated by XBP1u during disturbed flow that would lead to increased EC survival.

3.2 XBP1u Promotes EC Survival through the expression of HO-1

3.2.1 Identification of XBP1u-influenced candidate genes

As previously stated XBP1u contains a functional DNA-binding domain and is capable of binding to genomic DNA. We hypothesised that XBP1u responds to disturbed flow and increases EC proliferation through the activation or repression of gene expression. Specifically, we hypothesised that this occurs through the regulation of anti-oxidant and oxidising molecules. We identified potential candidate genes via microarray analysis. XBP1u was overexpressed in HUVECs from three independent human umbilical cord isolations. These were kindly provided by Gillian Cockerill. Adenoviral transduction was used to overexpress XBP1u for 24 and 72 hours. Any gene expression changes were identified via external microarray analysis. All genes demonstrating an up- or downregulated of more than 2-fold were selected for further analysis. The overexpression of XBP1u for 24 hours resulted in the upregulation of 121 genes and the downregulation of 1263 genes. The overexpression of XBP1u for 72 hours resulted in the upregulation of 699 and the downregulation of 52 genes.

The microarray data was performed only once due to budgetary reasons, there is therefore no heat-map distribution; however the main purpose of the microarray was

to identify candidate genes for further study, a library of 23,000 genes were screened for expression changes.

A

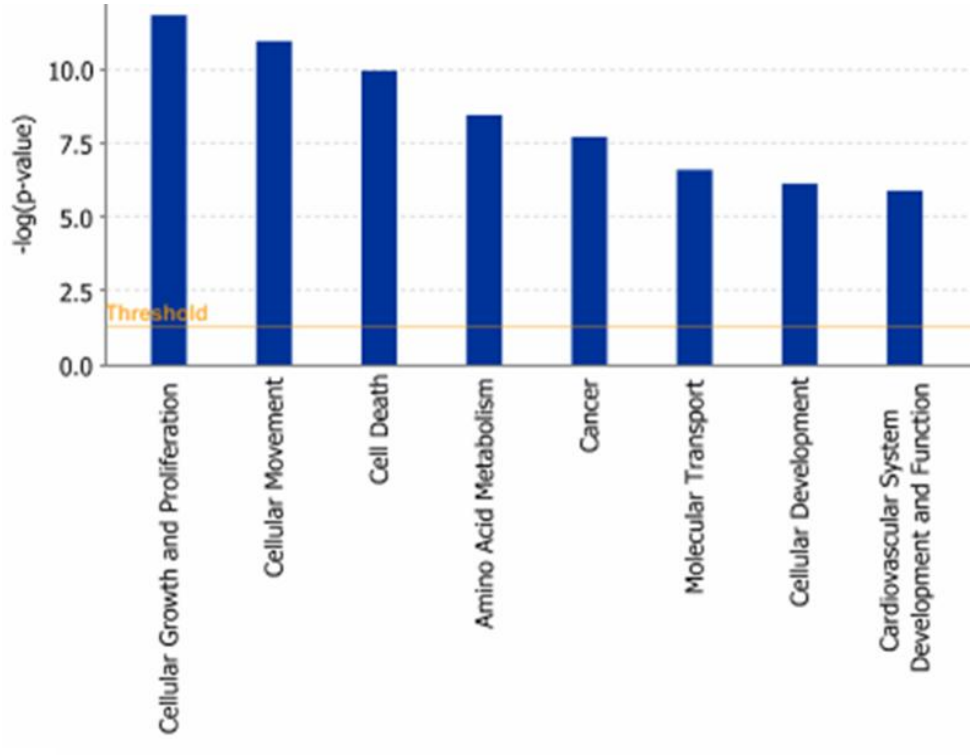

B

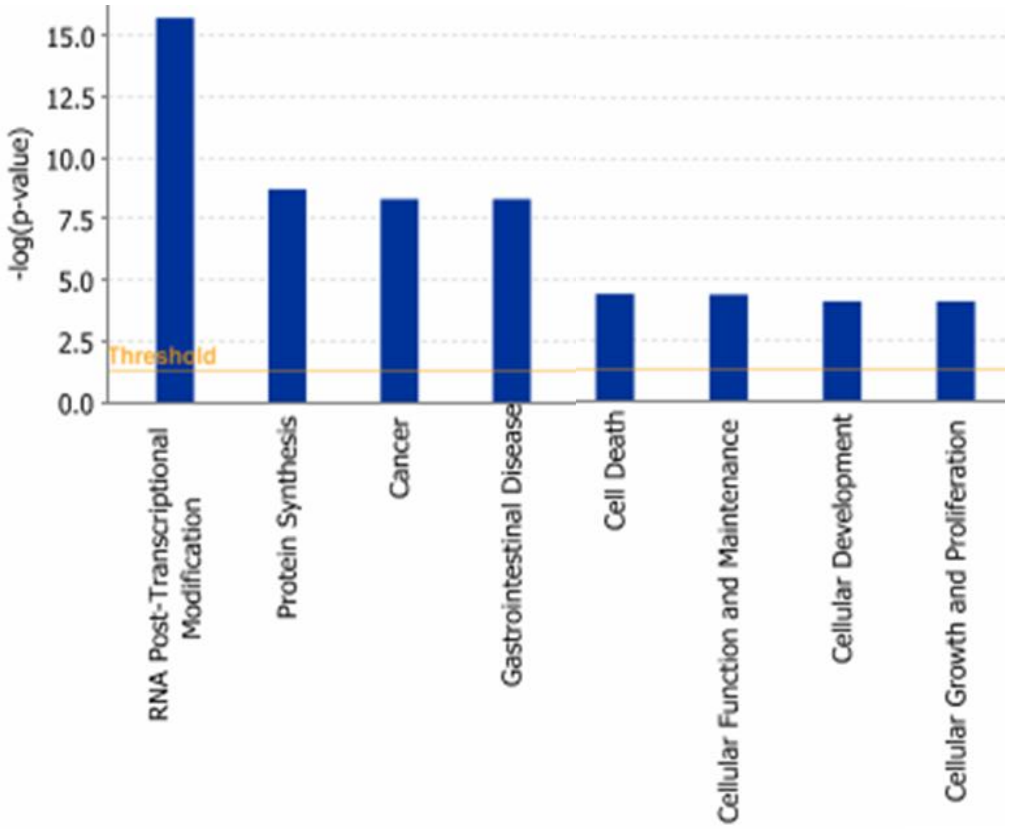

C

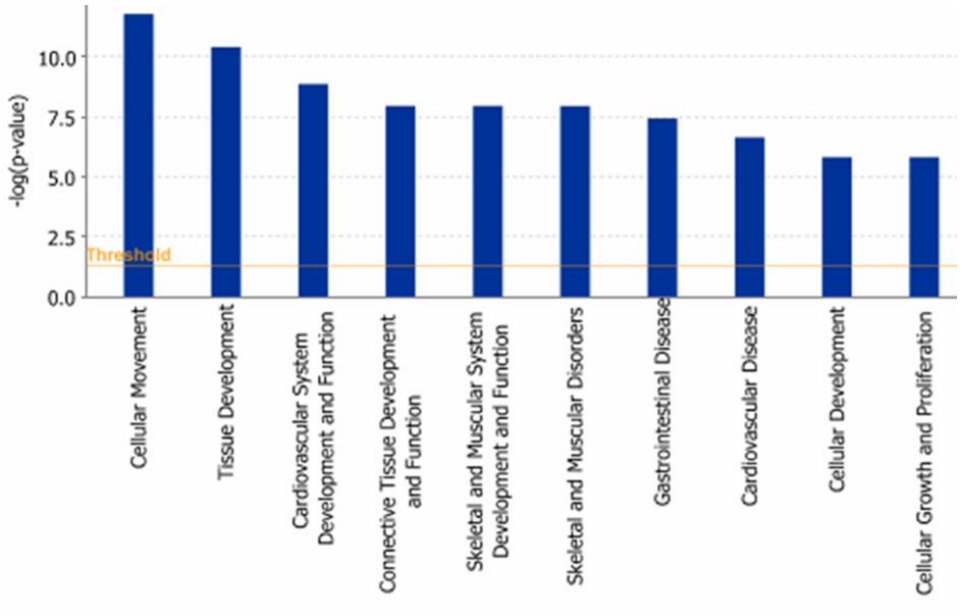
-log(p-value)
10.0
7.5
5.0
2.5
0.0
Threshold
Cellular Movement
Tissue Development
Cardiovascular System Development and Function
Connective Tissue Development and Function
Skeletal and Muscular System Development and Function
Skeletal and Muscular Disorders
Gastrointestinal Disease
Cardiovascular Disease
Cellular Development
Cellular Growth and Proliferation

D

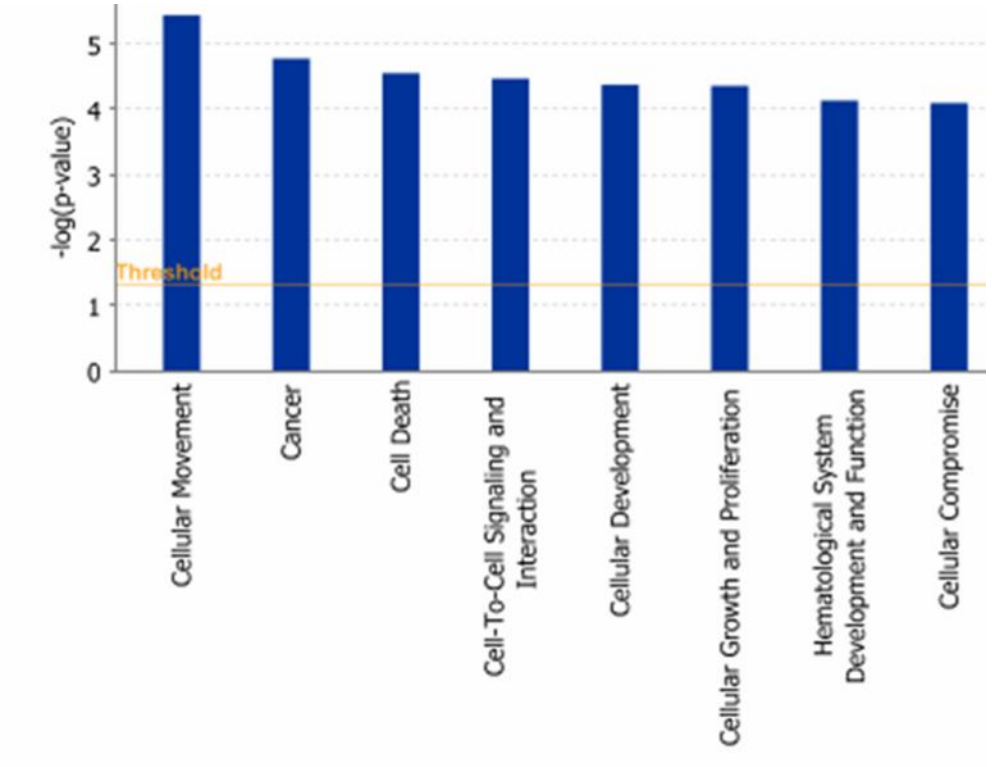
-log(p-value)
5
4
3
2
1
0
Threshold
Cellular Movement
Cancer
Cell Death
Cell-To-Cell Signaling and Interaction
Cellular Development
Cellular Growth and Proliferation
Hematological System Development and Function
Cellular Compromise

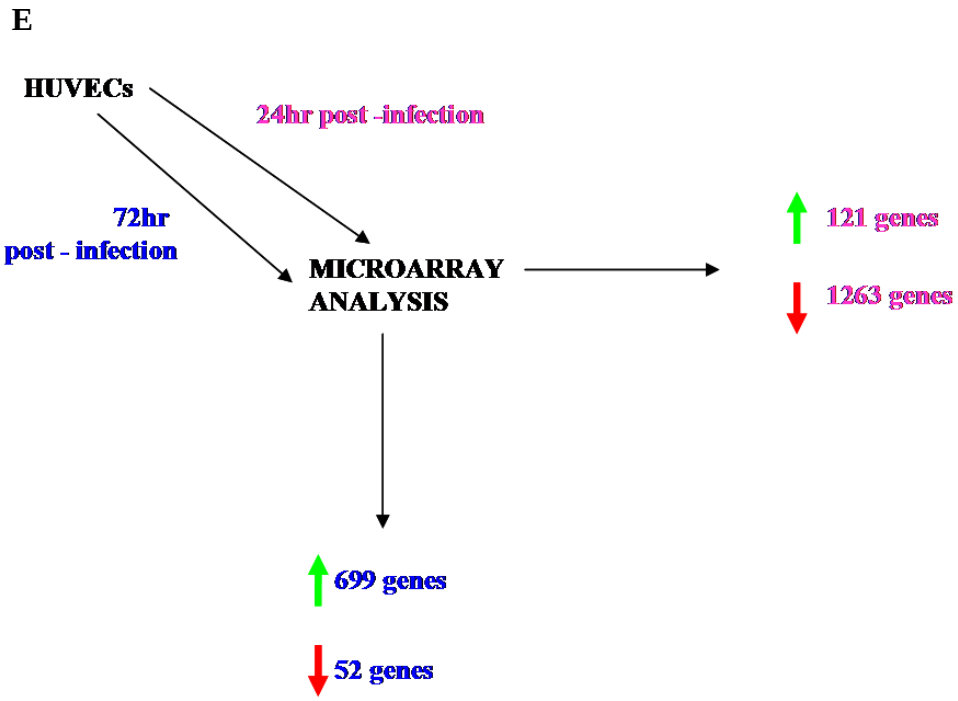

Figure 18: Overexpression of XBP1u influences the expression of genes involved in proliferation, death and cardiovascular disease.

Overexpression of XBP1u for 24 (**A** and **B**) and 48 (**C** and **D**) hours resulted in increased (**A** and **C**) and decreased (**B** and **D)** expression of genes responsible for specific cellular functions. Statistical analysis is calculated using a right-tailed Fishers exact test. The threshold demonstrates the point above which the likelihood of XBP1u influencing these processes is significant. **E.** Schematic diagram depicting the upregulation and downregulation of genes by XBP1u overexpression after 24 and 72 hours.

Potential candidate genes for regulation by XBP1u were identified via three mechanisms. Firstly, the Ingenuity programme was used to determine the cellular processes, such as proliferation, metabolism, transport, etc. most influenced by XBP1u (figure 18). Overexpression of XBP1u significantly influenced the expression of genes involved in cell growth and proliferation, cell death, cardiovascular system development and function and cell function and maintenance (figure 18A, 18C). This result supports our previous data linking XBP1u to EC proliferation and survival. Secondly, we identified the genes that were consistently regulated at both 24 and 72 hours of exogenous XBP1u overexpression. Thirdly, a manual analysis of the remaining genes identified several candidates for further study (table 3).

Table 3: Candidate target genes for regulation by XBP1u.

Gene	Function
Haem oxygenase 1 (HO-1)	The products of haem oxygenase; CO, biliverdin and iron(II) have been extensively characterised (Ryter et al., 2007). HO-1 was also demonstrated to be a potential therapeutic target for atherosclerosis.
Activating transcription factor 3 (ATF3)	ATF3 can be induced by NO in response to stress and represses p53 to protect against TNF-mediated apoptosis (Kawauchi et al., 2002).
Adrenomedullin 2 (ADM2)	ADM2 protects cells against hydrogen peroxide-induced damage through induction of cAMP and NO production (Chen et al., 2006).
Peroxisome proliferator activated receptor γ (PPAR γ)	PPARγ agonists were demonstrated to prevent atherosclerosis through a reduction in inflammation; however the role of PPARγ is controversial as clinical trials with agonists were not successful.
Calcitonin receptor-like receptor (CRLR)	CRLR acts as a receptor for ADM2 and therefore mediates the signalling pathway involved in cAMP and NO production.

One of the key candidate genes induced by XBP1u was haem oxygenase 1 (HO-1). HO-1 is an extensively studied antioxidant molecule and was therefore of further interest to us. Of the remaining candidate genes only ATF3 was selected for further study due to its induction by stress and ability to protect HUVECs against apoptosis (Kawauchi et al., 2002).

3.2.2 Confirmation of XBP1u candidate genes

To further confirm the microarray data the regulation of HO-1, ATF3, PPARγ, CRLR, COX-1, COX-2 and p53 gene expression by XBP1u was confirmed by real-time PCR and Western (figure 19). Overexpression of XBP1u for 24 hours caused a 5-fold increase in the level of HO-1 mRNA when compared to Ad-Null infected control cells. The overexpression of XBP1u also caused a significant 2-fold increase in ATF3 and COX-1 expression at the mRNA level. Western blotting confirmed that overexpression of XBP1u enhances the expression of HO-1, ATF3 and PPARγ. HO-1 and ATF3 have been linked to cell survival and therefore they were selected for further study (Kawauchi et al., 2002; Ryter et al., 2006).

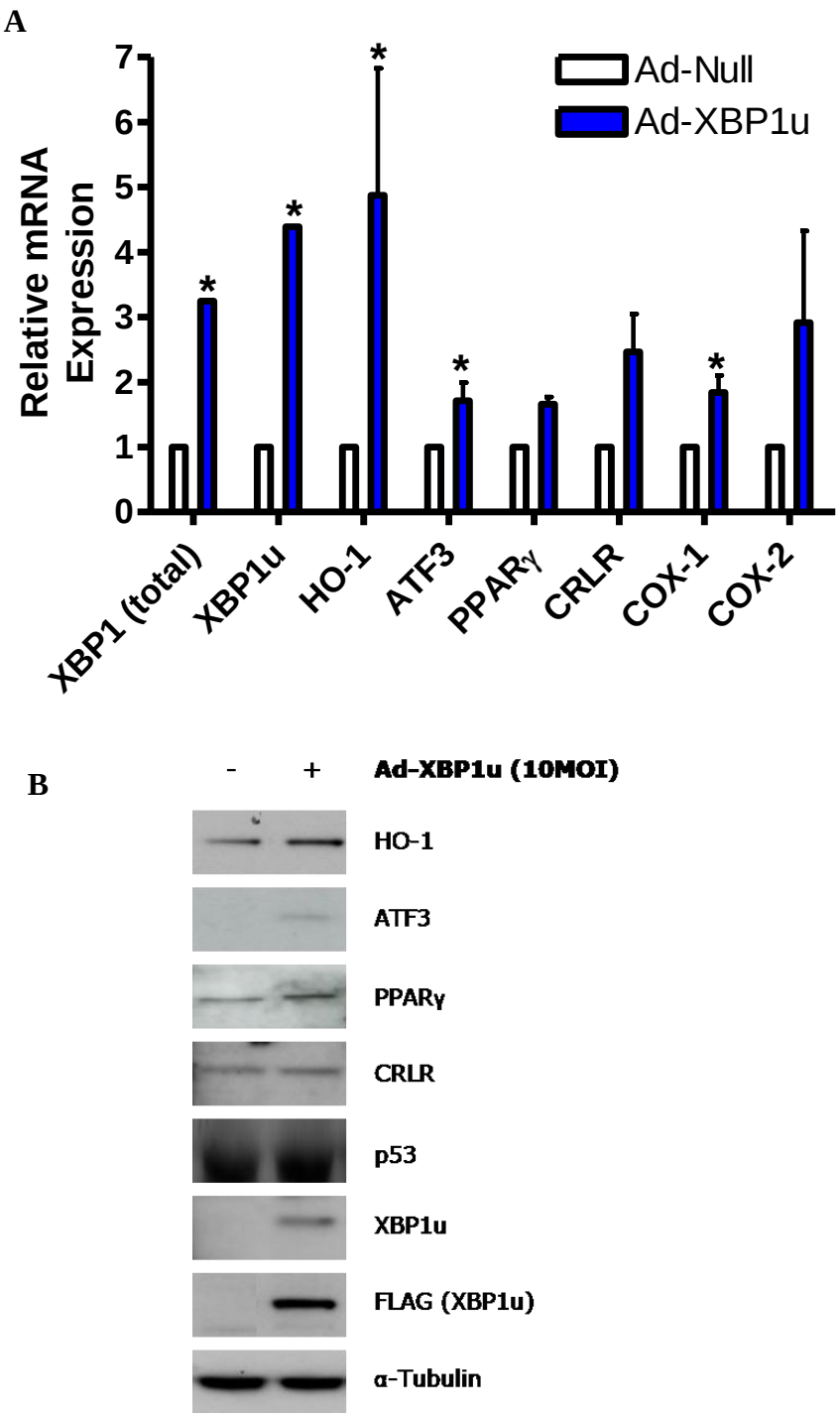

Figure 19: Overexpression of XBP1u enhances the expression of HO-1, ATF3, PPARγ, CRLR, COX-1 and COX-2.

HUVECs were transduced with 10 MOI Ad-Null or Ad-XBP1u adenoviral vectors. The (**A**) mRNA and (**B**) protein was harvested 24 hours post-transduction and the relative expression of XBP1 (total), XBP1u, HO-1, ATF3, PPARγ, CRLR, COX-1, COX-2 and p53 was determined by real-time PCR and Western blotting respectively. The histogram depicts the average and standard deviation from three independent experiments. * $P < 0.05$.

3.2.3 ATF3 is regulated by disturbed flow, however XBP1u is not crucial for its expression

Activating transcription factor 3 (ATF3) is a member of the ATF/cyclic AMP response element-binding (ATF/CREB) family of transcription factors. ATF3 has been shown to bind to other members of the bZIP transcription family, of which XBP1 is a member. However, binding of ATF3 to XBP1 has not yet been detected. ATF3 is suggested to regulate the delicate balance between proliferative and apoptotic signals that contribute to cell survival. This effect is cell type and context specific as overexpression of ATF3 has also been shown to protect cells from apoptosis and enhance cellular apoptosis (Yin et al., 2008). Specifically, overexpression of ATF3 in HUVECs has been demonstrated to protect against TNFα-mediated apoptosis at least partially through transcriptional regulation of p53 expression (Kawauchi et al., 2002). We hypothesised that XBP1u and ATF3 could interact and promote EC survival. To determine if ATF3 is regulated by disturbed flow in a manner similar to XBP1u, HUVECs were subjected to static or disturbed flow for 0.5, 2, 4 and 24 hours and the expression of ATF3 was determined by Western blotting (figure 20A-B). There is a non-significant trend towards increased ATF3 expression during disturbed flow.

To determine if the expression of ATF3 requires XBP1u, XBP1u was knocked down through the addition of shRNA-XBP1 and the expression of ATF3 was detected by Western blotting. (figure 20C). Lentiviral-mediated knockdown of XBP1u for 72 hours did not result in any significant changes to ATF3 mRNA expression. These data demonstrate that the expression of ATF3 is linked to XBP1u and may be linked to disturbed flow. Further study into the interaction between XBP1u and ATF3 could reveal a novel method through which ECs activate survival pathways.

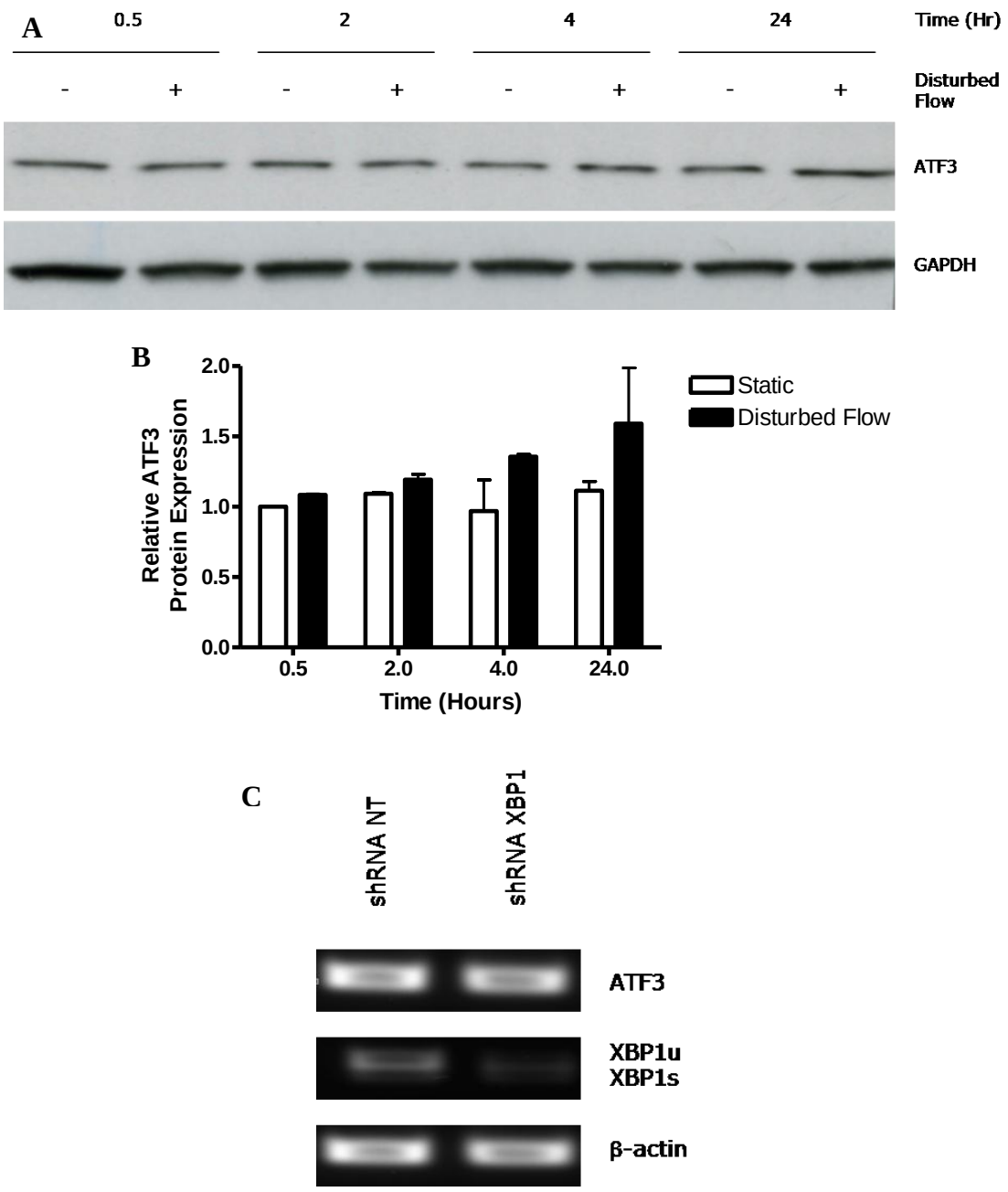

Figure 20: Disturbed flow and knockdown of XBP1 do not significantly impact ATF3 expression. **A.** and **B.** HUVECs were subjected to static or disturbed flow stress for 0.5, 2, 4 and 24 hours. **A.** The protein was harvested and the expression of ATF3 was determined by Western blotting. **B.** Histogram depicting densitometry of ATF3 protein expression during disturbed flow**.** Relative ATF3 expression is calculated in relation to the 0.5 hour static sample and the densitometry is normalised against the expression of GAPDH. The image is representative and the histogram depicts averages and standard deviation of three experiments. **C.** HUVECs were transduced with 100 TU/cell of shRNA-NT or shRNA-XBP1 lentiviral particles. The mRNA was harvested 72 hours post-transduction and the expression of ATF3 was assessed by semi-quantitative PCR. The data is representative of three independent experiments.

3.2.4 Overexpression of XBP1u enhances HO-1 expression

HO-1 has been widely reported to mediate antioxidant and anti-apoptotic responses in diverse cell types. HO-1 has also been shown to protect against hypoxia-induced oxidative stress *in vivo* (Ryter et al., 2006). The products of HO-1 mediated degradation of haem include: biliverdin and bilirubin, which scavenge free ROS; Fe^{2+}, which acts as a cofactor to induce transcription of several anti-apoptotic proteins through NF-κβ; and CO, which inhibits pro-inflammatory cytokine activation (Ryter et al., 2007).

Our microarray data demonstrated that XBP1u upregulates HO-1 mRNA expression. To confirm this, exogenous XBP1u was overexpressed by adenoviral gene transfer. The mRNA and protein level of HO-1 was determined 24, 48 and 72 hours after transduction by semi-quantitative PCR, real-time PCR and Western blotting (figure 21A-B and 22A-B). Overexpression of XBP1u resulted in a 4-fold increase in HO-1 mRNA expression after 24 hours and a 3-fold increase after 48 hours when compared to the Ad-Null transduced control samples. This was result was replicated at the protein level.

XBP1u was also overexpressed in a dose-dependent manner and the expression of HO-1 at the mRNA and protein level was determined after 24 hours (figure 21C-D and figure 22C-D). The overexpression of XBP1u results in a step-wise increase in HO-1 at the mRNA and the protein level. Overexpression of XBP1u resulted in a 4-fold increase in HO-1 mRNA expression. The effect of XBP1u was even more dramatic at the protein level. Overexpression of XBP1u resulted in a 10-fold increase in HO-1 protein levels. These data confirm that XBP1u regulates the expression of XBP1u at both the mRNA and protein level. Furthermore, these experiments demonstrate the reciprocal regulation of XBP1s expression by XBP1u. It was previously reported that XBP1u binds to XBP1s and targets it for proteosome-mediated degradation (Yoshida et al., 2006). Overexpression of exogenous XBP1u promotes the degradation of the XBP1s isoform (figure 21D). At the highest level of XBP1u expression, the XBP1s isoform can no longer be detected.

A

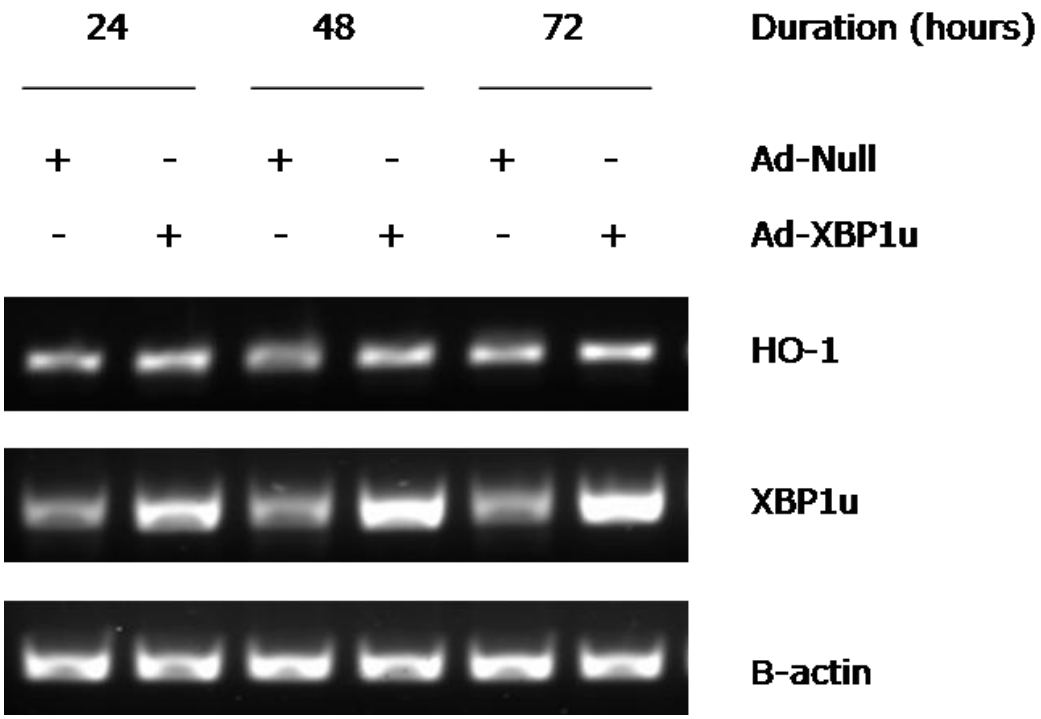
24
48
72
Duration (hours)
+ - + - + -
Ad-Null
- + - + - +
Ad-XBP1u
HO-1
XBP1u
B-actin

B

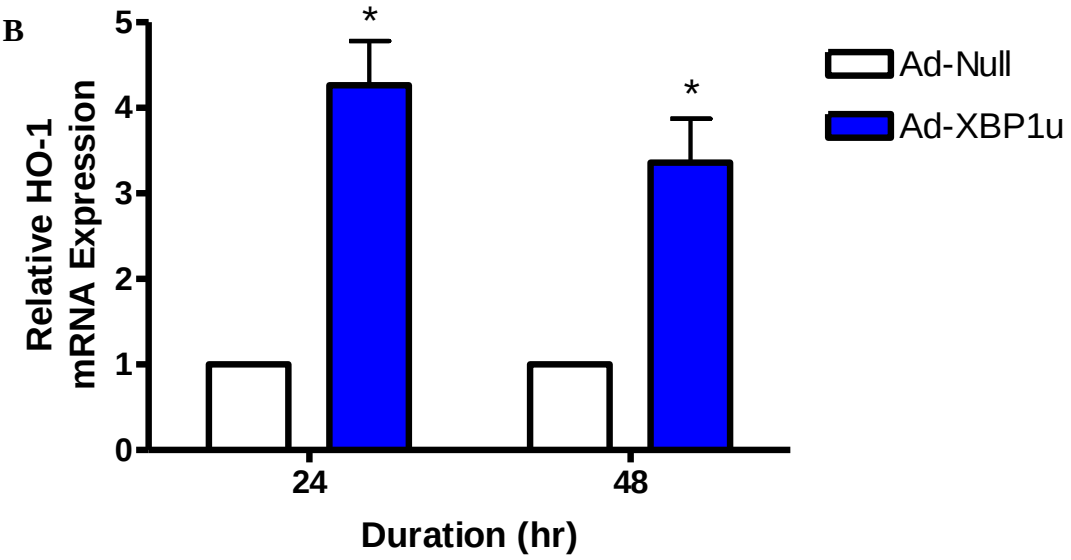
Relative HO-1 mRNA Expression
0
1
2
3
4
5
*
*
24
48
Duration (hr)
Ad-Null
Ad-XBP1u

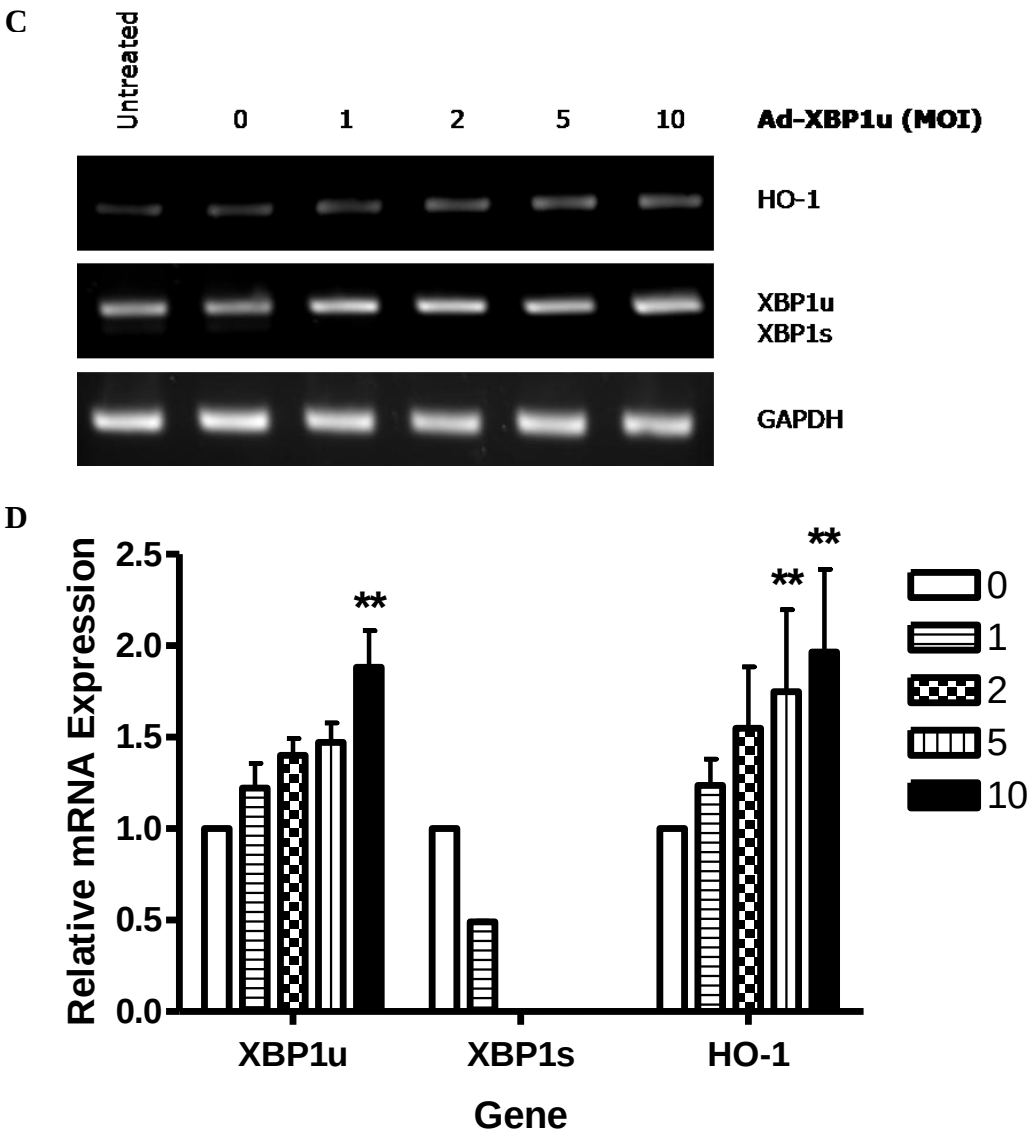

Figure 21: Overexpression of XBP1u increases HO-1 at the mRNA level.

A. and **B.** HUVECs were transduced with 10 MOI of Ad-Null or Ad-XBP1u adenoviruses. The mRNA was harvested 24, 48 and 72 hours after transduction. The effect of exogenous XBP1u overexpression on HO-1 mRNA levels was determined by (**A**) semi-quantitative PCR and (**B**) real-time PCR. **C.** and **D.** HUVECs were transduced with 0, 1, 2, 5 and 10 MOI of Ad-XBP1u adenoviruses with Ad-Null used to control for infectious particle concentration. The mRNA was harvested 24 hours after transduction. **C.** The effect of exogenous overexpression of XBP1u on HO-1 at the mRNA level was determined by semi-quantitative PCR. **D.** Densitometry analysis was performed on the semi-quantitative PCR images to assess the expression changes in XBP1u, XBP1s and HO-1 mRNA levels as compared to Ad-Null infected control cells. The images are representative and the histograms depict mean and standard deviation of three independent experiments. * $P < 0.01$., ** $P < 0.05$.

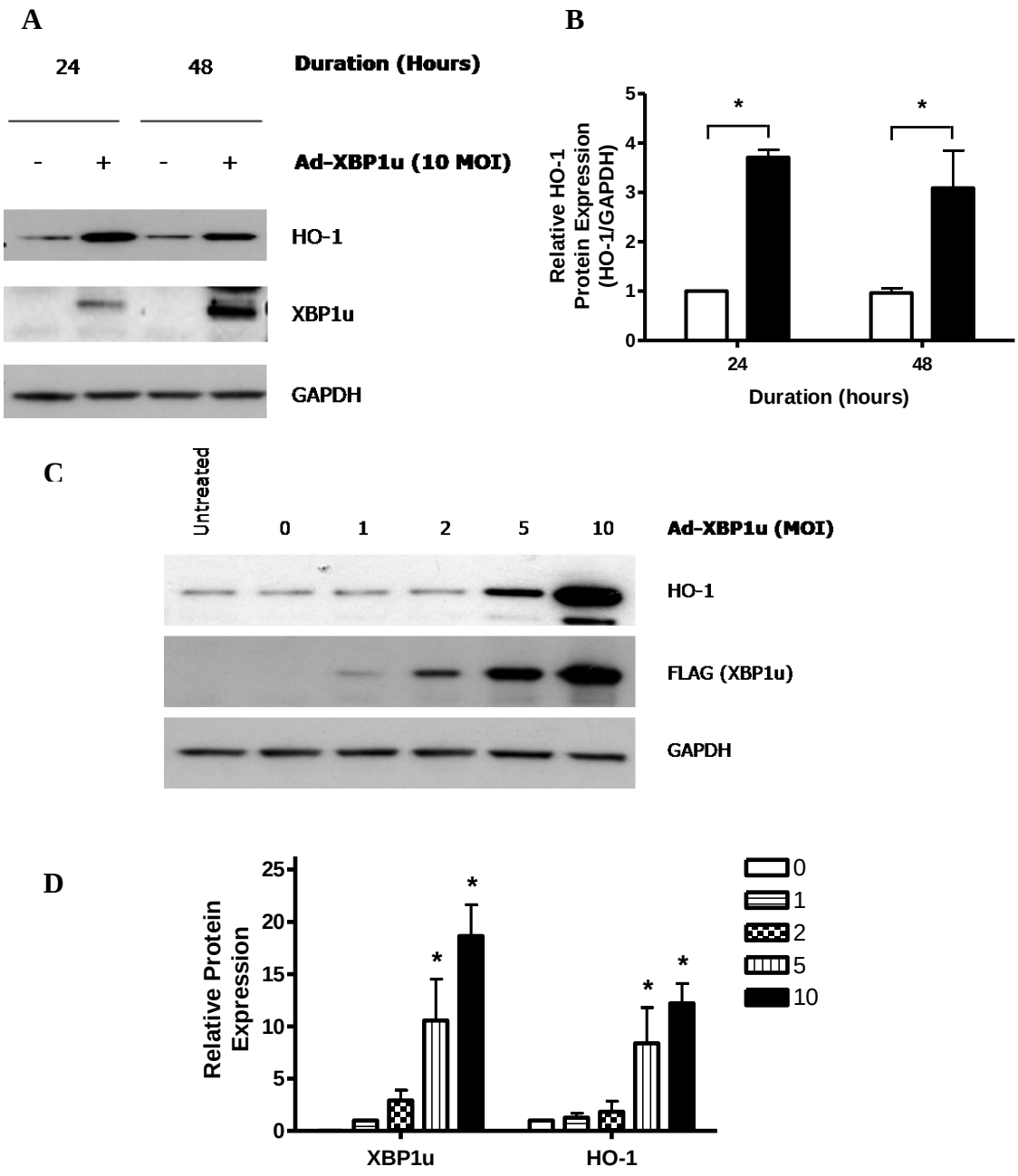

Figure 22: Overexpression of XBP1u increases HO-1 expression at the protein level.

A. HUVECs were transduced with 10 MOI of Ad-Null or Ad-XBP1u adenovirus. The protein was harvested 24, 48 and 72 hours post-transduction and the level of HO-1 was determined by Western blotting. **B.** Densitometry was performed to assess changes in HO-1 protein levels. The expression changes in HO-1 are calculated against the HO-1 expression level in Ad-null transduced cells. **C.** HUVECs were transduced with 0, 1, 2, 5 and 10 MOI of Ad-XBP1u adenoviruses with Ad-Null supplemented to ensure the quantity of infectious particles remained constant. The protein was harvested 24 hours post-transduction and the expression of HO-1 was determined by Western blotting. **D.** Densitometry was performed to assess changes in HO-1 protein levels. The expression changes in HO-1 are calculated against the HO-1 expression level in Ad-null transduced cells. The images are representative of three independent experiments. * $P < 0.01$.

3.2.5 XBP1u regulates HO-1 expression independently of UPR activation

XBP1s is a known activator of the unfolded protein response (UPR) in cells (Yoshida, 2007; Yoshida et al., 2001). CHOP and BiP are both upregulated by XBP1s and are used to demonstrate if UPR signalling is active. The expression of XBP1u has only recently been demonstrated to promote protein expression, previously only XBP1s had been identified as an active transcription factor (Liu et al., 2009). In order to determine if XBP1u activates the expression of HO-1 independently of XBP1s and UPR activation we overexpressed exogenous XBP1s in HUVECs (figure 23). The overexpression of XBP1s did not increase HO-1 expression at the mRNA level (figure 23A). Secondly, exogenous XBP1u and XBP1s were overexpressed in HUVECs and the mRNA level of CHOP, BiP and HO-1 was determined by real-time PCR (figure 23B). Only overexpression of XBP1s was sufficient to drive the upregulation of CHOP and BiP, which were upregulated by 5-fold and 8-fold, respectively. XBP1u had no effect on CHOP and BiP expression. In contrast, exogenous overexpression of XBP1s could not drive the induction of HO-1 expression. The expression of HO-1 was solely induced by XBP1u. This data indicates that XBP1u drives the expression of HO-1 independently to the production of XBP1s. Furthermore, the upregulation of HO-1 expression occurs independently of UPR activation. Through the tandem overexpression of XBP1u and XBP1s we have demonstrated that only the XBP1u isoform is able to activate the expression of HO-1. This implies that XBP1u functions as an activator of transcription distinctly to the role of XBP1s in promoting transcription.

3.2.6 XBP1 is required for the expression of HO-1

We have demonstrated that XBP1u is sufficient to induce the expression of HO-1. However, is XBP1u also necessary for basal HO-1 expression? HUVECs were transduced with 100 TU / cell of shRNA-NT and shRNA-XBP1 lentiviruses for 72 hours. The mRNA and protein were harvested and the expression of HO-1 was detected by semi-quantitative RT-PCR (figure 24A) real-time PCR (figure 24C) and Western blotting (figure 24B). Knockdown of XBP1 resulted in significantly

abrogated HO-1 expression at the mRNA and protein level as detected by both semi-quantitative and real-time PCR. Indeed, knockdown of XBP1 resulted in a 40% reduction in basal HO-1 mRNA levels in comparison with shRNA-NT transduced control cells. Knockdown of XBP1 had an even more significant impact on the protein level of HO-1 as it resulted in a 5-fold reduction in HO-1 protein. This data indicates that XBP1 is required for the basal expression of HO-1 at both the mRNA and protein level.

Overexpression of exogenous XBP1s results in reduced detection of XBP1u at the mRNA level. Exogenous overexpression of XBP1s results in the activation of the ER stress response and increased activity of the IRE-1α endoribonuclease (Back et al., 2005). IRE-1α endoribonuclease activity cleaves XBP1u pre-mRNA resulting in XBP1s pre-mRNA (Lee et al., 2002). Therefore, the detection of the XBP1u pre-mRNA is reduced alongside the expression of the XBP1u protein.

A

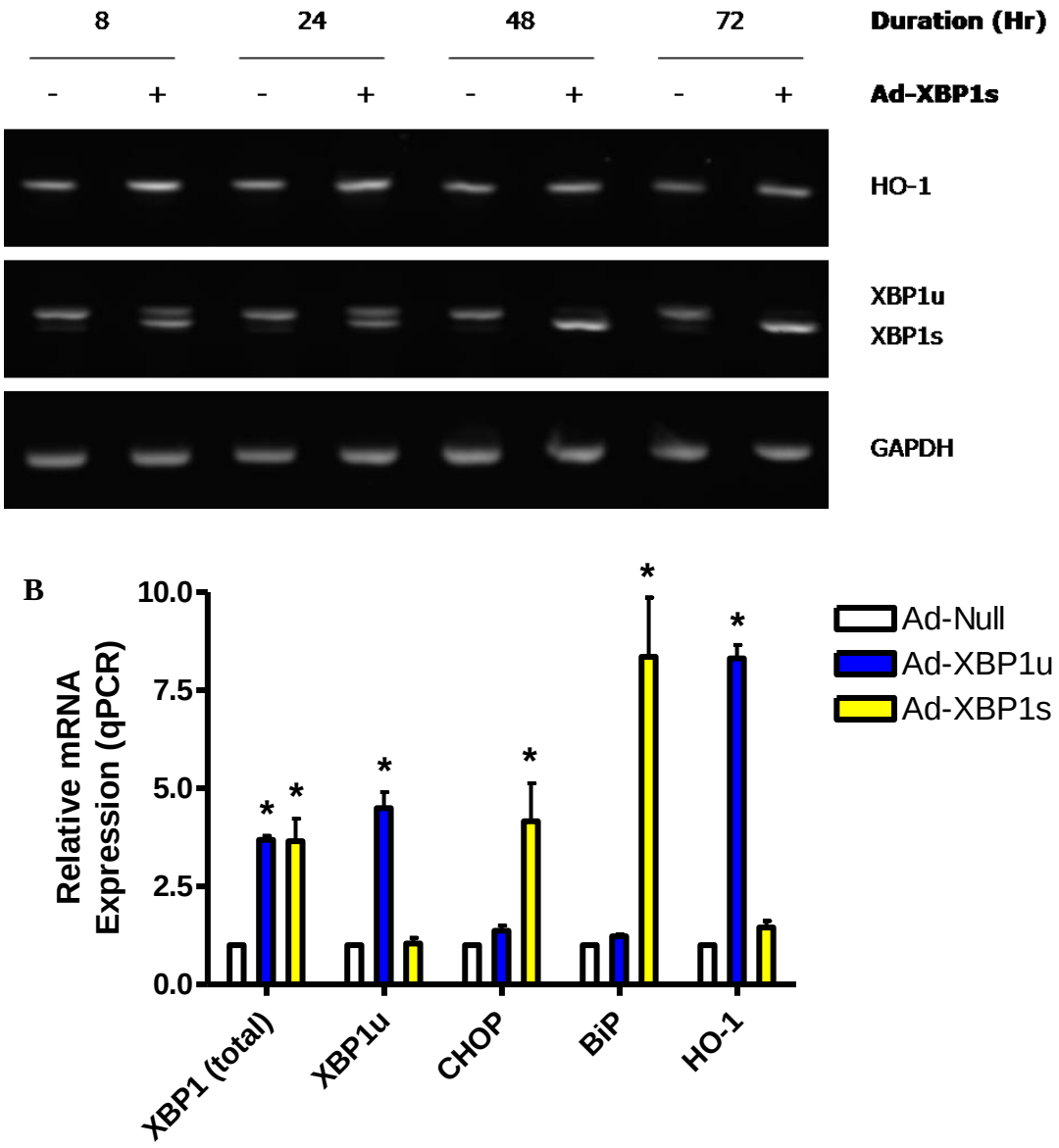

Figure 23: XBP1u increases the expression of HO-1 independently to UPR activation.

A. HUVECs were transduced with 10 MOI of Ad-Null or Ad-XBP1s adenovirus. The mRNA was harvested 8, 24, 48 and 72 hours after transduction. The mRNA level of HO-1 was determined by semi-quantitative PCR. The images are representative of three independent experiments. **B.** HUVECs were transduced with 10 MOI of Ad-Null, Ad-XBP1u or Ad-XBP1s adenoviruses. The mRNA from the HUVECs was harvested 24 hours post-transduction. The expression of XBP1 (total), XBP1u, CHOP, BiP and HO-1 was assessed by real time PCR. The histogram depicts the mean and standard deviation of three independent experiments. * $P < 0.01$.

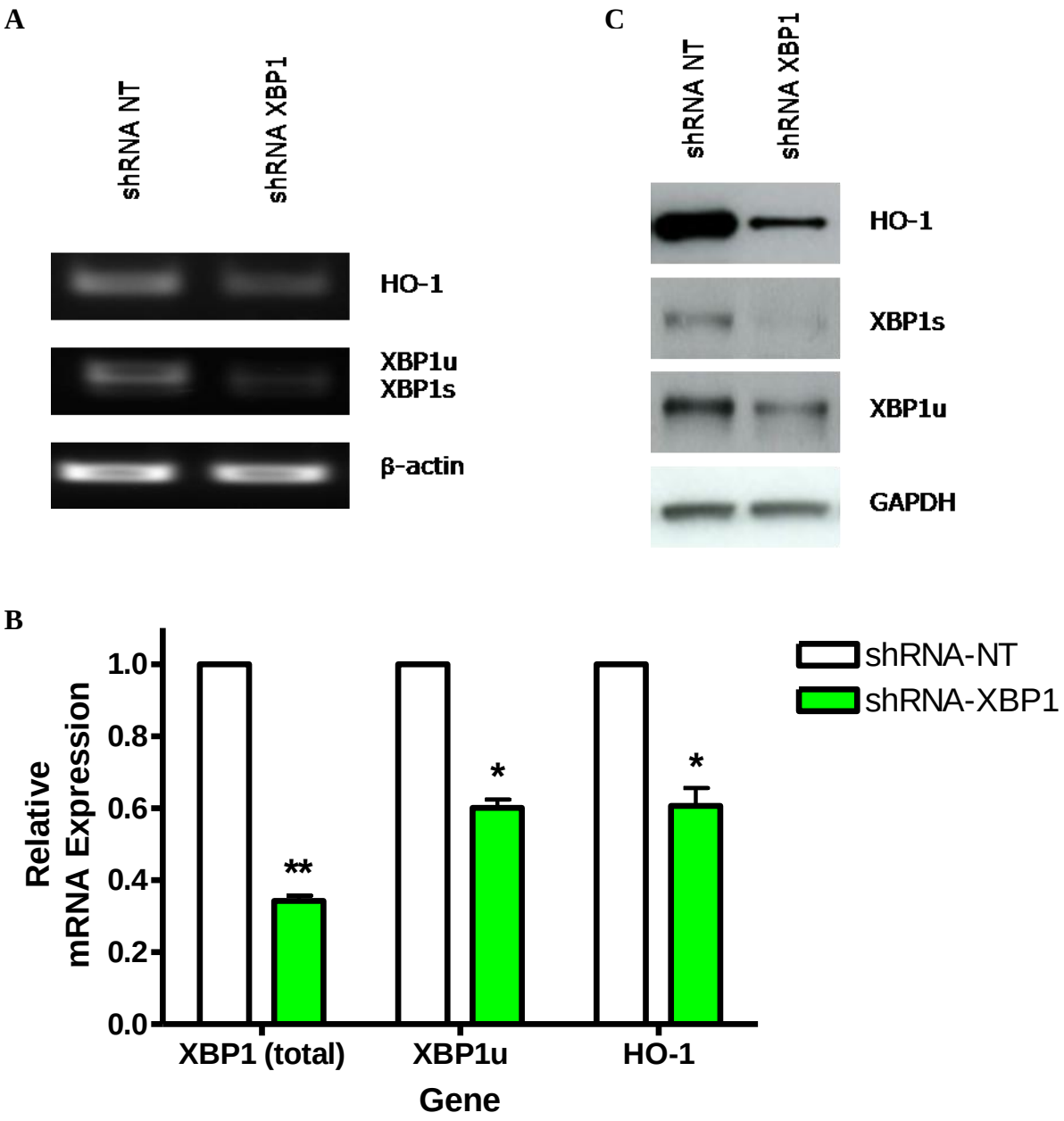

Figure 24: Knockdown of XBP1 reduces basal HO-1 expression.

HUVECs were transduced with 100 TU / cell of shRNA-NT and shRNA-XBP1 lentivirus. The mRNA and protein was harvested 72 hours post-transduction. The expression of HO-1 was determined by (**A**) semi-quantitative PCR, (**B**) real-time PCR and (**C**) Western blotting. The relative mRNA expression changes in total XBP1, XBP1u and HO-1 were calculated between shRNA-NT and shRNA-XBP1 infected HUVECs. The histogram depicts mean and standard deviation of five independent experiments. * $P < 0.05$, ** $P < 0.001$.

3.2.7 HO-1 levels are normal in XBP1-null ECs

We have demonstrated that XBP1u is both sufficient and necessary for the expression of HO-1 in HUVECs. To determine if HO-1 levels are reduced in XBP1-null ECs *in vivo*, we developed a conditional knockout XBP1 mouse, where the expression of XBP1 is abolished in cells expressing the Tie2 protein. Generation of these mice required the crossbreeding of mice containing *loxP* sites (floxed mice) in the XBP1 gene with mice containing a *Tie2-Cre* recombinase insert. Therefore, in *Tie2-Cre / XBP1$^{f/f}$* mice Cre recombinase will be expressed in cells that express Tie2 and result in abrogated XBP1 expression. The generation of these mice was performed externally and the genotyping has been demonstrated in figure 11. These mice have been characterised by Dr. Lingfang Zeng. He has demonstrated that there are no physiological differences between the wild type and *Tie2-Cre / XBP1$^{f/f}$* mice (data not shown). Data on the characterised mice will be published in Margariti, A. *et al. 2013* and Zeng, L. *et al.* 2013.

Aorta sections were harvested from 10 week old wild type and *Tie2-Cre / XBP1$^{f/f}$* mice, fixed and then double-immunostained for HO-1 and CD31. The sections were then analysed by fluorescence microscopy (Figure 25). Merged images are shown as the individual images are not available. CD31 was detected at the cell membranes, whilst HO-1 was present at the cell membranes and within the cytoplasm. We observed no significant differences in the expression of HO-1 between wild type and *Tie2-Cre / XBP1$^{f/f}$* mice. This data demonstrates that XBP1 is not necessary for the basal expression of HO-1 *in vivo*. It is possible that other signalling pathways can compensate for the lack of XBP1. When we knockdown XBP1 the effect is instantaneous and the cells do not have time to compensate. In the conditional knockout animal the cells have several weeks to adapt and activate several compensatory pathways that replicate Akt phosphorylation. This would explain the discrepancy between the *in vitro* and *in vivo* results.

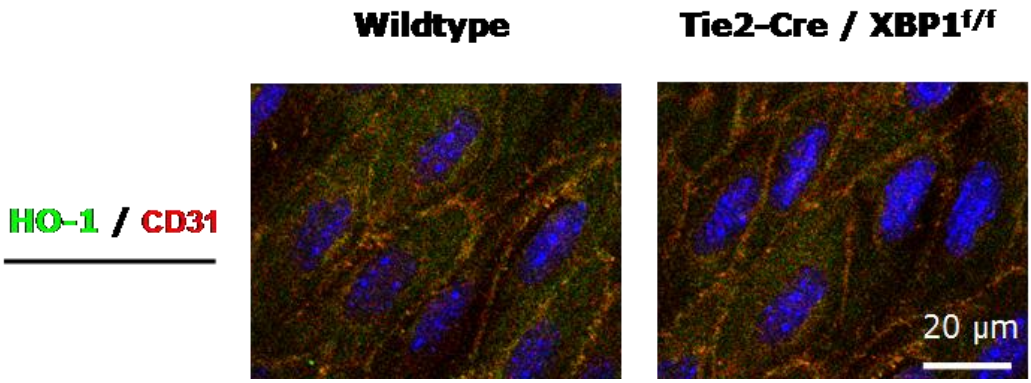

Figure 25: HO-1 levels are normal in XBP1-null cells.
Aorta sections from wild type and *Tie2-Cre / XBP1$^{f/f}$* mice were harvested for *en face* immunostaining. ECs were double-immunostained with HO-1 and CD31 antibodies and then stained with DAPI to identify the nuclei. Scale bar = 20 µm. These images are representative of independent experiments performed on three aortic segments taken from three separate mice for each of genotype.

3.2.8 Overexpression of XBP1u does not enhance the activity of the HO-1 or the ARE promoter

Unspliced XBP1 drives the expression of HO-1 at both the mRNA and the protein level. We hypothesised that XBP1u could directly regulate the expression of HO-1 through binding to its promoter and activating gene transcription through the recruitment of the polymerase complex. The activation of HO-1 transcription is driven by a large variety of transcription factors and co-activator elements. PPARα, PPARγ and the co-activator RXR bind and activate transcription from a region 1.8kb upstream of the HO-1 transcription start site (Kronke et al., 2007). Enhancer elements have also been detected in the internal region of the HO-1 gene (Hill-Kapturczak et al., 2003). The majority of the identified activation sites are present within 4kb of the transcription start site.

To study the activation of HO-1 gene expression by XBP1u the 1kb and 4kb upstream promoter regions of HO-1 were cloned into a PGL3-luciferase plasmid. The cloned regions were sequenced externally and compared to the UCSC genome browser for sequence verification. HUVECs were transfected with the HO-1 promoter reporter plasmids and the relative luciferase activity was used to assess

activation of the HO-1 promoter after exogenous overexpression of XBP1u (figure 26B). The expression of XBP1u was demonstrated by semi-quantitative PCR (figure 26A). However, the activation of the HO-1 promoter by Akt activation or shear stress was not demonstrated. These experiments would have strengthened the conclusions that can be drawn from this data. In this study we demonstrate that overexpression of XBP1u could not activate the transcription of HO-1 through the 1kb upstream promoter region. Overexpression of XBP1u slightly increased the activity and therefore the expression driven by the 4kb HO-1 promoter; however this result was not significant. This data suggests that XBP1u either does not directly regulate HO-1 expression, or that the XBP1u binding site is further upstream or is present in the internal gene structure, or that the confirmation of the DNA has altered through the cloning processes and prevented XBP1u binding. Further experiments to confirm that the cloned transcription site is functional would enhance the robustness of this data.

Nrf2 is a key-regulator of HO-1 expression and binds directly to antioxidant response elements (AREs) in conjunction with several bZIP activators. We hypothesised that XBP1u and Nrf2 may interact to activate transcription through binding to AREs. The ARE promoter region was kindly provided by Professor Jozef Dulak and its function has previously been demonstrated (Loboda et al., 2009). Overexpression of XBP1u in conjunction with cells transfected with an ARE-containing luciferase reporter plasmid demonstrated no activation by XBP1u (figure 26B). These data imply that XBP1u does not directly bind to the HO-1 promoter or AREs. However, it remains unknown if XBP1u interacts with other regions of the HO-1 gene.

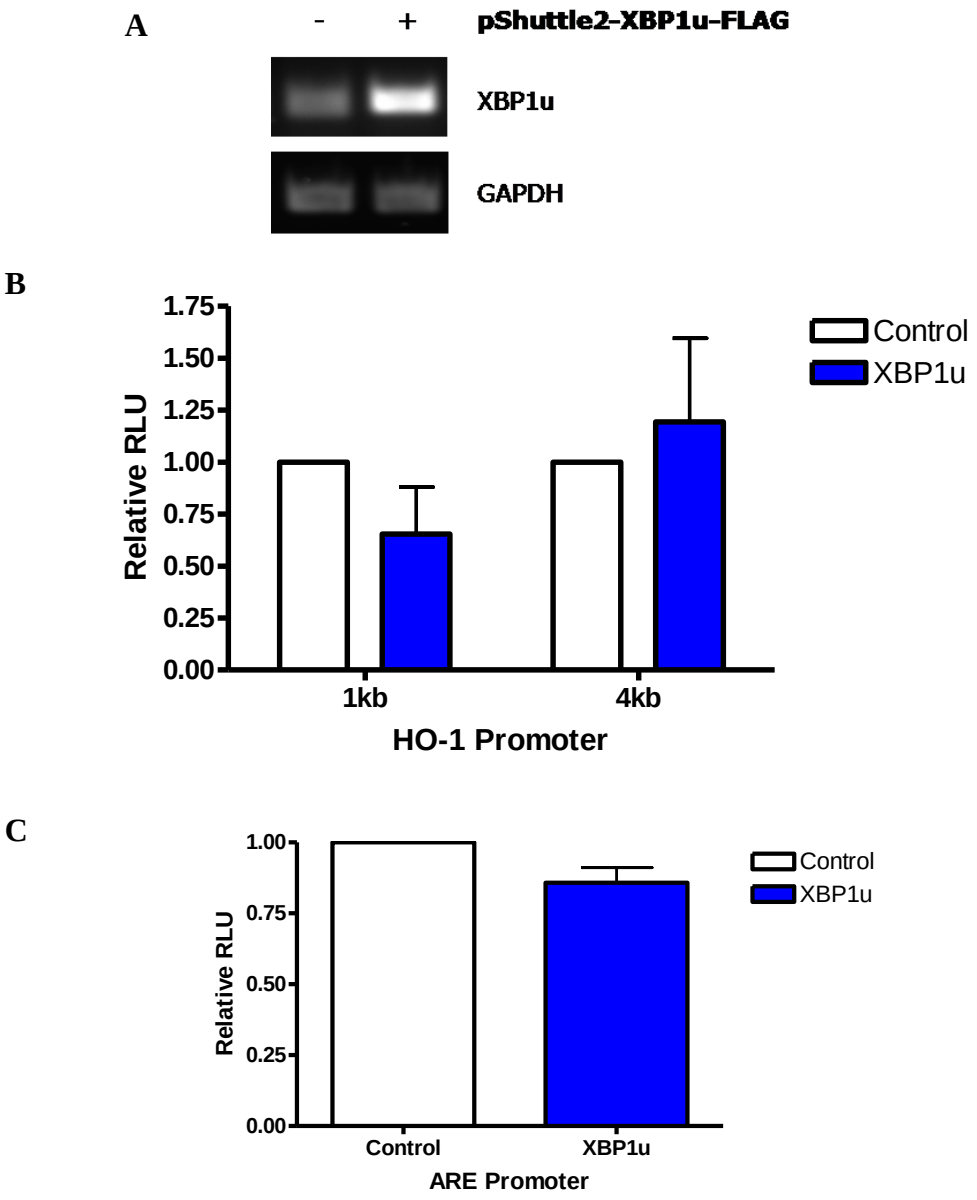

Figure 26: Overexpression of XBP1u and XBP1s does not influence the activity from the HO-1 or ARE Promoter.

A. Overexpression of XBP1u was demonstrated by semi-quantitative PCR. **B.** HUVECs were transfected with PGL3-HO1-1kb or PGL3-HO1-4kb plasmids alongside pShuttle2-Control or pShuttle2-XBP1u plasmids. PGL3-Renilla was used as a control for transfection efficiency. The RLU for each sample was assessed and normalised to renilla activation. The RLU detected was then normalised to the empty vector control for each promoter construct. The histogram depicts mean and standard deviation of three independent experiments. **C.** HUVECs were transfected with PGL3-ARE alongside pShuttle2-Control or pShuttle2-XBP1u plasmids. PGL3-Renilla was used as a control for transfection efficiency. The RLU for each sample was assessed and normalised to the renilla activation to control for transfection efficiency. The RLU detected was then normalised to the empty vector control for each promoter construct. The histogram depicts mean and standard deviation of three independent experiments.

3.2.9 Disturbed flow upregulates HO-1

We have demonstrated that XBP1u is upregulated under disturbed flow and leads to enhanced EC survival during oxidative stress. We hypothesised that XBP1u promotes EC survival through the upregulation of HO-1. HO-1 has previously been shown to be upregulated by shear stress; however we wished to confirm this under our conditions (Zeng et al., 2009). HUVECs were subjected to static or disturbed flow shear stress for 0, 1, 2, 4, 12 and 24 hours (Figure 27). The effect of disturbed flow on the expression of HO-1 at the mRNA level was determined by real-time PCR. HUVECs exposed to disturbed flow showed a trend towards increased HO-1 mRNA expression (figure 20A). Disturbed flow of 2, 4 and 24 hours resulted in significant upregulation of HO-1 at the protein level (figure 27B-C). These data indicate that disturbed flow increases the expression of HO-1 in comparison to static controls. The upregulation of HO-1 after 2 and 4 hours correlates with the observed increases in XBP1u expression during disturbed flow.

To determine if the induction of XBP1u and HO-1 by disturbed flow is dependent on *de novo* transcription or translation; HUVECs were treated with actinomycin D and cyclohexamide to inhibit transcription and translation, respectively (Figure 28). HUVECs were subjected to 8 hours of disturbed flow after pre-treatment with the inhibitors. The inhibition of transcription and translation completely abolished *de novo* production of XBP1u and HO-1 protein. Indeed the basal levels of these proteins were also abolished suggesting there is a fast turnover of protein production.

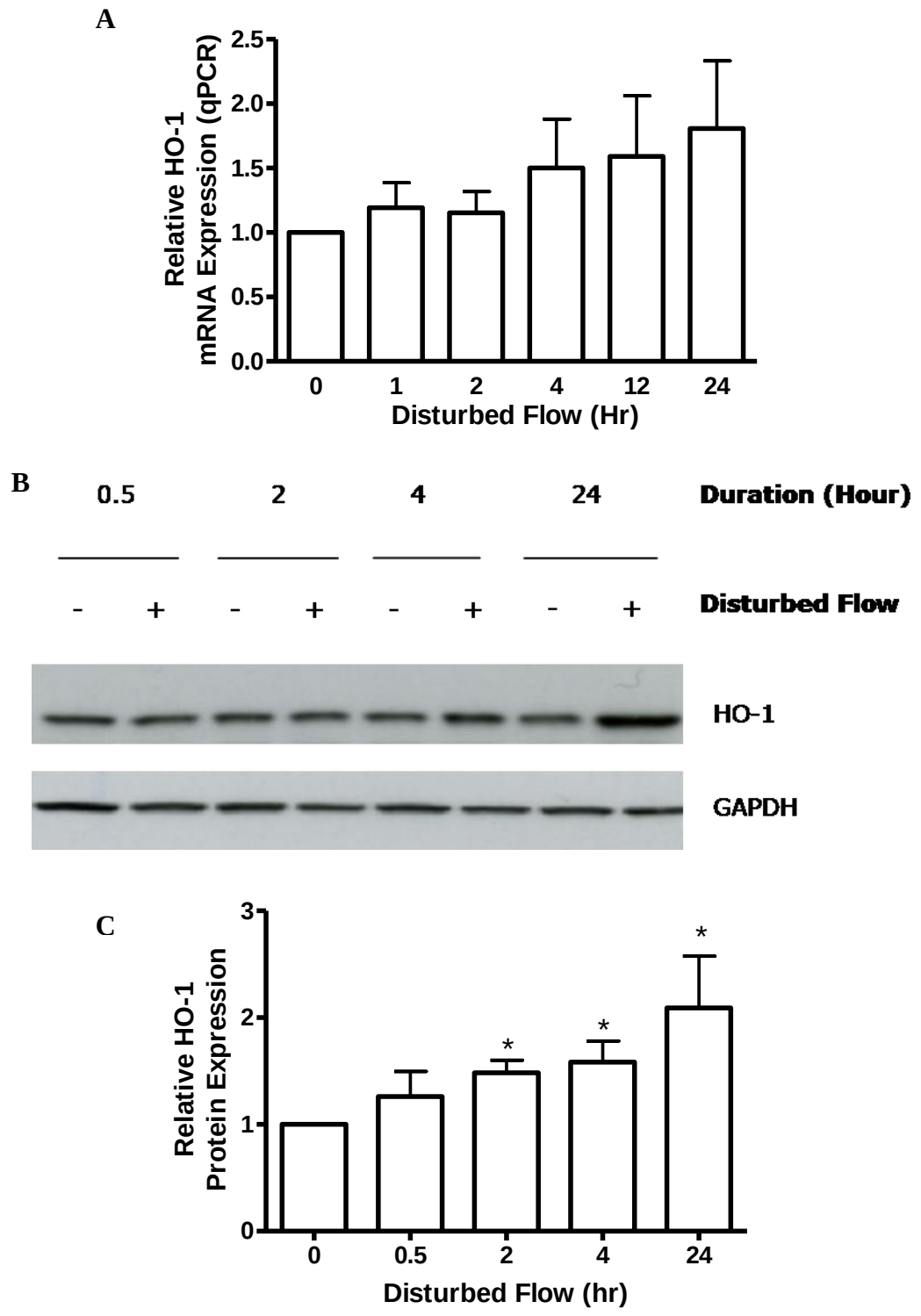

Figure 27: Disturbed flow upregulates HO-1.

HUVECs were subjected to static or disturbed flow for 0, 0.5, 2, 4 and 24 hours. **A.** The mRNA was harvested and the expression of HO-1 was determined by real-time PCR. **B.** The protein was harvested and the expression of HO-1 was determined by Western blotting. **C.** Histogram depicting densitometry of HO-1 protein expression after disturbed flow**.** The data is representative of and the histogram depicts averages and standard deviation of three independent experiments. * $P < 0.05$.

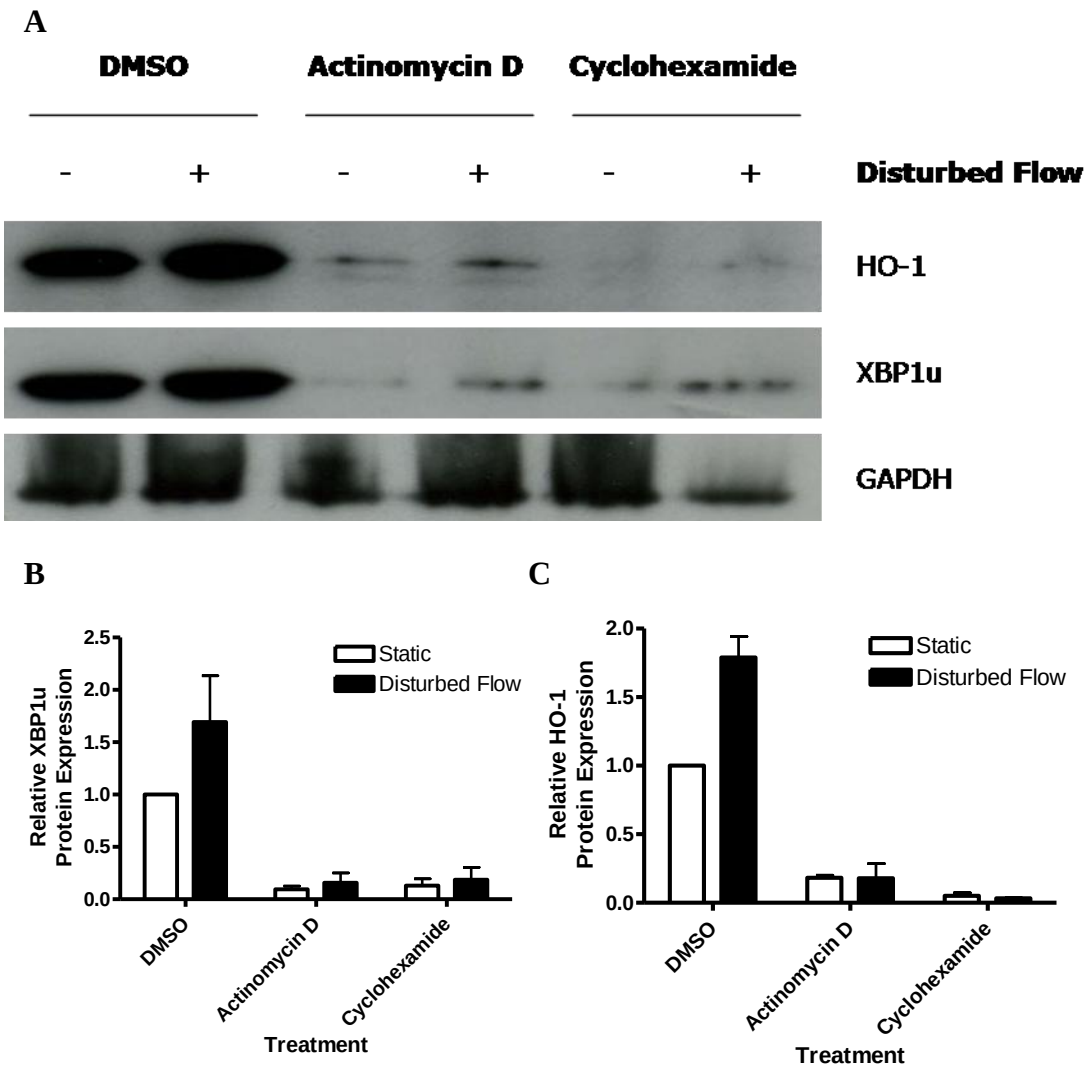

Figure 28: Disturbed flow-mediated upregulation of HO-1 and XBP1u is dependent on transcription and translation.

A. HUVECs were pre-treated with the relative inhibitors for 6 hours prior to their exposure to disturbed flow. HUVECs were subjected to static or disturbed flow for 8 hours. The protein was harvested and the expression of XBP1u and HO-1 was determined by Western blotting. The data is representative of three independent experiments. **B.** and **C.** Densitometry analysis of XBP1u and HO-1 expression after actinomycin D and cyclohexamide treatment.

3.2.10 Knockdown of XBP1 abolishes disturbed flow-induced upregulation of HO-1

We hypothesised that XBP1u is responsible for the induction of HO-1 by disturbed flow. The expression of XBP1 was knocked down in HUVECs via

transduction of shRNA-XBP1 particles using lentiviral vectors. The HUVECs were subjected to 8 hours of static or disturbed flow conditions. The protein was harvested and the expression of XBP1u, XBP1s and HO-1 was determined by Western blotting (figure 29). Knockdown of XBP1 completely abolished the induction of HO-1 by disturbed flow when compared to static controls. This data indicates that XBP1u is required for basal and disturbed flow-induced expression of HO-1 at the protein level.

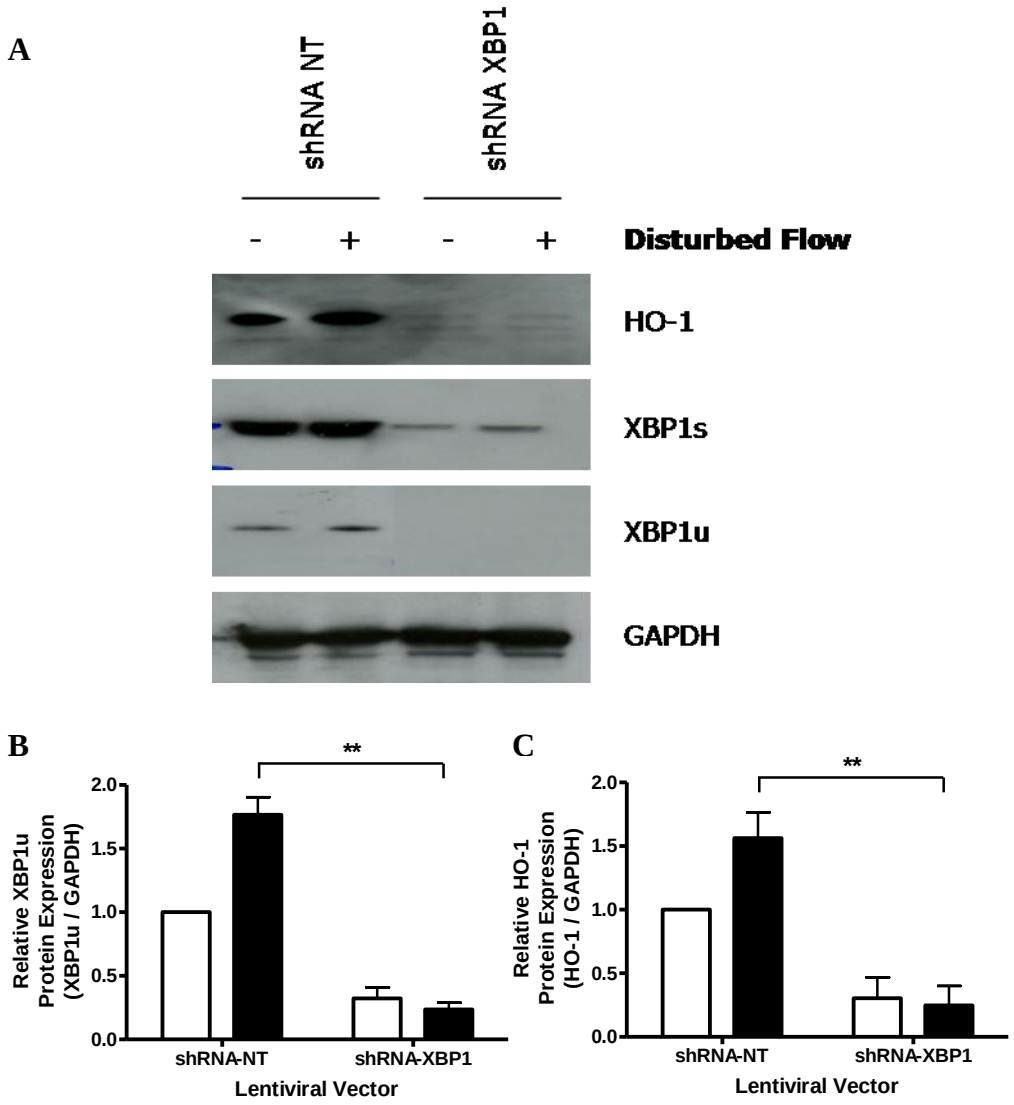

Figure 29: Knockdown of XBP1 abolishes disturbed flow-induced upregulation of HO-1.

A. HUVECs were transduced with 100 TU / cell of shRNA-NT and shRNA-XBP1 lentiviruses. HUVECs were then subjected to static or disturbed flow stress for 8 hours. The protein was harvested and the expression of HO-1 was assessed by Western blotting. The images are representative of three independent experiments. **B.** and **C.** Densitometry analysis of XBP1u and HO-1 expression after actinomycin D and cyclohexamide treatment. ** $P < 0.01$. White bars = static conditions, black bars = disturbed flow.

3.2.11 Inhibition of HO-1 ablates XBP1u-mediated protection of HUVEC apoptosis during oxidative stress

We have demonstrated that XBP1u promotes EC survival in response to oxidative stress and is crucial for the expression of HO-1. We hypothesised that XBP1u upregulates HO-1 and that this in turn increases the ability of ECs to mitigate oxidative stress. To determine if the regulation of HO-1 by XBP1 is crucial to its ability to promote EC survival, the activity of HO-1 was inhibited by a competitive inhibitor, tin protoporphyrin (SnPPIX). HUVECs were transduced with Ad-Null and Ad-XBP1u adenoviruses. The HUVECs were then pre-treated for 24 hours with 50μM SnPPIX before the application of 50μM hydrogen peroxide for 24 hours. The proliferation of the surviving ECs was then assessed by an MTS tetrazolium assay (Figure 30). Similarly to our previous experiments the overexpression of XBP1u promotes EC survival compared with Ad-Null treated cells. Additionally the overexpression of XBP1u protects ECs against apoptosis after hydrogen peroxide treatment as double the proliferation rate observed is double that of the control cells. Crucially, after the inhibition of HO-1 and hydrogen peroxide treatment of cells overexpressing exogenous XBP1u the survival rate of HUVECs is significantly reduced by 30%. This data demonstrates that inhibition of HO-1 prevents XBP1u-mediated promotion of HUVEC survival. The activation of HO-1 by XBP1u is therefore crucial in eliciting the protective effect of XBP1u.

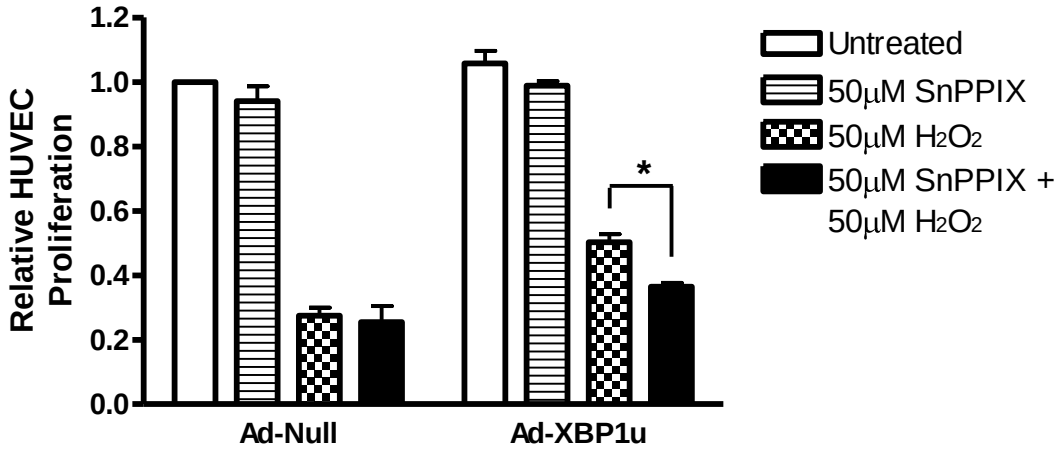

Figure 30: Inhibition of HO-1 abolishes XBP1u-mediated protection of HUVEC survival in response to oxidative stress.

HUVECs were transduced with 10 MOI Ad-Null or Ad-XBP1u adenoviral vectors. The HUVECs were subsequently treated with 50μM hydrogen peroxide for 24 hours, 48 hours after transduction. Prior to the application of hydrogen peroxide HUVECs were pre-treated with 50μM tin protoporphyrin (SnPPIX) for 24 hours. HUVEC proliferation was assessed using an MTS tetrazolium compound assay. The data is an average of three independent experiments. ***** $P < 0.05$.

We have demonstrated a clear and crucial connection between XBP1u and HO-1 during the EC response to disturbed flow and oxidative stress. Overexpression of XBP1u enhances the expression of HO-1 and this occurs independently of UPR activation. The expression of both XBP1u and HO-1 is augmented by disturbed flow and XBP1u is crucial for the disturbed flow mediated upregulation of HO-1. Furthermore, the activation of HO-1 by XBP1u is crucial in XBP1u-mediated protection of ECs during oxidative stress. However, we were unable to determine the exact mechanisms of HO-1 activation by XBP1u, in terms of transcriptional regulation. Our future studies will focus on elucidating how XBP1u signalling results in HO-1 expression and activation.

3.3 XBP1u promotes the expression of HO-1 by enhancing Akt phosphorylation

Akt is a crucial component of an anti-apoptotic survival pathway. The activation of Akt through phosphorylation is regulated by many growth factors and cytokines. Akt is fully functional when phosphorylated at two sites: T308 in the

catalytic domain and S473 in the hydrophobic motif. Akt has previously been shown to induce HO-1 expression (Chen et al., 2012; Martin et al., 2004). Akt has also been found to phosphorylate HO-1 directly (Salinas et al., 2004). Most reports show that Akt activates HO-1 expression through phosphorylation of the ARE-binding element Nrf2. Nrf2 dissociates from Keap2, localises to the nucleus and binds to the ARE in the HO-1 promoter (Paine et al.). We hypothesised that XBP1u may promote HO-1 expression through modulation of Akt expression or phosphorylation.

3.3.1 Overexpression of XBP1u enhances the phosphorylation of Akt on S473

To determine the effect of XBP1u overexpression on Akt expression and phosphorylation exogenous XBP1u was expressed in HUVECs in both a time and dose-dependent manner (figure 31). HUVECs were transduced with 10 MOI Ad-Null and Ad-XBP1u adenoviruses and the expression of Akt at the protein level and the phosphorylation of S473 and T308 of Akt was determined by Western blotting after 24 and 48 hours (figure 31A). Overexpression of XBP1u for 24 hours increased phosphorylation of Akt at S473, when compared to HUVECs transduced with Ad-Null adenovirus. The overexpression of XBP1u for 48 hours produced an even greater increase in the phosphorylation of Akt at S473. The protein level of Akt and phosphorylation of Akt at T308 remained constant throughout the experiment. Secondly, HUVECs were transduced with 0, 1, 2, 5 and 10 MOI Ad-XBP1u for 24 hours and the expression of Akt and the phosphorylation status of S473 of Akt was observed by Western blotting (figure 31B). Overexpression of XBP1u significantly increased Akt-S473 phosphorylation (figure 31C). A 5-fold increase in Akt-S473 phosphorylation was observed after overexpression of XBP1u for 24 hours. These data demonstrate that XBP1u enhances the phosphorylation of Akt-S473.

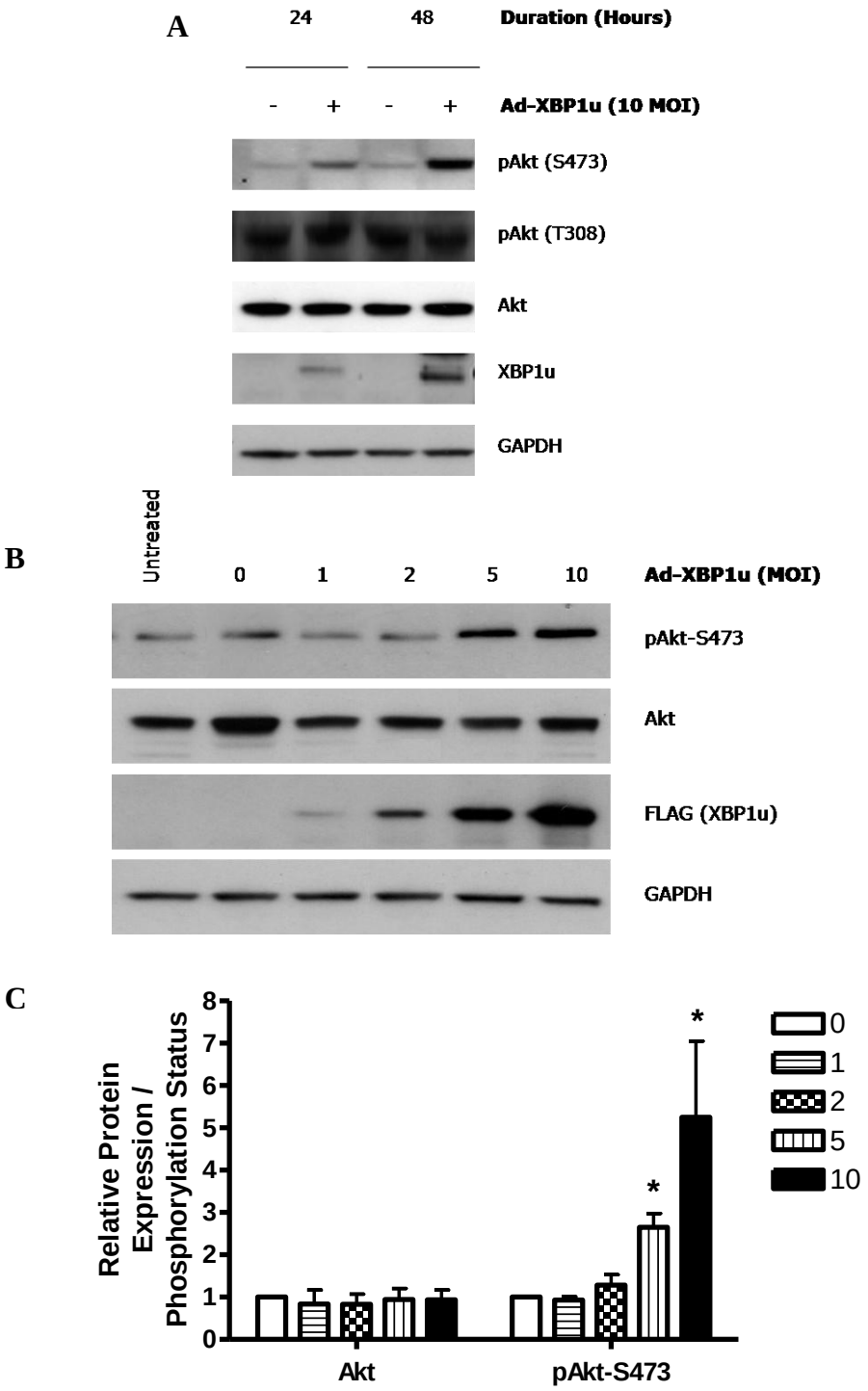

Figure 31: XBP1u increases the phosphorylation of Akt-S473.

A. HUVECs were transduced with 10 MOI of Ad-Null or Ad-XBP1u adenoviruses. The protein was harvested 24 and 48 hours after transduction and the expression and phosphorylation status of Akt was determined by Western blotting. **B.** HUVECs were transduced with 0, 1, 2, 5 and 10 MOI of Ad-XBP1u adenoviruses with Ad-Null supplemented to ensure a constant quantity of infectious particles. The protein was harvested 24 hours after transduction for Western blotting. **C.** Densitometry analysis of changes in Akt phosphorylation. The images are representative and the histogram depicts means and standard deviations of three independent experiments. * $P < 0.05$.

3.3.2 Overexpression of XBP1u increases the presence of phosphorylated Akt at the cell membrane

Most studies report that Akt phosphorylation occurs subsequently to its recruitment to the plasma membrane. PDK1 is responsible for T308 phosphorylation, whereas the Akt-kinases responsible for S473 phosphorylation have only been extensively studied more recently. Candidates for this role include mTORC2 and DNA-PK. It has been reported that the subcellular localisation and interacting partners of Akt may enhance the activation of particular downstream pathways (Bozulic and Hemmings, 2009). To determine the localisation of phosphorylated Akt after the overexpression of exogenous XBP1u we isolated the nuclear and cytoplasmic fractions were separated of HUVECs (Figure 32A). The majority of phosphorylated Akt is present in the cytoplasmic fraction. There was slight contamination of the nuclear samples with cytoplasmic markers; therefore it is possible that all the phosphorylated Akt is found in the cytoplasm.

To determine if XBP1u enhances Akt phosphorylation at the cell membrane we overexpressed exogenous XBP1u in HUVECs and isolated the cell membrane proteins (Figure 32B-C). The cell membrane proteins and any interacting intracellular partners were isolated through biotinylation of the cell surface and integral membrane proteins. Overexpression of XBP1u enhanced the quantity of phosphorylated Akt-S473 at the cell membrane. We also detected a large increase in phosphorylated Akt-S473 in the cytoplasm. However, this would be anticipated because of its other functions and due to the instability of its interaction with the integral membrane proteins of the plasma membrane. These data demonstrate that XBP1u Overexpression of XBP1u increases the phosphorylation of Akt at S473 and the newly phosphorylated protein is enhanced both at the cell membrane and within the cytoplasm.

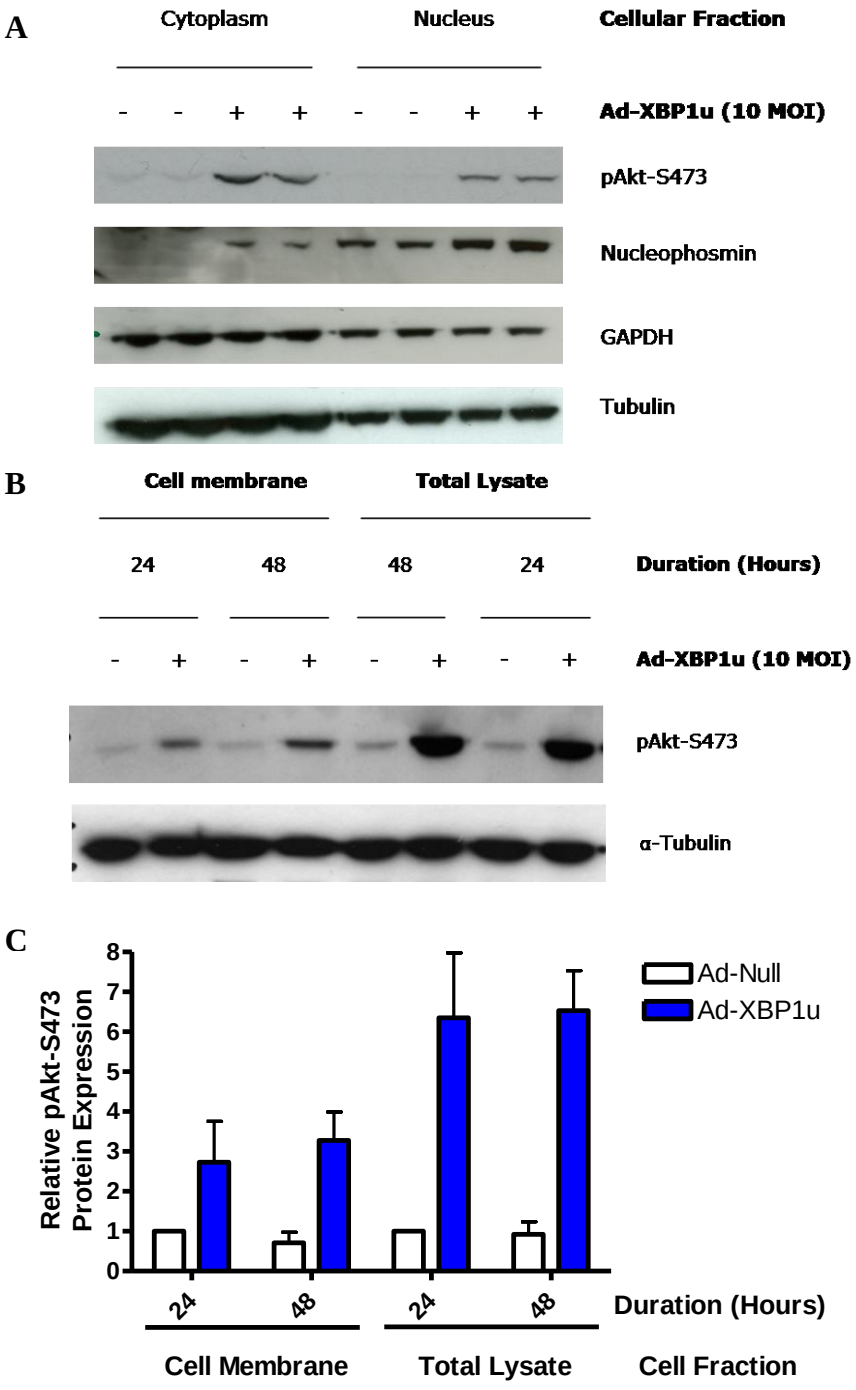

Figure 32: XBP1u increases the presence of phosphorylated Akt at the cell membrane.

A. HUVECs were transduced with 10 MOI Ad-Null or Ad-XBP1u adenovirus. Protein from the nuclear and cytoplasmic fractions was isolated 48 hours after transduction and the expression of Akt and pAkt-S473 was assessed by Western Blotting. **B.** HUVECs were infected with 10MOI of Ad-Null or Ad-XBP1u adenoviral vectors. The proteins associated with the cell membrane were isolated after 24 and 48 hours and HO-1 and pAkt-S473 at the cell membrane and in the total lysate were detected by Western blotting. **C.** Densitometry analysis of HO-1 and pS473 at the cell membrane and in the total lysate. The samples were normalised against HUVECs treated with 10MOI ad-Null for 24 hours. The data is representative and depicts means from two independent experiments.

3.3.3 XBP1 is required for Akt-S473 phosphorylation

We have determined that XBP1u is sufficient to induce an increase in Akt phosphorylation at S473; however it is also important to know if normal Akt phosphorylation can occur without XBP1u present. To determine if XBP1u is necessary for Akt phosphorylation, XBP1 was knocked down through lentiviral transfer of XBP1-targeted shRNA. The protein was harvested 72 hours after transduction and the expression of Akt and S473-phosphorylated Akt was determined by Western blotting (Figure 33). The knockdown of XBP1 significantly reduced the ability of Akt to be phosphorylated at S473.

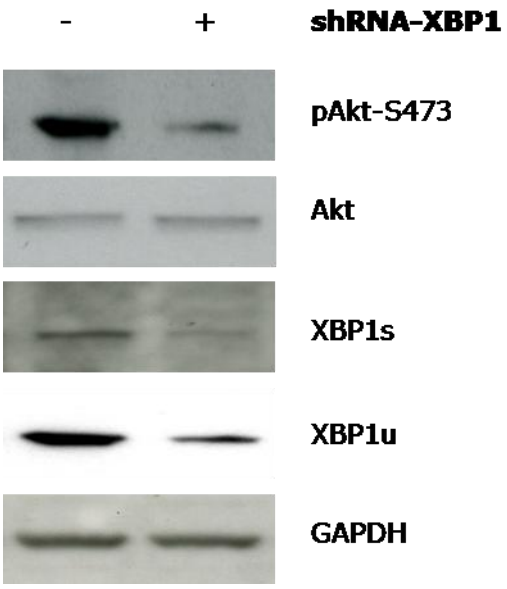

Figure 33: Knockdown of XBP1 abrogates Akt phosphorylation.
HUVECs were transduced with 100 TU / cell of shRNA-NT and shRNA-XBP1 lentivirus. Protein was harvested 72 hours post-transduction and the expression of XBP1u, XBP1s, Akt, pS473-Akt and GAPDH was determined by Western blotting. The images are representative of three independent experiments.

3.3.4 XBP1u does not induce Akt phosphorylation through PI-3-Kinase or VEGFR2 activity

In general Akt is phosphorylated through the activation of phosphatidylinositol-3-kinase (PI-3-kinase). When activated PI-3-kinase phosphorylates phosphatidylinositol-3,4-bisphosphate to create phosphatidylinositol-3,4,5-trisphosphate (PIP_3) in the cell membrane. Akt is recruited, through interactions between the lipids and the plekstrin homology domain of Akt (Duronio, 2008). Downstream kinases are then responsible for phosphorylation of Akt at T308 and S473 of which PDK-mediated phosphorylation of T308 is the more widely studied (Bozulic and Hemmings, 2009). It has been reported that VEGF signalling can also induce activation of Akt signalling and that this is important in EC angiogenesis (Olsson et al., 2006; Somanath et al., 2006).

In order to determine the mechanism behind the induction of Akt phosphorylation by XBP1u we used inhibitors VEGF receptor 2 (VEGFR2) and PI-3-kinase, both upstream regulators of Akt activation. HUVECs were treated with DMSO, 5μM LY294002 (a PI-3-kinase inhibitor) or 5μM SU1498 (a VEGFR2 inhibitor). These inhibitors have previously been demonstrated to inactivate their respective targets at these concentrations in HUVECs (Zampetaki et al., 2010). The HUVECs were subsequently transduced with 10 MOI Ad-Null or Ad-XBP1u adenoviral vectors and the protein was harvested after 48 hours. The phosphorylation of Akt-S473 was determined by Western blotting (figure 34). The inhibition of VEGFR2 or PI-3-kinase did not reduce XBP1u-mediated induction of Akt-S473 phosphorylation. Although PI-3-kinase is the most commonly studied method of inducing Akt activation a PI-3-kinase independent method has been suggested (Kamimura et al., 2008). This data demonstrates that XBP1u activates Akt-S473 phosphorylation independently of VEGFR2 and PI-3-kinase. This experiment does not address the ability of XBP1u to activate Akt phosphorylation at different time points and doses. To conclusively determine that XBP1u activates Akt phosphorylation independently of VEGFR2 and PI-3-Kinase it would be necessary to perform a time and dose-dependent treatment of the HUVECs with the inhibitors before the application of exogenous XBP1u.

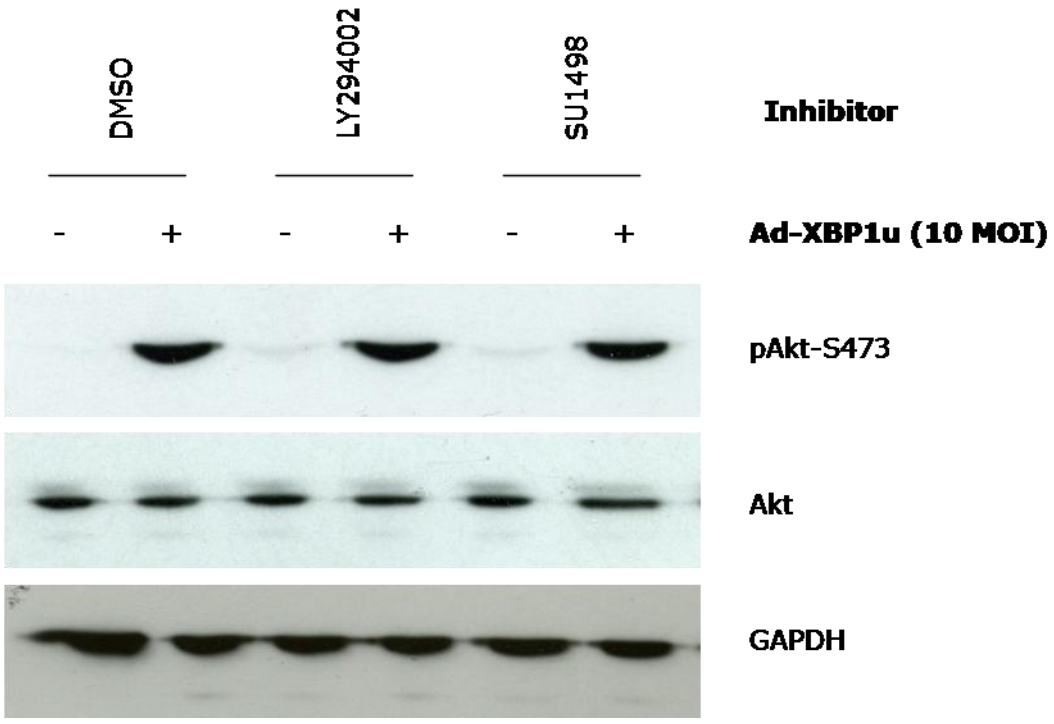

Figure 34: Inhibition of PI-3-kinase and VEGFR2 had no effect on XBP1u-induced Akt phosphorylation.

HUVECs were transduced with 10 MOI of Ad-Null or Ad-XBP1u adenoviral vectors. Six hours prior to transduction the HUVECs were treated with DMSO, 5μM LY294002 or 5μM SU1498. The HUVECs were harvested 48 hours after transduction and the protein was isolated. The phosphorylation status of Akt was detected by Western Blotting. The images are representative of three independent experiments.

3.3.5 Phosphorylated Akt-S473 levels are normal in XBP1-null ECs

We hypothesised that XBP1-null ECs would have a reduction in Akt-S473 phosphorylation compared to wild type controls. Arterial sections from wild type and *Tie2-Cre / XBP1*$^{f/f}$ mice were harvested from 10 week old mice. The aorta segments were then fixed and double-immunostained for phosphorylated Akt-S473 and CD31. The sections were then analysed by fluorescence microscopy (Figure 35). CD31 was detected at the cell membranes alongside the majority of phosphorylated Akt-S473. Pockets of phosphorylated Akt were also present in specific cytoplasmic subcellular locations. There were no significant differences in the phosphorylation of Akt-S473 between wild type and *Tie2-Cre / XBP1*$^{f/f}$ mice. Individual staining is not available.

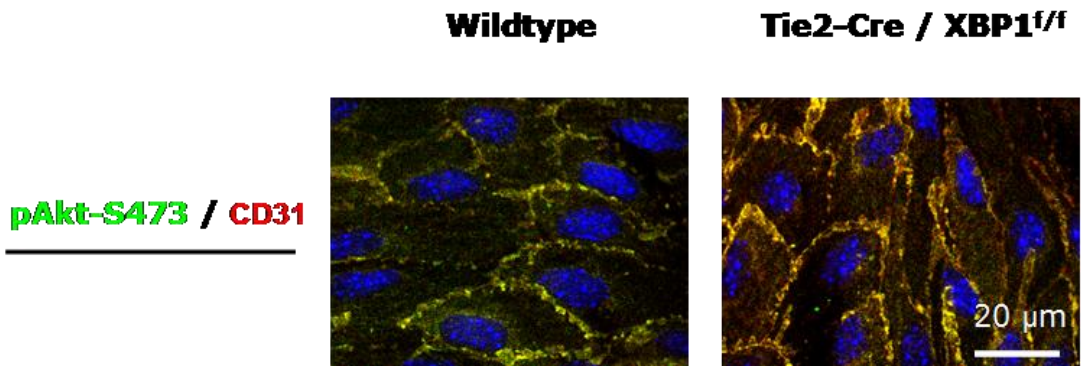

Figure 35: Phosphorylated Akt levels are normal in XBP1-null cells.
Aorta sections from wild type and Tie2-Cre / XBP1$^{f/f}$ mice were harvested for *en face* immunostaining. ECs were double-immunostained with phosphorylated S473-Akt and CD31 antibodies and then stained with DAPI to identify the nuclei. Scale bar = 20 µm. These images are representative of three experiments performed on aortic segments taken from three independent mice for each genotype.

3.3.6 Overexpression of constitutively active Akt increases XBP1u, XBP1s and HO-1 expression

We have demonstrated that overexpression of XBP1u enhances the expression of HO-1 and we predict that this occurs through the activation of Akt phosphorylation. A constitutively active isoform of Akt (donated by Professor Justin Mason, Imperial College, London) was used to further our studies. Exogenous constitutively active Akt was overexpressed in a time and dose-dependent manner. HUVECs were treated with 10 MOI Ad-Null and Ad-Akt adenovirus and the protein was harvested after 24 and 48 hours. The protein level of HO-1, XBP1u, XBP1s and Akt was determined by Western blotting (figure 36). As has previously been shown the overexpression of constitutively active Akt drastically increases HO-1 protein. The overexpression of constitutively active Akt also resulted in increased levels of XBP1u and XBP1s. HUVECs were also treated with 0, 5 and 10 MOI Ad-Akt for 24 hours and the protein level of HO-1, XBP1u, XBP1s and Akt was determined by Western blotting (figure 36B). The overexpression of constitutively active Akt enhanced the expression of HO-1, XBP1u and XBP1s at the protein level. These data indicate that phosphorylated Akt can induce the expression of HO-1 as well as XBP1u and XBP1s.

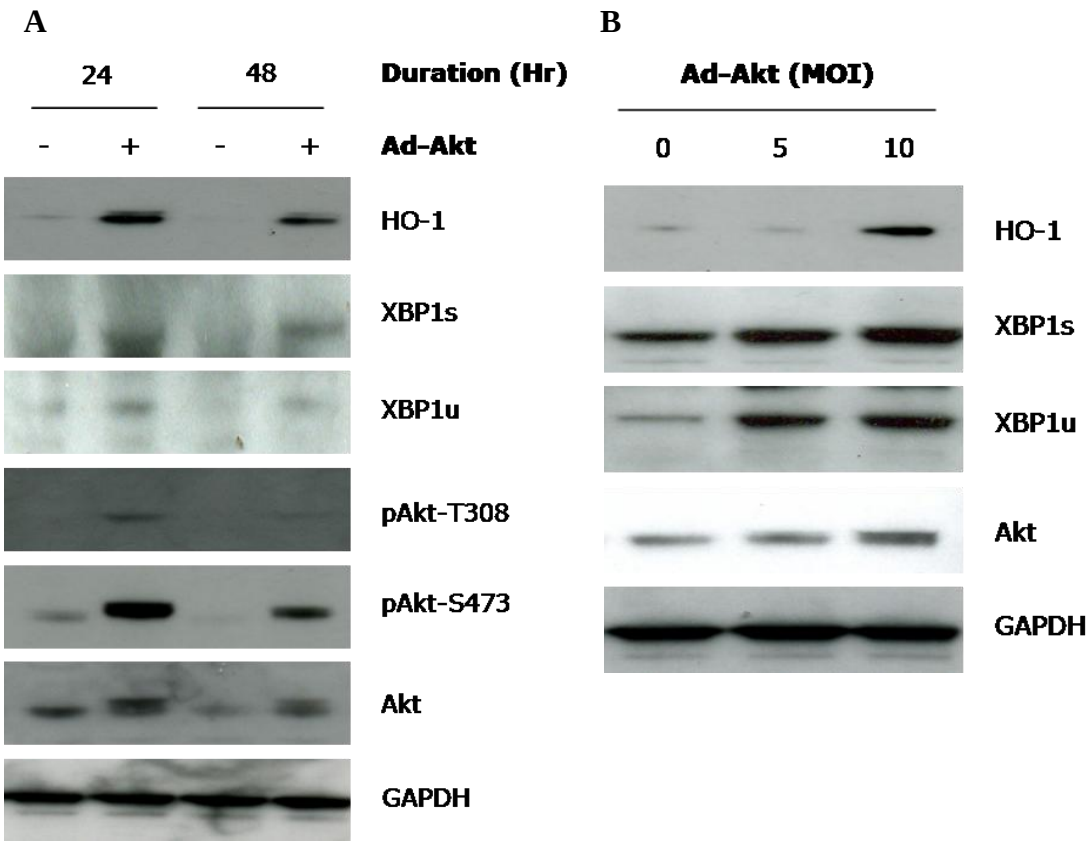

Figure 36: Constitutively active Akt increases XBP1u, XBP1s and HO-1 protein.

A. HUVECs were transduced with 10 MOI Ad-Null or Ad-Akt adenovirus. Protein was harvested 24 and 48 hours after transduction. The expression of HO-1, XBP1u, XBP1s, Akt, pAkt-T308, pAkt-S473 and GAPDH was assessed by Western blotting. **B.** HUVECs were transduced with 0, 5 and 10MOI of Ad-Akt adenovirus alongside compensating quantities of Ad-Null adenovirus to control for viral transduction. The expression of HO-1, XBP1u, XBP1s, Akt and GAPDH was assessed by Western blotting. The images are representative of three independent experiments.

3.3.7 Knockdown of XBP1 ablates Akt-mediated induction of HO-1

To determine if XBP1u is important for Akt-mediated regulation of HO-1, the expression of XBP1 was abolished through targeted shRNA transduction prior to overexpression of constitutively active Akt (Figure 37). HUVECs were treated with 100 TU/cell of shRNA-XBP1 lentivirus. 48 hours after transduction the HUVECs were treated with 10 MOI Ad-Akt. The protein was harvested and the expression of HO-1, Akt and XBP1u was determined by Western blotting. Knockdown of XBP1 resulted in a significant decrease in HO-1 expression. Furthermore, transduction of

constitutively active Akt increased the expression of XBP1u and HO-1. However, after knockdown of XBP1, the application of constitutively active Akt was unable to continue to increase the expression of HO-1. This data implies that XBP1u plays a crucial role in the activation of HO-1 expression. The expression of XBP1u is crucial for Akt-mediated activation of HO-1 expression.

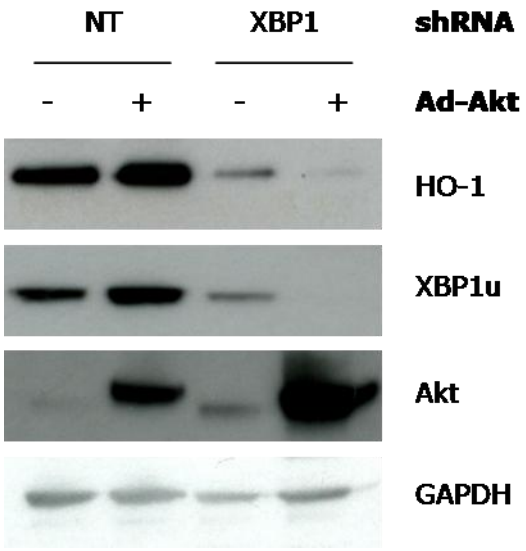

Figure 37: Knockdown of XBP1 ablates Akt-induced upregulation of HO-1.
HUVECs were transduced with 100 TU / cell of shRNA-NT and shRNA-XBP1 lentivirus. The HUVECs were further transduced with Ad-Null and Ad-Akt adenoviruses 48 hours post-transduction. The protein was harvested 48 hours later. The expression of HO-1, XBP1u, Akt and GAPDH was determined by Western blotting. The images are representative of three independent experiments.

3.3.8 Inhibition of Akt does not prevent XBP1u-induced upregulation of HO-1

To clarify the role of XBP1u in the upregulation of HO-1 a dominant-negative isoform of Akt (Akt(d/n)), which acts as a competitive inhibitor of activated Akt was kindly provided by Professor Justin Mason, Imperial College London. Exogenous Akt(d/n) and XBP1u were simultaneously overexpressed and the expression of HO-1 was determined. HUVECs were transduced with 10 MOI of Ad-XBP1u and Ad-Akt(d/n) alongside compensatory quantities of Ad-null adenovirus. The protein was harvested 48 hours after transduction and the level of HO-1 was determined by Western blotting (figure 38). The overexpression of exogenous XBP1u increased the level of HO-1 protein. Individually, the overexpression of the dominant negative

isoform of Akt had no effect on the protein level of HO-1 and reduced the quantity of Akt phosphorylated at S473. Overexpression of XBP1u is still able to induce the expression of HO-1 in the presence of inactive Akt. This data demonstrates that XBP1u functions downstream of Akt and is crucial in promoting basal HO-1 expression.

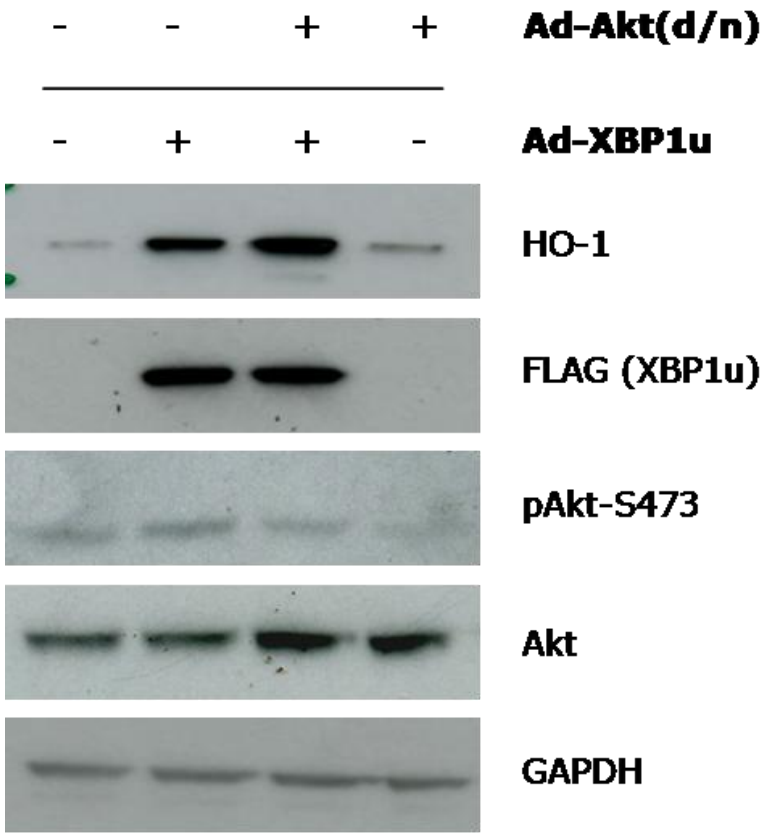

Figure 38: Inhibition of Akt does not prevent XBP1u-induced upregulation of HO-1.
HUVECs were transduced with 10 MOI of Ad-XBP1u, Ad-Akt(d/n) and 10 MOI of both Ad-XBP1u and Ad-Akt(d/n). MOI was compensated for with the addition of Ad-Null adenovirus. The protein was harvested 48 hours after transduction. The protein expression of HO-1, FLAG (XBP1u), pAkt-S473, Akt and GAPDH was assessed by Western blotting. The images are representative of three independent experiments.

3.3.9 Knockdown of XBP1 abolished the induction of Akt phosphorylation by disturbed flow

Our previous experiments with disturbed flow demonstrated that XBP1u and HO-1 are both upregulated through the application of disturbed flow onto a confluent HUVEC monolayer. Previously Akt has been shown to respond to shear stress in ECs. To confirm this in our model HUVECs were subjected to disturbed flow for 0, 0.25, 0.5, 1, 2, 4, 8 and 24 hours. The protein was harvested and the level of phosphorylated Akt-S473, phosphorylated Akt-T308 and Akt was determined by Western blotting (Figure 39A). Disturbed flow had very little effect on the phosphorylation status of Akt-T308; however, the application of disturbed flow very quickly (15 minutes) induced the phosphorylation of Akt-S473. The phosphorylation of Akt-S473 remained increased at all time points, however the intensity had decreased after 24 hours.

To determine if XBP1u is required for Akt phosphorylation during disturbed flow, XBP1 was knocked down by targeted shRNA prior to stimulation of the HUVECs with disturbed flow. HUVECs were treated with 100 TU / cell shRNA-XBP1. Disturbed flow was then applied for 8 hours, as previous experiments suggested that this is the optimal time to see upregulation of XBP1u, HO-1 and phosphorylated Akt-S473, and the expression of these proteins was detected through Western blotting (figure 39B). Disturbed flow induced the upregulation of XBP1u, HO-1 and phosphorylated S473-Akt. After knockdown of XBP1, no upregulation of HO-1, XBP1u or phosphorylated S473-Akt was observed. These data confirm that XBP1u is crucial in disturbed flow mediated upregulation of HO-1 and phosphorylation of Akt at S473.

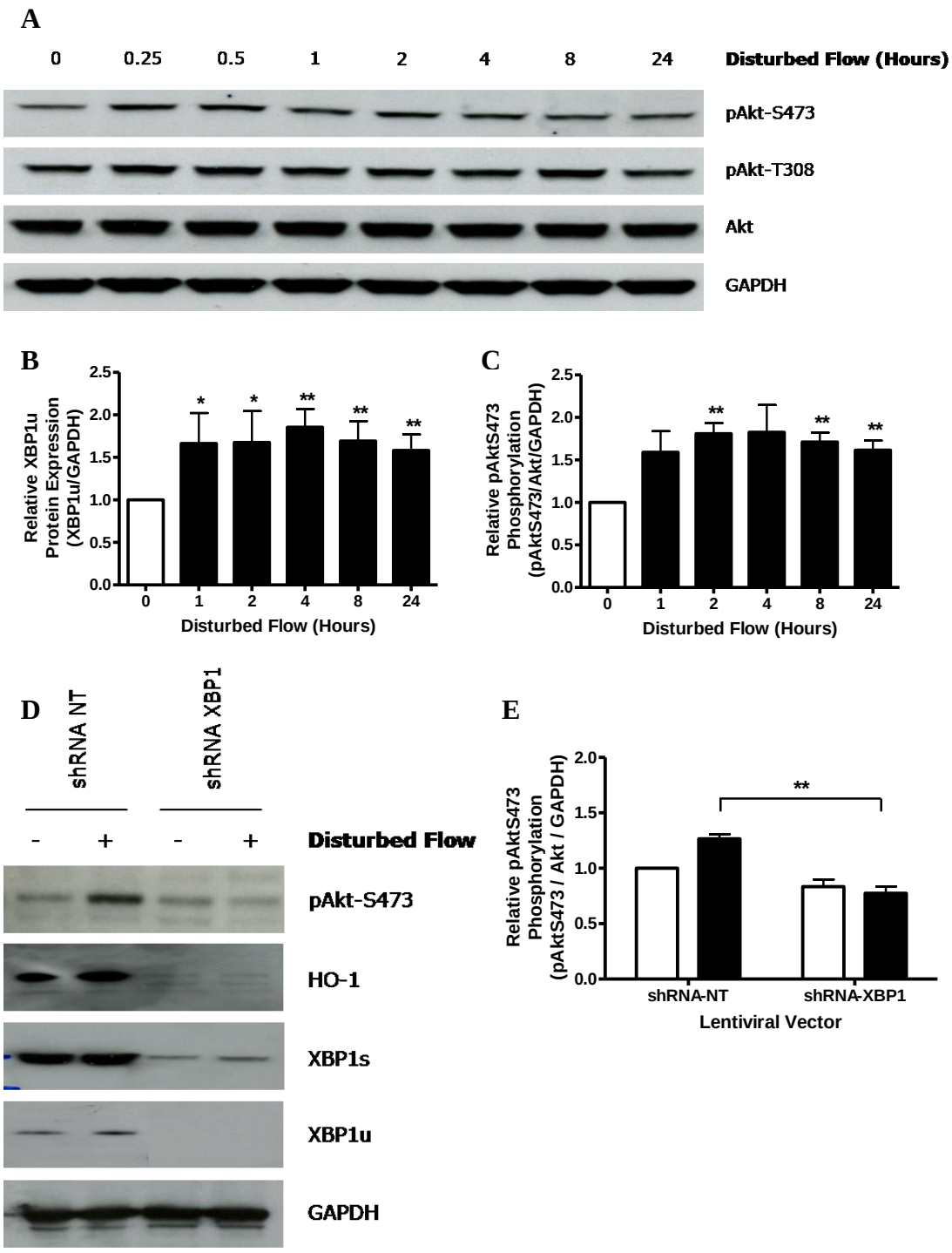

Figure 39: Knockdown of XBP1 abolishes disturbed flow-induced upregulation of pAkt-S473.

A. HUVECs were subjected to static or disturbed flow for 0.25, 0.5, 1, 2, 4, 8 and 24 hours. The protein was harvested and the expression and phosphorylation status of Akt was assessed by Western blotting. **B.** and **C.** Densitometry analysis of XBP1u and pAkt-S473 expression. **D.** HUVECs were transduced with 100 TU / cell of shRNA-NT and shRNA-XBP1 lentivirus. HUVECs were then subjected to static or disturbed flow for 8 hours. The protein was harvested and the expression of HO-1 and pAkt-S473 was assessed by Western blotting. The images are representative of three independent experiments. **E.** Densitometry analysis of pAkt-S473 expression.

Our results demonstrate that disturbed flow upregulates the expression of XBP1u and HO-1 and leads to increased phosphorylation of Akt at serine 473. Additionally, overexpression of XBP1u results in increased Akt S473 phosphorylation, HO-1 expression and EC survival under both normal and oxidative stress conditions. Akt has previously been shown to upregulate the expression of HO-1, which we have also confirmed. In addition, we have demonstrated that constitutively active Akt can induce the expression of XBP1u. Interestingly, we have shown that XBP1u is required for Akt-mediated augmentation of HO-1 expression. We hypothesise that XBP1u is upregulated in ECs in an attempt to mediate against the damaging effects of disturbed flow. Our experiments also demonstrate that an increase in XBP1u can enhance the phosphorylation, and thereby activation, of Akt. Indicating a potential positive feedback loop, whereby activated Akt increases the expression of XBP1u which in turns acts to promote the phosphorylation of Akt.

3.4 HDAC3 interacts with XBP1u and is required for XBP1u-mediated regulation of HO-1 expression and Akt phosphorylation

Our lab has demonstrated that HDAC3 is critical in EC survival and atherosclerosis development in response to disturbed flow (Zampetaki et al.). *En face* staining of mouse aortas showed that HDAC3 expression is predominantly increased in the branching areas *in vivo*. HDAC3 was also shown to be upregulated by disturbed flow and in turn upregulation of HDAC3 increased the phosphorylation of S473 of Akt. Furthermore, Akt was found to bind HDAC3 and form a complex that localises to the cell membrane. Finally knockdown of HDAC3 resulted in increased EC apoptosis *in vitro* and increased atherosclerotic development in aortic isografts (Zampetaki et al., 2010). These functions were remarkably similar to those we determined for XBP1u. Therefore, due to the similarities we observed between the role of XBP1u and HDAC3 in ECs we investigated the relationship between HDAC3 and XBP1u.

A second microarray experiment was performed by Dr. Anna Zampetaki, on samples subjected to the overexpression of HDAC3, through adenoviral transfer, for

24 and 72 hours. A significant overlap (40-50%) in gene regulation was observed between in the gene expression pattern after XBP1u and HDAC3 overexpression (the HDAC3 microarray data cannot be shown in this thesis). Due to these studies our investigation focused on a potential interaction between XBP1u and HDAC3 signalling pathways. We hypothesised that HDAC3 is also crucial in the XBP1u-Akt-HO-1 signalling pathway.

3.4.1 XBP1u has no impact on the expression of HDAC3

To determine if XBP1u can regulate the expression of HDAC3 exogenous XBP1u was overexpressed in HUVECs through the transduction of 10 MOI of Ad-XBP1u adenovirus. The protein was harvested after 24 and 48 hours and the expression of HDAC3 was detected by Western blotting (figure 40). Overexpression of XBP1u had no impact on HDAC3 protein levels after 24 or 48 hours.

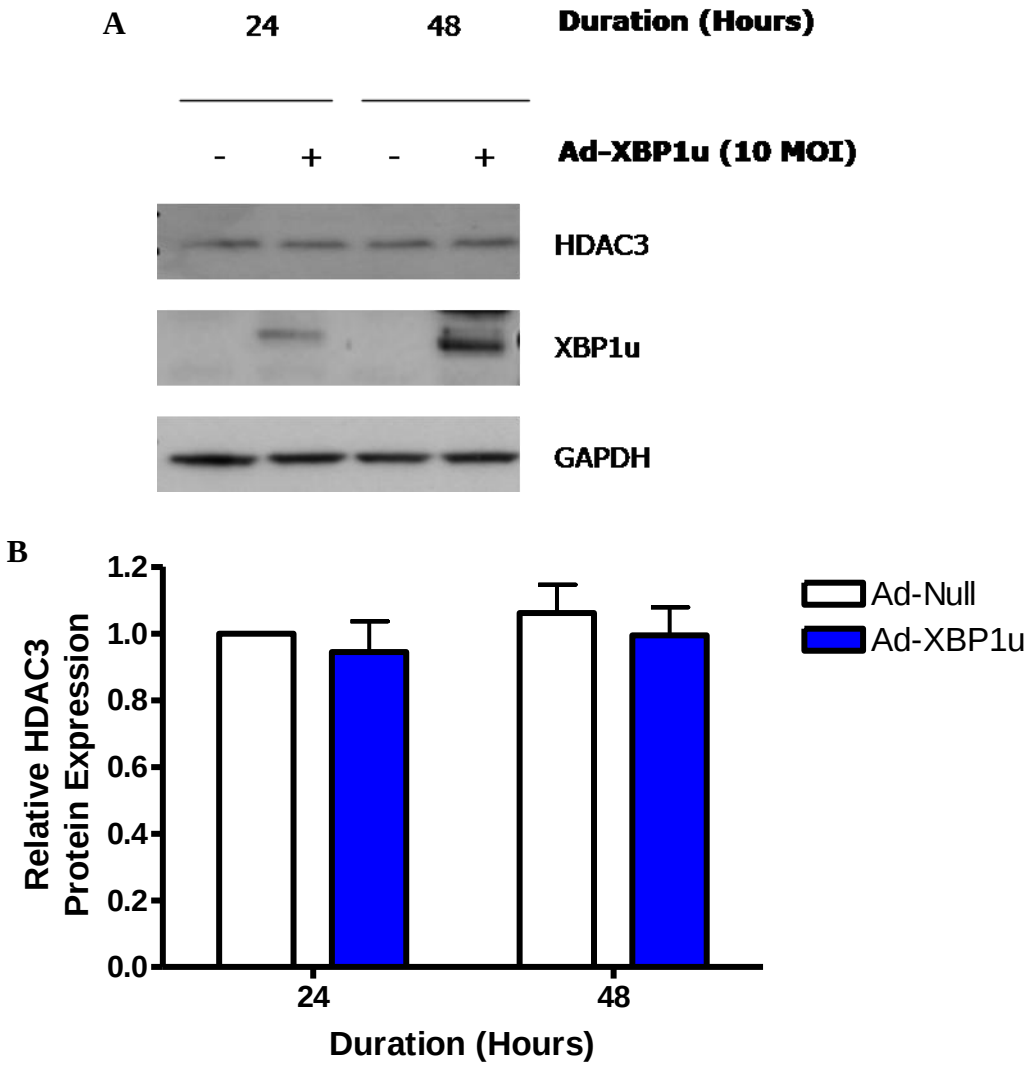

Figure 40: XBP1u has no effect on HDAC3 protein expression.

HUVECs were transduced with 10 MOI of Ad-Null or Ad-XBP1u adenoviruses. The protein was harvested 24 and 48 hours post-transduction. **A.** The expression of HDAC3 was assessed by Western blotting. **B.** The histogram depicts the effect of exogenous XBP1u overexpression on HDAC3 at the protein level. It depicts the mean and standard deviation of. three independent experiments.

To determine if the expression of XBP1u is required for basal HDAC3 expression the expression of XBP1 was knocked down by transducing HUVECs with 100 TU / cell of shRNA-XBP1 alongside a null shRNA-NT control. The protein was harvested after 72 hours and the expression of HDAC3 was determined by Western blotting (figure 41). Knockdown of XBP1 has no significant effect on the expression of HDAC3 at the protein level. These data demonstrate that XBP1u does not influence the expression of HDAC3.

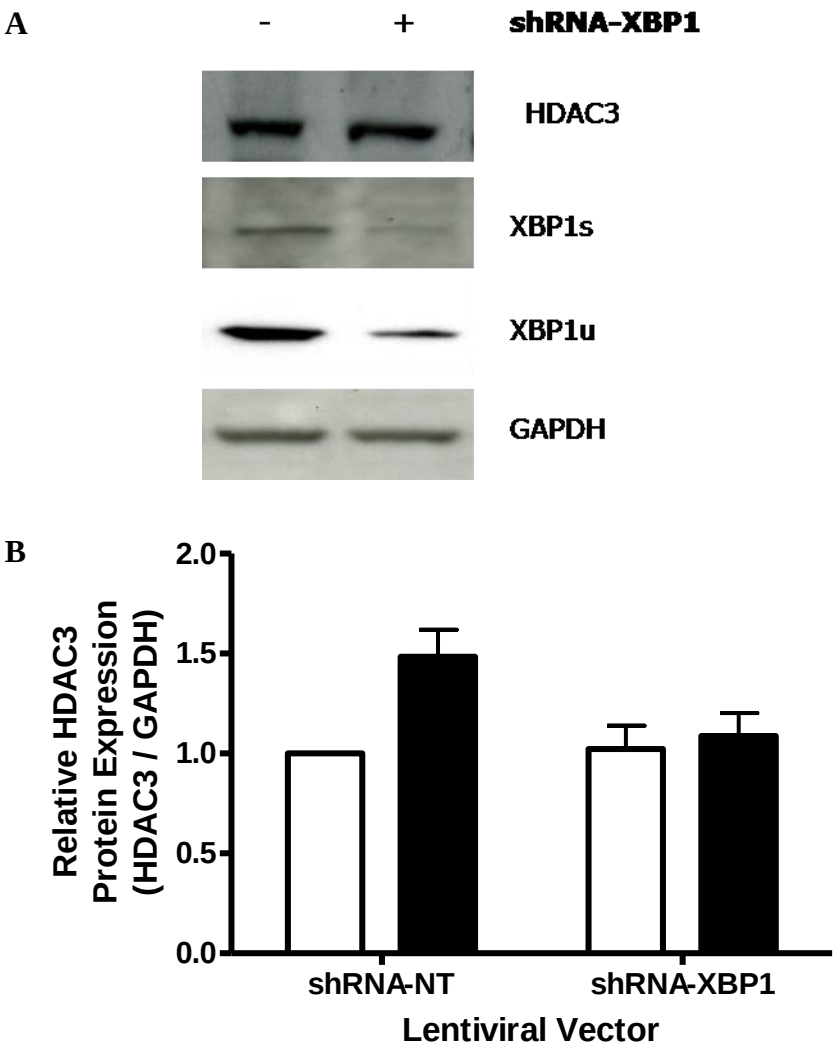

Figure 41: Knockdown of XBP1 has no effect on HDAC3 protein level.

A. HUVECs were transduced with 100 TU / cell of shRNA-NT and shRNA-XBP1 lentivirus. The protein was harvested 72 hours post-transduction and the expression of HDAC3, XBP1u, XBP1s and GAPDH was determined by Western Blotting. The images are representative of three independent experiments. **B.** Densitometry analysis of the HDAC3 protein level.

Furthermore, we examined the expression of HDAC3 in endothelial sections of wild type and *Tie2-Cre / XBP1*$^{f/f}$ mice. Aortic sections were harvested and subjected to immunostaining with CD31 and HDAC3 antibodies (figure 42). HDAC3 is expressed in ECs in specific subcellular locations within the cytoplasm; around the nucleus and at the cell membrane. There was no difference observed between the expression of HDAC3 in wild type and *Tie2-Cre / XBP1*$^{f/f}$ mice.

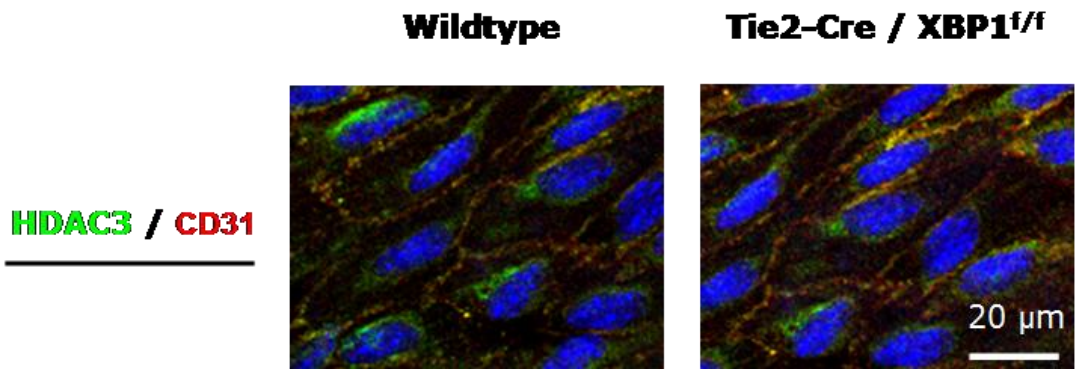

Figure 42: HDAC3 levels are normal in XBP1-null ECs.

Aorta sections from wild type and *Tie2-Cre / XBP1*$^{f/f}$ mice were harvested for *en face* immunostaining. ECs were double-immunostained with HDAC3 and CD31 antibodies and then stained with DAPI to identify the nuclei. Scale bar = 20 µm. These images are representative of three experiments performed on aortic segments taken from three independent mice for each genotype.

3.4.2 HDAC3 is transiently increased by disturbed flow

Our data has linked the expression of XBP1u and HO-1 to disturbed flow. To investigate the influence of disturbed flow on HDAC3, HUVECs were exposed to disturbed flow for 0, 1, 2, 4, 8 and 24 hours. The expression of HDAC3 protein was determined by Western blotting (figure 43). The expression of HDAC3 at the protein level was transiently increased by disturbed flow between 1 and 8 hours. This confirms the previous experiments performed in our lab demonstrating that a transient stabilisation of the HDAC3 protein occurs during disturbed flow (Zampetaki et al., 2010).

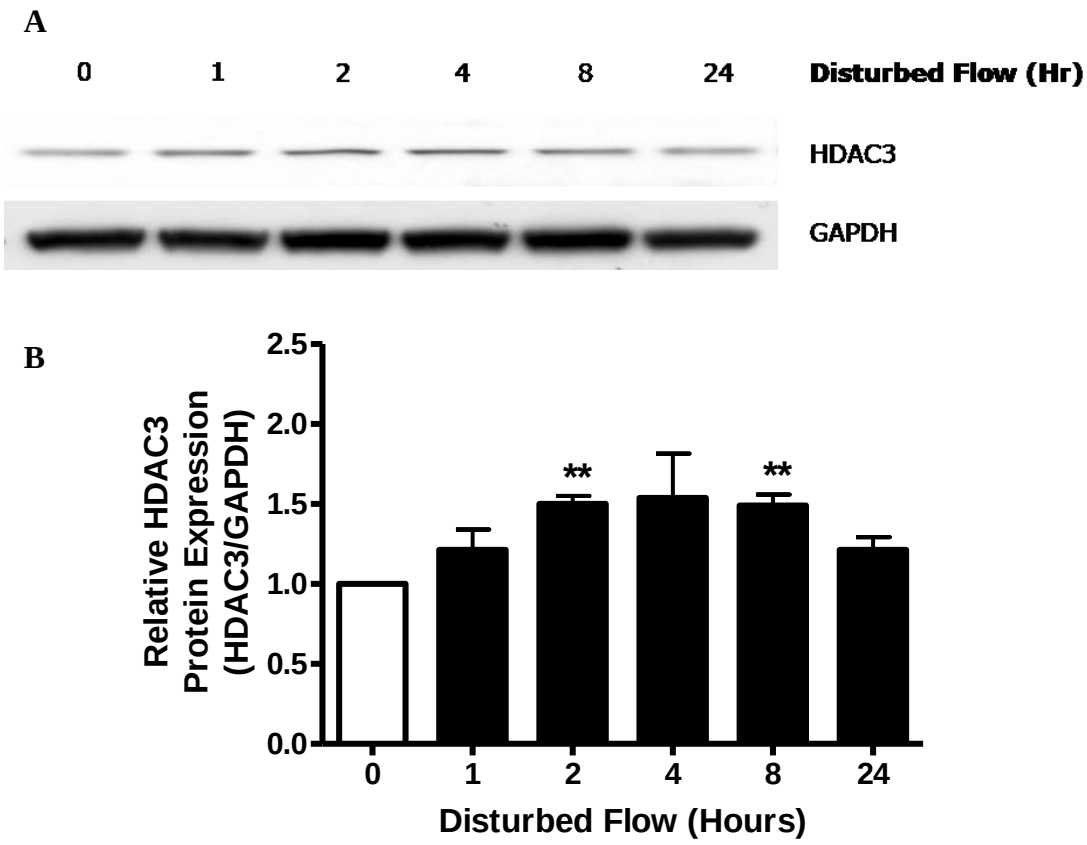

Figure 43: Disturbed flow transiently increases HDAC3 at the protein level.

A. HUVECs were subjected to static or disturbed flow for 0, 1, 2, 4, 8 and 24 hours. The protein was subsequently harvested and the expression of HDAC3 was assessed by Western blotting. The images are representative of three independent experiments. **B.** Densitometry analysis of HDAC3 expression. ** $P < 0.01$.

3.4.3 Knockdown of XBP1 prevents the stabilisation of HDAC3 by disturbed flow

The expression of XBP1u and HDAC3 is enhanced by disturbed flow and XBP1u has no effect on the basal HDAC3 expression. We hypothesised that XBP1u could stabilise HDAC3 protein during disturbed flow. To this end, XBP1 was knocked down in HUVECs using a lentiviral vector and then subjected to disturbed flow. The protein was harvested and the expression of HDAC3 and XBP1 was determined by Western blotting (figure 44). Disturbed flow enhances XBP1u, XBP1s and HDAC3 at the protein level. However, after knockdown of XBP1, disturbed flow is no longer able to induce an increase in HDAC3. This data demonstrates that XBP1 is crucial in mediating the post-disturbed flow stabilisation of HDAC3 protein.

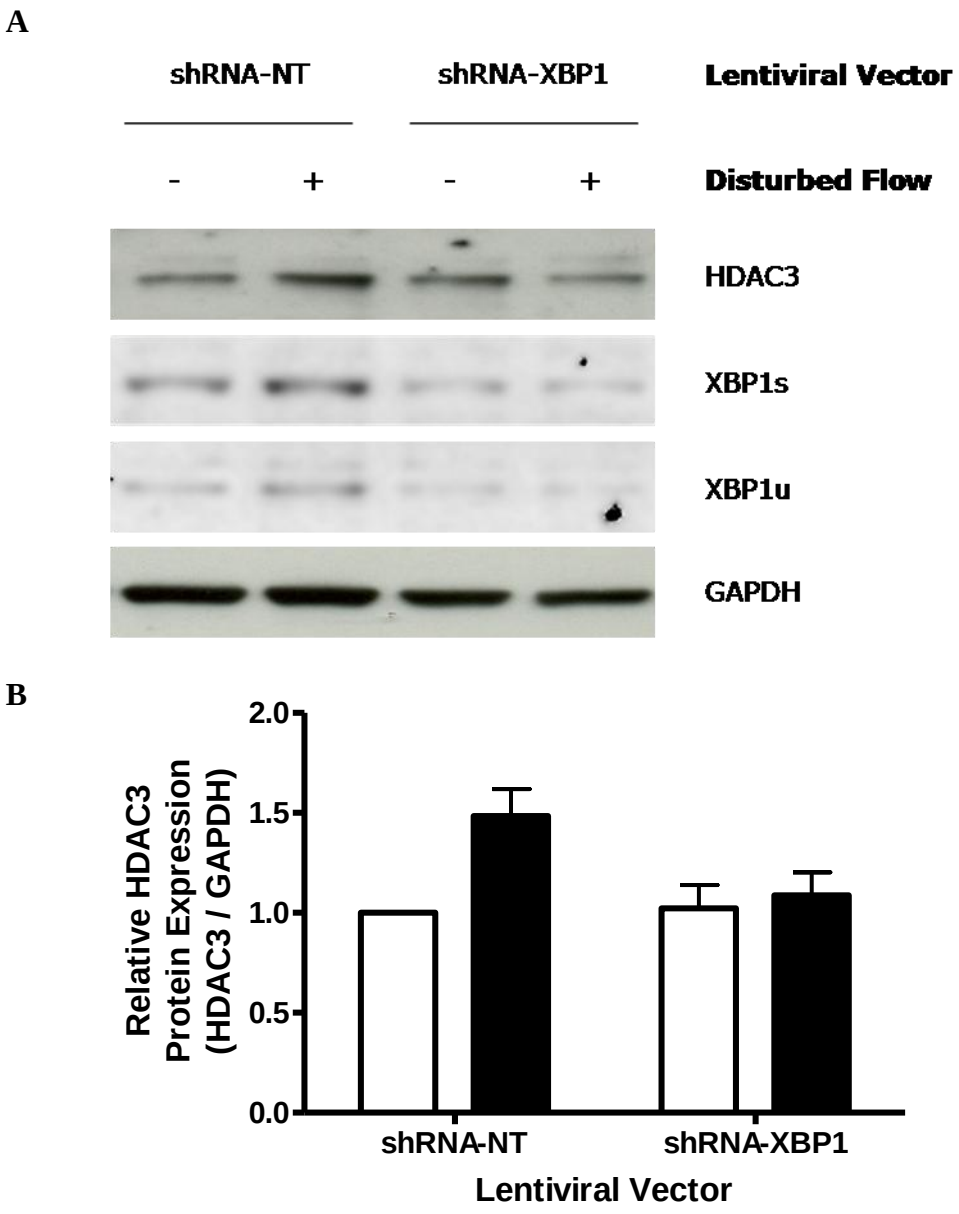

Figure 44: Knockdown of XBP1 abolishes disturbed flow-induced upregulation of HDAC3.
A. HUVECs were subjected to static or 4.5dyn/cm^2 disturbed flow stress for 8 hours. The protein was then harvested and the level of HDAC3, XBP1u, XBP1s and GAPDH was assessed by Western blotting. The images are representative of three independent experiments. **B.** Densitometry analysis of HDAC3 protein expression.

3.4.4 Disturbed flow-mediated upregulation of XBP1u and HDAC3 is abrogated by inhibition of VEGFR2 and PI-3-Kinase

XBP1u and HDAC3 are both upregulated by disturbed flow, but how? Having shown that Akt is also activated by disturbed flow we were interesting in determining the mechanism of activation. VEGFR2, PI-3-kinase and MEK1 have all been shown to activate, or respond to, Akt phosphorylation in ECs (Bozulic and Hemmings, 2009; Duronio, 2008; Olsson et al., 2006). HUVECs were treated with DMSO, 5μM SU4098, 10μM PD98059 (a MEK1 inhibitor) or 5μM LY294002 for 6 hours, prior to their exposure to disturbed flow for 8 hours. The protein was harvested and the expression of HDAC3 and XBP1u was determined by Western blotting (figure 45). The inhibition of MEK1 has no effect on disturbed flow-mediated upregulation of HDAC3 and XBP1u. However, when VEGFR2 and PI-3-kinase are inhibited, disturbed flow is unable to upregulate the expression of HDAC3 or XBP1u. These data demonstrate that disturbed flow must acts through VEGFR2 and PI-3-kinase to promote the stabilisation of XBP1u and HDAC3.

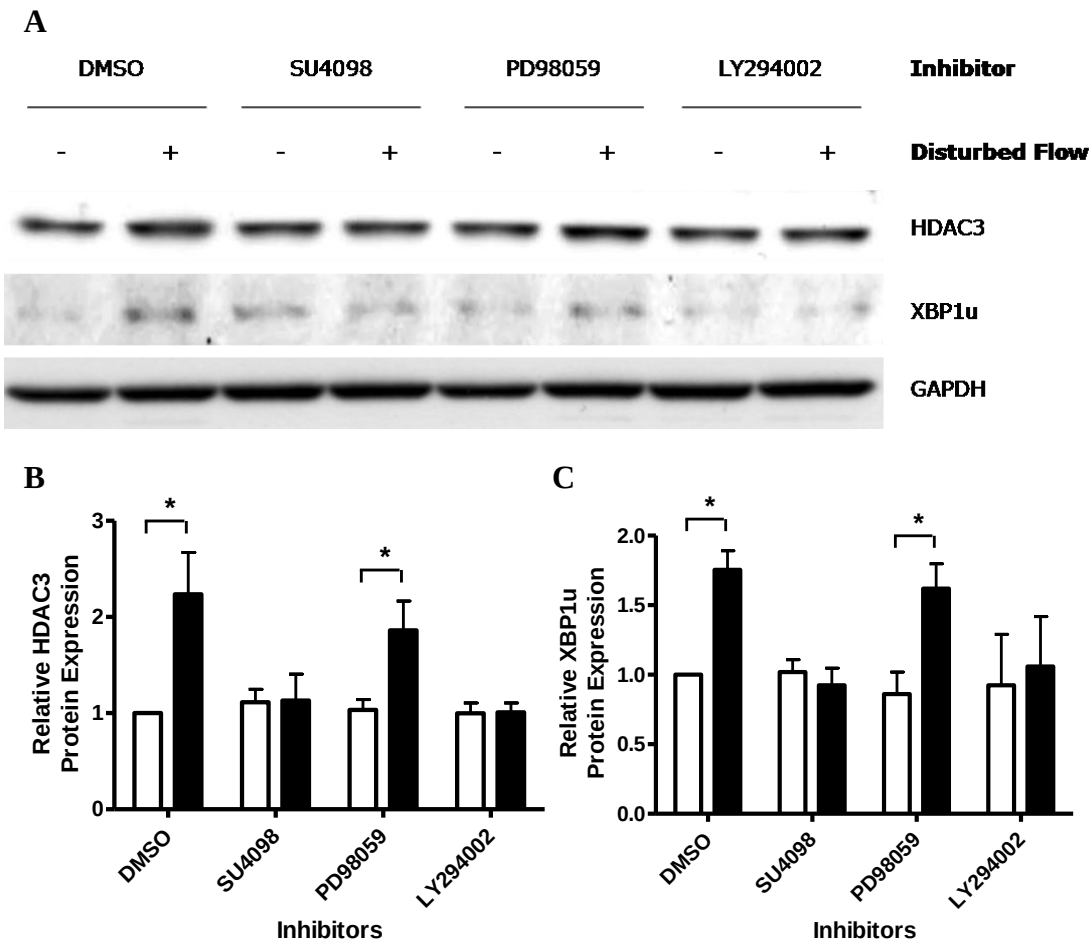

Figure 45: Disturbed flow-mediated upregulation of XBP1u and HDAC3 is abrogated by inhibition of VEGFR2 and PI-3-Kinase.

A. HUVECs were subjected to 8 hours of 4.5 dyn / cm^2 disturbed flow after a 6 hour pre-treatment with DMSO, 5μM SU4098, 10μM PD98059 or 5μM LY294002. The protein was harvested and the expression of HDAC3, XBP1u and GAPDH was assessed by Western blotting. The images are representative of three independent experiments. **B.** and **C.** Densitometry analysis of HDAC3 and XBP1u protein levels. White bars = static conditions, blacks bars = disturbed flow.

3.4.5 Knockdown of HDAC3 ablated XBP1u-mediated Akt phosphorylation and HO-1 expression

How do HDAC3 and XBP1u interact? We hypothesised that HDAC3 was necessary for XBP1u-mediated activation of Akt phosphorylation or HO-1 expression. HDAC3 was knocked down using an shRNA particle targeted against HDAC3 mRNA (shRNA-HDAC3). HUVECs were treated shRNA-HDAC3 alongside a non-targeting shRNA control. After 48 hours the HUVECs were transduced with 10 MOI of Ad-XBP1u adenovirus and the protein was harvested a further 48 hours later for examination by Western blotting (figure 46). The efficiency of HDAC3 knockdown was very effective (approximately 95%). The overexpression of XBP1u resulted in increased phosphorylation of Akt at S473 and HO-1 protein levels, but had no impact on Akt or HDAC3 levels. After knockdown of HDAC3, overexpression of XBP1u was only partially able to induce the phosphorylation of Akt-S473 and HO-1 expression. In the presence of HDAC3, XBP1u resulted in a 7-fold increase in HO-1 expression and a 6-fold increase in Akt-S473 phosphorylation. In the absence of HDAC3, XBP1u was only able to induce 2-fold increase in HO-1 expression and a 3-fold increase in Akt-S473 phosphorylation. These data demonstrate that HDAC3 is crucial for the correct induction of Akt-phosphorylation and HO-1 expression by XBP1u.

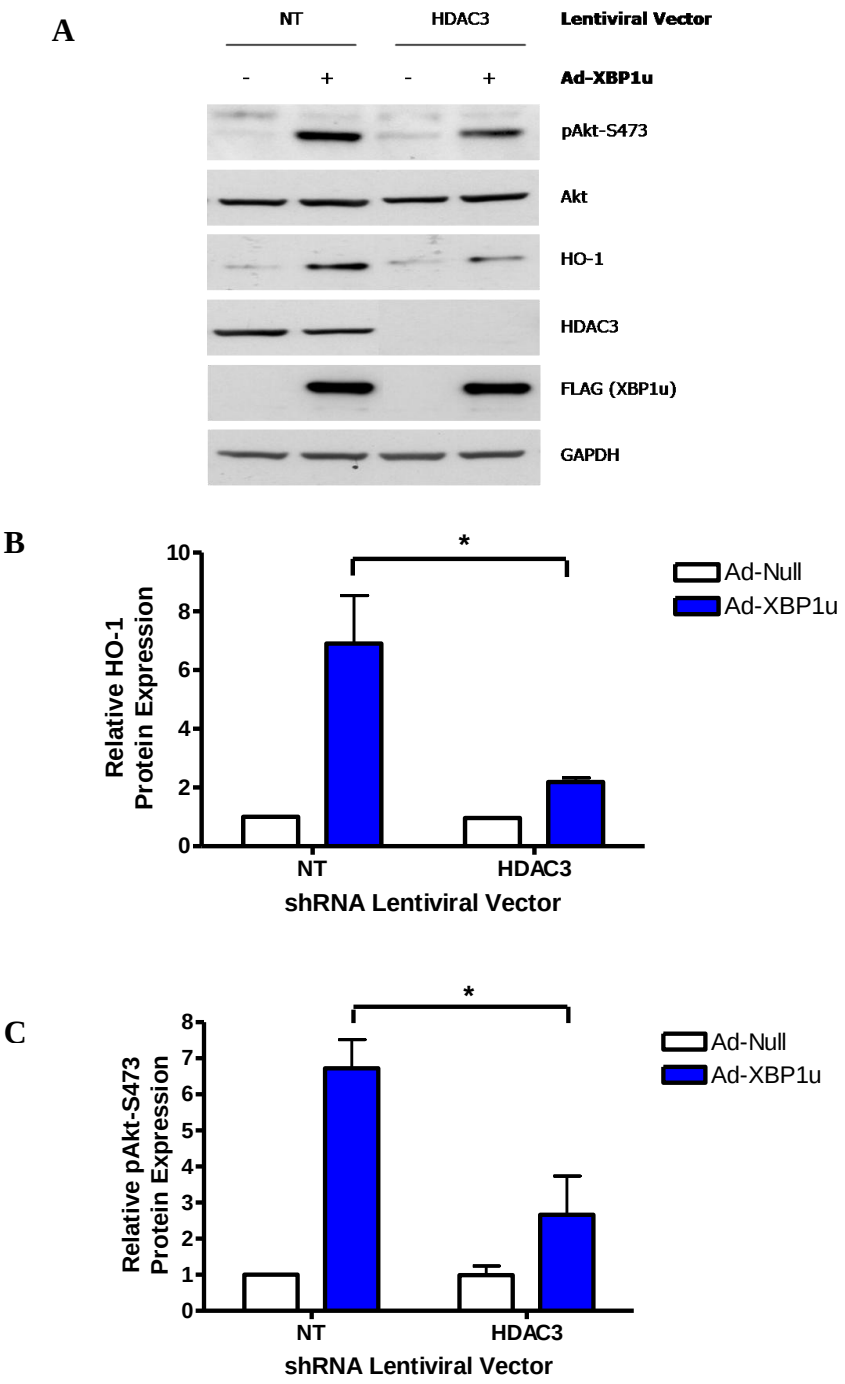

Figure 46: XBP1u-mediated induction of HO-1 expression and phosphorylation of Akt-S473 is inhibited by knockdown of HDAC3.

HUVECs were transduced with 100 TU / cell of shRNA-NT and shRNA-HDAC3 lentivirus and then again with 10MOI of Ad-Null or Ad-XBP1u adenovirus 48 hours post-transduction. **A.** The protein was harvested 48 hours after the second transduction for Western Blotting of phosphorylated S473-Akt, Akt, HDAC3, HO-1 and XBP1u (FLAG) expression. Densitometry analysis was performed on the protein expression of **(B)** HO-1 and **(C)** pAkt-S473 to determine relative protein expression changes. The images are representative and the histogram depicts mean and standard deviation of three independent experiments. * $P < 0.01$.

3.4.6 XBP1u and HDAC3 physically interact

We have demonstrated that XBP1u and HDAC3 play a very similar role in ECs. Firstly, overexpression of both XBP1u and HDAC3 is sufficient to induce Akt-S473 phosphorylation. Secondly, overexpression of XBP1u and HDAC3 results in very similar changes to gene expression patterns. Finally, XBP1u and HDAC3 are both induced by disturbed flow; however neither protein influences the expression of the other. We hypothesised that HDAC3 and XBP1u physically interact and that this interaction might activate signalling pathways involving Akt. Several XBP1u and HDAC3 expression constructs were created to aid these studies (figure 47A, 47C, 48A and 49A).

Initially HA-tagged XBP1u and Flag-tagged HDAC3 were overexpressed in HUVECs through FUGENE-mediated transfection. The protein was harvested 72 hours after transfection and protein was immunoprecipitated with anti-HA agarose beads. The presence of HDAC3 (Flag) and XBP1u (HA) was detected by Western blotting (figure 47B). Flag-tagged HDAC3 was able to bind to XBP1u and interact within HUVECs.

This experiment was repeated using Flag-tagged HDAC3, Flag-tagged XBP1u, anti-HDAC3 agarose beads and anti-Flag agarose beads. Both Flag-tagged HDAC3 and XBP1u were transfected into HUVECs. The protein was harvested after 72 hours. The sample was then incubated with anti-Flag conjugated agarose beads and anti-HDAC3 conjugated agarose beads. The control is performed using agarose beads conjugated to an anti-IgG antibody. The proteins were then eluted and the presence of HDAC3 and XBP1u (Flag) was detected by Western blotting (figure 47D). These data demonstrate that HDAC3 and XBP1u interact within HUVECs.

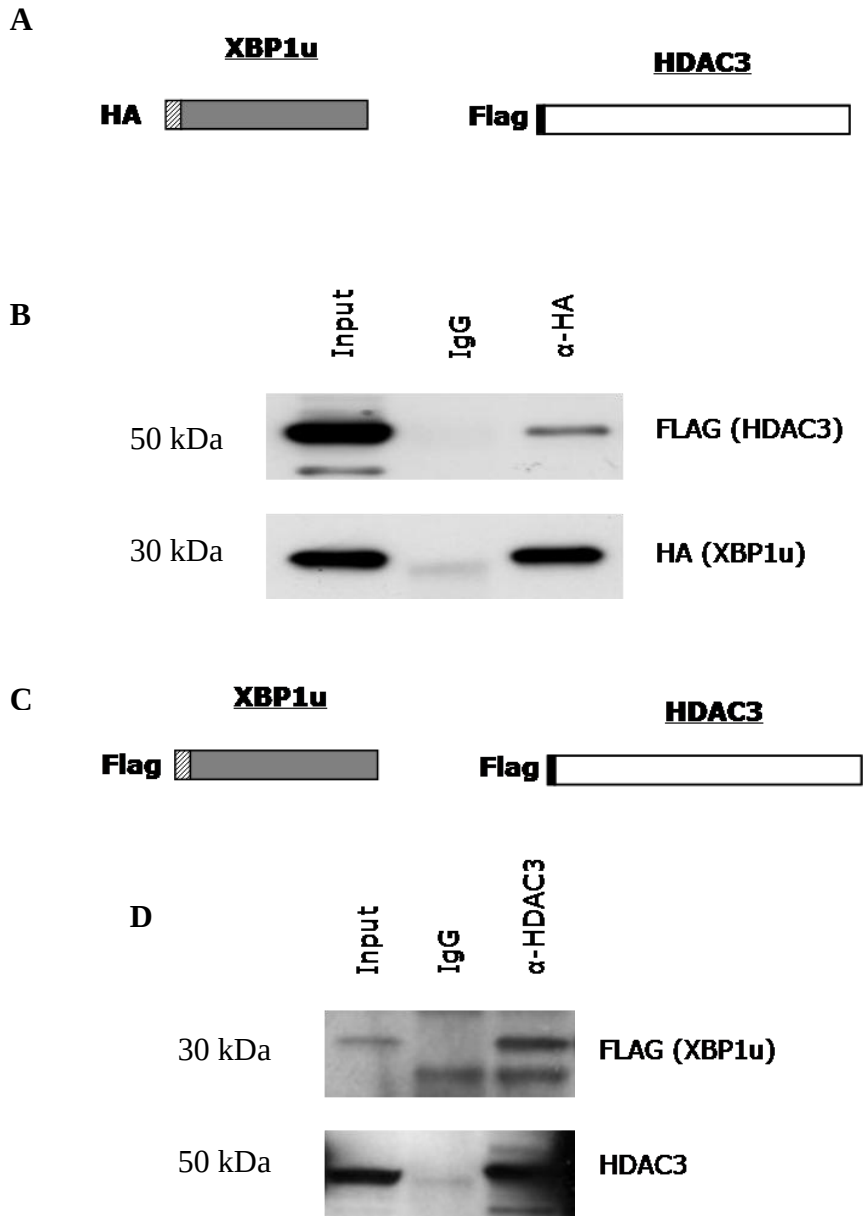

Figure 47: XBP1u interacts with HDAC3.

The interaction between XBP1u and HDAC3 was assessed through co-immunoprecipitation of the protein. **A.** Schematic diagram of the transfected XBP1u and HDAC3 proteins with their attached N-terminal tags. **B.** HUVECs were transfected with 1.5µg pShuttle2-HDAC3-FLAG and 1.5µg pShuttle2-XBP1u-HA vectors. The protein was harvested for co-immunoprecipitation 72 hours after transfection. The protein sample was precipitated with anti-HA agarose beads. The attached proteins were then eluted from the beads and XBP1u and HDAC3 were detected by Western blotting. **C.** Schematic diagram of the transfected XBP1u and HDAC3 proteins with their attached N-terminal tags. **D.** HUVECs were transfected with 1.5µg pShuttle2-HDAC3-FLAG and 1.5µg pShuttle2-XBP1u-FLAG vectors. The protein was harvested for co-immunoprecipitation 72 hours after transfection. The protein sample was precipitated with anti-HDAC3 and anti-FLAG agarose beads. The attached proteins were then eluted from the beads and XBP1u and HDAC3 were detected by Western blotting.

Having identified that XBP1u and HDAC3 are able to interact, we attempted to determine the HDAC3 domain responsible for the interaction. Previously our lab has demonstrated that HDAC3 interacts with Akt through residues 136-206 of HDAC3 (Zampetaki et al., 2010). We cloned two N-terminal and three C-terminal HDAC3 deletion mutations. These were Flag-tagged at the N-terminus and co-transfected with HA-tagged XBP1u (figure 48A). Immunoprecipitation experiments were performed using anti-HA conjugated agarose beads to collect XBP1u from the sample. Western blots were then performed with antibodies targeted against the Flag tag, to detect the HDAC3 mutations and the HA-tag to detect XBP1u (figure 48B). Both HDAC3 N-terminal deletion constructs (HD3C1 and HD3C2) were able to interact normally with XBP1u. Of the C-terminal deletion constructs, only the largest C- (HD3N3) was able to interact with XBP1u. Therefore residues 201-323 are crucial in mediating the interaction between HDAC3 and XBP1u. These results are very interesting as XBP1u interacts with HDAC3 through a completely different site on the HDAC3 protein. There is therefore the possibility that XBP1u and Akt can interact with HDAC3 at the same time and possibly binding of one may promote or hinder the interaction of the other.

3.4.7 HDAC3 interacts with Akt and this occurs in the presence of XBP1u

HDAC3 has already been identified to interact with Akt (Zampetaki et al., 2010). We sought to repeat this experiment and investigate the effect of XBP1u on this interaction. HA-tagged HDAC3 was overexpressed in HUVECs and the protein was harvested, purified and incubated with anti-HDAC3 conjugated agarose beads. The proteins bound to the anti-HDAC3 antibody were eluted and the presence of HDAC3 and Akt was determined by Western blotting (figure 49A). Akt was pulled down and therefore interacts with HDAC3.

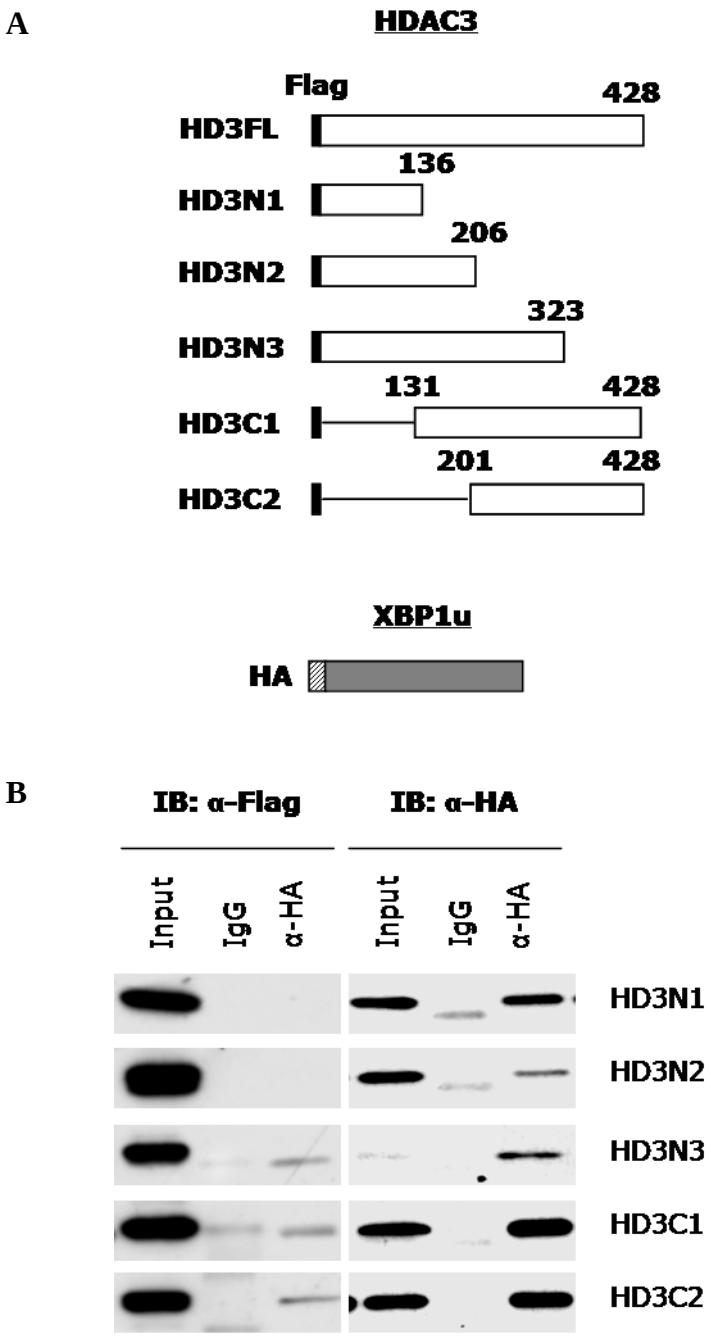

Figure 48: XBP1u interacts with residues 131-206 of HDAC3.

A. Schematic diagram of the HDAC3 deletion mutations and XBP1u and the attached N-terminal tags. **B.** HUVECs were transfected with 1.5µg pShuttle2-HDAC3-FLAG (and mutation variants) and 1.5µg pShuttle2-XBP1u-HA vectors. The protein was harvested for co-immunoprecipitation 72 hours after transfection. The protein sample was precipitated with anti-HA agarose beads. The attached proteins were then eluted from the beads and XBP1u (HA) and HDAC3 mutations (Flag) were detected by Western blotting. The images are representative of three independent experiments.

To determine the effect of XBP1u on the interaction between HDAC3 and Akt we overexpressed XBP1u and looked to see if any differences were observed in the ability of Akt to bind HDAC3. HA-tagged HDAC3 was transfected into HUVECs and then HUVECs were transduced with 10 MOI of Ad-XBP1u adenovirus. After 48 hours the protein was collected and co-immunoprecipitated with anti-HDAC3 conjugated agarose beads. The protein was eluted and the presence of HDAC3, Akt and XBP1u (Flag) was detected by Western blotting (figure 49B). In the presence of XBP1u, HDAC3 still interacts with Akt. We also found that XBP1u binds to HDAC3 at the same time. Therefore, HDAC3 is able to bind Akt and XBP1u and the overexpression of XBP1u does not inhibit the binding of Akt. Indeed, there is also a slight indication that the presence of XBP1u might enhance the ability of Akt to interact with HDAC3, although this cannot be confirmed through this experiment.

Our results have demonstrated that XBP1u is crucial in maintaining EC integrity and survival. During disturbed flow XBP1u is upregulated and plays a critical role in stabilising HDAC3. We demonstrate that XBP1u and HDAC3 enhance the phosphorylation, and thereby the activation, of Akt at S473. Activated Akt induces the expression of HO-1 and XBP1u is also crucial for this. Furthermore, XBP1u and Akt interact with HDAC3 and the overexpression of XBP1u does not complete with Akt for a binding site. HDAC3 is crucial in XBP1u-mediated activation of Akt phosphorylation and HO-1 expression as this is prevented by ablation of HDAC3 expression. We hypothesise that under disturbed flow conditions the expression (transcription and translation) of XBP1u is augmented. XBP1u can then bind to HDAC3 and promote its stabilisation. Akt is then recruited to HDAC3 and undergoes phosphorylation activating downstream anti-apoptotic signalling pathways. In particular we have demonstrated that Akt-mediated upregulation of HO-1 requires XBP1u and that disturbed flow acts through VEGFR2 and PI-3-kinase to initiate the stabilisation of HDAC3 and augment the expression of XBP1u. The blots have been modified as they have been performed alongside another experiment which is not relevant to this story.

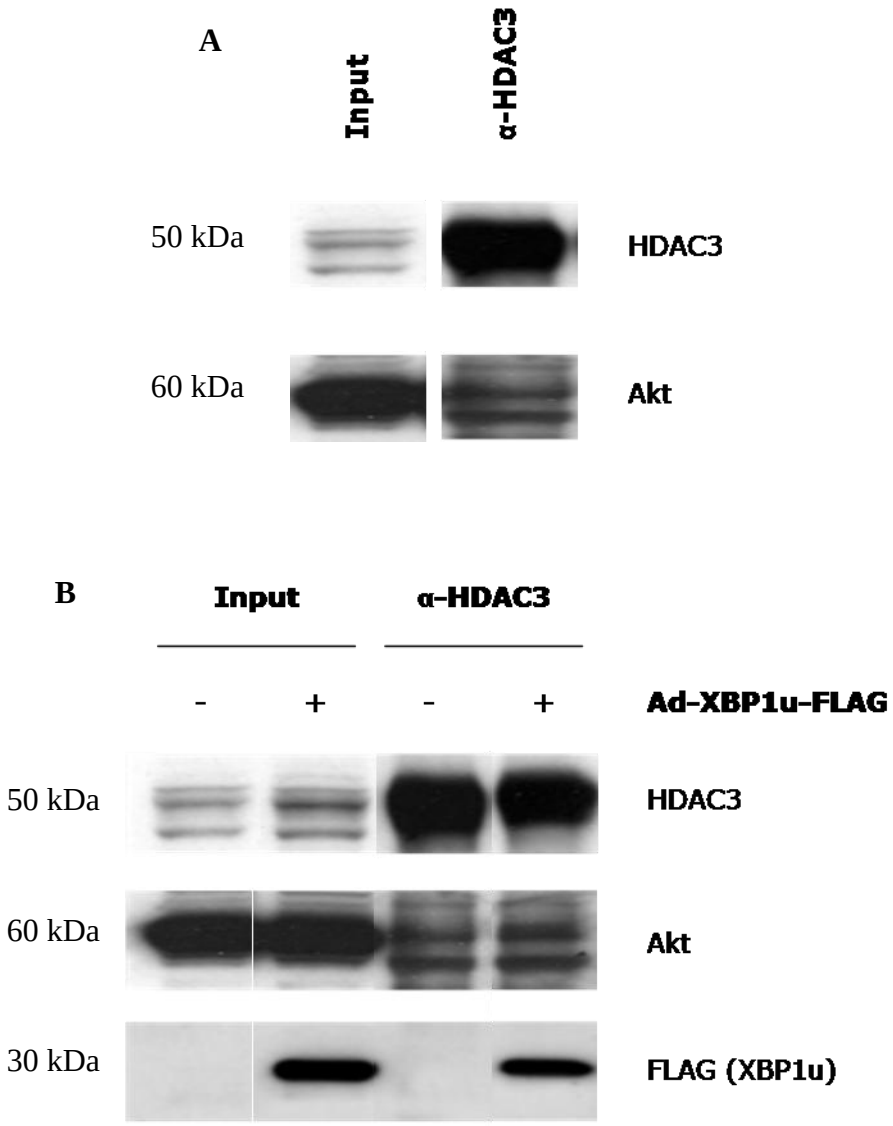

Figure 49: HDAC3 interacts with Akt and XBP1u simultaneously.

A. HUVECs were transfected with pShuttle2-HDAC3-HA plasmid. The protein from the HUVECs was harvested 72 hours post-transfection. The ability of HDAC3 to bind Akt was assessed by co-immunoprecipitation using anti-HDAC3 agarose beads and subsequent Western blotting with HDAC3 and Akt antibodies. **B.** HUVECs were transfected with pShuttle2-HDAC3-HA plasmid. They were then transduced with 10 MOI of Ad-XBP1u adenovirus. The protein from the HUVECs was harvested 72 hours post-transfection. The ability of HDAC3 to bind Akt and XBP1u was assessed by co-immunoprecipitation using anti-HDAC3 agarose beads and subsequent Western blotting with HDAC3, Akt and FLAG (XBP1u) antibodies. The images have been cropped from an original single Western blot for ease of analysis. The images are representative of three independent experiments.

3.5 XBP1 promotes EC migration

Microarray analysis of gene expression pattern alterations after overexpression of XBP1u demonstrated that several genes related to cell migration were affected (figure 18A, 18C and 18D). It was also apparent that overexpression of XBP1u influences the alignment and morphology of HUVECs under standard conditions (figure 13A). We hypothesised that XBP1u influences cell pathways involved in attachment and movement. Therefore the role of both isoforms of XBP1 in EC migration was investigated.

3.5.1 XBP1u influences HUVEC morphology

We have demonstrated that overexpression of XBP1u results in a 'healtheir' EC phenotype. The effect of XBP1 knockdown on HUVEC morphology was investigated after treating HUVECs with shRNA-XBP1 lentiviral constructs. The morphology of the cells was determined 72 hours after transduction via light microscopy (figure 50B). Overexpression of XBP1u elongates the appearance of the EC monolayer. After knockdown of XBP1 the ECs again have a more elongated morphology. These cells also appeared to be larger and demonstrated increased directionality. The cell number and size of HUVECs transduced with shRNA-XBP1 as compared to shRNA-NT transduced control cells was determined (figure 50C-D). These data demonstrate that knockdown of XBP1 creates an altered EC morphology and reduces EC number.

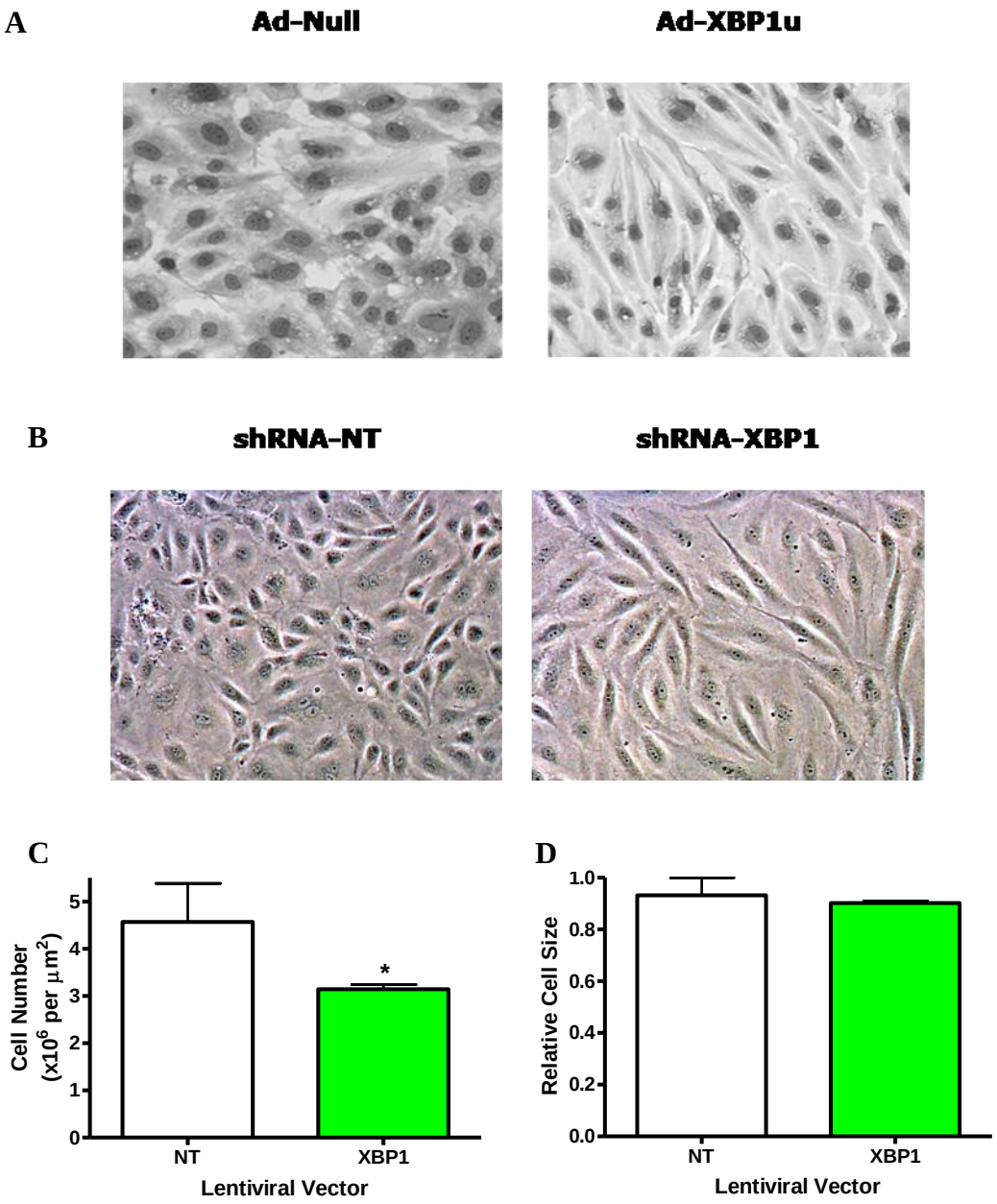

Figure 50: Overexpression and knockdown of XBP1 influence HUVEC morphology and cell number.

A. HUVECs were transduced with 10 MOI of Ad-Null or Ad-XBP1u adenoviral vectors and observed under a light microscope 48 hours post-transduction. **B.** HUVECs were transduced with 100 TU / cell of shRNA-NT and shRNA-XBP1 lentivirus. 48 hours post-transduction the HUVECs were observed and pictures were taken through a light microscope. The (**C**) cell number and (**D**) cell size were calculated after knockdown of XBP1. The images and data are representative of three independent experiments. * $P < 0.01$.

3.5.2 Overexpression of XBP1 increases the rate of HUVEC migration

To determine if XBP1 influences EC migration we performed wound healing assays. HUVECs were transduced with 10 MOI of Ad-Null, Ad-XBP1u or Ad-XBP1s adenoviruses. The ability of HUVECs to migrate was calculated subsequent to transduction and wound formation (figure 51A). The distance migrated was then calculated for each time point and treatment as compared against the distance covered by Ad-Null transduced cells migrating for 4 hours (figure 51B). Overexpression of XBP1u and XBP1s increased the speed of EC migration by 20% after 4 hours. A similar increase of 20% was observed after the cells were left to migrate for 8 hours. These data demonstrate that XBP1u and XBP1s significantly increase the speed of EC migration, particularly immediately after the wound has been created. These experiments were repeated in low serum (2%) media to reduce the influence of cell proliferation on the results. The data is not shown, but the same response was observed.

3.5.3 Knockdown of XBP1 reduces the speed of EC migration

Overexpression of exogenous XBP1u and XBP1s increase the rate of EC migration. Does knockdown of XBP1 also reduce the ability of HUVECs to migrate? HUVECs were transduced with shRNA-NT and shRNA-XBP1 lentiviruses and the ability of HUVECs to migrate was determined via wound healing assay (figure 52A). The relative speed of migration was calculated by comparing the area covered by HUVECs at the 4 and 8 hour time points with the area migrated by HUVECs transduced with shRNA-NT after 4 hours (figure 52B). Knockdown of XBP1 resulted in a 30-35% decrease in the speed of HUVEC migration. This decrease was significant and implies that XBP1 promotes normal cell migration. These experiments were repeated in low serum (2%) media to reduce the effects of cell proliferation on the results. The data is not shown here but the same response was observed.

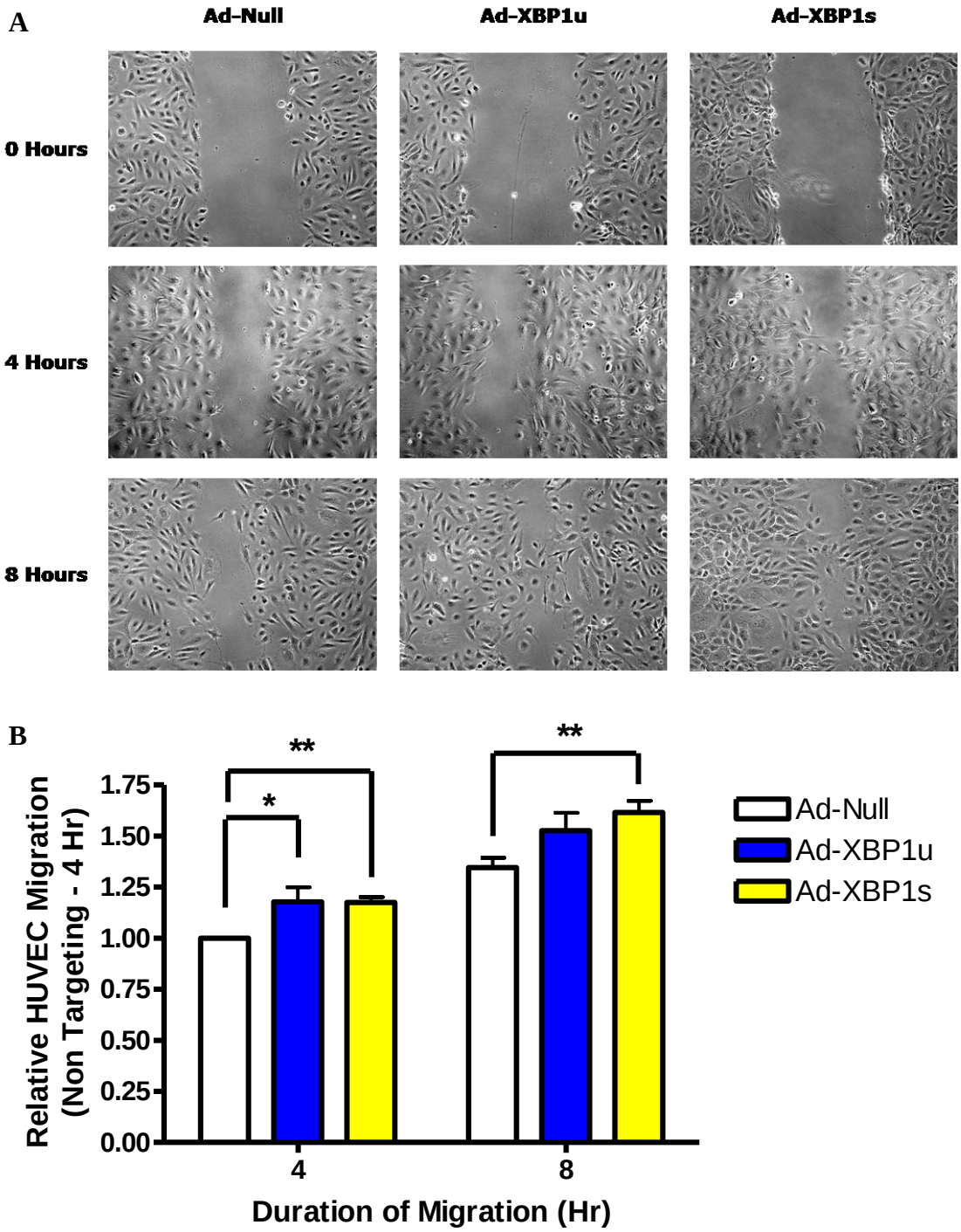

Figure 51: Overexpression of XBP1u and XBP1s increases HUVEC migration.

HUVECs were transduced with 10 MOI Ad-Null, Ad-XBP1u and Ad-XBP1s adenovirus. **(A)** HUVEC migration was assessed at 4 and 8 hour time points by scratch assay, 24 hours post-transduction. **(B)** The degree of HUVEC migration was determined relative to the migration of Ad-Null transduced cells after four hours. The images are representative and the histogram shows the mean and standard deviation of eight independent experiments. * $P < 0.05$, ** $P < 0.005$.

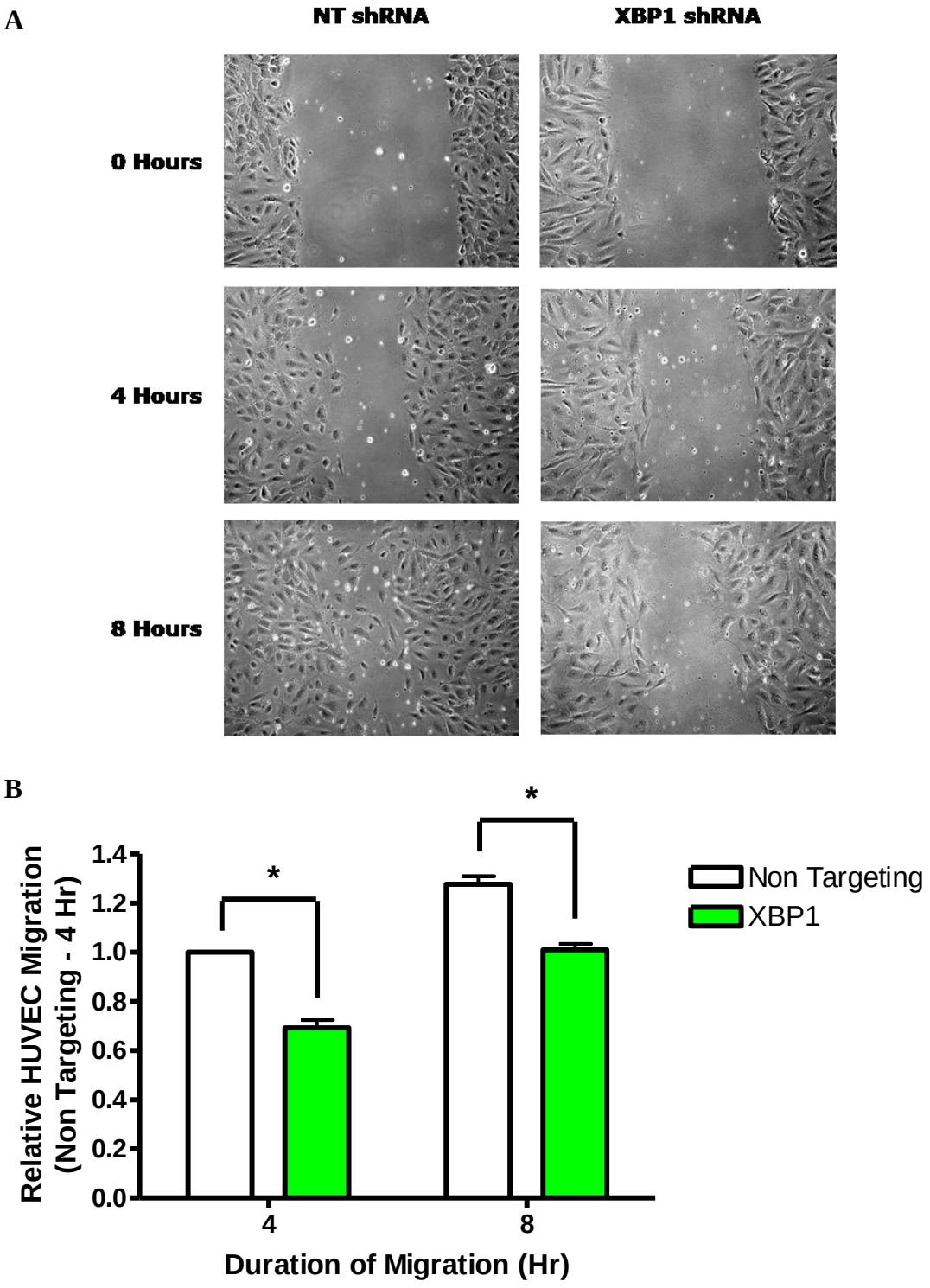

Figure 52: Knockdown of XBP1 decreases HUVEC migration.

HUVECs were transduced with 100 TU / cell of shRNA-NT and shRNA-XBP1 lentivirus. **(A)** HUVEC migration was assessed at 4 and 8 hour time points by scratch assay, 72 hours post-transduction. **(B)** The degree of HUVEC migration was determined relative to the migration of shRNA-NT transduced cells after four hours. The images are representative and the histogram shows the mean and standard deviation of nine independent experiments. * $P < 0.0001$.

3.5.4 Knockdown of IRE-1α reduces EC migration

Both isoforms of XBP1 appear to promote EC migration, although XBP1s appears to have a stronger effect. EC migration promotes high levels of stress in the cellular environment and requires a morphological change between cell types (De Smet et al., 2009). This requires the transcription of novel proteins and therefore there is the potential for the ER stress response to activate. IRE-1α is crucial in mediating the conversion of XBP1u into XBP1s. If the splicing process is crucial for EC migration then knock down of IRE-1α would adversely effect EC migration. HUVECs were transduced with shRNA-NT and shRNA-IRE-1α lentivirus. The ability of HUVECs to migrate was subsequently assessed via wound healing assay (figure 53A). The relative speed of migration was calculated by comparing the area covered by HUVECs at the 4 and 8 hour time points with the area migrated by HUVECs transduced with shRNA-NT after 4 hours (figure 53B). Knock down of IRE-1α resulted in a significant (20%) decrease in the ability of HUVECs to migrate. This response was especially pronounced during the initial stages of migration. These data demonstrate that XBP1, and the splicing of XBP1 in particular, is crucial for normal EC migration. These experiments were repeated in low serum (2%) media to reduce the effects of cell proliferation on the results. The data is not shown but the same response was observed.

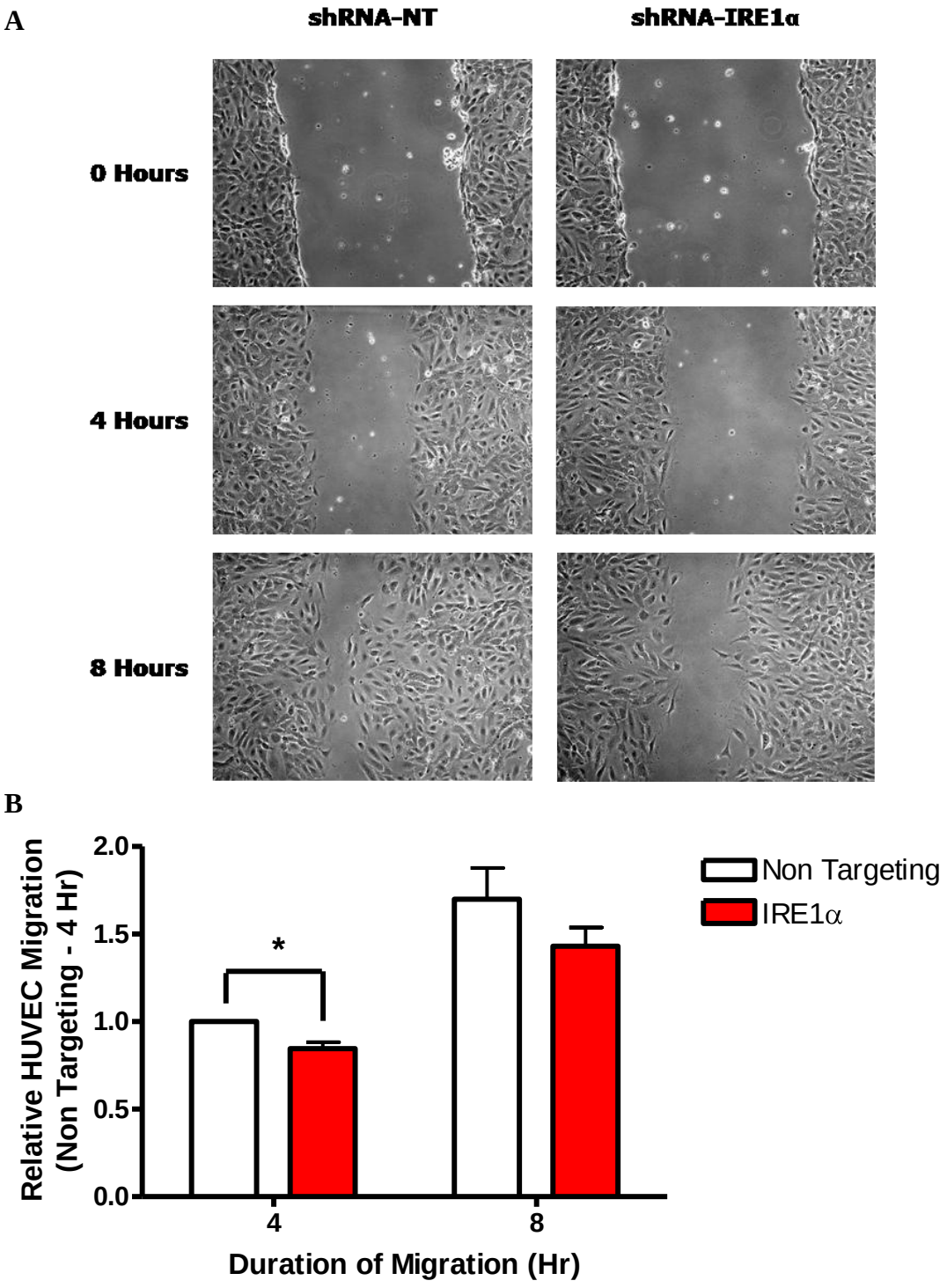

Figure 53: Knockdown of IRE-1α decreases HUVEC migration.

HUVECs were transduced with 100 TU / cell of shRNA-NT and shRNA-IRE1α lentivirus. **(A)** HUVEC migration was assessed at 4 and 8 hour time points by scratch assay, 72 hours post-transduction. **(B)** The degree of HUVEC migration was determined relative to the migration of shRNA-NT transduced cells after the four hour time point. The images are representative and the histogram shows the mean and standard deviation of six independent experiments. * $P < 0.005$.

3.5.4 XBP1 splicing is enhanced during EC migration

We have demonstrated that XBP1 splicing is crucial for proper EC migration, which implies that the expression of XBP1s would be increased during migration. To demonstrate this; HUVECs were induced to undergo migration and the expression of XBP1s was determined via Western blotting (figure 54). To determine if XBP1 splicing is enhanced during EC migration it was necessary to isolate ECs in a migratory phenotype. Over 100 scratch assays were performed on the same confluent HUVEC monolayer *in vitro*. Therefore, a large proportion of the ECs will be in a migratory phenotype in an attempt to close the gaps in the monolayer. The HUVECs were harvested 0, 6 and 24 hours after scratch assay induction and the expression of XBP1s was determined. The migration of ECs was assessed using microscopy. The expression of XBP1s is significantly enhanced during EC migration.

3.5.5 XBP1 does not influence eNOS expression or activity

Endothelial nitric oxide synthase (eNOS) plays a very important role in regulating vascular functions; from regulating vascular tone, to angiogenesis. eNOS has also been shown to be crucial in regulating endothelial progenitor cell mobilisation and angiogenic properties (Everaert et al., 2010). We were interested to see if XBP1 could influence the expression of eNOS and thereby regulate NO production. HUVECs were transduced with Ad-Null or Ad-XBP1u adenovirus and the mRNA and protein was harvested 24, 48 and 72 hours post-transduction. The expression of eNOS and XBP1u was determined by semi-quantitative PCR, real-time PCR and Western blotting (figure 55A-C). There were no significant changes in eNOS expression after overexpression of exogenous XBP1u. To determine the effect of XBP1 knockdown on eNOS expression HUVECs were transduced with shRNA-NT or shRNA-XBP1 lentivirus. The protein expression of eNOS and XBP1 was assessed 72 hours after transduction by Western blotting (figure 55D). Knock down of XBP1 did not affect eNOS protein expression. These data demonstrate that XBP1 does not influence the expression of eNOS at the transcriptional or translational level.

We hypothesised that XBP1 may exert an effect on NO activity. HUVECs were transduced with Ad-Null, Ad-XBP1u or Ad-XBP1s adenovirus and the level of nitrate in the supernatant was detected by ELISA (figure 56A). There were no significant differences in nitrate production after XBP1u and XBP1s overexpression. Next, HUVECs were transduced with shRNA-NT, shRNA-XBP1 (figure 56B) and shRNA-IRE-1α (figure 56C) lentivirus. There were no significant differences in nitrate production after knockdown of XBP1 or IRE-1α. To determine if NO production increases during EC migration HUVECs were induced to mass migrate via multiple scratch assays. NO production was detected via ELISA 0, 4, 8 and 24 hours after the wound induction. Migrating ECs produced more NO, although our previous experiments imply that this is not caused by increases in XBP1s.

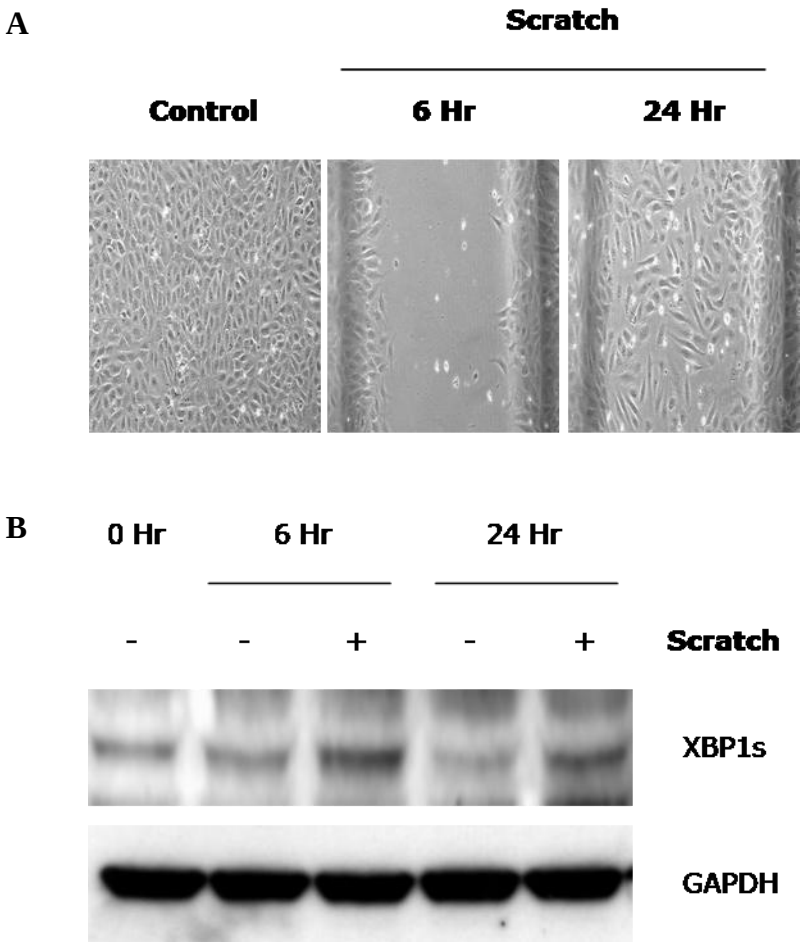

Figure 54: XBP1 splicing is increased during HUVEC migration.

A HUVEC monolayer was induced to migrate through creating multiple scratch wounds in the entire layer. The level of XBP1s mRNA was assessed by (**A**) semi-quantitative PCR and (**B**) real-time PCR. These images are representative of three independent experiments. * $P < 0.05$.

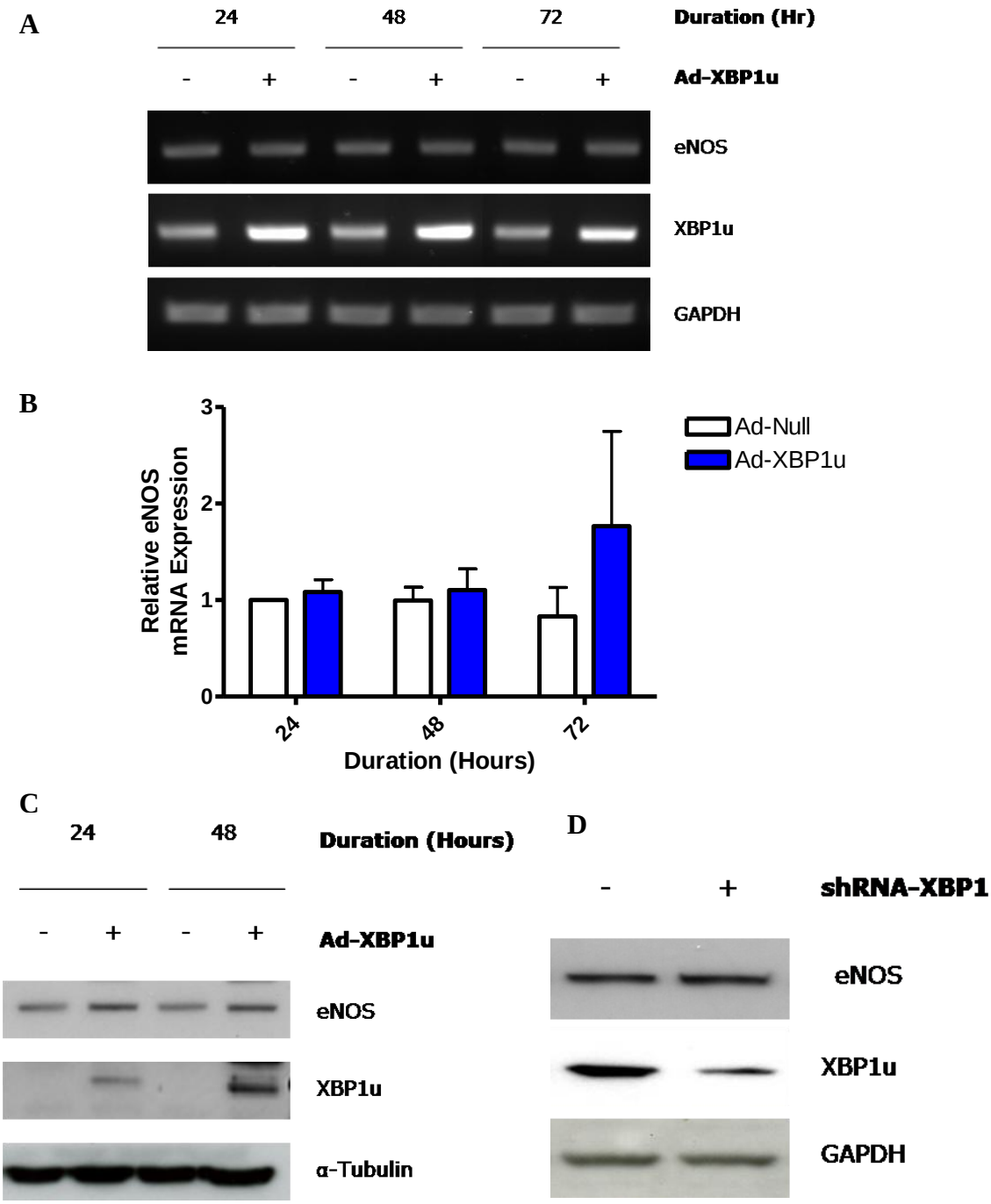

Figure 55: XBP1 has no effect on eNOS expression.

A. HUVECs were transduced with 10 MOI of Ad-Null or Ad-XBP1u adenoviruses. The mRNA and protein from the HUVECs was harvested 24, 48 and 72 (mRNA) hours post-transduction. The expression of eNOS was assessed by (**A**) semi-quantitative PCR (**B**) real-time PCR and (**C**) Western blotting. **D.** HUVECs were transduced with 100 TU / cell of shRNA-NT and shRNA-XBP1 lentivirus. Protein was harvested 72 hours post-transduction and the expression of eNOS, XBP1u, and GAPDH was determined by Western blotting. The images and histogram depicts mean and standard deviation of three independent experiments.

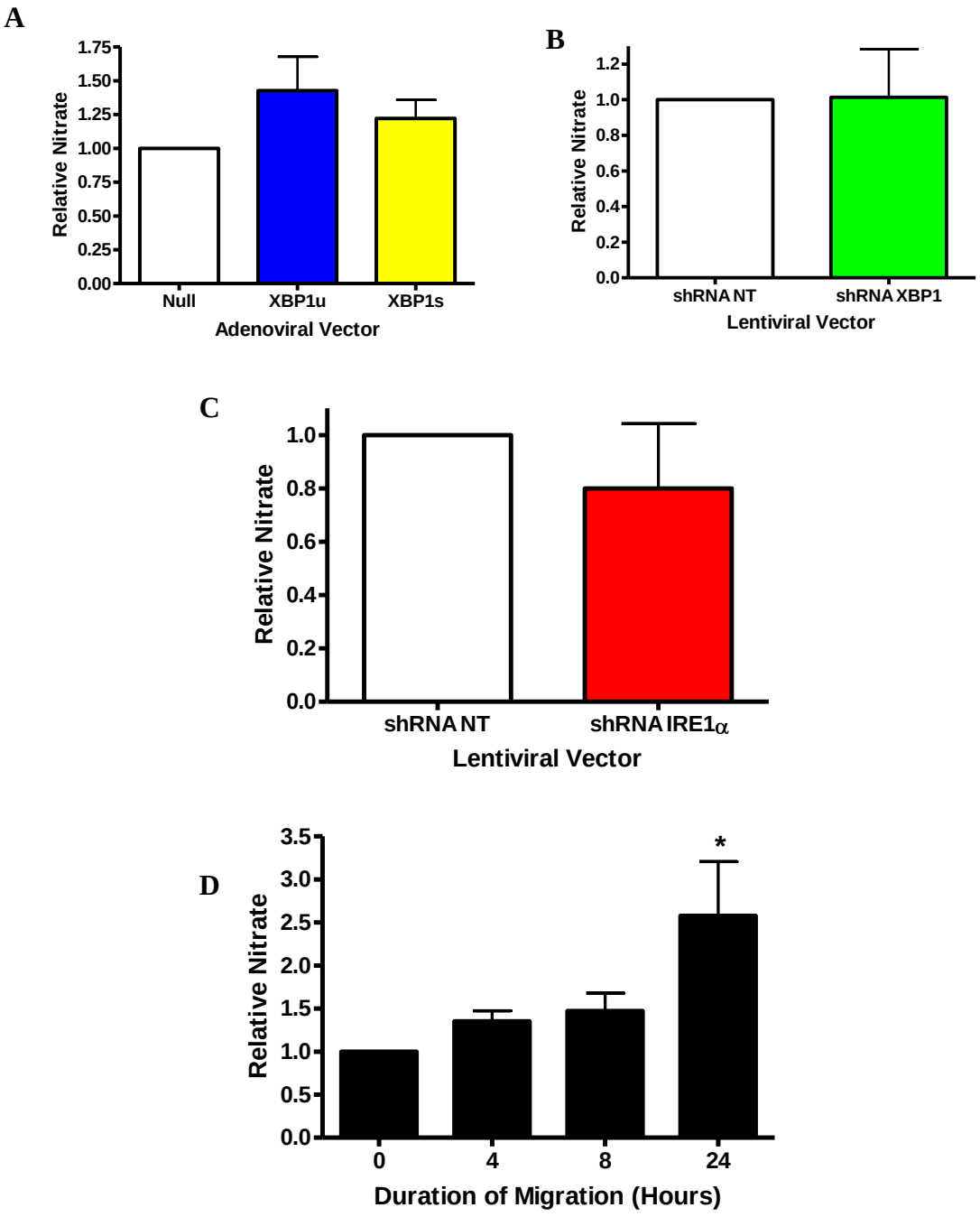

Figure 56: XBP1u and XBP1s do not influence the production of NO.

A. HUVECs were transduced with 10 MOI Ad-Null, Ad-XBP1u or Ad-XBP1s adenoviral vectors. The concentration of nitrate in the supernatant was detected via ELISA assay 48-hours post-transduction. The histograms depict mean and standard deviation of three independent experiments. HUVECs were transduced with 100 TU / cell of shRNA-NT and (**B**) shRNA-XBP1 lentivirus or (**C**) shRNA-IRE-1α lentivirus. The concentration of nitrate in the supernatant was detected via ELISA assay. **D.** The level of nitrate was assessed 0, 4, 8 and 24 hours after the induction of migration via scratch assay in HUVECs. The histograms depict mean and standard deviation of three independent experiments.

3.5.6 XBP1 heterozygous CMECs migrate normally

We wanted to determine if knockdown of XBP1 in primary ECs reduced their ability to migrate. We isolated wild type and XBP1 heterozygous coronary mouse ECs (CMECs) from 8-12 week old mice hearts. CMECs were isolated alongside Simon Walker according to the protocol designed in Professor Shah's (KCL, London) laboratory (Li et al., 2001). The morphology of the CMECs after 48 hours in culture is shown in figure 57A. The CMECs were characterised alongside Simon Walker and the expression of eNOS and CD31 was demonstrated in over 95% of the cells, whilst the expression of smooth muscle actin was absent (data not shown). Wild type and heterozygous XBP1 CMECs were subjected to wound healing assays (figure 57B). There was no significant difference in the ability of wild type and XBP1 heterozygous CMECs to migrate. It is impossible to compare CMECs from XBP1-null mice in this experiment as the global deletion of XBP1 is embryonic lethal. We were therefore unable to determine the effect of XBP1-knockdown in these cells on migration. In the case of the XBP1 heterozygous CMECs there remains one allele which contains a coding sequence for XBP1u, therefore in these cells it is possible that the quantity of XBP1u required in these cells is compensated for through increasing the activity of gene transcription at the remaining loci.

3.5.7 XBP1-null cells migrate less efficiently

To determine if XBP1-null cells migrate less efficiently we used cells from wild type and XBP1-null embryos. These cells are a mixed-population as described in the methods section. The morphology of these cells is shown in figure 58A. These cells were subjected to wound healing assays and the migration was characterised (figure 58B). XBP1-null cells had a significant reduction in their ability to migrate than their wild type compatriots. We have demonstrated that XBP1 is crucial for proper EC migration although the mechanism through which its effect is exerted remains to be determined.

3.5.8 Knockdown of XBP1 reduces EC migration and tube formation

To further confirm the role of XBP1 in EC migration Aortas from wild type and *Tie2-Cre / XBP1$^{f/f}$* mice were harvested and a 1-2mm ring segment was cut and cultured *in vitro.* The aortic ring was placed on low growth factor matrigel which had been incubated at 37°C for 30 minutes to allow it to harden and form a basement layer. The ring was then cultured in growth media for 72 hours and the area of EC outgrowth was calculated (figure 59A, 59C). The area was calculated by subtracting the area covered by endothelial cells from the total area of the matrigel basement. XBP1-null ECs were less able to migrate than their wild type counterparts.

One of the main functions of ECs is to form tubular structures. We knocked down XBP1 and IRE-1α and then plated the HUVECs on a low-growth factor matrigel and observed their ability to form tubular structures. Knock down of XBP1 significantly reduced the ability of HUVECs to form tubular structures. These data demonstrate that XBP1 is crucial in mediating EC migration.

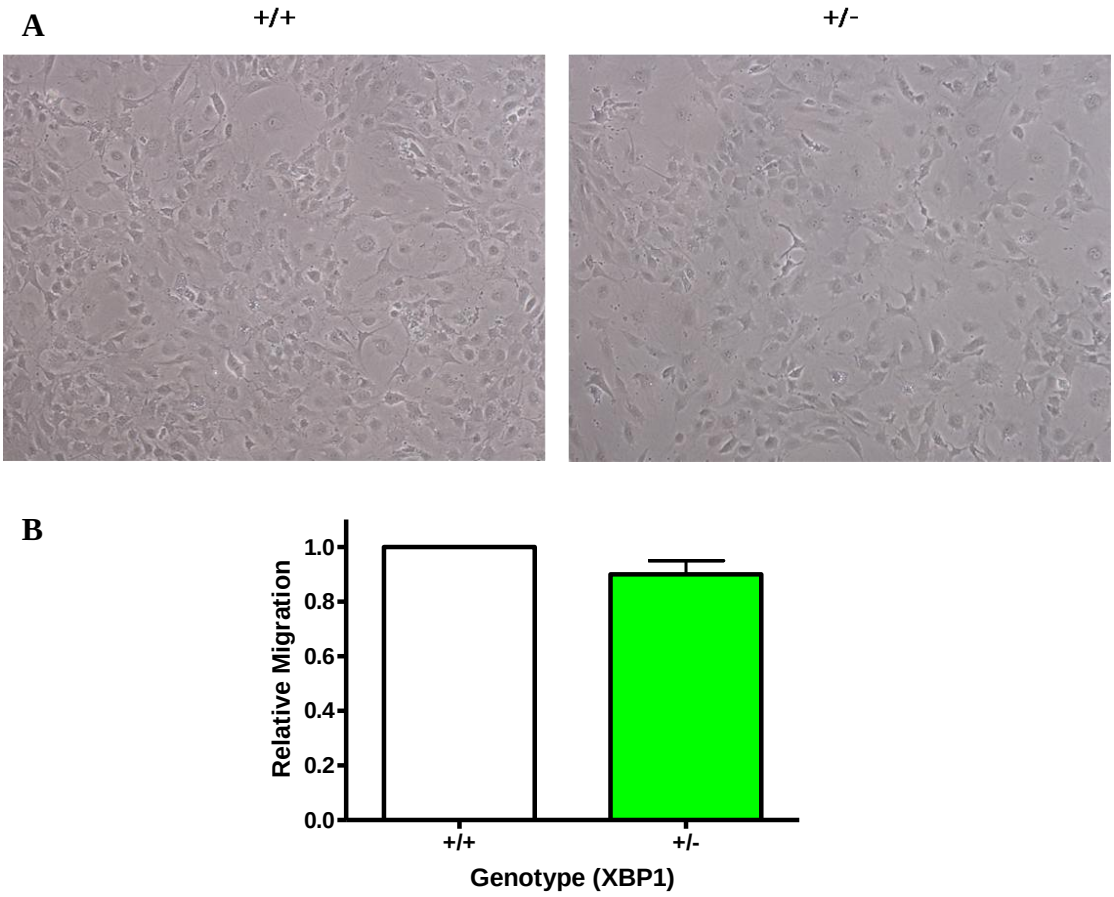

Figure 57: The ability of wild type and XBP1 heterozygous CMECs to migrate is similar.

A. The morphology of wild type and heterozygous CMECs. **B.** CMECs were induced to undergo migration through a scratch assay. The relative distance covered by wild type and heterozygous CMECs, after 4 hours of migration, was calculated and presented as a histogram. The images and histogram depict averages standard deviation of 6 independent experiments.

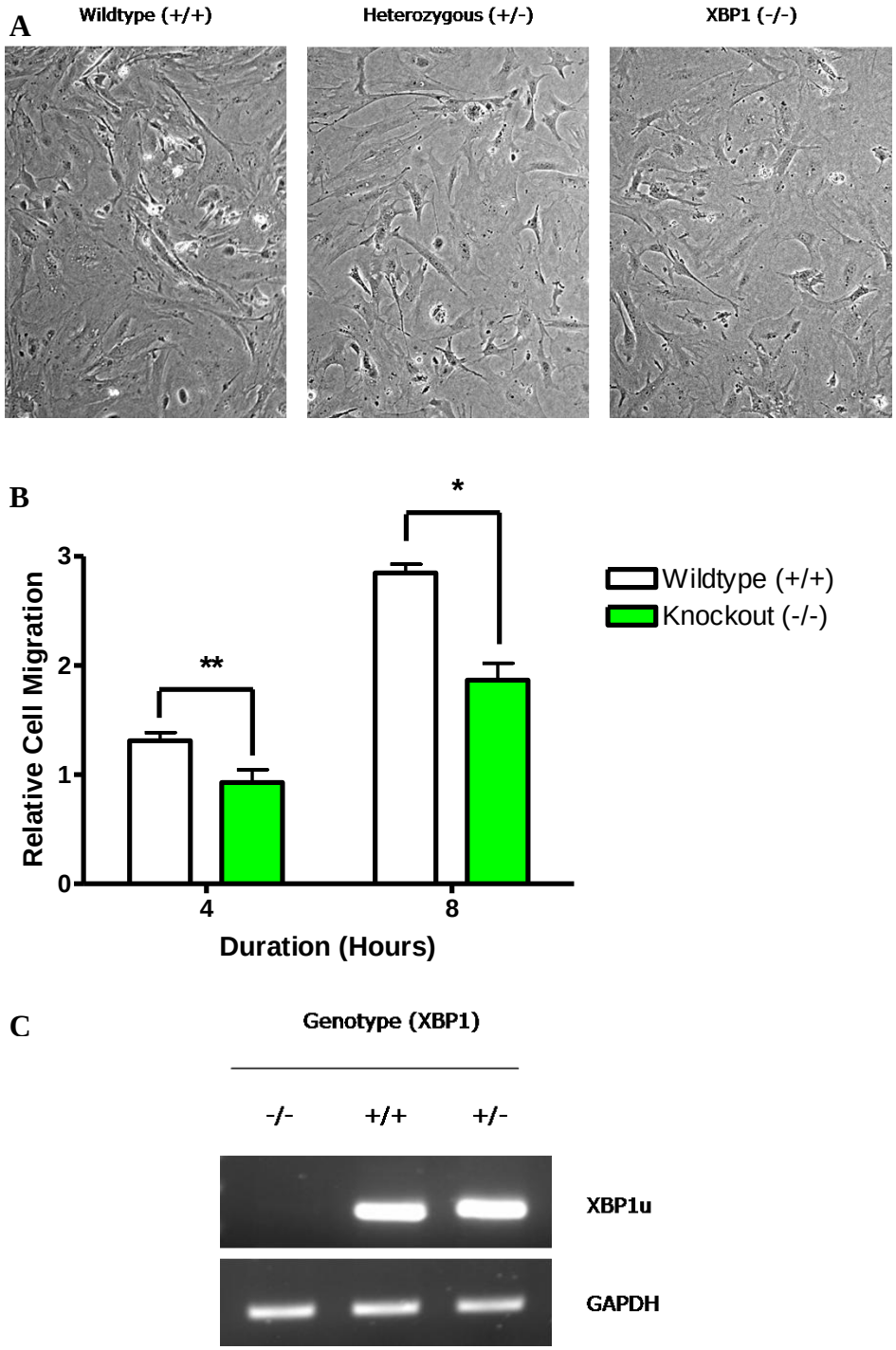

Figure 58: XBP1-Null embryonic cells migrate slower than wild type cells.

Embryonic day 13.5 embryos were removed from the mothers bred as XBP1 heterozygous crosses. **A.** The morphology of wild type, heterozygous and XBP1-null cell populations. **C.** The cells isolated from the embryo were cultured and the mRNA extracted for genotype analysis by semi-quantitative PCR. **B.** The cells were also subjected to migration analysis by scratch assay for 4 and 8 hours, where the migration was determined relative to that obtained from wild type cells after 4 hours of migration. The histogram depicts mean and standard deviation of 3 independent experiments performed on each of the cell lines from the 6 mice of each genotype. * $P < 0.0001$, ** $P < 0.01$.

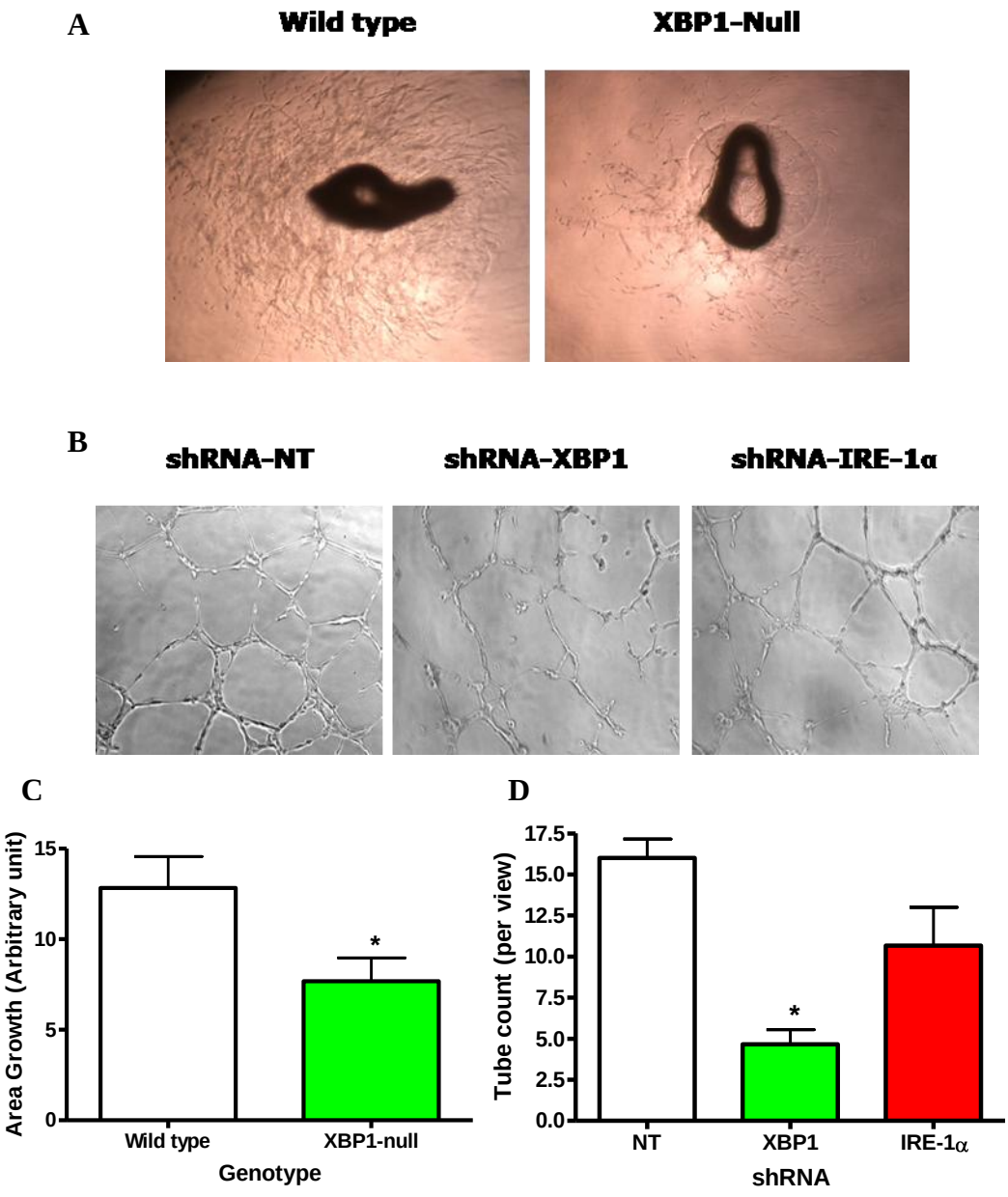

Figure 59: Knockdown of XBP1 reduces EC migration and tube formation.

A. Ring outgrowth assay. Aortas were harvested from wild type and *Tie2-Cre / XBP1$^{f/f}$* mice and ring sections were cut and grown in culture. The outgrowth of ECs was determined after 24 hours. **B.** Tube formation assay. HUVECs were transduced with shRNA-NT, shRNA-XBP1 or shRNA-IRE-1α lentiviruses. The HUVECs were then plated on low growth factor matrigel and tube formation was detected after 24 hours. **C.** Analysis of ring growth assay, the area migrated has been calculated relative to the size of the image. **D.** Analysis of tube formation. The tube count has been calculated as tubes per image. The images and histograms depict mean and standard variation of 5 independent experiments. * $P < 0.05$.

3.5.9 Knockdown of XBP1 reduces FAK expression

FAK, is crucial in mediating the signalling pathways involved in the migration of tip cells at the start of angiogenesis, therefore we investigated the role of XBP1 in mediating its expression. Endothelial sections from wild type and *Tie2-Cre / XBP1$^{f/f}$* mice were harvested and double immunofluorescence staining of CD31 and FAK was performed (figure 60). Knockdown of XBP1 resulted in significant decreases in the detection of expressed FAK. These data indicate that XBP1 may influence EC migration through mediating the FAK signalling pathway. In order to fully confirm the effect of XBP1u on FAK expression future studies will focus on Western blotting studies and semi- and real-time PCR. Negative staining controls were not performed therefore conclusions from this data are not as stringent as they could be. In future all staining will have negative controls alongside the staining.

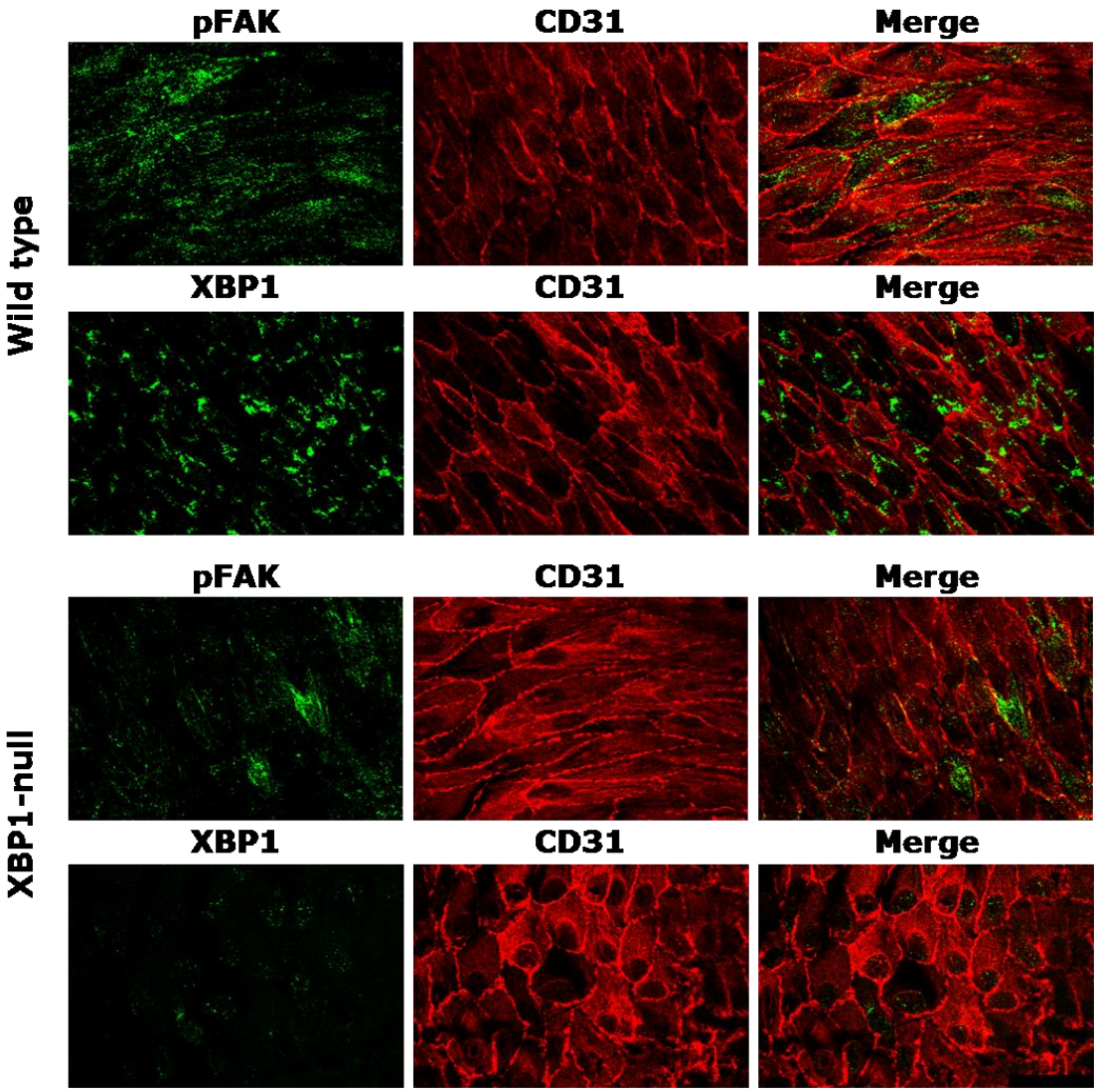

Figure 60: Knockdown of XBP1 reduces FAK expression.

Artery sections from wild type and *Tie2-Cre / XBP1*$^{f/f}$ mice were harvested and double immunostained for CD31 and FAK (or XBP1). The images are representative of five independent experiments.

We have demonstrated that XBP1 is crucial in mediating EC migration. Overexpression of XBP1 enhances the speed of migration, whilst knock down results in abrogated migration. We have also shown that XBP1 may mediate these effects through its influence of FAK expression.

Chapter 4 - Discussion

In the present study, the requirement of XBP1u for the constitutive expression of HO-1 is reported. We demonstrate that the expression of XBP1u is sufficient to induce the expression of HO-1 and the phosphorylation of Akt at serine 473. This study also demonstrates that there is a requirement for the expression of XBP1u to promote HO-1 expression via Akt activation. Furthermore, overexpression of XBP1u enhances the ability of ECs to survive under both normal and oxidative stress conditions, a state that is impaired through the loss of XBP1 expression. XBP1u-mediated induction of HO-1 expression is crucial for promoting EC survival under oxidative stress conditions. Moreover, the expression of XBP1u and HO-1 and the phosphorylation of Akt at serine 473 are enhanced in ECs under disturbed flow conditions. The expression of XBP1u is crucial for mediating the disturbed flow-induced upregulation of HO-1 expression and Akt phosphorylation at serine 473. Our findings indicate that XBP1u is crucial in promoting EC survival during oxidative stress, through activation of Akt signalling pathways and expression of HO-1. This study sheds new light on the mechanisms involved in protective signalling under flow and oxidative stress and provides evidence that XBP1u may be a novel target for therapeutic intervention in vascular disease.

This study has also identified a collaborative role between XBP1 and HDAC3. Knockdown of XBP1u prevents the disturbed flow-mediated upregulation of HDAC3, whilst knockdown of HDAC3 prevents XBP1u-mediated induction of Akt phosphorylation and HO-1 expression. This study demonstrates that XBP1u and Akt physically interact with HDAC3 and that this interaction can occur simultaneously. These data identify novel HDAC3 binding partners, further enhancing our knowledge of the role of HDAC3 externally to the nucleus.

Furthermore, this study demonstrates a requirement for XBP1 in promoting EC migration. The overexpression of XBP1u and XBP1s is sufficient to enhance the EC migration, whilst the knockdown of XBP1 and IRE-1α slows EC migration. We demonstrate that XBP1 splicing is enhanced during the initial stages of EC migration. Moreover, the expression of XBP1 is crucial in mediating the migration of primary ECs and in promoting EC tube formation. Our preliminary studies indicate that

XBP1-mediated regulation of FAK is responsible for mediating its effects on migration. Our findings indicate that XBP1 is crucial for proper EC migration. This data sheds new light on the mechanisms involved during the initial stages of angiogenesis and implicates XBP1 as a mediator of EC migration and integrity. This study provides evidence that XBP1 may be a novel target for therapeutic intervention during vascular disease.

4.1 XBP1 as a mediator of EC survival during shear stress

The study of ECs and their function is inherently complex due to the nature of their environment. The human vasculature is a highly adaptable and mobile organ, which is subjected to a wide range of stresses. One of the key features of ECs is their ability to sense and respond to shear stress. The effect that shear stress exerts on ECs differs due to the location, pressure, direction and speed of the force detected. ECs in linear regions of the vasculature are exposed to strong, pulsatile, unidirectional shear stress. ECs exposed to high time-averaged, unidirectional shear stress are less susceptible to EC apoptosis and atherosclerosis (Cheng et al., 2006; Kadohama et al., 2007). The protective response of ECs to normal blood flow is predicted to involve mechanoreceptors, which transmit signals across the cell membrane, inducing gene transcription (Chien, 2008a, b; Johnson et al., 2011). Laminar flow also induces the expression of antioxidant molecules, such as peroxiredoxin, which reduce the oxidative stress in the endothelium (Mowbray et al., 2008). In contrast, regions of the endothelium that experience low time-averaged shear stress and oscillatory or disturbed flow have only transient activation of these protective signalling pathways and are more susceptible to apoptosis and atherosclerotic lesion formation (Tricot et al., 2000; White et al., 2001). Importantly, the variations in shear stress promote different outcomes in ECs. Low shear stress and oscillatory shear stress are both associated with atherosclerotic lesion formation, however only low shear stress was associated with inflammatory responses and correlated with the likelihood of lesion rupture (Cheng et al., 2006). Disturbed flow has also been implicated in promoting oxidative stress through the promotion of ROS via upregulation and activation of NADPH oxidase (Hwang et al., 2003a; Hwang et al., 2003b). Increased production of ROS also reduces the bioavailability of NO, an atheroprotective molecule, through

incorporation as peroxynitrate, further exacerbating oxidative stress (Harrison et al., 2006). Disturbed flow and sustained production of ROS can result in EC apoptosis (Tricot et al., 2000). Hydrogen peroxide is commonly used to study oxidative stress-induced apoptosis, due to its ability to permeate aqueous and lipid environments. Oxidative stress induces apoptosis through caspase-3 activation, upregulation of p53 and sustained activation of JNK MAP kinase pathway signalling (Cook et al., 1999; Purdom and Chen, 2005). Oxidative stress can induce apoptosis and increase EC turnover and lipid deposition, leading to a greater risk of atherogenesis. The expression and activation of many atheroprotective and atherogenic genes has been linked to flow patterns (Dekker et al., 2006; Dekker et al., 2002; Dekker et al., 2005; Surapisitchat et al., 2001).

In this study, we explored the role of XBP1 in the vascular system. Previous studies have demonstrated that the expression of XBP1 in ECs during the ER stress response mediates vascular inflammation and EC dysfunction during atherosclerosis development (Gargalovic et al., 2006). We were curious to clarify the role of XBP1 in maintaining EC integrity and atherosclerotic lesion formation. Our studies demonstrate that the expression of XBP1 is intricately linked to flow pattern. Very little XBP1 was detected in ECs comprising linear regions of the vasculature. In contrast, XBP1 was highly expressed in bifurcation regions, subjected to disturbed flow, and around atherosclerotic lesions, which also create altered flow patterns. XBP1 has been shown to be ubiquitously expressed; however our data is the first to link the expression of XBP1 to shear stress (Clauss et al., 1993). To clarify the role of flow in the expression of XBP1u we used an *in vitro* disturbed flow model. Our flow model results in reduced, oscillatory time-averaged shear stress, although the range of shear stress experienced by individual ECs can range from 0 to 20 dyn/cm^2. Other methods that can be used to study the effects of disturbed flow *in vitro* include the step-flow chamber that allows a comparison between disturbed and laminar flow (Chien, 2008a). Our model of disturbed flow was used as it is easy to replicate the identical conditions for multiple experiments and the equipment is more widely available. Disturbed flow resulted in transient increases to XBP1s expression and a stable increase in the expression of XBP1u. Our studies previously identified that chronic expression of XBP1s results in EC apoptosis and atherosclerotic lesion formation (Zeng et al., 2009). These studies also demonstrated that laminar flow only

induced a transient activation of XBP1u expression. These results correlate as the onset of laminar flow is sensed by ECs as disturbed flow, as it is an environmental state to which they have not adapted. Combined, these data demonstrate that XBP1u is uniquely upregulated by disturbed flow conditions.

The role of XBP1u in cells remains poorly defined, although a functional role has previously been computationally predicted (Nekrutenko and He, 2006). However, a recent study demonstrated that XBP1u acts as a negative regulator of XBP1s (Yoshida et al., 2006). In an elegant series of experiments it was demonstrated that the expression of XBP1u is increased during the recovery phase, after ER stress has been ablated. Using XBP1u mutation constructs it was determined that XBP1u contains a conventional nuclear export signal and can shuttle between the nucleus and the cytoplasm. It was subsequently demonstrated that XBP1u and XBP1s form a complex that localises to the cytoplasm. This complex is targeted for proteosome-mediated degradation by the degradation domain present on XBP1u (Yoshida et al., 2006). We have also confirmed that XBP1u prevents EC apoptosis through targeted degradation of XBP1s. However, our data also demonstrates that XBP1u is functional in its own right and promotes EC survival. Knockdown of XBP1 was sufficient to reduce EC survival under normal culture conditions. Furthermore, overexpression of XBP1u increased the ability of ECs to survive under oxidative stress conditions. These data imply that the balance between XBP1u and XBP1s is altered by differing flow conditions and the acute overexpression of XBP1u during the initial stages of disturbed flow promotes EC survival. However, sustained stimulation by disturbed flow enhances XBP1 splicing resulting in EC apoptosis (figure 61). EC survival was assessed via MTS tetrazolium assay. This assay calculates cell number based on the detection of metabolically active and therefore viable cells. Secondly, viable ECs were identified via TUNEL assay, where the terminal ends of nucleic acids, which occur more frequently during apoptosis, are identified via the addition of labelled dUTP molecules. The role of XBP1 in cell survival was investigated for several reasons. Sustained overexpression of XBP1s resulted in EC apoptosis and atherosclerotic lesion formation. XBP1 was also demonstrated to promote cell survival during hypoxia in a tumour microenvironment (Koong et al., 2006). We therefore hypothesised that XBP1u could promote EC survival in response to oxidative stress.

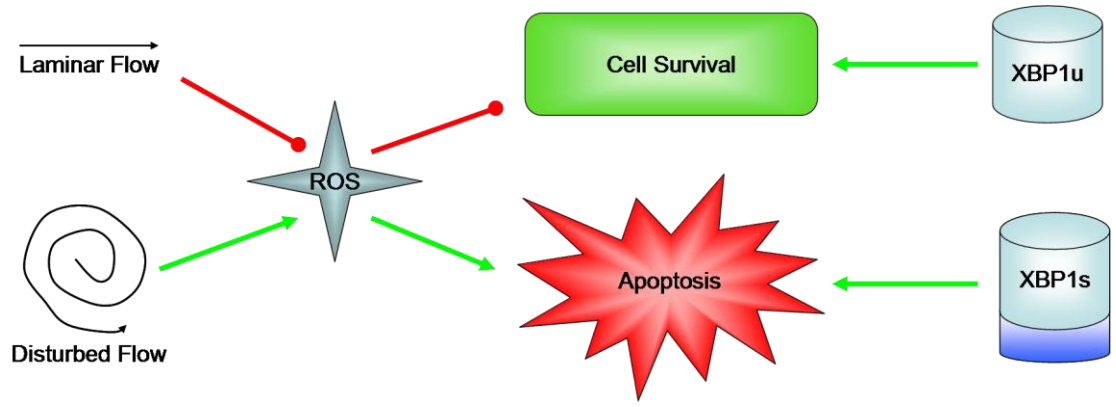

Figure 61: Schematic diagram depicting the influence of shear stress, XBP1u and XBP1s on EC survival and apoptosis.

Laminar flow reduces ROS generation and promotes EC quiescence and survival. Disturbed flow induces ROS generation which in turn promotes EC apoptosis and atherosclerotic lesion formation. Prolonged overexpression of XBP1s promotes EC apoptosis through caspase activation. Overexpression of XBP1u promotes EC survival and reduces ROS-mediated EC apoptosis.

4.2 XBP1u enhances EC survival through Akt and HO-1

Microarray analysis of genes regulated by XBP1u overexpression identified several target genes that could be responsible for mediating the protection of ECs against oxidative stress. HO-1 was identified as a prime target for further analysis. HO-1 catalyses the enzymatic conversion of haem into biliverdin, iron and carbon monoxide. The products of haem degradation have all been demonstrated to initiate or perform anti-apoptotic or antioxidant functions. HO-1 induces the export of iron from the cell and formation of ferritin, which neutralises the reactive iron and reduces apoptosis. Iron has also been shown to activate NF-κB which initiates anti-apoptotic signalling (Choi et al., 2004). Biliverdin protects against apoptosis through an antioxidant mechanism by scavenging ROS. Recent studies have demonstrated a role for CO in many cell signalling events (Kaczorowski and Zuckerbraun, 2007). CO inhibits TNFα-mediated apoptosis in mouse ECs through activation of MKK3 and p38 MAPK (Brouard et al., 2000). CO has a direct role in anti-inflammatory signalling by inhibiting cytokine-mediated apoptosis. HO-1 is upregulated during laminar flow in response to Nrf2 activation. One of the main regulators of Nrf2 is NO; however, the upregulation of HO-1 is independent of eNOS (Warabi et al., 2007).

These studies demonstrate for the first time that XBP1u enhances the expression of HO-1 at both the mRNA and protein level. We demonstrate that the upregulation of HO-1 is uniquely activated by XBP1u and does not require the activation of the ER stress response. Knockdown of XBP1 and the subsequent loss of HO-1 expression imply that XBP1u is required for the basal expression of HO-1. These studies imply that the expression of XBP1u is crucial for HO-1 expression. HO-1 expression is under the control of multiple enhancer elements, these include NF-κB, AP-1, BVR, Nrf2, CREB and ATF2 (Kim et al., 2011). The expression of HO-1 has previously been shown to protect ECs from apoptosis, regulate vascular tone, attenuate the inflammatory response and participates in angiogenesis and vasculogenesis (Morsi et al., 2006; Otterbein et al., 2003a; Otterbein et al., 2003b). Together these studies suggest that HO-1 is a perfect candidate to mediate XBP1u-dependent protection of ECs.

The total XBP1 knockout mouse is embryonic lethal, therefore we were unable to study the effects of XBP1 knockdown exclusively in the vascular system. To further our studies we developed a conditional XBP1 knockout mouse. The ablation of XBP1 expression is dependent upon the expression of Cre recombinase, which we have linked to the Tie2 promoter. Tie2 was initially identified as a specific vascular growth factor that governed several properties of ECs. However, Tie2 has more recently been identified to maintain the quiescent status of haematopoietic stem cells in the bone marrow and it is expressed outside the vascular compartment in several cancers (Martin et al., 2008). Tie2-expressing monocytes have also been identified which promote tumour angiogenesis and growth in mouse models (De Palma et al., 2003; Venneri et al., 2007). Therefore, although XBP1 is not exclusively knocked out in ECs, there are very few other cell types and functions that will be affected by this deletion. Our studies demonstrated that the expression of HO-1 was not ablated in XBP1-null ECs. These contrasts with our *in vitro* data that implies XBP1 is essential for HO-1 expression. It is likely that XBP1 is sufficient to induce the expression of HO-1; however, *in vivo* compensatory mechanisms may be activated to promote adequate HO-1 expression.

Our *in vitro* data demonstrates that XBP1u can enhance the expression of HO-1 at the mRNA and protein level. As XBP1u contains a functional DNA-binding

domain we hypothesised that XBP1u might directly activate the transcription of HO-1 by binding to the HO-1 promoter. After cloning the HO-1 promoter into a luciferase reporter vector and subsequent overexpression of XBP1u, we did not detect any activity from the HO-1 promoter. This suggests that XBP1u does not bind directly to the HO-1 promoter but may induce its activity in an indirect manner. Furthermore, the cloning of the HO-1 promoter may have modified the structural requirements for XBP1u binding.

XBP1u is upregulated in regions of disturbed flow and can enhance the ability of ECs to survive during oxidative stress and increases the expression of HO-1. We hypothesised that XBP1u promotes EC survival during oxidative stress, which can be induced by disturbed flow, through the activation of HO-1 expression. Although we do not demonstrate that our model of disturbed flow induces oxidative stress, this has been extensively determined previously (De Keulenaer et al., 1998; Laurindo et al., 1994; Nigro et al., 2011). Our data confirms that the expression of HO-1, as well as XBP1u, is enhanced during disturbed flow. The upregulation of HO-1 and XBP1u is transcriptionally and translationally dependent. The expression of HO-1 has already been linked with shear stress patterns. Pulsatile, laminar flow of 19 dynes / cm^2 increased the expression of KLF2 and Nrf2, a key promoter of HO-1 expression (Fledderus et al., 2008). In contrast to our data a report has been published stating that whilst laminar flow enhances the expression of HO-1, disturbed flow impairs the activation of HO-1 expression (Ali et al., 2009). However, when compared in isolation their data is remarkably similar to our own. When HUVECs under disturbed flow conditions for 24 hours are compared to HUVECs under static conditions they show a 3 fold induction in the expression of HO-1 mRNA. In our hands the exposure of HUVECs to disturbed flow for 24 hours results in a 2-fold increase in HO-1 at the mRNA level and a significant 2-fold increase in the protein level of HO-1. Their disturbed flow conditions of +/- 5 dynes / cm^2 are similar to our conditions of 4.5 dynes / cm^2. However, they show that laminar shear stress further enhances the expression of HO-1 and that the upregulation of HO-1 under disturbed flow is due to intermittent activation of the upstream signalling pathway. We hypothesise that two separate signalling pathways are activated; one occurs under laminar shear stress conditions; whilst the second is activated in response to disturbed flow to attempt to mitigate against oxidative stress. This second pathway involves the activation of

XBP1u expression. Evidence for distinct pathways activated by disturbed flow, in comparison to static controls and laminar flow, has previously been suggested. ECs exposed to disturbed flow exhibit increased levels of localised NF-κB, c-Jun and c-fos in their nuclei (Nagel et al., 1999). Moreover, knock down of XBP1 prior to the induction of disturbed flow demonstrates that XBP1u is required for shear stress-mediated upregulation of HO-1. This is the first time that XBP1u has been identified as a shear stress mediated factor.

In the present study, we have used SnPPIX to inhibit HO-1 and determine if this impairs the ability of XBP1u to promote EC survival. Indeed, inhibition of HO-1 completely abolished the protective effect of XBP1u on ECs. In accordance with these results XBP1u has previously been shown to prevent oxidative stress in mouse embryonic fibroblast (MEF) cells (Liu et al., 2009). It was demonstrated that XBP1-null cells were more sensitive to a loss in mitochondrial membrane potential and subsequent cell death after the application of hydrogen peroxide. In these studies the MEFs were treated with 1 mM hydrogen peroxide for 12 hours as opposed to our experiments where the HUVECs were treated with 50 μM hydrogen peroxide for 24 hours, which reflects the different abilities of these cells to deal with oxidative stress. Furthermore, in XBP1-deficeint cells there was a greater increase in ROS production after hydrogen peroxide treatment and the expression of several antioxidant enzymes was lower, including catalase. It was demonstrated that XBP1u enhances the expression of catalase through the CCAAT box present in the catalase promoter. Moreover, it was demonstrated that knockdown of XBP1 ablated catalase expression and enhanced ROS generation. These effects were reversed upon the addition of exogenous XBP1u.

These results, combined with our data indicate a protective role of XBP1 against oxidative stress. The positive regulation of catalase and HO-1 may account for part of this function. These results indicate that XBP1u is a crucial mediator of the response to oxidative stress during disturbed flow (figure 62).

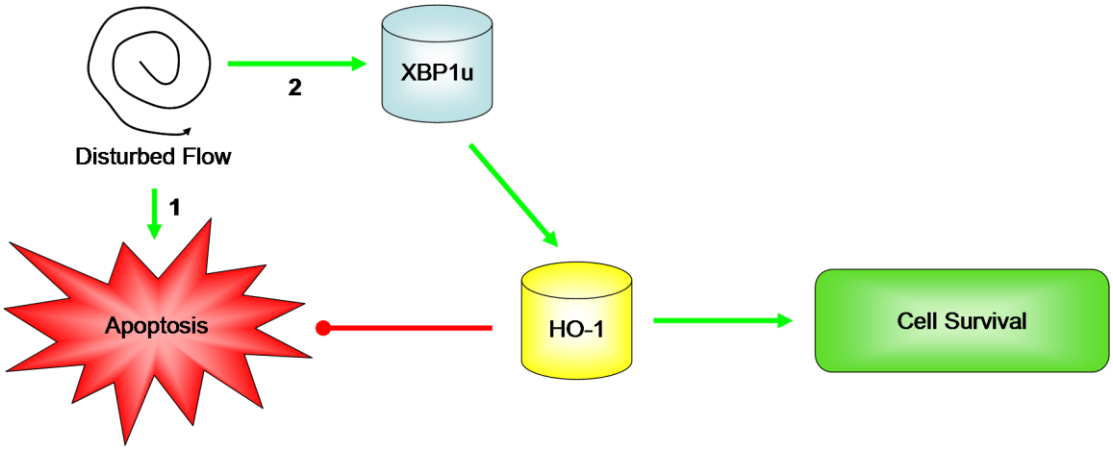

Figure 62: Schematic diagram depicting the influence of disturbed flow shear stress on XBP1u, HO-1 and EC survival and apoptosis.

1. Disturbed flow induces the formation of an apoptotic, atheroprone phenotype in ECs that results in EC apoptosis. One of the mechanisms that induces EC apoptosis is increased oxidative stress. **2.** To promote EC survival, disturbed flow enhances the expression of both XBP1u and HO-1. The expression of HO-1 is dependent on the presence of XBP1. The expression of HO-1 promotes a non-apoptotic EC phenotype and promotes EC survival. Presumably a balance in XBP1u expression is in operation, potentially the sustained stimulation with disturbed flow will result in levels of oxidative stress that an upregulation of XBP1u is insufficient to deal with.

Having determined that XBP1u does not directly enhance the expression of HO-1 through interactions with its promoter region we searched for other candidates. Akt is a known activator of HO-1 expression. We hypothesised that XBP1u may enhance the phosphorylation of Akt and thereby enhance the expression of HO-1. Akt regulates essential cellular functions such as migration, proliferation, apoptosis and metabolism. Akt is a serine/threonine kinase activated by PI-3-kinase signalling. Activated PI-3-kinase mediates the conversion of phosphatidylinositol-4,5-bisphosphate into phosphatidylinositol-3,4,5-trisphosphate (PIP_3). PIP_3 recruits PDK1 and Akt to the membrane through their plekstrin homology domains. PDK1 is a known activator of Akt, which then translocates to subcellular compartments where it phosphorylates substrates and interacts with binding partners (Cantley, 2002). For example, Akt-mediated phosphorylation of the apoptotic factor Bad, allows recruitment of 14-3-3 proteins, preventing the interaction of Bad with Bcl-2. Phosphorylation of Bad and the subsequent release of Bcl-2 prevents cell death induced by various stimuli, including hydrogen peroxide (Aikawa et al., 2000). Akt phosphorylation occurs at threonine 308, which is present in the activation domain

and at serine 473, in the carboxyl terminus. Phosphorylation of both sites contributes towards Akt activation (Alessi et al., 1996). Akt phosphorylated at T308 alone is only 10% as active as the fully phosphorylated form (O'Neill et al., 2012). Phosphorylation of Akt at S473 stabilises the active conformation and allows for full Akt activation (O'Neill et al., 2012).

In this study, we demonstrated that exogenous overexpression of XBP1u resulted in the enhanced phosphorylation of Akt at serine 473, but had no effect either on the expression level of Akt or the phosphorylation of Akt at threonine 308. Furthermore XBP1u promoted the accumulation of phosphorylated Akt at the cell membrane. The presence of XBP1 is crucial for basal Akt phosphorylation at serine 473, as knock down of XBP1 abolishes Akt phosphorylation under normal conditions. Previously XBP1u has not been linked to the activation of Akt phosphorylation. Indeed, inhibition of XBP1 splicing has been shown to have no effect on Akt phosphorylation induced by subtilase cytotoxin (Yamazaki et al., 2009). However, we are the first to look at the effect of XBP1u on the phosphorylation status of Akt.

Using inhibitors of PI-3-kinase and VEGFR2 activity we demonstrated that XBP1u enhances the phosphorylation of Akt independently to this classical pathway. We used the pan-PI-3-kinase inhibitor LY294002, which can also cross-react with PI-3-kinase related kinase such as mTOR and DNA-dependent protein kinases. There are also problems with its solubility and high toxicity due to its ability to target a broad range of PI-3-kinase-related enzymes (Marone et al., 2008). The general consensus is that Akt activation requires recruitment to the cell membrane via activation of PI-3-kinase (Polak and Buitenhuis, 2012). However, several recent studies have identified several kinases that can activate Akt independently of PI-3-kinase. These include the tyrosine kinases; Ack1, Src and PTK6 and the serine / threonine kinases; TBK1, IKBKE and DNAPKcs. These kinases activate Akt and promote its pro-proliferative signalling functions (Mahajan and Mahajan, 2012). These data imply that XBP1u promotes the phosphorylation of Akt through activation of a PI-3-kinase independent mechanism.

Our studies demonstrated that the activation of Akt phosphorylation was not ablated in XBP1-null ECs. These contrasts with our *in vitro* data that implies XBP1u

is essential for Akt phosphorylation at serine 473. It is likely that XBP1u is sufficient to induce the activation of Akt phosphorylation; however, *in vivo* compensatory mechanisms may be activated to promote adequate Akt phosphorylation.

In the present study, we demonstrate that constitutively active Akt promotes the expression of XBP1u and HO-1 at the protein level. The upregulation of HO-1 by XBP1u was shown to be dependent on XBP1. Moreover, Akt is not required for the induction of HO-1 by XBP1u. These data show that XBP1u functions downstream of Akt (figure 3). Activated Akt must interact with XBP1u to promote the expression of HO-1 in our system. Previous reports have demonstrated that the activation of Akt is required for HO-1-mediated protection against carnosol-induced oxidative stress (Martin et al., 2004). The levels of the ARE-binding transcription factor Nrf2 are also raised during the protective response against carnosol. Recent studies have also shown that HO-1 expression is mediated by activation of Akt signalling by a mitochondrial redox-dependent pathway in ECs. Celecoxib, a cyclooxygenase-2 selective inhibitor, activates HO-1 expression through an Akt-dependent manner (Hamdulay et al., 2010). These results indicate that activation of Akt is a key event in regulating the induction of HO-1 in response to cytokines and growth factors. In combination these data demonstrate that XBP1u is crucial in mediating the activation of HO-1 expression by Akt. We suggest that XBP1u may interact with a promoter element or an enhancer of HO-1 transcription to induce its expression.

In this study we also demonstrate that Akt phosphorylation can be enhanced by disturbed flow and that this can be abrogated by knockdown of XBP1, in a similar manner to that observed on the expression of HO-1 (figure 63). Disturbed flow, which predominantly occurs in the bifurcation regions of the vasculature, predisposes these regions to atherosclerosis. The lack of laminar shear stress detected by ECs in these regions leads to their transformation towards an atheroprone phenotype. These cells undergo a higher degree of turnover than ECs in vascular regions subjected to laminar flow, allowing for increased macrophage penetration of the endothelium and thereby increasing the likelihood of lesion formation. One of the main causes for EC turnover in these regions is an increase in oxidative stress, from inconsistent activation of cell survival pathways. We also predict that there are several pathways which are activated within these cells to combat the increases in oxidative stress. In

accordance with our findings, oscillatory flow has been determined to induce activation of Akt signalling in osteoblast-like cells (Lee et al., 2010). Together these data demonstrate that disturbed flow induces the phosphorylation of Akt at serine 473 in an XBP1-dependent manner.

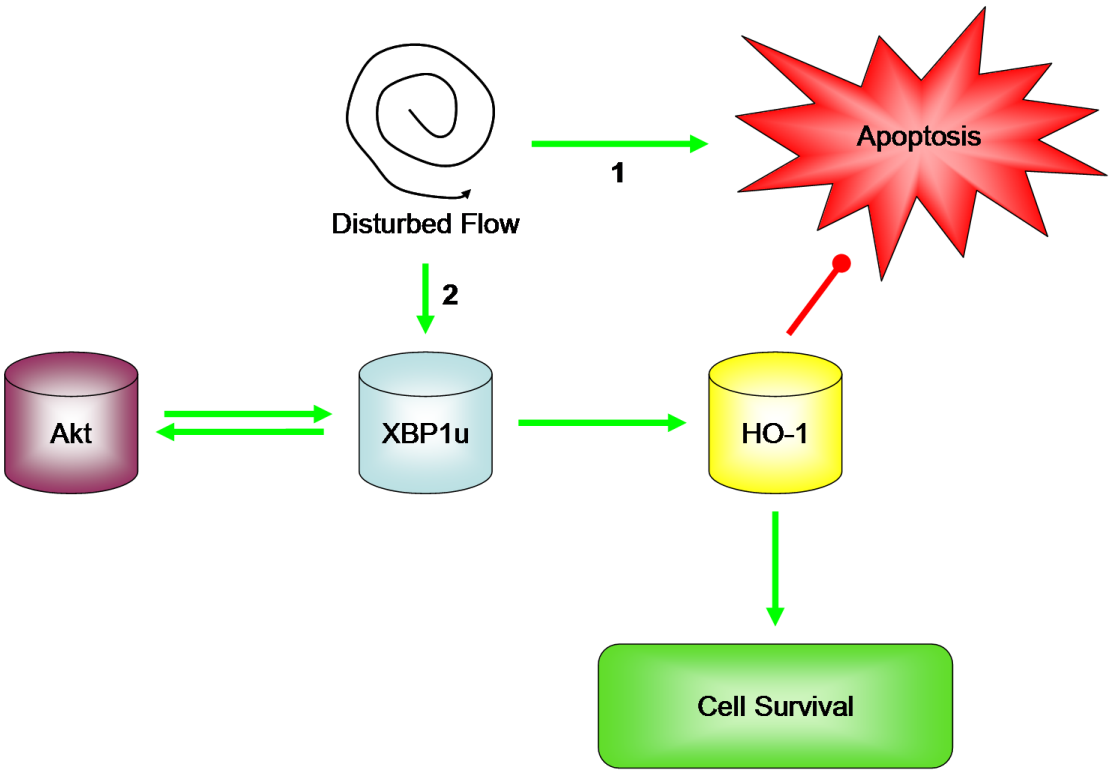

Figure 63: Schematic diagram depicting the influence of XBP1u on Akt activation.
1. Disturbed flow induces the formation of an apoptotic, atheroprone phenotype in ECs that results in EC apoptosis. One of the mechanisms that induces EC apoptosis is increased oxidative stress. **2.** To promote EC survival, disturbed flow enhances the expression of both XBP1u and HO-1 and enhances the phosphorylation of Akt. The expression of HO-1 and the phosphorylation of Akt is dependent on the presence of XBP1. Independently of disturbed flow, the activation of HO-1 expression by Akt is also dependent upon XBP1. The expression of HO-1 promotes a non-apoptotic EC phenotype and promotes EC survival.

The results discussed above demonstrate for the first time the involvement of XBP1u in promoting EC survival during disturbed flow and oxidative stress. XBP1u is crucial in mediating a protective signalling response through Akt phosphorylation and HO-1 expression. Modulation of XBP1u activity may serve to increase EC integrity in a therapeutic setting.

4.3 HDAC3 is crucial for promoting XBP1u-mediated EC survival

Previous studies in our lab have identified a role for HDAC3 in promoting EC survival (Zampetaki et al., 2010). HDAC3 has already been demonstrated to play an important role in the biology of endothelial progenitor cells (Rossig et al., 2005). It is expressed ubiquitously and its activity depends on its association with multisubunit repressor complexes. HDAC3 is present in both the nucleus and the cytoplasm of ECs (Longworth and Laimins, 2006). Our lab has demonstrated that HDAC3 is predominantly expressed in endothelial bifurcation regions. *In vitro* studies showed that disturbed flow enhanced the stability of HDAC3 and overexpression of HDAC3 increases Akt phosphorylation. Furthermore Akt was demonstrated to interact with Akt, whilst knock down of HDAC3 induced EC dysfunction and atherosclerotic lesion formation (Zampetaki et al., 2010). In our studies, we demonstrate that there is a significant overlap in the genes influenced by overexpression of exogenous XBP1u and HDAC3. We have also seen that both proteins enhance the phosphorylation of Akt at serine 473. We therefore investigated the ability of XBP1u and HDAC3 to interact in the protective signalling pathway. These studies show that XBP1u does not influence the expression of HDAC3 under normal conditions. We confirm previous data that demonstrated that the expression of HDAC3 at the protein level is enhanced by disturbed flow. Furthermore, the expression of XBP1u is crucial for the disturbed flow-mediated upregulation of HDAC3.

We were interested in determining how XBP1u and HDAC3 are upregulated during disturbed flow. One of the main pathways predicted to influence Akt activation is through VEGFR2 / PI-3-kinase. Therefore we inhibited these proteins as well as MEK1 and looked at the effect of disturbed flow on the expression of XBP1u and HDAC3. Disturbed flow-mediated upregulation of HDAC3 and XBP1u is dependent on VEGFR2 and PI-3-kinase signalling. Moreover, knockdown of HDAC3 ablated XBP1u-meditaed increases in Akt phosphorylation and HO-1 expression, implying that there is a crucial interaction between these proteins that promotes EC survival. Previously HDAc3 has been found to bind to several other proteins in the cytoplasm. HDAC3 was found to localise to the plasma membrane independently of its NES, through interaction with the membrane bound tyrosine kinase, c-Src (Longworth and Laimins, 2006). Furthermore, HDAC3 was found to

interact with Akt through residues 136-201 (Zampetaki et al., 2010). Our studies confirm that HDAC3 can interact with Akt. Furthermore, we demonstrate that XBP1u is able to interact with HDAC3 through residues 131-206 of HDAC3. In addition the overexpression of XBP1u does not displace Akt from its interaction with HDAC3, suggesting that these molecules can interact at the same time.

Our results have demonstrated that HDAC3 and XBP1u are crucial in maintaining EC integrity and survival. Under disturbed flow conditions, both HDAC3 and XBP1u are upregulated. XBP1u plays a critical role in mediating the stabilisation of HDAC3 during disturbed flow. Our experiments also demonstrate that XBP1u and HDAC3 enhance the phosphorylation, and thereby the activation, of Akt at S473. Activated Akt can induce the expression of HO-1, and under our experimental conditions XBP1u is also crucial in this role. Our most recent studies demonstrate that both XBP1u and Akt can physically interact with HDAC3, and that overexpression of XBP1u does not displace or complete with Akt for a binding site with HDAC3. Furthermore, knockdown of HDAC3 prevents XBP1u-mediated Akt phosphorylation and increased expression of HO-1. We hypothesise that under disturbed flow conditions the expression (transcription and translation) of XBP1u is augmented. XBP1u can then bind to HDAC3 and promote its stabilisation. It is through this means that more Akt can be recruited to HDAC3 and undergo phosphorylation. The subsequent cell survival pathways can then be activated. Our particular area of interest demonstrated that Akt-mediated upregulation of HO-1 requires XBP1u to be present (figure 64). Furthermore disturbed flow acts through VEGFR2 and PI-3-kinase to initiate the stabilisation of HDAC3 and augment the expression of XBP1u.

We hypothesise that the interaction between HDAC3 and XBP1u occurs in the cytoplasm. The binding of XBP1u to HDAC3 may serve to mask the nuclear localisation signal present on both molecules. Akt is activated at the cell membrane and we therefore hypothesize that these proteins form a complex that stabilises the recruitment and retention of Akt at the cell membrane. Our data demonstrates that the presence of phosphorylated Akt is enhanced after overexpression of XBP1u, however we were unable to determine if XBP1u and HDAC3 are enhanced in our cell membrane isolations. The stabilisation of this complex through mutual interactions

serves to promote the phosphorylation, and thereby the activation, of Akt at serine residue 473.

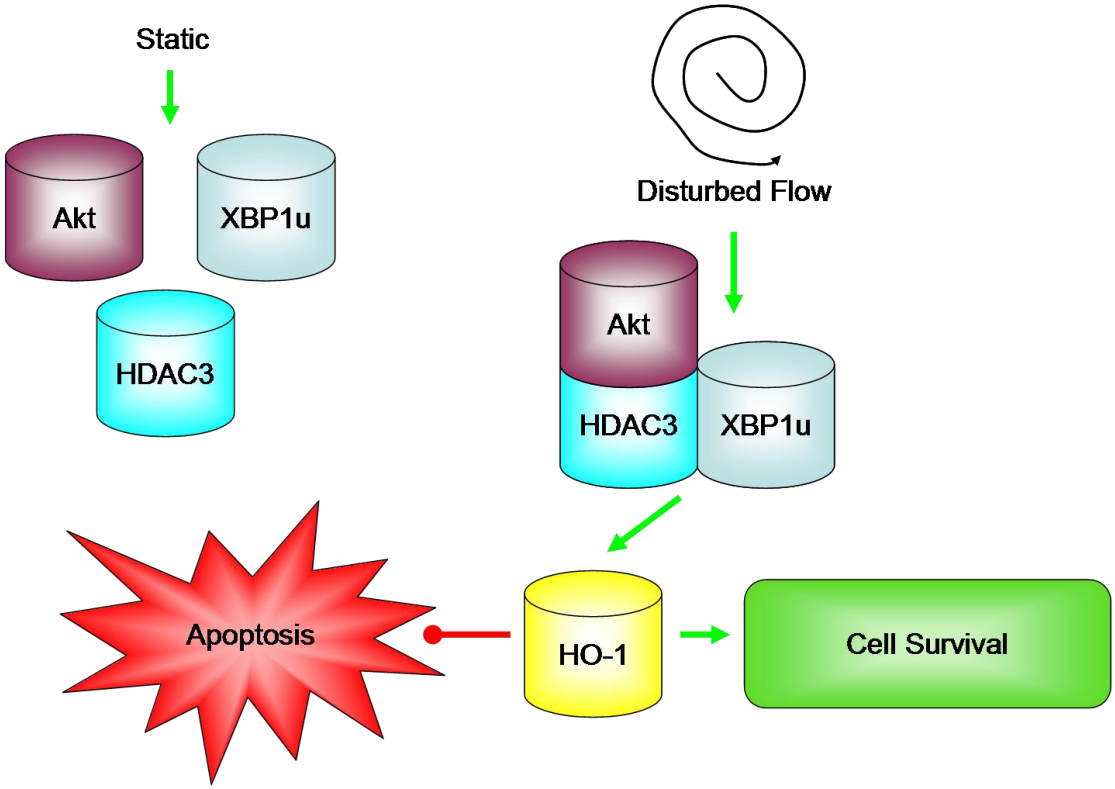

Figure 64: HDAC3 interacts with XBP1u and Akt to induce activation of HO-1.
HDAC3 is required for XBP1u-mediated phosphorylation of S473-Akt and upregulation of HO-1 expression. HDAC3 also interacts with Akt and XBP1u in order for this process to occur.

4.4 XBP1u promotes EC survival in response to disturbed flow

Disturbed flow induces endothelial cell apoptosis through increased oxidative stress. One of the cells responses is to try and reduce oxidative stress through the expression of antioxidant molecules. We have found that XBP1u can interact with HDAC3 to promote the recruitment and phosphorylation of Akt-S473. Both activated Akt and XBP1u promote the expression of HO-1, thereby reducing oxidative stress and apoptosis. All of these functions are physiologically relevant as XBP1u, HDAC3 and phosphorylation of Akt all occur under disturbed flow conditions. In addition disturbed flow-mediated regulation of XBP1u requires VEGFR2 and PI-3-kinase activity as inhibition of these molecules prevents upregulation of XBP1u (figure 65).

The impact of these studies and exploration of the mechanism will take place in a later chapter.

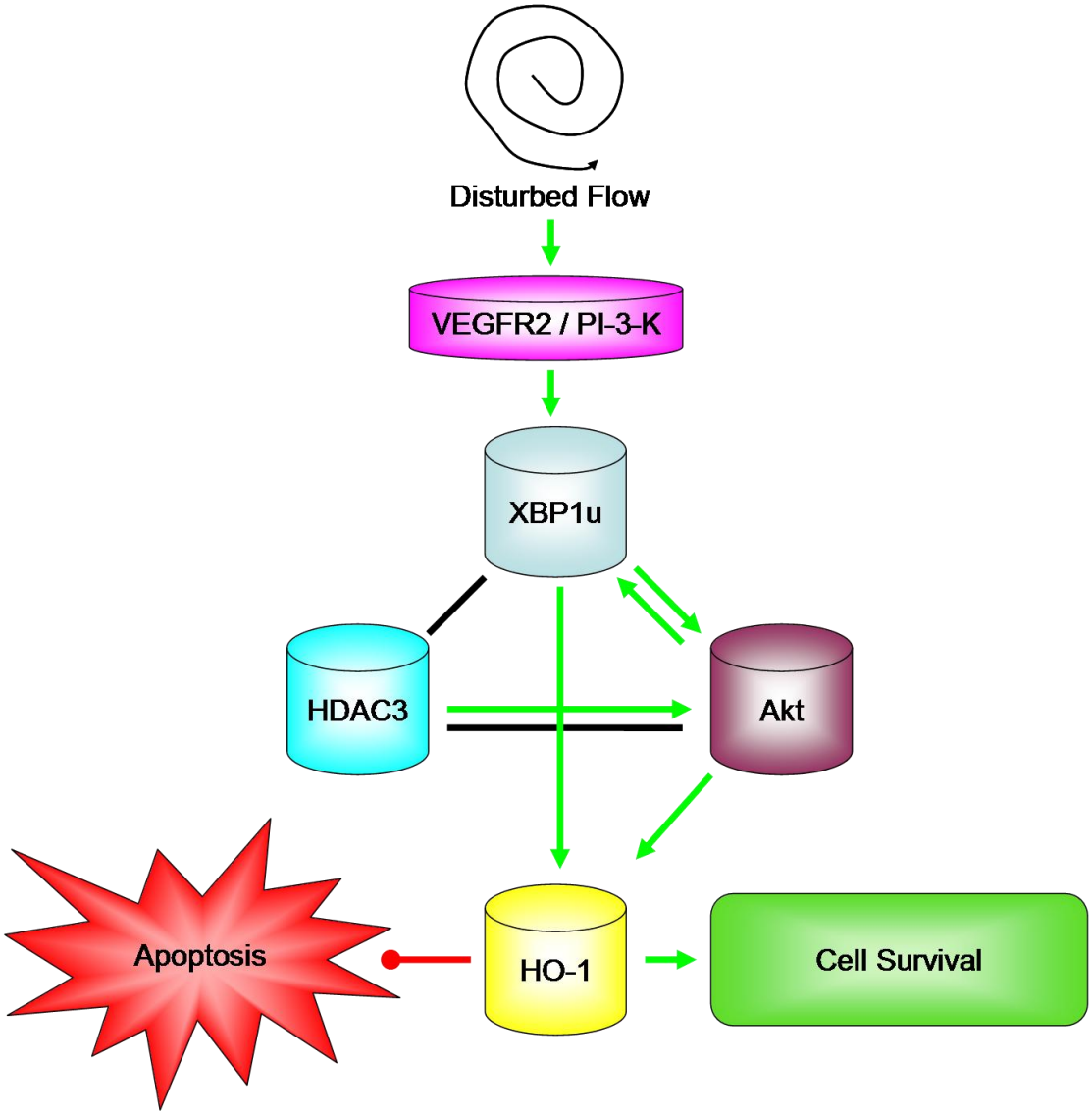

Figure 65: XBP1u promotes EC survival in response to disturbed flow.

Disturbed flow induces endothelial cell apoptosis through increased oxidative stress. One of the cells responses is to try and reduce oxidative stress through the expression of antioxidant molecules. We have found that XBP1u can interact with HDAC3 to promote the recruitment and phosphorylation of Akt-S473. Both activated Akt and XBP1u promote the expression of HO-1, thereby reducing oxidative stress and apoptosis. All of these functions are physiologically relevant as XBP1u, HDAC3 and phosphorylation of Akt all occur under disturbed flow conditions. In addition disturbed flow-mediated regulation of XBP1u requires VEGFR2 and PI-3-kinase activity as inhibition of these molecules prevents upregulation of

In summary, we have shown that XBP1u enhances the survival of ECs during oxidative stress. XBP1u-mediates this effect through an interaction with HDAC3 to promote Akt activation and the expression of HO-1. This process may be crucial during disturbed flow and targeting XBP1u and HDAC3 may provide novel therapeutic interventions for vascular disease.

4.5 XBP1 is crucial for EC migration

The occlusion of a blood vessel by thrombosis, atherosclerosis or injury will cause ischemia to local tissues, leading to cell death and loss of organ function (Kirton and Xu, 2010). Angiogenesis contributes to the restoration of blood flow in ischemic tissues, in which EC migration and proliferation plays an important role. In this study we demonstrated a crucial role for XBP1 in mediating EC migration.

Overexpression of both XBP1 isoforms was sufficient to enhance EC migration under normal and low serum (2%) conditions. Furthermore knockdown of XBP1 ablated the ability of ECs to migrate during wound healing assays. It was interesting to see that both isoforms of XBP1 enhanced EC migration. These data were the first to link the expression of XBP1 with EC migration. To determine if the splicing of XBP1u is crucial, the expression of IRE-1α was ablated via lentiviral transfer of shRNA. We demonstrated that IRE-1α is crucial for proper EC migration. Furthermore, the expression of XBP1s is enhanced during the initial stages of migration. Together these data demonstrate that XBP1s plays an important role in EC migration.

To confirm the importance of XBP1 *in vivo* endothelial-like cells were harvested from wild type and XBP1-null embryos. The migration of XBP1-null cells was dramatically reduced compared to wild type controls. Furthermore knockdown of XBP1 *in vitro* reduced the ability of ECs to form tube-like structures. Moreover, EC outgrowth from arterial rings taken from *Tie2-Cre-XBP1*$^{f/f}$ mice demonstrated significantly less movement than wild type controls. Our experiments remain at an early stage, although we have investigated the influence of XBP1 on the expression of FAK, a crucial mediator of EC migration (Hung et al., 2012; Shi et al., 2011). Knock

down of XBP1 abrogates the expression of FAK in aortic sections from *Tie2-Cre-XBP1$^{f/f}$* mice. Further experimentation will serve to enhance our understanding of the link between XBP1s and FAK.

Thus, the present study provides for the first time phenotypic evidence by which XBP1 plays a significant role in maintaining endothelial integrity physiologically and promotes angiogenesis under pathophysiologic conditions.

4.6 Importance of the study

This study demonstrates for the first time that XBP1u is crucial in promoting EC survival in response to oxidative stress. This occurs through the activation of Akt phosphorylation and enhancing the expression of HO-1. Furthermore, we demonstrate that XBP1u and HDAC3 are enhanced by disturbed flow and that this occurs in a VEGFR2 / PI-3-kinase dependent manner. These studies implicate XBP1u as a potential therapeutic target for vascular disease. Modulation of XBP1u function could enhance EC integrity and reduce atherosclerotic lesion formation.

4.7 Limitations of the study

Although we have demonstrated that XBP1u and HDAC3 promote EC survival, several of our hypotheses require further experimentation. We have not demonstrated that XBP1u promotes EC survival under disturbed flow conditions, only that survival is promoted in response to oxidative stress. We have made the assumption that disturbed flow induces oxidative stress and that the signalling pathway we have uncovered functions during disturbed flow stimulation.

The interaction that we have demonstrated between XBP1u and HDAC3 is also crucial to our conclusions. However, although we have demonstrated that XBP1u and HDAC3 are both responsible for promoting EC survival and phosphorylation of Akt, we have not shown that an interaction between the two proteins is crucial for this event. In order to determine this it would be necessary to identify the sequence responsible for mediating the binding of XBP1u to HDAC3 and

mutate it so that the interaction could no longer occur. If the overexpression of XBP1u is no longer able to induce EC survival in response to oxidative stress then we will have demonstrated that the interaction is crucial for EC survival.

4.8 Future work

In order to more fully understand the role of XBP1u in promoting EC survival several experiments could be performed. Firstly to confirm that HO-1 is indeed the transducer of XBP1u-mediated EC survival, knockdown of XBP1, which induces increased EC apoptosis, could potentially be rescued through the application of a CO donor. We would predict that the application of a CO donor to XBP1-null ECs would promote EC survival in response to oxidative stress.

We have shown that XBP1u and HDAC3 are important in mediating the activation of Akt, however the kinase responsible for phosphorylation of Akt has not been identified. It would be interesting to see if this kinase is recruited to the HDAC3-XBP1u-Akt complex and this is the mechanism through which EC survival is enhanced.

We have demonstrated that XBP1u and HDAC3 interact. To more completely define the interaction it would be necessary to create several XBP1 deletion mutation constructs. These could then be used to identify the particular region of XBP1u responsible for mediating the binding to HDAC3. We would predict that the C-terminal domain would most likely be responsible as the N-terminal domain is required for the interaction with DNA.

Our preliminary data implicates FAK in XBP1-mediated migration. Further studies on the role of XBP1 in mediating the expression and function of FAK are required. Cloning of the promoter region of FAK into luciferase vectors will allow us to determine if XBP1 can bind directly to the FAK promoter and stimulate its expression. Furthermore, rescue experiments where XBP1 is knocked down and exogenous FAK is added to the HUVECs to determine if EC migration reverts back to

normal levels would enable a determination of the role of XBP1u and FAK in EC migration.

To demonstrate that migration promotes XBP1 splicing we have attempted to attach a GFP-tag to the XBP reading frame, such that the coding sequence for GFP would only be translated during XBP1 splicing. We would therefore be able to monitor the splicing of XBP1 in EC tip cells during the initial stages of migration. To convincing separate the role of proliferation from migration, the effect of XBP1 knock down on EC migration will be assessed using a Bowden chamber assay.

In the present study we demonstrated that knockdown of XBP1 impairs EC migration. It would be interesting to determine if this impairment in migration has any physiological roles. We have only recently obtained the conditional XBP1 knockout mice. These animals could be subjected to a hindlimb ischemia experiment. Here the femoral artery is ligated and lateral vessel growth is observed. We would anticipate that vessel growth in the XBP1-null mice would be impaired, demonstrating that XBP1 is crucial in mediating *in vivo* EC migration.

Furthermore to identify the function of XBP1 on *in vivo* EC migration it would be interesting to perform a retinal vasculogenesis assay. $XBP1^{loP/loxP}$ mice bred to Tie2-Cre (Kisanuki et al., 2001) transgenic mice, which express Cre recombinase in ECs and bone marrow progenitor cells, which allows for the generation of EC conditional knockout mice. Retinal vasculogenesis could then be observed. We would predict that the avascular area would be significantly larger in XBP1-null mice as compared to wild type mice. This would imply that XBP1-null mice have delayed retinal vascular development. Current studies have already implicated XBP1 in the anti-oxidant defence in retinal pigment epithelium (Zhong et al., 2012).

Chapter 5 - Publications and awards

Publications:

Alam S, Li H, Margariti A, ***Martin D****, Zampetaki A, Habi O, Cockerill G, Hu Y, Xu Q, Zeng L.* Galectin-9 Expression in Endothelial Cells is Positively Regulated by Histone Deacetylase 3. Journal of Biological Chemistry, 2011.

Zhou B, Margariti A, Zeng L, Habi O, Xiao Q, ***Martin D****, Wang G, Hu Y, Wang X, Xu Q.* Splicing of Histone Deacetylase 7 Modulates Smooth Muscle Cell Proliferation and Neointima Formation Through Nuclear β-Catenin Translocation. Arteriosclerosis, Thrombosis and Vascular Biology, 2011.

Margariti A, Zampetaki A, Xiao Q, Zhou B, Karamariti E, ***Martin D****, Yin X, Mayr M, Li H, Zhang Z, De Falco E, Hu Y, Cockerill G, Xu Q, Zeng L.* Histone Deacetylase 7 Controls Endothelial Cell Growth through Modulation of β-Catenin. Circulation Research, 2010.

Zeng L, Zampetaki A, Margariti A, Pepe AE, Alam S, ***Martin D****, Xiao Q, Wang W, Jin ZG, Cockerill G, Mori K, Li YS, Hu Y, Chien S, Xu Q.* Sustained Activation of XBP1 Splicing leads to Endothelial Apoptosis and Atherosclerosis Development in Response to Disturbed Flow. PNAS, 2009.

Margariti A, Xiao Q, Zampetaki A, Zhang Z, Li H, ***Martin D****, Hu Y, Zeng L, Xu Q.* Splicing of HDAC3 Modulates the SRF-Myocardin Complex during Stem Cell Differentiation towards Smooth Muscle Cells. Journal of Cell Science, 2009.

Awards:

Finalist for the Young Investigator Award at the British Atherosclerosis Society Conference, 2010

Chapter 6 References

Aikawa, R., Nawano, M., Gu, Y., Katagiri, H., Asano, T., Zhu, W., Nagai, R., and Komuro, I. (2000). Insulin prevents cardiomyocytes from oxidative stress-induced apoptosis through activation of PI3 kinase/Akt. Circulation *102*, 2873-2879.

Alessi, D.R., Andjelkovic, M., Caudwell, B., Cron, P., Morrice, N., Cohen, P., and Hemmings, B.A. (1996). Mechanism of activation of protein kinase B by insulin and IGF-1. EMBO J *15*, 6541-6551.

Alessi, D.R., James, S.R., Downes, C.P., Holmes, A.B., Gaffney, P.R., Reese, C.B., and Cohen, P. (1997). Characterization of a 3-phosphoinositide-dependent protein kinase which phosphorylates and activates protein kinase Balpha. Curr Biol *7*, 261-269.

Ali, F., Zakkar, M., Karu, K., Lidington, E.A., Hamdulay, S.S., Boyle, J.J., Zloh, M., Bauer, A., Haskard, D.O., Evans, P.C., *et al.* (2009). Induction of the cytoprotective enzyme heme oxygenase-1 by statins is enhanced in vascular endothelium exposed to laminar shear stress and impaired by disturbed flow. J Biol Chem *284*, 18882-18892.

Antico Arciuch, V.G., Galli, S., Franco, M.C., Lam, P.Y., Cadenas, E., Carreras, M.C., and Poderoso, J.J. (2009). Akt1 intramitochondrial cycling is a crucial step in the redox modulation of cell cycle progression. PLoS One *4*, e7523.

Asahara, T., Murohara, T., Sullivan, A., Silver, M., van der Zee, R., Li, T., Witzenbichler, B., Schatteman, G., and Isner, J.M. (1997). Isolation of putative progenitor endothelial cells for angiogenesis. Science *275*, 964-967.

Assmann, G., Cullen, P., Jossa, F., Lewis, B., and Mancini, M. (1999). Coronary heart disease: reducing the risk: the scientific background to primary and secondary prevention of coronary heart disease. A worldwide view. International Task force for the Prevention of Coronary Heart disease. Arterioscler Thromb Vasc Biol *19*, 1819-1824.

Back, S.H., Schroder, M., Lee, K., Zhang, K., and Kaufman, R.J. (2005). ER stress signaling by regulated splicing: IRE1/HAC1/XBP1. Methods *35*, 395-416.

Barry-Lane, P.A., Patterson, C., van der Merwe, M., Hu, Z., Holland, S.M., Yeh, E.T., and Runge, M.S. (2001). p47phox is required for atherosclerotic lesion progression in ApoE(-/-) mice. J Clin Invest *108*, 1513-1522.

Bazzoni, G., and Dejana, E. (2004). Endothelial cell-to-cell junctions: molecular organization and role in vascular homeostasis. Physiol Rev *84*, 869-901.

Bellacosa, A., Chan, T.O., Ahmed, N.N., Datta, K., Malstrom, S., Stokoe, D., McCormick, F., Feng, J., and Tsichlis, P. (1998). Akt activation by growth factors is a multiple-step process: the role of the PH domain. Oncogene *17*, 313-325.

Berk, B.C. (2008). Atheroprotective signaling mechanisms activated by steady laminar flow in endothelial cells. Circulation *117*, 1082-1089.

Bertolotti, A., Zhang, Y., Hendershot, L.M., Harding, H.P., and Ron, D. (2000). Dynamic interaction of BiP and ER stress transducers in the unfolded-protein response. Nat Cell Biol *2*, 326-332.

Bhaskara, S., Chyla, B.J., Amann, J.M., Knutson, S.K., Cortez, D., Sun, Z.W., and Hiebert, S.W. (2008). Deletion of histone deacetylase 3 reveals critical roles in S phase progression and DNA damage control. Mol Cell *30*, 61-72.

Bisoendial, R.J., Kastelein, J.J., and Stroes, E.S. (2007). C-reactive protein and atherogenesis: from fatty streak to clinical event. Atherosclerosis *195*, e10-18.

Boon, R.A., Fledderus, J.O., Volger, O.L., van Wanrooij, E.J., Pardali, E., Weesie, F., Kuiper, J., Pannekoek, H., ten Dijke, P., and Horrevoets, A.J. (2007). KLF2 suppresses TGF-beta signaling in endothelium through induction of Smad7 and inhibition of AP-1. Arterioscler Thromb Vasc Biol *27*, 532-539.

Boon, R.A., and Horrevoets, A.J. (2009). Key transcriptional regulators of the vasoprotective effects of shear stress. Hamostaseologie *29*, 39-40, 41-33.

Bozulic, L., and Hemmings, B.A. (2009). PIKKing on PKB: regulation of PKB activity by phosphorylation. Curr Opin Cell Biol *21*, 256-261.

Brouard, S., Otterbein, L.E., Anrather, J., Tobiasch, E., Bach, F.H., Choi, A.M., and Soares, M.P. (2000). Carbon monoxide generated by heme oxygenase 1 suppresses endothelial cell apoptosis. J Exp Med *192*, 1015-1026.

Brunsing, R., Omori, S.A., Weber, F., Bicknell, A., Friend, L., Rickert, R., and Niwa, M. (2008). B- and T-cell development both involve activity of the unfolded protein response pathway. J Biol Chem *283*, 17954-17961.

Butt, E., Bernhardt, M., Smolenski, A., Kotsonis, P., Frohlich, L.G., Sickmann, A., Meyer, H.E., Lohmann, S.M., and Schmidt, H.H. (2000). Endothelial nitric-oxide synthase (type III) is activated and becomes calcium independent upon phosphorylation by cyclic nucleotide-dependent protein kinases. J Biol Chem *275*, 5179-5187.

Cai, H. (2005). NAD(P)H oxidase-dependent self-propagation of hydrogen peroxide and vascular disease. Circ Res *96*, 818-822.

Cantley, L.C. (2002). The phosphoinositide 3-kinase pathway. Science *296*, 1655-1657.

Cardone, M.H., Roy, N., Stennicke, H.R., Salvesen, G.S., Franke, T.F., Stanbridge, E., Frisch, S., and Reed, J.C. (1998). Regulation of cell death protease caspase-9 by phosphorylation. Science *282*, 1318-1321.

Carmeliet, P. (2000a). Developmental biology. One cell, two fates. Nature *408*, 43, 45.

Carmeliet, P. (2000b). Mechanisms of angiogenesis and arteriogenesis. Nat Med *6*, 389-395.

Carmeliet, P. (2003). Angiogenesis in health and disease. Nat Med *9*, 653-660.

Chatzizisis, Y.S., Coskun, A.U., Jonas, M., Edelman, E.R., Feldman, C.L., and Stone, P.H. (2007). Role of endothelial shear stress in the natural history of coronary atherosclerosis and vascular remodeling: molecular, cellular, and vascular behavior. J Am Coll Cardiol *49*, 2379-2393.

Chen, H.H., Chen, Y.T., Huang, Y.W., Tsai, H.J., and Kuo, C.C. (2012). 4-Ketopinoresinol, a novel naturally occurring ARE activator, induces the Nrf2/HO-1 axis and protects against oxidative stress-induced cell injury via activation of PI3K/AKT signaling. Free Radic Biol Med *52*, 1054-1066.

Chen, L., Kis, B., Hashimoto, H., Busija, D.W., Takei, Y., Yamashita, H., and Ueta, Y. (2006). Adrenomedullin 2 protects rat cerebral endothelial cells from oxidative damage in vitro. Brain Res *1086*, 42-49.

Chen, X.L., Varner, S.E., Rao, A.S., Grey, J.Y., Thomas, S., Cook, C.K., Wasserman, M.A., Medford, R.M., Jaiswal, A.K., and Kunsch, C. (2003a). Laminar flow induction of antioxidant response element-mediated genes in endothelial cells. A novel anti-inflammatory mechanism. J Biol Chem *278*, 703-711.

Chen, X.L., Varner, S.E., Rao, A.S., Grey, J.Y., Thomas, S., Cook, C.K., Wasserman, M.A., Medford, R.M., Jaiswal, A.K., and Kunsch, C. (2003b). Laminar flow induction of antioxidant response element-mediated genes in endothelial cells. A novel anti-inflammatory mechanism. J Biol Chem *278*, 703-711.

Cheng, C., Tempel, D., van Haperen, R., van der Baan, A., Grosveld, F., Daemen, M.J., Krams, R., and de Crom, R. (2006). Atherosclerotic lesion size and vulnerability are determined by patterns of fluid shear stress. Circulation *113*, 2744-2753.

Chien, S. (2008a). Effects of disturbed flow on endothelial cells. Ann Biomed Eng *36*, 554-562.

Chien, S. (2008b). Role of shear stress direction in endothelial mechanotransduction. Mol Cell Biomech *5*, 1-8.

Choi, B.M., Pae, H.O., Jeong, Y.R., Oh, G.S., Jun, C.D., Kim, B.R., Kim, Y.M., and Chung, H.T. (2004). Overexpression of heme oxygenase (HO)-1 renders Jurkat T cells resistant to fas-mediated apoptosis: involvement of iron released by HO-1. Free Radic Biol Med *36*, 858-871.

Clauss, I.M., Gravallese, E.M., Darling, J.M., Shapiro, F., Glimcher, M.J., and Glimcher, L.H. (1993). In situ hybridization studies suggest a role for the basic region-leucine zipper protein hXBP-1 in exocrine gland and skeletal development during mouse embryogenesis. Dev Dyn *197*, 146-156.

Cook, S.A., Sugden, P.H., and Clerk, A. (1999). Regulation of bcl-2 family proteins during development and in response to oxidative stress in cardiac myocytes: association with changes in mitochondrial membrane potential. Circ Res *85*, 940-949.

Credle, J.J., Finer-Moore, J.S., Papa, F.R., Stroud, R.M., and Walter, P. (2005). On the mechanism of sensing unfolded protein in the endoplasmic reticulum. Proc Natl Acad Sci U S A *102*, 18773-18784.

Cunningham, K.S., and Gotlieb, A.I. (2005). The role of shear stress in the pathogenesis of atherosclerosis. Lab Invest *85*, 9-23.

Dai, G., Vaughn, S., Zhang, Y., Wang, E.T., Garcia-Cardena, G., and Gimbrone, M.A., Jr. (2007). Biomechanical forces in atherosclerosis-resistant vascular regions regulate endothelial redox balance via phosphoinositol 3-kinase/Akt-dependent activation of Nrf2. Circ Res *101*, 723-733.

De Keulenaer, G.W., Chappell, D.C., Ishizaka, N., Nerem, R.M., Alexander, R.W., and Griendling, K.K. (1998). Oscillatory and steady laminar shear stress differentially affect human endothelial redox state: role of a superoxide-producing NADH oxidase. Circ Res *82*, 1094-1101.

De Palma, M., Venneri, M.A., Roca, C., and Naldini, L. (2003). Targeting exogenous genes to tumor angiogenesis by transplantation of genetically modified hematopoietic stem cells. Nat Med *9*, 789-795.

De Smet, F., Segura, I., De Bock, K., Hohensinner, P.J., and Carmeliet, P. (2009). Mechanisms of vessel branching: filopodia on endothelial tip cells lead the way. Arterioscler Thromb Vasc Biol *29*, 639-649.

Dejana, E., Tournier-Lasserve, E., and Weinstein, B.M. (2009). The control of vascular integrity by endothelial cell junctions: molecular basis and pathological implications. Dev Cell *16*, 209-221.

Dekker, R.J., Boon, R.A., Rondaij, M.G., Kragt, A., Volger, O.L., Elderkamp, Y.W., Meijers, J.C., Voorberg, J., Pannekoek, H., and Horrevoets, A.J. (2006). KLF2 provokes a gene expression pattern that establishes functional quiescent differentiation of the endothelium. Blood *107*, 4354-4363.

Dekker, R.J., van Soest, S., Fontijn, R.D., Salamanca, S., de Groot, P.G., VanBavel, E., Pannekoek, H., and Horrevoets, A.J. (2002). Prolonged fluid shear stress induces a distinct set of endothelial cell genes, most specifically lung Kruppel-like factor (KLF2). Blood *100*, 1689-1698.

Dekker, R.J., van Thienen, J.V., Rohlena, J., de Jager, S.C., Elderkamp, Y.W., Seppen, J., de Vries, C.J., Biessen, E.A., van Berkel, T.J., Pannekoek, H., *et al.* (2005). Endothelial KLF2 links local arterial shear stress levels to the expression of vascular tone-regulating genes. Am J Pathol *167*, 609-618.

Diehl, J.A., Cheng, M., Roussel, M.F., and Sherr, C.J. (1998). Glycogen synthase kinase-3beta regulates cyclin D1 proteolysis and subcellular localization. Genes Dev *12*, 3499-3511.

Duronio, V. (2008). The life of a cell: apoptosis regulation by the PI3K/PKB pathway. Biochem J *415*, 333-344.

Everaert, B.R., Van Craenenbroeck, E.M., Hoymans, V.Y., Haine, S.E., Van Nassauw, L., Conraads, V.M., Timmermans, J.P., and Vrints, C.J. (2010). Current perspective of pathophysiological and interventional effects on endothelial progenitor cell biology: focus on PI3K/AKT/eNOS pathway. Int J Cardiol *144*, 350-366.

Favatier, F., and Polla, B.S. (2001). Tobacco-smoke-inducible human haem oxygenase-1 gene expression: role of distinct transcription factors and reactive oxygen intermediates. Biochem J *353*, 475-482.

Ferri, K.F., and Kroemer, G. (2001). Organelle-specific initiation of cell death pathways. Nat Cell Biol *3*, E255-263.

Fledderus, J.O., Boon, R.A., Volger, O.L., Hurttila, H., Yla-Herttuala, S., Pannekoek, H., Levonen, A.L., and Horrevoets, A.J. (2008). KLF2 primes the antioxidant transcription factor Nrf2 for activation in endothelial cells. Arterioscler Thromb Vasc Biol *28*, 1339-1346.

Fledderus, J.O., van Thienen, J.V., Boon, R.A., Dekker, R.J., Rohlena, J., Volger, O.L., Bijnens, A.P., Daemen, M.J., Kuiper, J., van Berkel, T.J., *et al.* (2007). Prolonged shear stress and KLF2 suppress constitutive proinflammatory transcription through inhibition of ATF2. Blood *109*, 4249-4257.

Gargalovic, P.S., Gharavi, N.M., Clark, M.J., Pagnon, J., Yang, W.P., He, A., Truong, A., Baruch-Oren, T., Berliner, J.A., Kirchgessner, T.G., *et al.* (2006). The unfolded protein response is an important regulator of inflammatory genes in endothelial cells. Arterioscler Thromb Vasc Biol *26*, 2490-2496.

Gerhardt, H., and Betsholtz, C. (2003). Endothelial-pericyte interactions in angiogenesis. Cell Tissue Res *314*, 15-23.

Gerhardt, H., Golding, M., Fruttiger, M., Ruhrberg, C., Lundkvist, A., Abramsson, A., Jeltsch, M., Mitchell, C., Alitalo, K., Shima, D., *et al.* (2003). VEGF guides angiogenic sprouting utilizing endothelial tip cell filopodia. J Cell Biol *161*, 1163-1177.

Glass, C.K., and Witztum, J.L. (2001). Atherosclerosis. the road ahead. Cell *104*, 503-516.

Golubovskaya, V., Kaur, A., and Cance, W. (2004). Cloning and characterization of the promoter region of human focal adhesion kinase gene: nuclear factor kappa B and p53 binding sites. Biochim Biophys Acta *1678*, 111-125.

Haberland, M., Montgomery, R.L., and Olson, E.N. (2009). The many roles of histone deacetylases in development and physiology: implications for disease and therapy. Nat Rev Genet *10*, 32-42.

Hahn, C., and Schwartz, M.A. (2009). Mechanotransduction in vascular physiology and atherogenesis. Nat Rev Mol Cell Biol *10*, 53-62.

Hamdulay, S.S., Wang, B., Birdsey, G.M., Ali, F., Dumont, O., Evans, P.C., Haskard, D.O., Wheeler-Jones, C.P., and Mason, J.C. (2010). Celecoxib activates PI-3K/Akt and mitochondrial redox signaling to enhance heme oxygenase-1-mediated anti-inflammatory activity in vascular endothelium. Free Radic Biol Med *48*, 1013-1023.

Harrison, D.G., Widder, J., Grumbach, I., Chen, W., Weber, M., and Searles, C. (2006). Endothelial mechanotransduction, nitric oxide and vascular inflammation. J Intern Med *259*, 351-363.

Heil, M., Eitenmuller, I., Schmitz-Rixen, T., and Schaper, W. (2006). Arteriogenesis versus angiogenesis: similarities and differences. J Cell Mol Med *10*, 45-55.

Hetz, C., Martinon, F., Rodriguez, D., and Glimcher, L.H. (2011). The unfolded protein response: integrating stress signals through the stress sensor IRE1alpha. Physiol Rev *91*, 1219-1243.

Hill-Kapturczak, N., Sikorski, E., Voakes, C., Garcia, J., Nick, H.S., and Agarwal, A. (2003). An internal enhancer regulates heme- and cadmium-mediated induction of human heme oxygenase-1. Am J Physiol Renal Physiol *285*, F515-523.

Hobbs, H.H., and Rader, D.J. (1999). ABC1: connecting yellow tonsils, neuropathy, and very low HDL. J Clin Invest *104*, 1015-1017.

Hojo, Y., Saito, Y., Tanimoto, T., Hoefen, R.J., Baines, C.P., Yamamoto, K., Haendeler, J., Asmis, R., and Berk, B.C. (2002). Fluid shear stress attenuates hydrogen peroxide-induced c-Jun NH2-terminal kinase activation via a glutathione reductase-mediated mechanism. Circ Res *91*, 712-718.

Hollien, J., Lin, J.H., Li, H., Stevens, N., Walter, P., and Weissman, J.S. (2009). Regulated Ire1-dependent decay of messenger RNAs in mammalian cells. J Cell Biol *186*, 323-331.

Hollien, J., and Weissman, J.S. (2006). Decay of endoplasmic reticulum-localized mRNAs during the unfolded protein response. Science *313*, 104-107.

Hung, H.S., Chu, M.Y., Lin, C.H., Wu, C.C., and Hsu, S.H. (2012). Mediation of the migration of endothelial cells and fibroblasts on polyurethane nanocomposites by the activation of integrin-focal adhesion kinase signaling. J Biomed Mater Res A *100*, 26-37.

Hwang, J., Ing, M.H., Salazar, A., Lassegue, B., Griendling, K., Navab, M., Sevanian, A., and Hsiai, T.K. (2003a). Pulsatile versus oscillatory shear stress regulates NADPH oxidase subunit expression: implication for native LDL oxidation. Circ Res *93*, 1225-1232.

Hwang, J., Saha, A., Boo, Y.C., Sorescu, G.P., McNally, J.S., Holland, S.M., Dikalov, S., Giddens, D.P., Griendling, K.K., Harrison, D.G., *et al.* (2003b). Oscillatory shear stress stimulates endothelial production of O2- from p47phox-dependent NAD(P)H oxidases, leading to monocyte adhesion. J Biol Chem *278*, 47291-47298.

Ilic, D., Kovacic, B., McDonagh, S., Jin, F., Baumbusch, C., Gardner, D.G., and Damsky, C.H. (2003). Focal adhesion kinase is required for blood vessel morphogenesis. Circ Res *92*, 300-307.

Inoue, K., Kobayashi, M., Yano, K., Miura, M., Izumi, A., Mataki, C., Doi, T., Hamakubo, T., Reid, P.C., Hume, D.A., *et al.* (2006). Histone deacetylase inhibitor

reduces monocyte adhesion to endothelium through the suppression of vascular cell adhesion molecule-1 expression. Arterioscler Thromb Vasc Biol *26*, 2652-2659.

Ishikawa, K., Sugawara, D., Wang, X., Suzuki, K., Itabe, H., Maruyama, Y., and Lusis, A.J. (2001). Heme oxygenase-1 inhibits atherosclerotic lesion formation in ldl-receptor knockout mice. Circ Res *88*, 506-512.

Ishizaka, N., de Leon, H., Laursen, J.B., Fukui, T., Wilcox, J.N., De Keulenaer, G., Griendling, K.K., and Alexander, R.W. (1997). Angiotensin II-induced hypertension increases heme oxygenase-1 expression in rat aorta. Circulation *96*, 1923-1929.

Jakobsson, L., Franco, C.A., Bentley, K., Collins, R.T., Ponsioen, B., Aspalter, I.M., Rosewell, I., Busse, M., Thurston, G., Medvinsky, A., *et al.* (2010). Endothelial cells dynamically compete for the tip cell position during angiogenic sprouting. Nat Cell Biol *12*, 943-953.

Johnson, B.D., Mather, K.J., and Wallace, J.P. (2011). Mechanotransduction of shear in the endothelium: basic studies and clinical implications. Vasc Med *16*, 365-377.

Jung, S.B., Kim, C.S., Naqvi, A., Yamamori, T., Mattagajasingh, I., Hoffman, T.A., Cole, M.P., Kumar, A., Dericco, J.S., Jeon, B.H., *et al.* (2010). Histone deacetylase 3 antagonizes aspirin-stimulated endothelial nitric oxide production by reversing aspirin-induced lysine acetylation of endothelial nitric oxide synthase. Circ Res *107*, 877-887.

Kaczorowski, D.J., and Zuckerbraun, B.S. (2007). Carbon monoxide: medicinal chemistry and biological effects. Curr Med Chem *14*, 2720-2725.

Kadohama, T., Nishimura, K., Hoshino, Y., Sasajima, T., and Sumpio, B.E. (2007). Effects of different types of fluid shear stress on endothelial cell proliferation and survival. J Cell Physiol *212*, 244-251.

Kamimura, Y., Xiong, Y., Iglesias, P.A., Hoeller, O., Bolourani, P., and Devreotes, P.N. (2008). PIP3-independent activation of TorC2 and PKB at the cell's leading edge mediates chemotaxis. Curr Biol *18*, 1034-1043.

Kaser, A., Lee, A.H., Franke, A., Glickman, J.N., Zeissig, S., Tilg, H., Nieuwenhuis, E.E., Higgins, D.E., Schreiber, S., Glimcher, L.H., *et al.* (2008). XBP1 links ER stress to intestinal inflammation and confers genetic risk for human inflammatory bowel disease. Cell *134*, 743-756.

Kawauchi, J., Zhang, C., Nobori, K., Hashimoto, Y., Adachi, M.T., Noda, A., Sunamori, M., and Kitajima, S. (2002). Transcriptional repressor activating transcription factor 3 protects human umbilical vein endothelial cells from tumor necrosis factor-alpha-induced apoptosis through down-regulation of p53 transcription. J Biol Chem *277*, 39025-39034.

Khan, B.V., Parthasarathy, S.S., Alexander, R.W., and Medford, R.M. (1995). Modified low density lipoprotein and its constituents augment cytokine-activated vascular cell adhesion molecule-1 gene expression in human vascular endothelial cells. J Clin Invest *95*, 1262-1270.

Kim, Y.M., Pae, H.O., Park, J.E., Lee, Y.C., Woo, J.M., Kim, N.H., Choi, Y.K., Lee, B.S., Kim, S.R., and Chung, H.T. (2011). Heme oxygenase in the regulation of vascular biology: from molecular mechanisms to therapeutic opportunities. Antioxid Redox Signal *14*, 137-167.

Kirton, J.P., and Xu, Q. (2010). Endothelial precursors in vascular repair. Microvasc Res *79*, 193-199.

Kisanuki, Y.Y., Hammer, R.E., Miyazaki, J., Williams, S.C., Richardson, J.A., and Yanagisawa, M. (2001). Tie2-Cre transgenic mice: a new model for endothelial cell-lineage analysis in vivo. Dev Biol *230*, 230-242.

Koong, A.C., Chauhan, V., and Romero-Ramirez, L. (2006). Targeting XBP-1 as a novel anti-cancer strategy. Cancer Biol Ther *5*, 756-759.

Kronke, G., Kadl, A., Ikonomu, E., Bluml, S., Furnkranz, A., Sarembock, I.J., Bochkov, V.N., Exner, M., Binder, B.R., and Leitinger, N. (2007). Expression of

heme oxygenase-1 in human vascular cells is regulated by peroxisome proliferator-activated receptors. Arterioscler Thromb Vasc Biol *27*, 1276-1282.

Ku, D.N., Giddens, D.P., Zarins, C.K., and Glagov, S. (1985). Pulsatile flow and atherosclerosis in the human carotid bifurcation. Positive correlation between plaque location and low oscillating shear stress. Arteriosclerosis *5*, 293-302.

Kumar, A., Lin, Z., SenBanerjee, S., and Jain, M.K. (2005). Tumor necrosis factor alpha-mediated reduction of KLF2 is due to inhibition of MEF2 by NF-kappaB and histone deacetylases. Mol Cell Biol *25*, 5893-5903.

Lamalice, L., Le Boeuf, F., and Huot, J. (2007). Endothelial cell migration during angiogenesis. Circ Res *100*, 782-794.

Laurindo, F.R., Pedro Mde, A., Barbeiro, H.V., Pileggi, F., Carvalho, M.H., Augusto, O., and da Luz, P.L. (1994). Vascular free radical release. Ex vivo and in vivo evidence for a flow-dependent endothelial mechanism. Circ Res *74*, 700-709.

Lee, A.H., Scapa, E.F., Cohen, D.E., and Glimcher, L.H. (2008). Regulation of hepatic lipogenesis by the transcription factor XBP1. Science *320*, 1492-1496.

Lee, D.Y., Li, Y.S., Chang, S.F., Zhou, J., Ho, H.M., Chiu, J.J., and Chien, S. (2010). Oscillatory flow-induced proliferation of osteoblast-like cells is mediated by alphavbeta3 and beta1 integrins through synergistic interactions of focal adhesion kinase and Shc with phosphatidylinositol 3-kinase and the Akt/mTOR/p70S6K pathway. J Biol Chem *285*, 30-42.

Lee, K., Tirasophon, W., Shen, X., Michalak, M., Prywes, R., Okada, T., Yoshida, H., Mori, K., and Kaufman, R.J. (2002). IRE1-mediated unconventional mRNA splicing and S2P-mediated ATF6 cleavage merge to regulate XBP1 in signaling the unfolded protein response. Genes Dev *16*, 452-466.

Li, H., Korennykh, A.V., Behrman, S.L., and Walter, P. (2010). Mammalian endoplasmic reticulum stress sensor IRE1 signals by dynamic clustering. Proc Natl Acad Sci U S A *107*, 16113-16118.

Li, J.M., Mullen, A.M., and Shah, A.M. (2001). Phenotypic properties and characteristics of superoxide production by mouse coronary microvascular endothelial cells. J Mol Cell Cardiol *33*, 1119-1131.

Liou, H.C., Boothby, M.R., Finn, P.W., Davidon, R., Nabavi, N., Zeleznik-Le, N.J., Ting, J.P., and Glimcher, L.H. (1990). A new member of the leucine zipper class of proteins that binds to the HLA DR alpha promoter. Science *247*, 1581-1584.

Liu, Y., Adachi, M., Zhao, S., Hareyama, M., Koong, A.C., Luo, D., Rando, T.A., Imai, K., and Shinomura, Y. (2009). Preventing oxidative stress: a new role for XBP1. Cell Death Differ *16*, 847-857.

Loboda, A., Stachurska, A., Florczyk, U., Rudnicka, D., Jazwa, A., Wegrzyn, J., Kozakowska, M., Stalinska, K., Poellinger, L., Levonen, A.L., *et al.* (2009). HIF-1 induction attenuates Nrf2-dependent IL-8 expression in human endothelial cells. Antioxid Redox Signal *11*, 1501-1517.

Longworth, M.S., and Laimins, L.A. (2006). Histone deacetylase 3 localizes to the plasma membrane and is a substrate of Src. Oncogene *25*, 4495-4500.

Mahajan, K., and Mahajan, N.P. (2012). PI3K-independent AKT activation in cancers: a treasure trove for novel therapeutics. J Cell Physiol *227*, 3178-3184.

Malek, A.M., Alper, S.L., and Izumo, S. (1999). Hemodynamic shear stress and its role in atherosclerosis. JAMA *282*, 2035-2042.

Marone, R., Cmiljanovic, V., Giese, B., and Wymann, M.P. (2008). Targeting phosphoinositide 3-kinase: moving towards therapy. Biochim Biophys Acta *1784*, 159-185.

Martin, D., Rojo, A.I., Salinas, M., Diaz, R., Gallardo, G., Alam, J., De Galarreta, C.M., and Cuadrado, A. (2004). Regulation of heme oxygenase-1 expression through the phosphatidylinositol 3-kinase/Akt pathway and the Nrf2 transcription factor in response to the antioxidant phytochemical carnosol. J Biol Chem *279*, 8919-8929.

Martin, V., Liu, D., Fueyo, J., and Gomez-Manzano, C. (2008). Tie2: a journey from normal angiogenesis to cancer and beyond. Histol Histopathol *23*, 773-780.

Marui, N., Offermann, M.K., Swerlick, R., Kunsch, C., Rosen, C.A., Ahmad, M., Alexander, R.W., and Medford, R.M. (1993). Vascular cell adhesion molecule-1 (VCAM-1) gene transcription and expression are regulated through an antioxidant-sensitive mechanism in human vascular endothelial cells. J Clin Invest *92*, 1866-1874.

Mayo, L.D., and Donner, D.B. (2001). A phosphatidylinositol 3-kinase/Akt pathway promotes translocation of Mdm2 from the cytoplasm to the nucleus. Proc Natl Acad Sci U S A *98*, 11598-11603.

McNally, J.S., Davis, M.E., Giddens, D.P., Saha, A., Hwang, J., Dikalov, S., Jo, H., and Harrison, D.G. (2003). Role of xanthine oxidoreductase and NAD(P)H oxidase in endothelial superoxide production in response to oscillatory shear stress. Am J Physiol Heart Circ Physiol *285*, H2290-2297.

Mehta, D., and Malik, A.B. (2006). Signaling mechanisms regulating endothelial permeability. Physiol Rev *86*, 279-367.

Metaxa, E., Meng, H., Kaluvala, S.R., Szymanski, M.P., Paluch, R.A., and Kolega, J. (2008). Nitric oxide-dependent stimulation of endothelial cell proliferation by sustained high flow. Am J Physiol Heart Circ Physiol *295*, H736-742.

Montgomery, R.L., Potthoff, M.J., Haberland, M., Qi, X., Matsuzaki, S., Humphries, K.M., Richardson, J.A., Bassel-Duby, R., and Olson, E.N. (2008). Maintenance of cardiac energy metabolism by histone deacetylase 3 in mice. J Clin Invest *118*, 3588-3597.

Morsi, W.G., Shaker, O.G., Ismail, E.F., Ahmed, H.H., El-Serafi, T.I., Maklady, F.A., Abdel-Aziz, M.T., El-Asmar, M.F., and Atta, H.M. (2006). HO-1 and VGEF gene expression in human arteries with advanced atherosclerosis. Clin Biochem *39*, 1057-1062.

Mowbray, A.L., Kang, D.H., Rhee, S.G., Kang, S.W., and Jo, H. (2008). Laminar shear stress up-regulates peroxiredoxins (PRX) in endothelial cells: PRX 1 as a mechanosensitive antioxidant. J Biol Chem *283*, 1622-1627.

Murata, H., Ihara, Y., Nakamura, H., Yodoi, J., Sumikawa, K., and Kondo, T. (2003). Glutaredoxin exerts an antiapoptotic effect by regulating the redox state of Akt. J Biol Chem *278*, 50226-50233.

Nagel, T., Resnick, N., Dewey, C.F., Jr., and Gimbrone, M.A., Jr. (1999). Vascular endothelial cells respond to spatial gradients in fluid shear stress by enhanced activation of transcription factors. Arterioscler Thromb Vasc Biol *19*, 1825-1834.

Nakashima, Y., Raines, E.W., Plump, A.S., Breslow, J.L., and Ross, R. (1998). Upregulation of VCAM-1 and ICAM-1 at atherosclerosis-prone sites on the endothelium in the ApoE-deficient mouse. Arterioscler Thromb Vasc Biol *18*, 842-851.

Nekrutenko, A., and He, J. (2006). Functionality of unspliced XBP1 is required to explain evolution of overlapping reading frames. Trends Genet *22*, 645-648.

Newby, A.C. (2007). Metalloproteinases and vulnerable atherosclerotic plaques. Trends Cardiovasc Med *17*, 253-258.

Newby, A.C. (2008). Metalloproteinase Expression in Monocytes and Macrophages and its Relationship to Atherosclerotic Plaque Instability. Arterioscler Thromb Vasc Biol.

Nigro, P., Abe, J., and Berk, B.C. (2011). Flow shear stress and atherosclerosis: a matter of site specificity. Antioxid Redox Signal *15*, 1405-1414.

Nilsson, J., and Hansson, G.K. (2008). Autoimmunity in atherosclerosis: a protective response losing control? J Intern Med *263*, 464-478.

Nilsson, J., Nordin Fredrikson, G., Schiopu, A., Shah, P.K., Jansson, B., and Carlsson, R. (2007). Oxidized LDL antibodies in treatment and risk assessment of atherosclerosis and associated cardiovascular disease. Curr Pharm Des *13*, 1021-1030.

Nusinzon, I., and Horvath, C.M. (2005). Histone deacetylases as transcriptional activators? Role reversal in inducible gene regulation. Sci STKE *2005*, re11.

O'Neill, A.K., Niederst, M.J., and Newton, A.C. (2012). Suppression of survival signalling pathways by the phosphatase PHLPP. FEBS J.

Oberoi, J., Fairall, L., Watson, P.J., Yang, J.C., Czimmerer, Z., Kampmann, T., Goult, B.T., Greenwood, J.A., Gooch, J.T., Kallenberger, B.C., *et al.* (2011). Structural basis for the assembly of the SMRT/NCoR core transcriptional repression machinery. Nat Struct Mol Biol *18*, 177-184.

Oh, W.J., and Jacinto, E. (2011). mTOR complex 2 signaling and functions. Cell Cycle *10*, 2305-2316.

Olsson, A.K., Dimberg, A., Kreuger, J., and Claesson-Welsh, L. (2006). VEGF receptor signalling - in control of vascular function. Nat Rev Mol Cell Biol *7*, 359-371.

Otterbein, L.E., Soares, M.P., Yamashita, K., and Bach, F.H. (2003a). Heme oxygenase-1: unleashing the protective properties of heme. Trends Immunol *24*, 449-455.

Otterbein, L.E., Zuckerbraun, B.S., Haga, M., Liu, F., Song, R., Usheva, A., Stachulak, C., Bodyak, N., Smith, R.N., Csizmadia, E., *et al.* (2003b). Carbon monoxide suppresses arteriosclerotic lesions associated with chronic graft rejection and with balloon injury. Nat Med *9*, 183-190.

Paine, A., Eiz-Vesper, B., Blasczyk, R., and Immenschuh, S. (2010). Signaling to heme oxygenase-1 and its anti-inflammatory therapeutic potential. Biochem Pharmacol *80*, 1895-1903.

Parmar, K.M., Larman, H.B., Dai, G., Zhang, Y., Wang, E.T., Moorthy, S.N., Kratz, J.R., Lin, Z., Jain, M.K., Gimbrone, M.A., Jr., *et al.* (2006). Integration of flow-dependent endothelial phenotypes by Kruppel-like factor 2. J Clin Invest *116*, 49-58.

Phng, L.K., and Gerhardt, H. (2009). Angiogenesis: a team effort coordinated by notch. Dev Cell *16*, 196-208.

Polak, R., and Buitenhuis, M. (2012). The PI3K/PKB signaling module as key regulator of hematopoiesis: implications for therapeutic strategies in leukemia. Blood *119*, 911-923.

Purdom, S., and Chen, Q.M. (2005). Epidermal growth factor receptor-dependent and -independent pathways in hydrogen peroxide-induced mitogen-activated protein kinase activation in cardiomyocytes and heart fibroblasts. J Pharmacol Exp Ther *312*, 1179-1186.

Rader, D.J., and Daugherty, A. (2008). Translating molecular discoveries into new therapies for atherosclerosis. Nature *451*, 904-913.

Reimold, A.M., Etkin, A., Clauss, I., Perkins, A., Friend, D.S., Zhang, J., Horton, H.F., Scott, A., Orkin, S.H., Byrne, M.C., *et al.* (2000). An essential role in liver development for transcription factor XBP-1. Genes Dev *14*, 152-157.

Risau, W. (1997). Mechanisms of angiogenesis. Nature *386*, 671-674.

Risau, W., and Flamme, I. (1995). Vasculogenesis. Annu Rev Cell Dev Biol *11*, 73-91.

Rodriguez, D., Rojas-Rivera, D., and Hetz, C. (2011). Integrating stress signals at the endoplasmic reticulum: The BCL-2 protein family rheostat. Biochim Biophys Acta *1813*, 564-574.

Romashkova, J.A., and Makarov, S.S. (1999). NF-kappaB is a target of AKT in anti-apoptotic PDGF signalling. Nature *401*, 86-90.

Ron, D., and Walter, P. (2007). Signal integration in the endoplasmic reticulum unfolded protein response. Nat Rev Mol Cell Biol *8*, 519-529.

Ross, R. (1999). Atherosclerosis--an inflammatory disease. N Engl J Med *340*, 115-126.

Rossig, L., Urbich, C., Bruhl, T., Dernbach, E., Heeschen, C., Chavakis, E., Sasaki, K., Aicher, D., Diehl, F., Seeger, F., *et al.* (2005). Histone deacetylase activity is essential for the expression of HoxA9 and for endothelial commitment of progenitor cells. J Exp Med *201*, 1825-1835.

Ryter, S.W., Alam, J., and Choi, A.M. (2006). Heme oxygenase-1/carbon monoxide: from basic science to therapeutic applications. Physiol Rev *86*, 583-650.

Ryter, S.W., Kim, H.P., Hoetzel, A., Park, J.W., Nakahira, K., Wang, X., and Choi, A.M. (2007). Mechanisms of cell death in oxidative stress. Antioxid Redox Signal *9*, 49-89.

Salinas, M., Wang, J., Rosa de Sagarra, M., Martin, D., Rojo, A.I., Martin-Perez, J., Ortiz de Montellano, P.R., and Cuadrado, A. (2004). Protein kinase Akt/PKB phosphorylates heme oxygenase-1 in vitro and in vivo. FEBS Lett *578*, 90-94.

Sandoo, A., van Zanten, J.J., Metsios, G.S., Carroll, D., and Kitas, G.D. (2010). The endothelium and its role in regulating vascular tone. Open Cardiovasc Med J *4*, 302-312.

Schebesta, M., Heavey, B., and Busslinger, M. (2002). Transcriptional control of B-cell development. Curr Opin Immunol *14*, 216-223.

Schroder, M., and Kaufman, R.J. (2005). The mammalian unfolded protein response. Annu Rev Biochem *74*, 739-789.

Shahbazian, M.D., and Grunstein, M. (2007). Functions of site-specific histone acetylation and deacetylation. Annu Rev Biochem *76*, 75-100.

Shelton, J.L., Wang, L., Cepinskas, G., Inculet, R., and Mehta, S. (2008). Human neutrophil-pulmonary microvascular endothelial cell interactions in vitro: differential effects of nitric oxide vs. peroxynitrite. Microvasc Res *76*, 80-88.

Shi, C., Lu, J., Wu, W., Ma, F., Georges, J., Huang, H., Balducci, J., Chang, Y., and Huang, Y. (2011). Endothelial cell-specific molecule 2 (ECSM2) localizes to cell-cell junctions and modulates bFGF-directed cell migration via the ERK-FAK pathway. PLoS One *6*, e21482.

Sima, A.V., Stancu, C.S., and Simionescu, M. (2009). Vascular endothelium in atherosclerosis. Cell Tissue Res *335*, 191-203.

Somanath, P.R., Razorenova, O.V., Chen, J., and Byzova, T.V. (2006). Akt1 in endothelial cell and angiogenesis. Cell Cycle *5*, 512-518.

Sorescu, D., Weiss, D., Lassegue, B., Clempus, R.E., Szocs, K., Sorescu, G.P., Valppu, L., Quinn, M.T., Lambeth, J.D., Vega, J.D., *et al.* (2002). Superoxide production and expression of nox family proteins in human atherosclerosis. Circulation *105*, 1429-1435.

Stocker, R., and Perrella, M.A. (2006). Heme oxygenase-1: a novel drug target for atherosclerotic diseases? Circulation *114*, 2178-2189.

Stokoe, D., Stephens, L.R., Copeland, T., Gaffney, P.R., Reese, C.B., Painter, G.F., Holmes, A.B., McCormick, F., and Hawkins, P.T. (1997). Dual role of phosphatidylinositol-3,4,5-trisphosphate in the activation of protein kinase B. Science *277*, 567-570.

Surapisitchat, J., Hoefen, R.J., Pi, X., Yoshizumi, M., Yan, C., and Berk, B.C. (2001). Fluid shear stress inhibits TNF-alpha activation of JNK but not ERK1/2 or p38 in human umbilical vein endothelial cells: Inhibitory crosstalk among MAPK family members. Proc Natl Acad Sci U S A *98*, 6476-6481.

Takabe, W., Warabi, E., and Noguchi, N. (2011). Anti-atherogenic effect of laminar shear stress via Nrf2 activation. Antioxid Redox Signal *15*, 1415-1426.

Takami, Y., and Nakayama, T. (2000). N-terminal region, C-terminal region, nuclear export signal, and deacetylation activity of histone deacetylase-3 are essential for the viability of the DT40 chicken B cell line. J Biol Chem *275*, 16191-16201.

Tamminen, M., Mottino, G., Qiao, J.H., Breslow, J.L., and Frank, J.S. (1999). Ultrastructure of early lipid accumulation in ApoE-deficient mice. Arterioscler Thromb Vasc Biol *19*, 847-853.

Taniyama, Y., and Griendling, K.K. (2003). Reactive oxygen species in the vasculature: molecular and cellular mechanisms. Hypertension *42*, 1075-1081.

Tirziu, D., Dobrian, A., Tasca, C., Simionescu, M., and Simionescu, N. (1995). Intimal thickenings of human aorta contain modified reassembled lipoproteins. Atherosclerosis *112*, 101-114.

Tricot, O., Mallat, Z., Heymes, C., Belmin, J., Leseche, G., and Tedgui, A. (2000). Relation between endothelial cell apoptosis and blood flow direction in human atherosclerotic plaques. Circulation *101*, 2450-2453.

Trivedi, C.M., Lu, M.M., Wang, Q., and Epstein, J.A. (2008). Transgenic overexpression of Hdac3 in the heart produces increased postnatal cardiac myocyte proliferation but does not induce hypertrophy. J Biol Chem *283*, 26484-26489.

Ushio-Fukai, M. (2006). Redox signaling in angiogenesis: role of NADPH oxidase. Cardiovasc Res *71*, 226-235.

van Hinsbergh, V.W. (2001). The endothelium: vascular control of haemostasis. Eur J Obstet Gynecol Reprod Biol *95*, 198-201.

van Thienen, J.V., Fledderus, J.O., Dekker, R.J., Rohlena, J., van Ijzendoorn, G.A., Kootstra, N.A., Pannekoek, H., and Horrevoets, A.J. (2006). Shear stress sustains atheroprotective endothelial KLF2 expression more potently than statins through mRNA stabilization. Cardiovasc Res *72*, 231-240.

Vandenbroucke, E., Mehta, D., Minshall, R., and Malik, A.B. (2008). Regulation of endothelial junctional permeability. Ann N Y Acad Sci *1123*, 134-145.

Venneri, M.A., De Palma, M., Ponzoni, M., Pucci, F., Scielzo, C., Zonari, E., Mazzieri, R., Doglioni, C., and Naldini, L. (2007). Identification of proangiogenic TIE2-expressing monocytes (TEMs) in human peripheral blood and cancer. Blood *109*, 5276-5285.

Vivanco, I., and Sawyers, C.L. (2002). The phosphatidylinositol 3-Kinase AKT pathway in human cancer. Nat Rev Cancer *2*, 489-501.

Wang, J., Mahmud, S.A., Bitterman, P.B., Huo, Y., and Slungaard, A. (2007). Histone deacetylase inhibitors suppress TF-kappaB-dependent agonist-driven tissue factor expression in endothelial cells and monocytes. J Biol Chem *282*, 28408-28418.

Warabi, E., Takabe, W., Minami, T., Inoue, K., Itoh, K., Yamamoto, M., Ishii, T., Kodama, T., and Noguchi, N. (2007). Shear stress stabilizes NF-E2-related factor 2 and induces antioxidant genes in endothelial cells: role of reactive oxygen/nitrogen species. Free Radic Biol Med *42*, 260-269.

Wary, K.K., Kohler, E.E., and Chatterjee, I. (2012). Focal adhesion kinase regulation of neovascularization. Microvasc Res *83*, 64-70.

Weiss, D., Kools, J.J., and Taylor, W.R. (2001). Angiotensin II-induced hypertension accelerates the development of atherosclerosis in apoE-deficient mice. Circulation *103*, 448-454.

White, C.R., Haidekker, M., Bao, X., and Frangos, J.A. (2001). Temporal gradients in shear, but not spatial gradients, stimulate endothelial cell proliferation. Circulation *103*, 2508-2513.

Wolinsky, H. (1980). A proposal linking clearance of circulating lipoproteins to tissue metabolic activity as a basis for understanding atherogenesis. Circ Res *47*, 301-311.

World, C.J., Garin, G., and Berk, B. (2006). Vascular shear stress and activation of inflammatory genes. Curr Atheroscler Rep *8*, 240-244.

Xiao, Q., Zeng, L., Zhang, Z., Hu, Y., and Xu, Q. (2007). Stem cell-derived Sca-1+ progenitors differentiate into smooth muscle cells, which is mediated by collagen IV-integrin alpha1/beta1/alphav and PDGF receptor pathways. Am J Physiol Cell Physiol *292*, C342-352.

Xiao, Q., Zeng, L., Zhang, Z., Margariti, A., Ali, Z.A., Channon, K.M., Xu, Q., and Hu, Y. (2006). Sca-1+ progenitors derived from embryonic stem cells differentiate into endothelial cells capable of vascular repair after arterial injury. Arterioscler Thromb Vasc Biol *26*, 2244-2251.

Xu, Q. (2008). Stem cells and transplant arteriosclerosis. Circ Res *102*, 1011-1024.

Xu, Q., Zhang, Z., Davison, F., and Hu, Y. (2003). Circulating progenitor cells regenerate endothelium of vein graft atherosclerosis, which is diminished in ApoE-deficient mice. Circ Res *93*, e76-86.

Xu, X., Gao, X., Potter, B.J., Cao, J.M., and Zhang, C. (2007). Anti-LOX-1 rescues endothelial function in coronary arterioles in atherosclerotic ApoE knockout mice. Arterioscler Thromb Vasc Biol *27*, 871-877.

Yamashita, J., Itoh, H., Hirashima, M., Ogawa, M., Nishikawa, S., Yurugi, T., Naito, M., and Nakao, K. (2000). Flk1-positive cells derived from embryonic stem cells serve as vascular progenitors. Nature *408*, 92-96.

Yamazaki, H., Hiramatsu, N., Hayakawa, K., Tagawa, Y., Okamura, M., Ogata, R., Huang, T., Nakajima, S., Yao, J., Paton, A.W., *et al.* (2009). Activation of the Akt-NF-kappaB pathway by subtilase cytotoxin through the ATF6 branch of the unfolded protein response. J Immunol *183*, 1480-1487.

Yanagitani, K., Imagawa, Y., Iwawaki, T., Hosoda, A., Saito, M., Kimata, Y., and Kohno, K. (2009). Cotranslational targeting of XBP1 protein to the membrane promotes cytoplasmic splicing of its own mRNA. Mol Cell *34*, 191-200.

Yang, W.M., Tsai, S.C., Wen, Y.D., Fejer, G., and Seto, E. (2002). Functional domains of histone deacetylase-3. J Biol Chem *277*, 9447-9454.

Yang, W.M., Yao, Y.L., Sun, J.M., Davie, J.R., and Seto, E. (1997). Isolation and characterization of cDNAs corresponding to an additional member of the human histone deacetylase gene family. J Biol Chem *272*, 28001-28007.

Yin, X., Dewille, J.W., and Hai, T. (2008). A potential dichotomous role of ATF3, an adaptive-response gene, in cancer development. Oncogene *27*, 2118-2127.

Yoshida, H. (2007). Unconventional splicing of XBP-1 mRNA in the unfolded protein response. Antioxid Redox Signal *9*, 2323-2333.

Yoshida, H., Matsui, T., Yamamoto, A., Okada, T., and Mori, K. (2001). XBP1 mRNA is induced by ATF6 and spliced by IRE1 in response to ER stress to produce a highly active transcription factor. Cell *107*, 881-891.

Yoshida, H., Oku, M., Suzuki, M., and Mori, K. (2006). pXBP1(U) encoded in XBP1 pre-mRNA negatively regulates unfolded protein response activator pXBP1(S) in mammalian ER stress response. J Cell Biol *172*, 565-575.

Zampetaki, A., Kirton, J.P., and Xu, Q. (2008). Vascular repair by endothelial progenitor cells. Cardiovasc Res *78*, 413-421.

Zampetaki, A., Zeng, L., Margariti, A., Xiao, Q., Li, H., Zhang, Z., Pepe, A.E., Wang, G., Habi, O., deFalco, E., *et al.* (2010). Histone deacetylase 3 is critical in endothelial survival and atherosclerosis development in response to disturbed flow. Circulation *121*, 132-142.

Zand, T., Hoffman, A.H., Savilonis, B.J., Underwood, J.M., Nunnari, J.J., Majno, G., and Joris, I. (1999). Lipid deposition in rat aortas with intraluminal hemispherical plug stenosis. A morphological and biophysical study. Am J Pathol *155*, 85-92.

Zeng, L., Xiao, Q., Margariti, A., Zhang, Z., Zampetaki, A., Patel, S., Capogrossi, M.C., Hu, Y., and Xu, Q. (2006). HDAC3 is crucial in shear- and VEGF-induced stem cell differentiation toward endothelial cells. J Cell Biol *174*, 1059-1069.

Zeng, L., Zampetaki, A., Margariti, A., Pepe, A.E., Alam, S., Martin, D., Xiao, Q., Wang, W., Jin, Z.G., Cockerill, G., *et al.* (2009). Sustained activation of XBP1 splicing leads to endothelial apoptosis and atherosclerosis development in response to disturbed flow. Proc Natl Acad Sci U S A *106*, 8326-8331.

Zhang, M.X., Zhang, C., Shen, Y.H., Wang, J., Li, X.N., Chen, L., Zhang, Y., Coselli, J.S., and Wang, X.L. (2008). Effect of 27nt small RNA on endothelial nitric-oxide synthase expression. Mol Biol Cell *19*, 3997-4005.

Zhang, X., Ozawa, Y., Lee, H., Wen, Y.D., Tan, T.H., Wadzinski, B.E., and Seto, E. (2005). Histone deacetylase 3 (HDAC3) activity is regulated by interaction with protein serine/threonine phosphatase 4. Genes Dev *19*, 827-839.

Zhao, J., and Guan, J.L. (2009). Signal transduction by focal adhesion kinase in cancer. Cancer Metastasis Rev *28*, 35-49.

Zhong, Y., Li, J., Wang, J.J., Chen, C., Tran, J.T., Saadi, A., Yu, Q., Le, Y.Z., Mandal, M.N., Anderson, R.E., *et al.* (2012). X-box binding protein 1 is essential for the anti-oxidant defense and cell survival in the retinal pigment epithelium. PLoS One *7*, e38616.

Zhuang, X., Cross, D., Heath, V.L., and Bicknell, R. (2011). Shear stress, tip cells and regulators of endothelial migration. Biochem Soc Trans *39*, 1571-1575.